THE PROCEEDINGS OF THE PHYSICAL SOCIETY

VOL. 47, PART 2 March 1, 1935 NO. 259

538.22:546.711

THE MAGNETIC PROPERTIES OF AMORPHOUS MANGANESE

BY L. F. BATES, D.SC., PH.D., F.INST.P., Reader in Physics,

AND

D. V. REDDI PANTULU, B.SC., University College, London

Received October 13, 1934. *Read in title December* 7, 1934.

ABSTRACT. A description is given of the preparation *in vacuo* of pure amorphous manganese. It is found to be paramagnetic, without trace of ferromagnetism, and to obey the Curie-Weiss law, $\chi = 2{\cdot}174 \times 10^{-2}/T + 1540$, over the range of temperature 90 to 600° K., the experimental value of χ at 20° C. being $11{\cdot}80 \times 10^{-6}$.

§ 1. INTRODUCTION

In recent years the magnetic properties of manganese have been investigated by many workers, for it is known to exist in several well-defined states and to combine readily with non-magnetic elements to form ferromagnetic substances. In 1912, Honda[6] used a specimen of fused manganese obtained from Kahlbaum, stated to contain about 3·4 parts of ferromagnetic impurity per 1000, and measured its susceptibility over a wide range of temperature, the value at room temperature being $9{\cdot}70 \times 10^{-6}$ e.m.u. per gram. A little later, Ishiwara[8], using a similar sample, obtained $9{\cdot}66 \times 10^{-6}$, and suggested that certain traces of ferromagnetism might be attributed to the combination of manganese with nitrogen.

Hadfield, Chéveneau and Géneau[5] prepared manganese from an amalgam and cast it in dry hydrogen. The grey powder which they obtained was slightly ferromagnetic with a susceptibility of $11{\cdot}2 \times 10^{-6}$, the traces of ferromagnetism being attributed to combination with hydrogen. Freese[3], however, found that manganese prepared in this way was non-ferromagnetic, and that specimens prepared by cathode disintegration in hydrogen showed no traces of ferromagnetism. Kapitza[9] found that a very pure specimen of manganese prepared by distillation and melted *in vacuo* by Miss Gayler[4] was perfectly paramagnetic with a susceptibility of $9{\cdot}66 \times 10^{-6}$ at room temperature. Miss Wheeler[20] prepared samples of α-manganese by distillation and obtained a sample of β-manganese by quenching an α specimen

at 1000° C. in water. She found susceptibilities of 9·60 and $8{\cdot}80 \times 10^{-6}$ for the α and β specimens respectively, with no traces of ferromagnetism. It must also be recorded that Shimizu[14] obtained specimens by distillation and followed the magnetic changes associated with the α to β and β to γ transitions, but his values for the susceptibilities are much lower than those recorded above, and the two magnetic transition points recorded by him do not appear to correspond with any of the four transition temperatures recorded by Miss Gayler.

It is generally stated that the susceptibility of manganese appears to be independent of the temperature over a wide range. Thus, Owen[12] used a fused Kahlbaum specimen and found a value of $8{\cdot}93 \times 10^{-6}$ which was practically independent of temperature over many hundreds of degrees. This value is, however, rather low compared with Miss Wheeler's, assuming that it refers to unquenched manganese. Again, Honda and Soné[7] made measurements with similar specimens and also found the susceptibility constant over a wide range. It does not appear to be profitable, however, to consider their results in detail, for their specimens contained considerable quantities of iron and appreciable amounts of aluminium, copper and silicon, and certain sudden changes in susceptibility and the temperature hysteresis phenomena exhibited by these specimens may not be attributed to pure manganese. It therefore seems that the statements concerning the constant susceptibility of manganese are open to question. As no record of the preparation of pure amorphous manganese from an amalgam heated *in vacuo* could be found, and its thermomagnetic properties were unknown, the following preparation and investigation were made.

§ 2. PREPARATION OF SPECIMENS

Manganese amalgam was prepared by electrolysis in the following manner. A saturated solution of manganese chloride was placed in a large glazed earthenware trough and crystals were added during the electrolysis to keep the solution saturated. The anode consisted of a platinum strip placed inside a porous pot containing saturated manganese sulphate solution. The cathode was a pool of mercury contained in a flat dish. During electrolysis the reactions at the anode were vigorous and could become unpleasant, but the latter tendency was counteracted by periodically transferring the platinum strip to a porous pot filled with fresh solution. A stream of manganese sulphate could, of course, be used in large-scale manufacture.

Usually, a current of six amperes was passed for thirty minutes. The method employed in stirring the mercury was important, for when it was vigorously stirred by a rotating glass vane the amalgam did not appear to be at all rich in manganese. Careful stirring with a glass stirrer, such that the portions of the amalgam richer in manganese were systematically pushed beneath the surface of the pool, gave very satisfactory yields.

The amalgam was quickly washed in water and squeezed in a linen bag. The heavy mass thus obtained was rapidly forced into the pyrex glass bulb *A* of figure 1 through the tube *a*, which was then sealed. The apparatus of figure 1 was placed inside a furnace up to the region *b*, and exhausted through drying tubes by a Hyvac

pump. When all traces of water had been removed the temperature was raised slowly to 370° C., when the mercury vapour driven off was condensed in a water-cooled bulb. After the bulb *A* had been maintained at 370° C. for a sufficient time a mercury-vapour pump and vapour-trap were used to remove the last traces of mercury from the manganese. The apparatus was sealed at the constriction *e* and allowed to cool slowly.

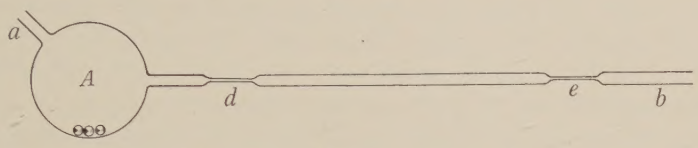

Figure 1.

The porous black lump of manganese was now powdered and forced into the tube *de*, which was of uniform cross-section of diameter 0·5 cm. Inside the bulb *A* were three pyrex beads, and on shaking of the bulb these easily smashed the manganese to a fine powder. The powder was shaken into the tube, the beads again being used to force it through the constriction *d*. Finally, when practically all the manganese had been forced into *de*, the tube was sealed at *d*, and glass hooks were formed at *d* and *e* as shown in figure 2. The tube *de* now contained a specimen of amorphous manganese prepared and sealed *in vacuo*. Its purity undoubtedly depended to some extent on the rapidity with which the amalgam was transferred from the electrolyte trough to the bulb *A*.

§ 3. MEASUREMENT OF MAGNETIC SUSCEPTIBILITY

The measurement of magnetic susceptibility was made by the Gouy method, the tube *de* being suspended vertically from the arm of a sensitive balance with its lower end in a uniform field between the flat pole pieces of an electromagnet, as shown in figure 2. A tube cut from the same piece of pyrex was evacuated, sealed and attached close to the lower end of *de*, in order to compensate for the magnetic effects of the tube *de* and the air displaced by it. Therefore, except for a small effect due to slight dissimilarities between the two tubes, the magnetic field acting on the system provided a downward force mg equal to $\frac{1}{2}k\alpha\,(H^2-H_0^2)$ dynes, where k is the susceptibility per cm.^{3} of the manganese, α the area of internal cross-section of the tube, and H and H_0 the strengths of the field at the lower and upper ends of *de*, respectively. In our experiments H_0^2 and the small effect just mentioned were found negligible. H was measured by a calibrated fluximeter and search coil.

mg

H

In the high-temperature measurements *de* was suspended from a copper wire inside the furnace, as shown in figure 2. The furnace consisted of a thick-walled copper tube suitably wound and lagged. The temperature in the neighbourhood of the lower end of *de* was recorded by a mercury thermometer inserted through *f*; it was calibrated *in situ* against a series of standard thermometers placed vertically in turn inside the furnace. In the low-temperature measurements the tubes were

suspended by a thread inside a copper tube surrounded by liquid oxygen or carbon dioxide and alcohol mixture contained in a Dewar flask. In the latter case the temperature was measured by a standard pentane thermometer.

After these measurements had been made, *de* was weighed and opened, and the manganese was removed. The area of internal cross-section and the volume previously occupied by manganese were found by suitable weighings. The suscepti-

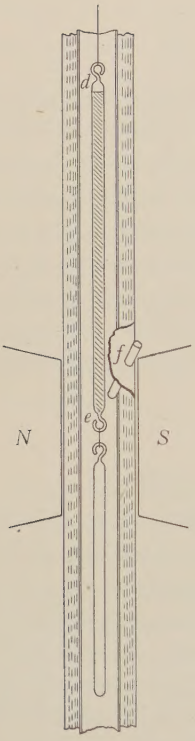

Figure 2.

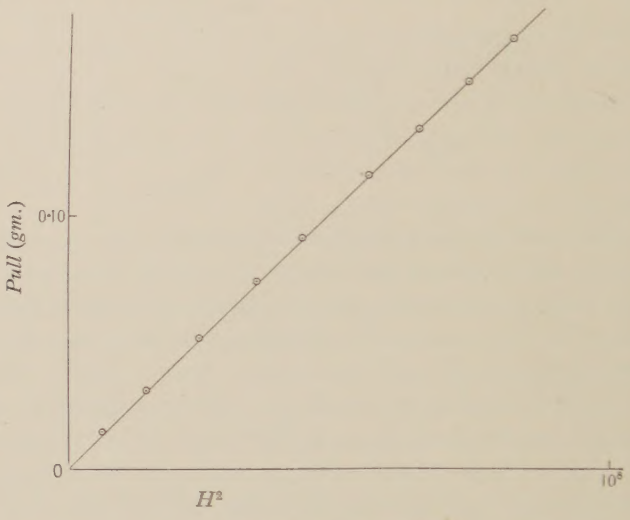

Figure 3 (*a*). Specimen No. 1.

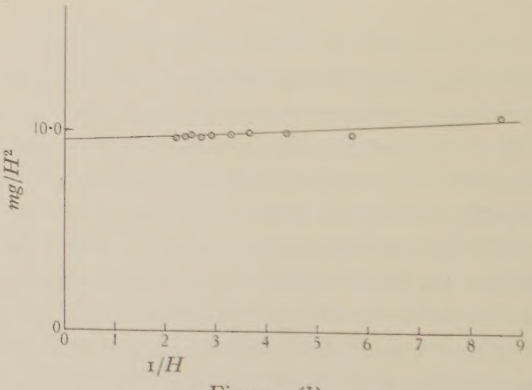

Figure 3 (*b*).

bility per gram could now be calculated. These operations meant the loss of the pure manganese, for we were unable satisfactorily to transfer the intensely pyrophoric material from one vessel to another. The method of poisoning with hydrogen which we tried to adopt in accordance with published information was found useless. Indeed, very little hydrogen appeared to be absorbed by the manganese. The above magnetic results were also checked against a standardized solution of nickel chloride of known susceptibility, kindly supplied by Professor Sugden.

§ 4. EXPERIMENTAL RESULTS

The most complete investigations were made with two chosen specimens of amorphous manganese. The first specimen, I, was made before the best arrangements had been effected for the rapid handling of the amalgam, so that it was in contact with air for a longer period than was desirable. Accordingly, it exhibited traces of ferromagnetism as shown by figures 3 (*a*) and 3 (*b*), where the downward force mg is plotted against H^2, and mg/H^2 against $1/H$, respectively. For small values of H^2 the curve of figure 3 (*a*) is not linear. Figure 3 (*b*) shows that Honda's method may be employed to eliminate the effect of the ferromagnetic impurity, provided that the values of H^2 are not so low that the measurements are liable to be inaccurate.

The second specimen, II, was made under very satisfactory conditions, and showed no traces of ferromagnetism, the curve corresponding to figure 3 (*a*) being strictly linear. Mr H. Terrey kindly analysed this specimen and found it entirely free of mercury and other metals. We therefore conclude that amorphous manganese properly prepared *in vacuo* is definitely non-ferromagnetic, and the traces of ferromagnetism exhibited by specimen I are attributed to the action of nitrogen; we propose to study this action in more detail at a later date.

The way in which the susceptibility of specimen II varied with temperature over the range -183 to 340° C. is shown in figure 4, where the reciprocal of the susceptibility per gram is plotted against the temperature. Figure 4 shows that over a considerable range the value of the susceptibility per gram is given by the Curie-Weiss law

$$\chi = C/(T+\Delta) = 2{\cdot}174 \times 10^{-2}/(T+1540), \qquad \Delta,\ T$$

from which it follows that the effective magnetic moment of a manganese atom is 3·09 Bohr magnetons. The actual susceptibility per gram at 20° was $11{\cdot}80 \times 10^{-6}$. All values in figure 4 have been corrected for the diamagnetism of the manganese atom, which was taken as 0·1 unit per gram[16].

Perhaps a more adequate conception of the rate of change of χ with T may be obtained by reference to figure 5, where the uncorrected experimental values of the susceptibility are plotted against the corresponding absolute temperatures.

In order to compare the paramagnetic properties of the two specimens, the effects of the ferromagnetic impurity in specimen I were eliminated by Honda's method; see figure 3 (*b*). It was considered unnecessary to apply the more complete form of correction given by Vogt[17, 18]. The susceptibility χ_∞ in an infinitely large field is assumed to be related to the susceptibility χ_H in a field H by the equation $\chi_\infty = \chi_H - \sigma/H$, where σ is the saturation magnetization of the ferromagnetic impurity. The values of χ_∞ were therefore obtained at chosen temperatures -183, 20, 166 and 299° C., from the corresponding values of χ_H for two suitable values of H. The graph of $1/\chi_\infty$ against T was strictly linear over the range -183 to 300° C. with a value 1541° of Δ. The value of the susceptibility at room-temperature corrected for diamagnetism of the manganese atom was $11{\cdot}83 \times 10^{-6}$. The agreement with the corresponding values of specimen II is very striking.

χ_∞ χ_H

Two further points of interest appear to merit record in connexion with specimen I. First, the mass of powder per cm^3 inside the tube was some 20 per cent greater than in the case of specimen II. Secondly, specimen I was far less pyro-

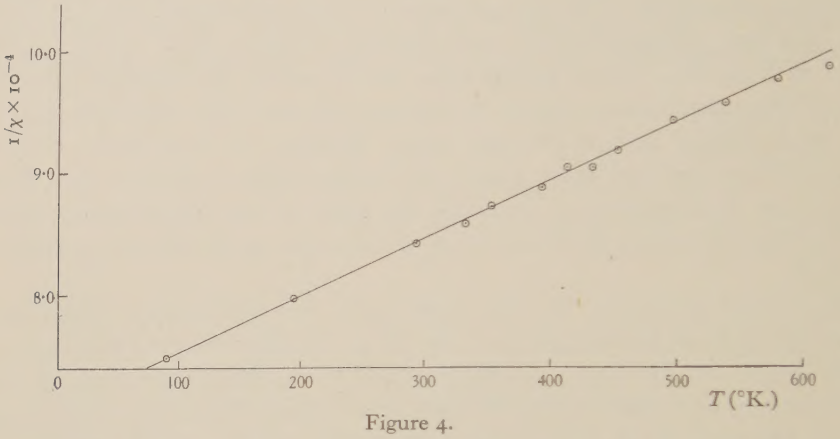

Figure 4.

phoric, and could be transferred from one tube to another with comparative ease in an atmosphere of hydrogen. These points deserve more extensive examination than we have so far been able to give them.

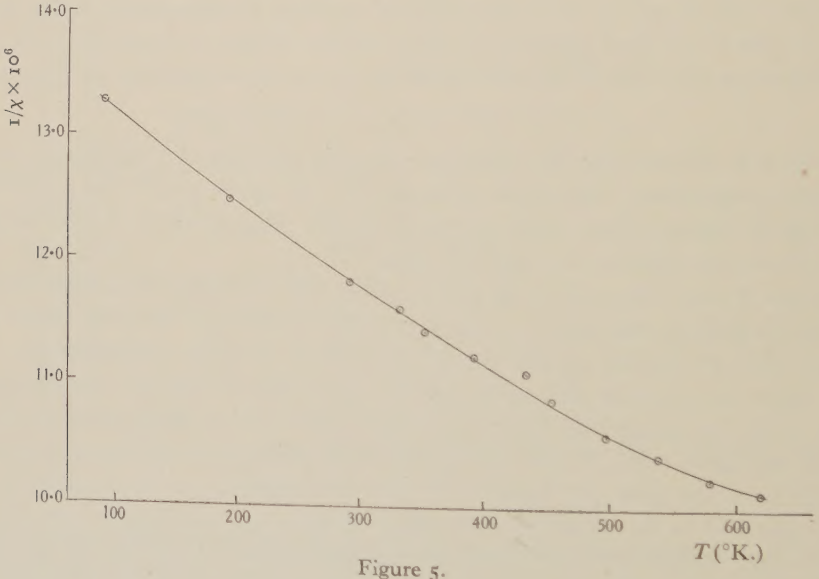

Figure 5.

§ 5. DISCUSSION OF RESULTS

The value obtained for the susceptibility at room temperature compares favourably with the corrected value $11{\cdot}3 \times 10^{-6}$ obtained by Hadfield and his collaborators, in view of the differences in the preparations. There is, however, a

considerable difference between our value and those of Kapitza and Miss Wheeler, which must be due to differences in crystalline structure. It would thus appear that in the case of amorphous manganese there is less quenching of the electron orbits than in the other forms. The value obtained for the effective atomic moment, 3·09 Bohr magnetons, agrees well with the value 3·05 given by Sadron[13], who finds that the manganese atom dissolves in manganese-nickel and manganese-cobalt alloys with a mean moment of this amount.

The value of Δ, 1540°, is remarkably high, and is very interesting in view of the value, 1720°, recently calculated by Néel[10]. He finds that a series of solid solutions of manganese in copper and silver obey Curie-Weiss laws, the appropriate values of the Curie constant in each case being directly proportional to the concentration of manganese. Hence the Curie constant for 1 gm.-mol. of manganese dissolved under these conditions can be computed. It is thus found that the manganese atom possesses an effective magnetic moment of 4·81 Bohr magnetons, which is considerably higher than any values hitherto recorded.

Néel[11] has recently given a theory of the constant paramagnetism of metals based on classical ideas. He supposes that in a specimen of pure manganese a negative molecular field causes alternate atoms to set with their moments oppositely directed so that the resultant magnetic moment of the specimen is zero. An applied magnetic field produces only a slight departure from this arrangement, and at high temperatures T greater than Δ the susceptibility is given by

$$\chi = C/T + \Delta;$$

while at low temperatures T less than Δ the susceptibility is given by

$$\chi_0 = C/3\Delta,$$

i.e. we have a constant susceptibility. Assuming that the value of χ_0 is $9{\cdot}9 \times 10^{-6}$ and taking his calculated value of C, Néel finds Δ to be 1720° from the last expression. It is therefore of some interest that a form of manganese exists which obeys a Curie-Weiss law even at low temperatures with Δ equal to 1540°.

The highest experimental values for the quantity Δ are found in the case of platinum. Föex and Miss Collet[2] have recently shown that platinum specimens behave in a very complicated way in different magnetic fields and over different ranges of temperature, and give different values for the effective magnetic moment for Δ. To a first approximation Δ was here directly proportional to the value of the Curie constant. The highest value of Δ, 3420°, was found with a specimen which possessed a moment of 13 Weiss magnetons over the range -180 to -110° C. Consequently, beyond a suggestion that a high value of Δ means the presence of an internal molecular field which opposes magnetization, no satisfactory explanation of these high values can at present be given.

The modern quantum theory of the magnetic properties of metals has recently been discussed in an illuminating manner by Stoner[15]. Paramagnetism, on this theory, is attributed to electron spins. In the absence of a magnetic field the number of spins pointing in one direction is balanced by an equal number pointing in the opposite direction. The establishment of a magnetic field causes an increase in the

number pointing along the lines of force. Now according to the Fermi-Dirac statistics, this increase can only occur by the transition of electrons from cells of lower to cells of higher energy. In a metal the conduction electrons must be regarded as occupying a series of energy bands, and accordingly the possibility of transfer depends on the energy-separation between successive bands.

The comparatively high susceptibilities of the transition elements may be considered to be due to a narrowing of these energy bands, which in these atoms are derived from five *d* and one *s* states. Stoner suggests that these bands probably overlap, and perhaps should more properly be treated as one composite band in which the number of electrons able to contribute to the paramagnetism is equal to the number of unpaired electron spins in the atom. From these views is derived an expression for the susceptibility of manganese which requires that the variation with temperature over the range investigated in the above experiments should be of the order of 2 per cent, assuming the critical temperature, i.e. the temperature above which the conduction electrons may be taken to obey classical laws, to be 3150° K. Our experiments may therefore be interpreted as showing that the critical temperature must be much lower than this, and that the composite band must be very narrow.

§ 6. ACKNOWLEDGMENTS

We wish to thank Prof. E. N. da C. Andrade for the facilities afforded us. The cost of the magnet[1] used in this investigation was fully covered by a grant from the Government Grants Committee of the Royal Society, to whom we express our thanks.

REFERENCES

(1) L. F. Bates and B. J. Lloyd-Evans. *Proc. phys. Soc.* **45**, 425 (1933).
(2) G. Föex and Miss Collet. *J. Phys. Radium*, **2**, 290 (1931).
(3) H. Freese. *Phys. Z.* **29**, 191 (1928).
(4) Marie Gayler. *J. Iron Steel Inst.* **115**, 393 (1929).
(5) R. Hadfield, C. Chéveneau and C. Géneau. *Proc. roy. Soc.* A, **94**, 65 (1917).
(6) K. Honda. *Sci. Rep. Tokio Imp. Univ.* **1**, 1 (1912).
(7) H. Honda and T. Soné. *Sci. Rep. Tokio Imp. Univ.* **2**, 27 (1913).
(8) T. Ishiwara. *Sci. Rep. Tokio Imp. Univ.* **1**, 51 (1912).
(9) P. Kapitza. *Proc. roy. Soc.* A, **131**, 266 (1931).
(10) M. L. Néel. *J. Phys. Radium*, **3**, 160 (1932).
(11) M. L. Néel. Thèse, Strasbourg (1932).
(12) H. Owen. *Ann. Phys.*, Lpz., **37**, 657 (1912).
(13) C. Sadron. *C. R. Acad. Sci.*, Paris, **192**, 1311 (1931), and **193**, 1070 (1931).
(14) Y. Shimizu. *Sci. Rep. Tokio Imp. Univ.* **19**, 411 (1930).
(15) E. C. Stoner. *Magnetism and Matter*, Chap. xiv (1934).
(16) J. H. van Vleck. *Electric and Magnetic Susceptibilities*, p. 225 (1932).
(17) E. Vogt. *Ann. Phys.*, Lpz., **14**, 1 (1932).
(18) E. Vogt. *Sci. Progr. Twent. Cent.* **27**, 110 (1933).
(19) P. Weiss. *Congrès International d'Electricité*, Section 1, Rapport 15, p. 26 (1932).
(20) Mary A. Wheeler. *Phys. Rev.* **41**, 351 (1932).

612.843.3

THE COLOUR-VISION CHARACTERISTICS OF TWO TRICHROMATS

By W. D. WRIGHT, D.Sc., Ph.D., A.R.C.S., D.I.C.

AND

F. H. G. PITT, A.R.C.S., D.I.C., B.Sc.

(Imperial College of Science and Technology)

Received September 14, 1934. *Read in title December* 7, 1934.

ABSTRACT. The authors' luminosity curves, trichromatic coefficients, mixture curves, complementary wave-lengths and their mixture in terms of luminosity, their hue-discrimination curves and some data on saturation discrimination have been obtained and the results tabulated. The importance, for visual research, of complete data for individual observers, rather than mean curves for different groups of observers, is emphasized.

§ 1. INTRODUCTION

In the discussion on a recent paper on hue-discrimination[5], the question was raised of the relation between the discrimination function and the colour-mixture data for individual eyes. This raises the larger question of the need, in visual research, of having complete information for each observer, rather than a number of mean curves, especially when these have been obtained for very different groups of observers. This need is of no particular concern in colorimetry, but visual problems can undoubtedly be attacked more profitably by investigating each individual observer completely, relating his various curves with each other, and then comparing the complete characteristics of different observers. This has led us to collect all the data we have for our own eyes and present it in a form suitable for comparing with other results as they become available. We believe this is the first time such complete information has been published for even one eye, but it is to be hoped that data for other observers will be forthcoming in the near future.

It will be realized that the larger part of the tables and curves given here do not represent new observations, but results that have been extracted from previous publications. This applies to the trichromatic coefficients, the hue-discrimination curves and, indirectly, the complementary colours. The luminosity curves and the saturation data represent new observations.

One or two points of interest are noted, but the results have not, as yet, been subjected to any detailed analytical study.

§ 2. APPARATUS

The apparatus used for all the measurements has been the Wright colorimeter, and as this has been described in detail elsewhere[3] no further description is given. The uses of the apparatus have also been given previously, so that, where further reference has been desirable in this paper, it has been made as brief as possible.

§ 3. LUMINOSITY

The evaluation of a luminosity curve involves two distinct measurements. We have first to compare the luminosities of narrow bands of a given spectrum and, secondly, we have to determine the relative amounts of energy in each band. There are three possible ways in which the first observations may be obtained, by direct comparison, by flicker, or by means of a trichromatic colour-match. The first method is useless for accurate work, the second is satisfactory if somewhat lengthy and tedious, while the third is very convenient and straightforward, provided the relative luminosities of the three primaries can be found. The latter method was adopted, as it was particularly convenient with our colorimeter, but it is surprising that the method is not more generally used in heterochromatic photometry. It should be very useful in these days, when gas discharge lamps of various colours are being used on such a large scale for illumination purposes.

The energy in the spectrum viewed in the colorimeter was computed from a knowledge of the colour temperature of the pointolite lamp, from measurements of the absorption of a filter that was used and whose transmission was not strictly uniform throughout the spectrum, from an approximate correction for the absorption in the prisms and lenses of the colorimeter, and from a further correction to allow for the varying width of spectrum transmitted through the exit pupil of the instrument.

The results for W.D.W. and F.H.G.P. are given in the second columns of tables 1 and 2 and in figures 1 and 6 respectively. They have been corrected to give the relative luminosity of an equal-energy spectrum and the ordinates have been adjusted so that the maximum luminosity is in each case 1·000. For W.D.W. the maximum is at 0·558 μ., while for F.H.G.P. it occurs at 0·562 μ.; these values compare with a maximum at 0·555 μ. for the standard luminosity curve. In the blue, both curves are somewhat higher than the normal curve, apparently owing to a less dense macular pigment, as will be shown below from the position of the white points in the colour triangle.

§ 4. TRICHROMATIC COEFFICIENTS

The trichromatic coefficients were obtained exactly as described elsewhere[4] and further description is unnecessary. It has, however, to be decided in what form the results shall be expressed. In 1931, the Commission Internationale de l'Éclairage defined the colorimetric characteristics of a standard observer in terms of three monochromatic radiations, 0·70 μ., 0·5461 μ. and 0·4358 μ., while the units of the

Wave-length	Relative luminosity of equal-energy spectrum	Trichromatic coefficients			Mixture curves for equal-energy spectrum			Complementary wave-lengths		Luminosity of λ to be mixed with unit luminosity of λ'	Saturation-discrimination; just-noticeable wave-length differences	Saturation-discrimination; luminosity of white to be mixed with unit luminosity of λ	Wave-length
λ (μ.)		B (0·46 μ.)	G (0·53 μ.)	R (0·65 μ.)	L_B	L_G	L_R	λ (μ.)	λ' (μ.)		(μ.)		λ (μ.)
0·40	0·010	1·022	−0·054	0·036	0·028	−0·030	0·012	0·40	0·5693	0·0160	—	—	0·40
0·41	0·014	1·021	−0·053	0·034	0·036	−0·038	0·016	0·41	0·5696	0·0164	—	—	0·41
0·42	0·019	1·020	−0·051	0·033	0·047	−0·047	0·019	0·42	0·5698	0·0175	—	—	0·42
0·43	0·027	1·019	−0·048	0·031	0·061	−0·057	0·023	0·43	0·5700	0·0183	0·0076	—	0·43
0·44	0·037	1·018	−0·046	0·028	0·080	−0·071	0·028	0·44	0·5702	0·0196	0·0031	—	0·44
0·45	0·056	1·016	−0·034	0·018	0·098	−0·064	0·022	0·45	0·5704	0·0248	0·0040	—	0·45
0·46	0·085	1·000	0·000	0·000	0·085	0·000	0·000	0·46	0·5722	0·0437	0·00335	0·128	0·46
0·47	0·133	0·955	0·080	−0·035	0·062	0·094	−0·023	0·47	0·5758	0·100	0·00235	—	0·47
0·48	0·186	0·861	0·209	−0·070	0·039	0·187	−0·040	0·48	0·5822	0·245	0·00160	—	0·48
0·49	0·254	0·678	0·424	−0·102	0·023	0·281	−0·050	0·49	0·6030	0·795	0·00118	0·031	0·49
0·50	0·409	0·380	0·755	−0·135	0·012	0·452	−0·055	—	—	—	0·00118	—	0·50
0·51	0·604	0·170	0·958	−0·128	0·006	0·653	−0·055	—	—	—	0·00142	0·024	0·51
0·52	0·772	0·064	1·010	−0·074	0·002	0·808	−0·038	—	—	—	0·00190	—	0·52
0·53	0·874	0·000	1·000	0·000	0·000	0·874	0·000	—	—	—	0·00235	0·033	0·53
0·54	0·951	−0·018	0·934	0·084	−0·0009	0·900	0·052	—	—	—	0·00240	—	0·54
0·55	0·994	−0·020	0·851	0·169	−0·0010	0·882	0·113	—	—	—	0·00204	—	0·55
0·56	0·998	−0·021	0·761	0·260	−0·0012	0·818	0·181	—	—	—	0·00165	0·024	0·56
0·57	0·982	−0·018	0·662	0·356	−0·0010	0·730	0·253	0·4320	0·57	0·0185	0·00140	—	0·57
0·58	0·904	−0·015	0·543	0·472	−0·0008	0·579	0·326	0·4770	0·58	0·190	0·00115	0·030	0·58
0·59	0·781	−0·010	0·416	0·594	−0·0005	0·407	0·376	0·4860	0·59	0·41	0·00100	—	0·59
0·60	0·639	−0·008	0·302	0·706	−0·0003	0·250	0·389	0·4896	0·60	0·69	0·00095	—	0·60
0·61	0·518	−0·004	0·198	0·806	−0·0001	0·143	0·375	0·4910	0·61	1·00	0·00115	-	0·61
0·62	0·400	−0·003	0·123	0·880	−0·0001	0·071	0·329	0·4924	0·62	1·28	0·00155	0·024	0·62
0·63	0·284	−0·002	0·066	0·936	0·0000	0·028	0·256	0·4926	0·63	1·50	0·00210	—	0·63
0·64	0·181	−0·001	0·029	0·972	0·0000	0·008	0·173	0·4928	0·64	1·64	0·00285	—	0·64
0·65	0·111	0·000	0·000	1·000	0·0000	0·000	0·111	0·4930	0·65	1·72	0·0060	0·028	0·65
0·66	0·0686	0·000	−0·013	1·013	0·0000	−0·0014	0·070	—	—	—	—	—	0·66
0·67	0·0408	0·000	−0·018	1·018	0·0000	−0·0011	0·0419	—	—	—	—	—	0·67
0·68	0·0205	0·000	−0·022	1·022	0·0000	−0·0007	0·0212	—	—	—	—	0·036	0·68
0·69	0·0082	0·000	−0·026	1·026	0·0000	−0·0003	0·0085	—	—	—	—	—	0·69
0·70	0·0024	0·000	−0·029	1·029	0·0000	−0·0001	0·0025	0·4932	0·70	1·89	—	0·116	0·70
1931 C.I.E. S_B source		0·421	0·363	0·216	Relative luminosities of trichromatic units of primaries								
λ=0·4940 μ.		0·558	0·558	−0·116	0·46 μ.	0·53 μ.	0·65 μ.						
λ=0·5825 μ.		−0·014	0·507	0·507	0·051	1·000	0·648						

Table 2. Colour characteristics for F.H.G.P.

Wave-length	Relative luminosity of equal-energy spectrum	Trichromatic coefficients			Mixture curves for equal-energy spectrum			Complementary wave-lengths		Luminosity of λ to be mixed with unit luminosity of λ'	Hue-discrimination; just-noticeable wave-length differences	Saturation-discrimination; luminosity of white to be mixed with unit luminosity of λ	Wave-length
λ (μ.)		B (0·46 μ.)	G (0·53 μ.)	R (0·65 μ.)	L_B	L_G	L_R	λ (μ.)	λ' (μ.)		(μ.)		λ (μ.)
0·40	0·012	1·028	−0·054	0·026	0·031	−0·028	0·009	0·40	0·5698	0·0175	—	—	0·40
0·41	0·016	1·027	−0·052	0·025	0·039	−0·036	0·013	0·41	0·5700	0·0180	—	—	0·41
0·42	0·020	1·027	−0·049	0·022	0·048	−0·041	0·013	0·42	0·5702	0·0189	—	—	0·42
0·43	0·026	1·026	−0·044	0·018	0·057	−0·044	0·013	0·43	0·5704	0·0204	0·0050	—	0·43
0·44	0·035	1·022	−0·037	0·015	0·065	−0·042	0·012	0·44	0·5707	0·0244	0·00275	—	0·44
0·45	0·045	1·016	−0·026	0·010	0·068	−0·031	0·008	0·45	0·5712	0·0306	0·00273	—	0·45
0·46	0·054	1·000	0·000	0·000	0·054	0·000	0·000	0·46	0·5721	0·0463	0·00260	0·033	0·46
0·47	0·073	0·938	0·082	−0·020	0·032	0·050	−0·009	0·47	0·5750	0·112	0·00189	—	0·47
0·48	0·120	0·829	0·221	−0·050	0·024	0·115	−0·019	0·48	0·5818	0·283	0·00146	—	0·48
0·49	0·196	0·647	0·445	−0·092	0·017	0·211	−0·032	0·49	0·6088	1·01	0·00118	0·035	0·49
0·50	0·336	0·387	0·729	0·116	0·011	0·367	−0·042	—	—	—	0·00104	—	0·50
0·51	0·508	0·164	0·928	0·092	0·0053	0·542	−0·039	—	—	—	0·00103	0·039	0·51
0·52	0·674	0·058	0·990	−0·048	0·0021	0·697	−0·025	—	—	—	0·00128	—	0·52
0·53	0·786	0·000	1·000	0·000	0·0000	0·786	0·000	—	—	—	0·00156	0·028	0·53
0·54	0·873	−0·023	0·952	0·071	−0·0011	0·829	0·045	—	—	—	0·00168	—	0·54
0·55	0·956	−0·024	0·866	0·158	−0·0013	0·845	0·112	—	—	—	0·00159	—	0·55
0·56	0·998	−0·019	0·771	0·248	−0·0012	0·810	0·189	—	—	—	0·00136	0·031	0·56
0·57	0·987	−0·015	0·668	0·347	−0·0009	0·717	0·271	0·410	0·57	0·0180	0·00115	—	0·57
0·58	0·908	−0·011	0·544	0·467	−0·0006	0·561	0·348	0·4780	0·58	0·234	0·00100	0·030	0·58
0·59	0·800	−0·009	0·418	0·591	−0·0005	0·396	0·405	0·4856	0·59	0·51	0·00085	—	0·59
0·60	0·665	−0·008	0·300	0·708	−0·0003	0·245	0·420	0·4886	0·60	0·80	0·00085	—	0·60
0·61	0·506	−0·006	0·202	0·804	−0·0002	0·130	0·376	0·4901	0·61	1·03	0·00089	—	0·61
0·62	0·371	−0·004	0·116	0·888	−0·0001	0·057	0·314	0·4915	0·62	1·18	0·00104	0·019	0·62
0·63	0·261	−0·003	0·060	0·943	0·0001	0·021	0·240	0·4920	0·63	1·31	0·00131	—	0·63
0·64	0·177	−0·001	0·021	0·980	0·0000	0·005	0·172	0·4922	0·64	1·42	0·00195	—	0·64
0·65	0·110	0·000	0·000	1·000	0·0000	0·000	0·110	0·4924	0·65	1·51	0·00275	0·015	0·65
0·66	0·062	0·000	−0·010	1·010	0·0000	−0·0009	0·063	—	—	—	0·0050	—	0·66
0·67	0·0312	0·000	0·018	1·018	0·0000	−0·0008	0·032	—	—	—	—	—	0·67
0·68	0·0159	0·000	0·021	1·021	0·0000	−0·0005	0·0164	—	—	—	—	0·026	0·68
0·69	0·0073	0·000	−0·022	1·022	0·0000	−0·0002	0·0075	—	—	—	—	—	0·69
0·70	0·0029	0·000	−0·023	1·023	0·0000	−0·0001	0·0030	0·4926	0·70	1·60	—	0·026	0·70
1931 C.I.E. S_B source		0·422	0·367	0·211	Relative luminosities of trichromatic units of primaries								
λ = 0·4940 μ.		0·552	0·552	−0·104	0·46 μ.	0·53 μ.	0·65 μ.						

hree stimuli were taken as equal when mixed together so as to match the colour possessed by a hypothetical source having an equal-energy spectral radiation.

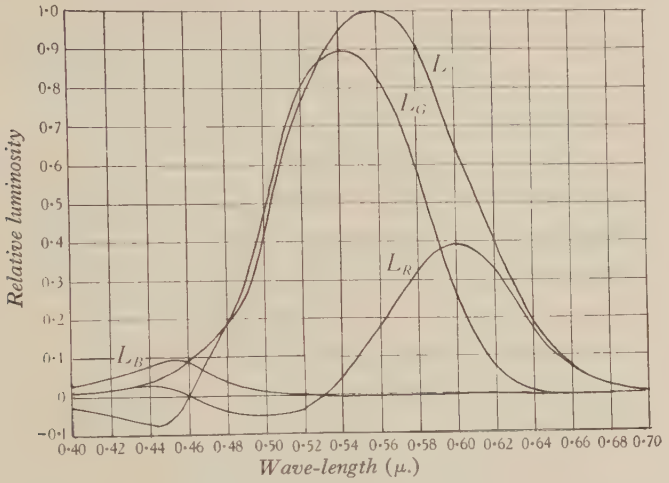

Figure 1. Luminosity curve and mixture curves for equal-energy spectrum (W.D.W.).

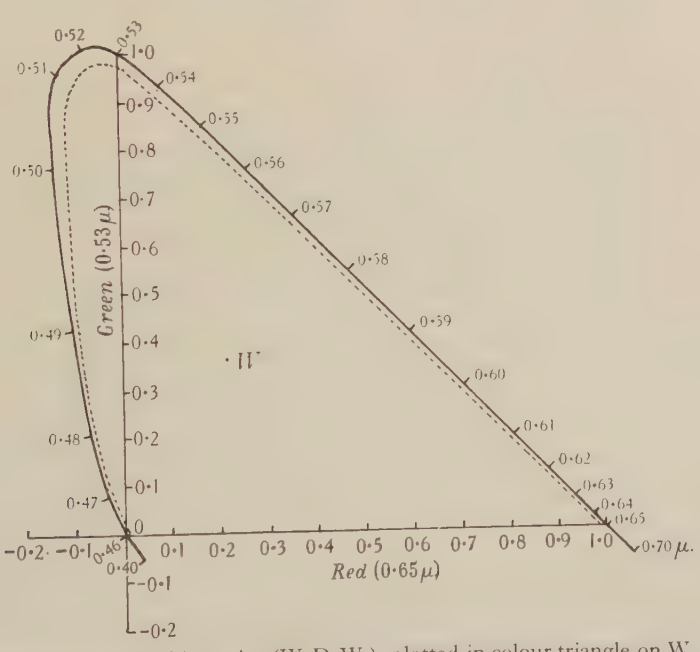

Figure 2. Spectral locus and white point (W.D.W.), plotted in colour triangle on W.D.W. system. Dotted curve shows the locus of points having a just-noticeable difference in saturation from the spectral colours.

Should the coefficients given here be expressed in the same framework? It would be convenient, for instance, to be able to compare the authors' coefficients with those of the standard observer and it is certainly desirable to keep the number of different

reference systems down to a minimum. On the other hand, the standard observer has been defined for use in colorimetry and is only indirectly of interest to the physiological side of the subject. The system of units used by Wright[4] in 1929 has

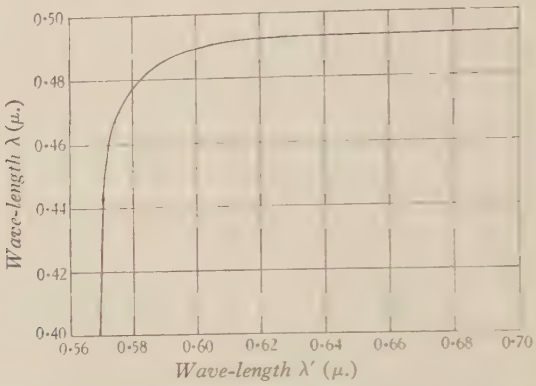

Figure 3. Curve showing relation between complementary wave-lengths λ and λ' (W.D.W.).

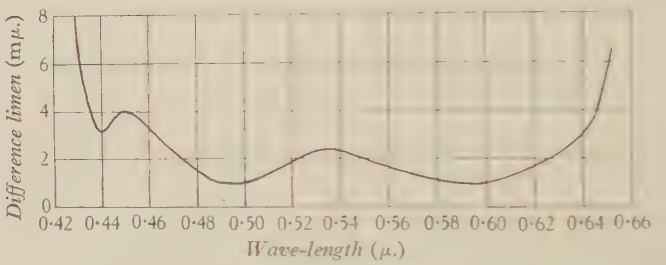

Figure 4. Hue-discrimination curve (W.D.W.).

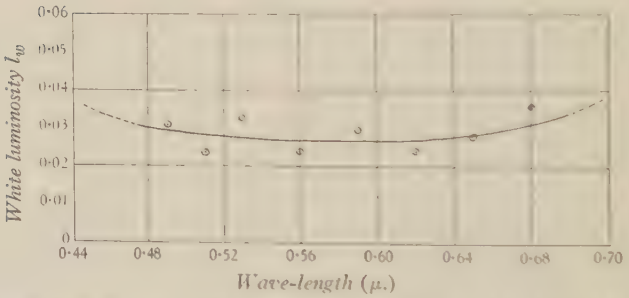

Figure 5. Saturation discrimination (W.D.W.). Luminosity of white (4800 K.) which has to be added to unit luminosity of spectral radiation to produce a just-noticeable difference in saturation from the spectral colour.

an advantage, from the latter point of view, that seems worth retaining. In this method the units of the primaries are based on matches of two monochromatic radiations, a yellow and a blue-green, instead of on a match with a source of continuous-energy radiation. The spectral coefficients so obtained are unaffected by the density of the macular pigment while, on the other hand, the position of the white

point in the colour triangle is a direct indication of the yellowness of the pigment. This feature, we feel, should be retained, and although it could be done while still retaining the primaries prescribed by the Commission Internationale de l'Éclairage, there would be little point in doing so if the units of the primaries were defined on another system. In fact, a hybrid arrangement of this sort would probably cause more confusion than two distinct systems. We therefore decided to retain the monochromatic basis, which we may perhaps be allowed to distinguish as the W.D.W. system, using the primaries we have employed for the past seven years, namely 0·65 μ., 0·53 μ., and 0·46 μ. In the W.D.W. system, the red and green units are adjusted to be equal when matched against a yellow, 0·5825 μ., and the blue and green units are corrected so that equal amounts of 0·46 μ. and 0·53 μ. are required in the match on 0·4940 μ.

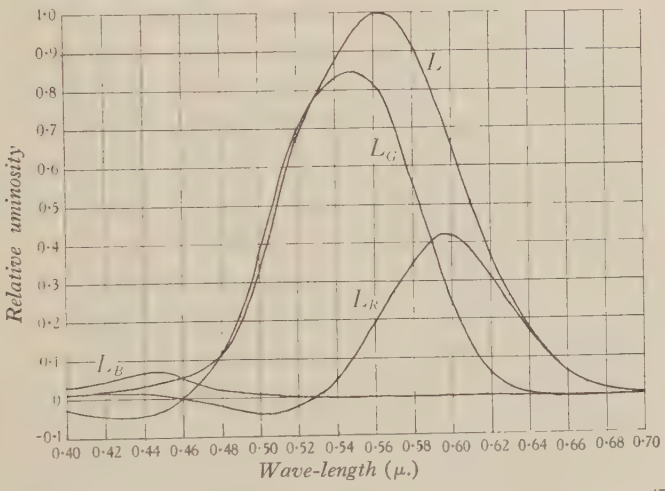

Figure 6. Luminosity curve and mixture curves for equal-energy spectrum (F.H.G.P.).

The authors' coefficients are given in columns 3, 4 and 5 of tables 1 and 2 and are shown in the colour triangle in figures 2 and 7. It is interesting to note that in the blue-green region, the slightly larger negative red coefficients for W.D.W. correspond to larger positive red values in the violet part of the spectrum. Also, the two white points, which by pure coincidence happen to be practically identical, are both on the blue side of the corresponding point for the standard observer, whose coefficients on this system are $R=0{\cdot}249$, $G=0{\cdot}399$, $B=0{\cdot}352$. This indicates that the authors' macular pigment is rather less dense than that of the standard observer, and this would in turn account for the higher ordinates found at the blue end of the luminosity curve. The illuminant used to provide this white point was the S_B source, having a colour temperature of 4800° K., of the Commission Internationale de l'Éclairage (1931).

§ 5. MIXTURE CURVES

The mixture curves, which merely express the colour-mixture data in terms of luminosity, have been computed from the luminosity curve, the trichromatic

coefficients and the relative luminosities of the three primaries, in the usual manner. The data is given for an equal-energy spectrum in columns 6, 7 and 8 of the two tables and diagrammatically in figures 1 and 6. The three mixture curves when added together give, of course, the luminosity curve. Some small differences in the two sets of results, such as the shape of the red curves, the position of the green maxima and, most of all, the differences at the blue end, are of interest.

§ 6. COMPLEMENTARY COLOURS

Once the spectral locus and the white point in the colour triangle are known, it is possible, from the geometry of the triangle, to locate complementary wave-lengths. If a straight line passing through the white point intersects the spectral locus at wave-lengths λ and λ', then these two wave-lengths are complementary. Pairs of complementary wave-lengths have been found in this manner and are given in columns 9 and 10 of the tables. The values obtained will depend on the white radiation to which they refer and, as in the rest of the work, the S_B source of the Commission Internationale de l'Éclairage has been used. For convenience, the complementaries have been given for radiations at intervals of $0{\cdot}010\,\mu$., both for the range between $0{\cdot}40\,\mu$. and $0{\cdot}49\,\mu$. and for that between $0{\cdot}57\,\mu$. and $0{\cdot}65\,\mu$. The green region has, of course, no complementary colour in the spectrum. In figures 3 and 8, the results are shown graphically.

Not only can the complementary wave-lengths be deduced, but the proportion in which they must be mixed can also be calculated and expressed in terms of luminosity, provided the luminosities of the primaries are known. The procedure involves merely the application of the well-known centre-of-gravity property of the colour triangle, combined with the luminosity values of trichromatic units of the radiations concerned. The results calculated in this way are given in column 11 of the tables and show the intensity of λ required to be mixed with unit intensity of λ' to match the white illuminant.

§ 7. HUE-DISCRIMINATION

The determination of the authors' hue-discrimination curves has been described recently[5] and the results given here have been extracted directly from the previous paper. In column 12 of the tables the wave-length difference required to produce a just-noticeable colour-difference has been tabulated for intervals of $0{\cdot}010\,\mu$. through the spectrum. The results are shown graphically in figures 4 and 9.

§ 8. SATURATION-DISCRIMINATION

We should have liked to include some measurements on the relative saturation of the spectral colours, similar to the curves given by Priest and Brickwedde[2] and by Martin, Warburton and Morgan[1]. These investigators have obtained curves showing the luminosity required by each monochromatic radiation to produce, when mixed with a given luminosity of white, a just-noticeable colour-difference from white. In figure 11 a mean curve taken from the paper by Martin, Warburton and

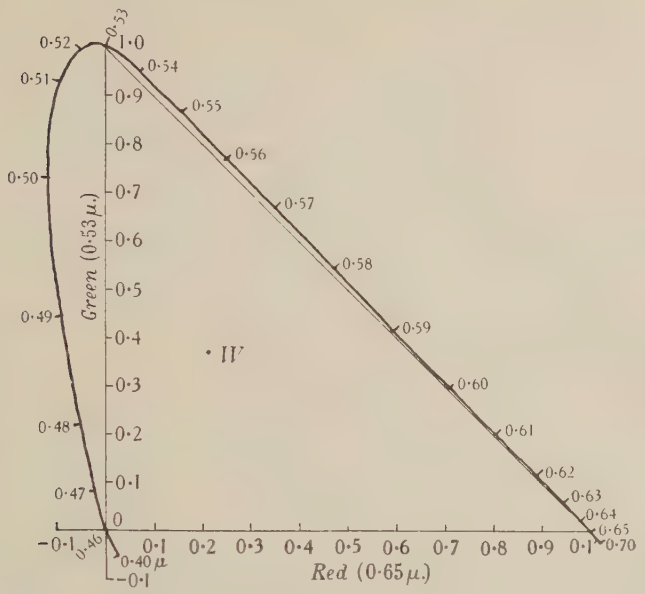

Figure 7. Spectral locus and white point (F.H.G.P.), plotted in colour triangle on W.D.W. system.

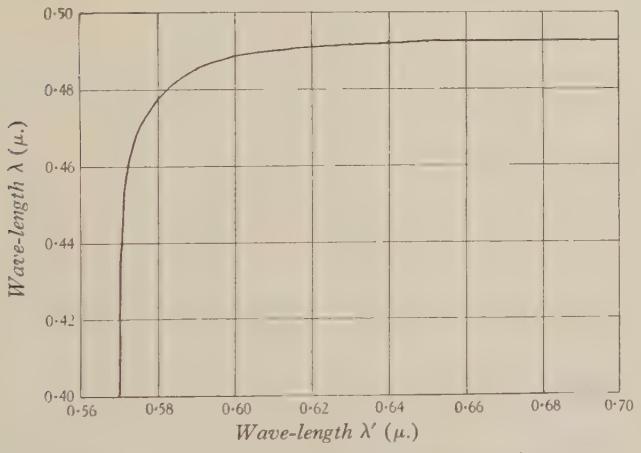

Figure 8. Curve showing relation between complementary wave-lengths λ and λ' (F.H.G.P.).

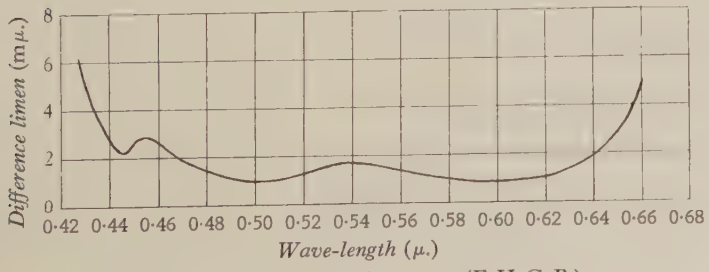

Figure 9. Hue-discrimination curve (F.H.G.P.).

Morgan is reproduced and shows one form of this relation. We can see, for instance, that the yellow region, 0·57 μ., is very much less saturated than the rest of the spectrum, since a greater intensity of the monochromatic beam has to be added to the white to produce a colour-difference. Pressure of other work prevented us from determining these curves for our own eyes, but we were able to obtain some results that we hoped would be equivalent by reversing the measurements and thus simplifying the experimental procedure. Instead of adding a small amount of monochromatic radiation to white, we added a small quantity of white light to the monochromatic radiation, to produce a difference from the spectral colour. This could be fairly easily carried out with our apparatus and we were able to get some results in a comparatively short space of time.

The optical system necessary in addition to the colorimeter is shown in figure 12. The two monochromatic beams a and b coming from the colorimeter pass into a photometer prism P and are brought to a focus at the exit pupil E by the lens O. When the eye is placed at E, a 2° -square field is seen, one half illuminated by beam and the other by beam b. Parallel to this system, an optical bench B was fixed on which a 1000-watt lamp L could be moved by the observer so as to vary the illumination on a magnesium oxide screen M placed at one end of the bench. A glass plate G mounted at 45° to the direction of beam b enabled a fraction of the light from the magnesium screen to be mixed with beam b, and the observer merely had to adjust the position of the lamp L until he could just notice a difference in saturation between a and b, assuming these had been previously adjusted to be of the same wave-length. Two sectors S_1 and S_2 provided further control of the intensities of the field if required. The intensity of beam a could, of course, be varied by the observer by using the photometer wedge belonging to the colorimeter. The 1000-watt lamp was run at the voltage required to give the S_B illuminant of the Commission Internationale de l'Éclairage, when used in conjunction with the appropriate filter at F.

The optical bench was calibrated against the colorimeter wedges and the relative intensities of the spectral radiation and the white light could be calculated readily. To ensure that a and b were accurately at the same wave-lengths, a preliminary hue-discrimination measurement was made. One half of the field was illuminated by λ, while the other was altered by a small amount to a wave-length $(\lambda+\delta\lambda_1)$, until $\delta\lambda_1$ was such that a just-noticeable colour-difference between the two halves of the field could be seen. The measurement was repeated on the short-wave side of λ, to a wave-length $(\lambda-\delta\lambda_2)$, and the value was again recorded. To a first approximation $\delta\lambda_1=\delta\lambda_2$, so that the mean value of $(\lambda+\delta\lambda_1)$ and $(\lambda-\delta\lambda_2)$ will be λ and the correct setting for identical wave-lengths can be found to within 1 or 2 A. This method was considered more accurate than independent calibration of the two wave-length scales on the apparatus.

The intensity at which the observations were made was maintained at an approximately constant level by the use of the sectors. Except for the wave-lengths of 0·70 μ. and 0·46 μ., the intensities never differed by more than 25 per cent from a mean value of about 50 photons.

The steps as measured for 10 wave-lengths are given in column 13 of the tables. The values give l_w, the small white luminosity that must be added to unit intensity of each spectral radiation to produce a just-noticeable saturation difference. The results are shown graphically in figures 5 and 10.

l_w

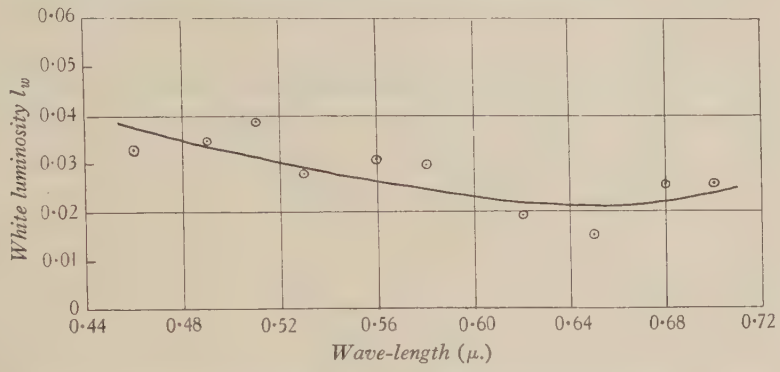

Figure 10. Saturation discrimination (F.H.G.P.). Luminosity of white (4800° K.) which has to be added to unit luminosity of spectral radiation to produce a just-noticeable difference in saturation from the spectral colour.

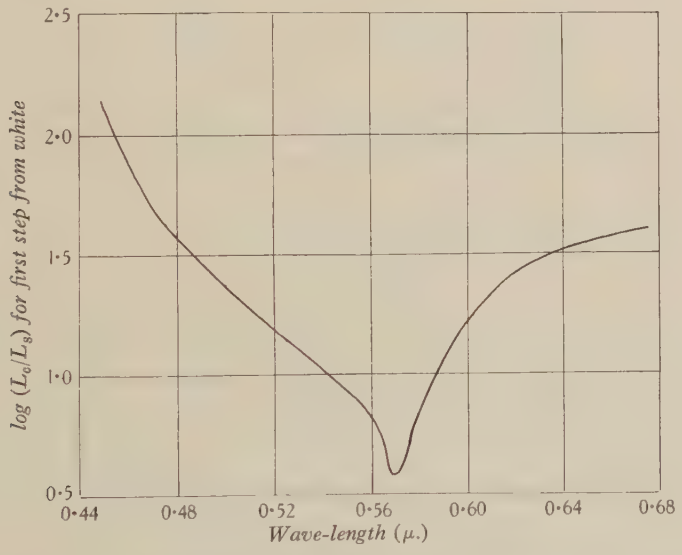

Figure 11. Saturation discrimination—mean curve taken from Martin, Warburton and Morgan, showing the relation between spectral radiation (luminosity L_s) which, when mixed with white (luminosity L_w), gives a colour (luminosity L_c, $L_c = L_s + L_w$) which has a just-noticeable saturation difference from white.

The rather unexpected result has been obtained that l_w remains very nearly constant for all wave-lengths. This result was quite definitely confirmed for W. D. W. on two or three occasions, and although time did not permit the observations for F. H. G. P. to be repeated so thoroughly, there was every reason to believe that more extensive observations would have produced equally constant results. The two end

values for W.D.W. were higher than the rest, possibly but not necessarily as a result of the lower intensity-level. It was of some interest to find that the intensity seemed to play a bigger part in changing the size of saturation-step than had been found in the case with hue-discrimination. This may be associated with the decreasing saturation (increasing whiteness) known to occur as the intensity of a radiation is increased.

There is a surprising difference between the saturation functions of figures 5 and 10 and that of figure 11, but we consider that the latter is the more correct measure of the saturation for two reasons. In the first place, when the spectral radiations are added to white, all the measurements are made in one part of the colour triangle and the sensitivity of the eye to colour-differences will be practically the same for all the observations. In the other method, not only is the saturation a variable, but at each

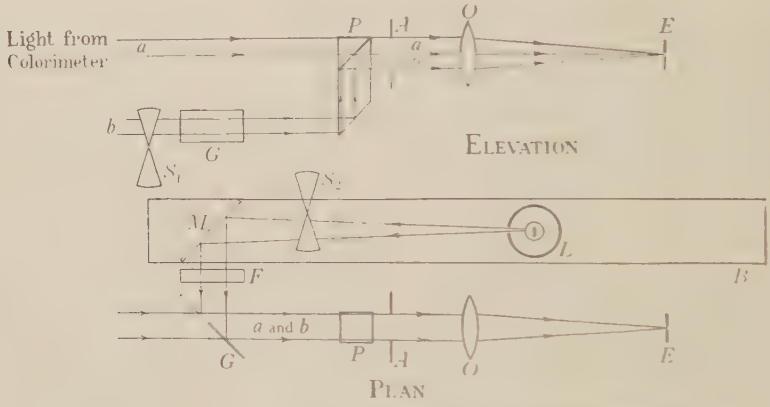

Figure 12. Diagram of optical system used for measurement of saturation discrimination.

wave-length the eye will have a different sensitivity and the results will measure the combined effect of variations of saturation and sensitivity. Secondly, when the steps from white are being measured, the eye will be in practically the same state of adaptation for all the experiments; but this is certainly not the case in the method we have adopted. Both these points suggest that figure 11 is the more reliable saturation function. Nevertheless, the more or less constant value we found for l_w has to be explained and there is evidently room for further investigation.

The saturation-steps plotted in the colour triangle are of some interest and we have therefore given, in figure 2, the first step from the spectral locus for W.D.W.'s colour triangle. It must be remembered when using this diagram that the colour difference is only a liminal one when measured along a line passing through the white point. It would be incorrect, for instance, to draw a normal to the spectral locus and regard the intersections with the locus and the dotted line as giving two points having a just-noticeable colour-difference.

§ 9. CONCLUSIONS

Several points of interest have been brought out in the course of the paper and these are probably sufficient to demonstrate the advantage of a complete series of results for each individual observer. The value of each item is undoubtedly enhanced by a knowledge of the remaining items, and when comparison is made with other observers, the manner in which the characteristics vary should be of particular value. These variations and their connexion with the more marked abnormalities of colour-vision, such as anomalous trichromatism, should also be of special interest.

§ 10. ACKNOWLEDGMENT

The authors desire to acknowledge their appreciation of the financial assistance given by the Medical Research Council.

REFERENCES

(1) L. C. Martin, F. L. Warburton and W. J. Morgan. *Spec. Rep. Ser. med. Res. Coun.* No. 188.
(2) I. G. Priest and F. G. Brickwedde. *J. opt. Soc. Amer.* **13**, 306 (1926).
(3) W. D. Wright. *Trans. opt. Soc.* **29**, 225 (1927–8).
(4) W. D. Wright. "A re-determination of the trichromatic coefficients of the spectral colours." *Trans. opt. Soc.* **30**, 141 (1928–9).
(5) W. D. Wright and F. H. G. Pitt. *Proc. phys. Soc.* **46**, 459 (1934).

551.594.12

THE POTENTIAL ACQUIRED IN THE NATURAL ELECTRIC FIELD BY A VERTICAL ROD STANDING ON THE GROUND, INSULATED AT THE BOTTOM AND CARRYING A COLLECTOR AT THE TOP

By L. H. G. DINES, M.A.

Received October 18, 1934. *Read in title December* 7, 1934.

ABSTRACT. This paper investigates the potential of a small cylindrical rod standing upon, and insulated from, a charged plane, and provided with a small collector at the top. Data of a direct observational comparison between such a rod and a standard piece of apparatus are given. The main part of the paper consists of a theoretical determination of the potential of the rod by means of an approximate solution of the integral equation involved. The investigation is extended to cover a certain range of values of the ratio of the diameter to the height of the rod. An attempt is made to indicate the distribution of charge on the surface of the rod in a special case. An estimate is made of the subsidiary error involved when the collector takes the form of a horizontal fuze which shortens as it burns away.

§ 1. STATEMENT OF THE PROBLEM

The measurement of the electric stress near the surface of the ground is a problem which has exercised the minds of meteorologists for several decades. The physical quantity which it is desired to measure is the vertical gradient of electric potential over a large horizontal surface, but in the earlier attempts the measuring apparatus employed itself distorted the field so much that the results obtained were subject to large error.

Several improved forms of apparatus were devised about twenty-five years ago, and one which was adopted by the late G. W. Walker was installed by him at Eskdalemuir Observatory, Dumfriesshire, and has been in use there since. It consists of a thin insulated vertical rod, of which the lower end passes through a small hole in a large horizontal plane into an underground chamber, in which sits an observer with an electrometer connected to the rod. A collector is attached to the top of the rod in the form of a small burning fuze placed horizontally.

It was originally assumed that when equilibrium had been attained the potential of the rod would be very nearly the same as the undisturbed potential at points in the horizontal plane passing through the top of the rod, and it is the object of the present paper to test the truth of this assumption.

Under normal conditions the surface of the ground is negatively charged, and a qualitative consideration of the problem shows that as the rod is mainly at a higher

potential than its surroundings it must have positive charges on its surface, and its potential must therefore be higher than the undisturbed potential in the neighbourhood of the burning fuze. In a paper by G. M. B. Dobson[1], published about twenty years ago, reference is made in a footnote to a comparison between the vertical rod and another form of apparatus employing a horizontal rod, which showed that the former gave readings about 4 per cent higher than the latter. Unfortunately very few details of this test are available.

Figure 1 shows in diagrammatic form the shape of the equipotential surfaces in the neighbourhood of a plain insulated rod fitted with an ideal small collector at the

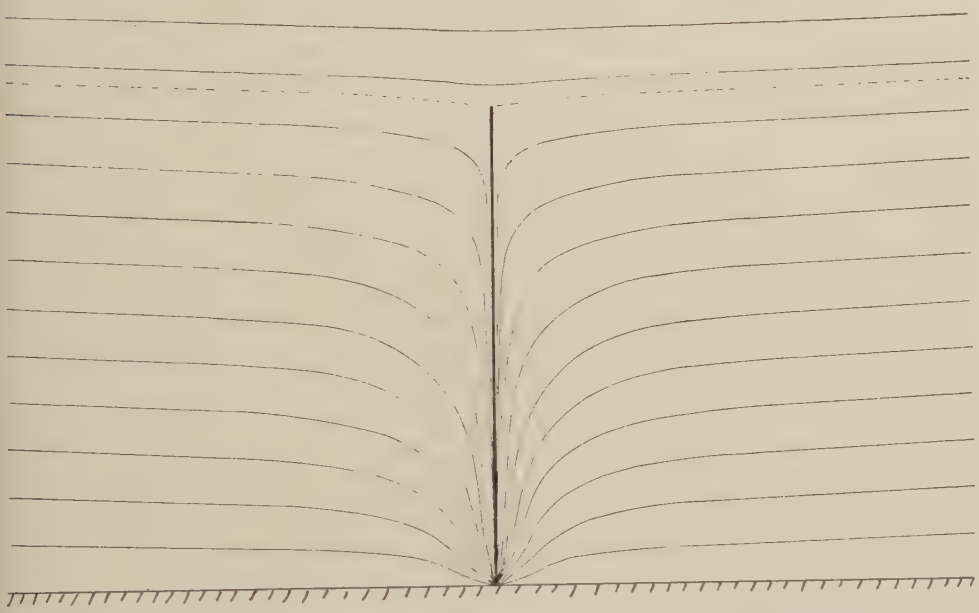

Figure 1. Approximate diagrammatic section of the equipotential surfaces in the neighbourhood of an insulated vertical rod 100 cm. in height and 4 mm. in diameter, standing upon a charged horizontal surface and provided with a collector at the top.

extreme top. It is demonstrated later that the critical equipotential which passes through the top of the rod takes a form in that region which departs little from that of a cone. This fact suggested that if the long thin fuze commonly used as a collector were placed on the slope so as to form a generator of the cone, then the presence of the fuze would not disturb the configuration of the equipotential surfaces, and observations so made would give results identical with those made with a plain rod and an ideal small collector. On this basis, a series of comparisons were made at Kew Observatory between a vertical rod with an inclined fuze and a modern form of apparatus substantially free from systematic error. This work was done subsequently to the theoretical investigation, but it seems best to give an account of it first.

§ 2. AN EXPERIMENTAL DETERMINATION

Early in the year 1933 a series of simultaneous readings of potential were made, use being made on the one hand of a vertical rod fitted with an inclined fuze, and on the other a long insulated horizontal wire provided with a fuze in the middle. On theoretical grounds it is demonstrable that the latter form of apparatus is not subject to appreciable error due to distortion of the electric field. A description of it is given by Dr R. E. Watson[3].

The site of the comparison was the roof of the underground electrical laboratory at Kew Observatory and the surrounding level lawn. The roof consists of a horizontal surface 10 m. square raised about 25 cm. above the level of the surrounding lawn. The vertical rod protruded from the roof near the middle of the square, through a small hole from the chamber below, where the electrometer was placed. The rod could be removed and in its place a horizontal wire 18 m. in length could be stretched across the flat roof; the middle portion of the wire passed through the same point in space as had been occupied by the top of the rod, and had a small fuze fixed to it concentrically. As a standard of comparison another stretched wire, observer, and electrometer were situated on the lawn a little distance away; the latter observer took readings of his electrometer simultaneously with every observation made on the roof, whether by means of the rod or the alternative stretched wire.

The reading of potential by rod or alternative wire referred to exactly the same point in space, and the same electrometer was used for both. Strictly speaking there was a slight difference between the exposures of the rod and the alternative wire in that the observer was underground in the former case and above ground in the latter. He was however about 9 m. distant from the fuze, and furthermore his presence would to some extent affect the other stretched wire also, and therefore tend to be cancelled out in a direct comparison.

The vertical rod employed was approximately 1 m. in height and 4·1 mm. in diameter. The theoretical investigation which follows shows that for such a rod the fuze should be inclined at 7° above the horizontal, and it was accordingly so fixed. At the point where it joined the vertical rod its axis was 1 m. above the roof, its diameter was $4\frac{1}{2}$ mm. and initial length from 7 to 10 cm., burning away to nothing at the end of the test in each case.

Seven complete comparative tests were made. In each case simultaneous readings were made by both observers at intervals of half a minute. Table 1 sets out the mean results of each portion of each comparison, the nomenclature adopted being as follows:

V_r V_r is the potential of the vertical rod;

V_a V_a the potential of the stretched wire over the roof; and

V_c V_c the potential of the control wire over the lawn.

The values of $V_r - V_a$ have been derived from the mean values of $V_r - V_c$ and $V_a - V_c$ in the rows above. The whole series was made under good conditions in dry weather

Table 1

Date, 1933	April 4	April 7	April 7	April 8	April 10	April 11	April 11	Mean
No. of readings	16	15	15	20	20	23	15	
Mean of V_r/V_c	1·08	1·09	1·11	1·10	1·08	1·09	1·10	1·09
No. of readings	18	11	17	17	21	23	19	
Mean of V_a/V_c	1·02	1·05	1·02	1·06	1·06	1·02	1·03	1·03
V_r/V_a	1·06	1·04	1·09	1·04	1·06	1·06	1·08	1·06

with a gentle breeze. The scatter of the individual values in the last row is too great to allow us to say with precision what the mean value of a very large number of similar observations would be, but it is fairly safe to say that it must lie between 1·05 and 1·07.

§ 3. THE THEORETICAL INVESTIGATION

In dealing with the potential of the rod from the theoretical point of view it is necessary to simplify the conditions. The fuze will be supposed to be replaced by a particle of ionizing material attached to the tip of the rod, and the shape of the latter will be regarded as a cylinder of length h and diameter $2a$, having plane orthogonal ends. The cylinder stands vertically upon, but is insulated from, an infinite horizontal plane which is uniformly charged with a surface density q. The only physical property of the collector which we need consider is that it produces a state of equilibrium in which the surface density of charge at the top of the rod is zero. The writer does not know of any published solution of this problem, nor of the more tractable case when the rod takes the form of a thin prolate spheroid. It can however be attacked by methods of approximation, and the method which has been adopted here was suggested by the description of a somewhat similar process given by L. F. Richardson in a paper entitled "How to solve differential equations approximately by arithmetic[2]."

h, a

q

The problem may be stated analytically thus. Take the axis of the rod as axis of Y, the positive direction being downwards with the origin at the top of the rod. Let σ be the surface density of the charge on the rod at the distance y from the top. At the top end of the rod the surface density is zero: at the bottom end, which is nearly in contact with the infinite plane, there will be a large charge. The latter will have in close proximity a corresponding charge on the plane, nearly equal and opposite to it, and the external effect of such pairs falls off as a high power of the distance. Its effect will be ignored in the present investigation. We are therefore solely concerned with charges on the cylindrical surface. The surface density of the charge on the infinite plane is disturbed by the presence of the charged rod; its effect may be dealt with by the method of images, so that we shall envisage the problem as that of a charged rod above the plane, the image of the rod below, and the plane having a uniform surface density q.

σ, y

y' Consider any point on the axis of Y inside the rod, and let y' denote its distance from the origin. Since it is inside a conductor the electric stress there is zero, and therefore from a consideration of all the elemental charges in the system and the vertical stresses which they individually produce at the point considered, we have the following integral equation which is true for all values of y' between zero and h.

$$2\pi a \left\{ \int_0^h \frac{\sigma\,(y'-y)}{((y'-y)^2+a^2)^{\frac{3}{2}}}\,dy + \int_0^h \frac{\sigma\,(2h-y'-y)}{((2h-y'-y)^2+a^2)^{\frac{3}{2}}}\,dy \right\} = 4\pi q.$$

We have to determine σ as a function of y, and thence determine the potential of the rod relative to the plane. The process being numerical it is necessary to start with a rod of definite dimensions. Assume a rod 1 m. in length and 4 mm. in diameter; it is also convenient to assume that q is equal to $-\frac{1}{4}\pi$, because this gives a vertical potential-gradient equal to unity in absolute units above the plane, and positive upwards. This case having been worked out any other will follow proportionally. The rod is supposed to be divided into n equal portions, and the assumption is made that $d\sigma/dy$ is constant throughout each portion. Our hypothetical distribution therefore involves discontinuities in $d\sigma/dy$ but not in σ. We shall assume that this hypothetical distribution makes the electric stress zero at certain convenient points on the axis of the rod, and then work out numerically for several values of n the values of the distribution constants which are required to meet these conditions. Lastly the potential of the rod will be evaluated, and from a series of values obtained from increasing values of n an approximation to the limiting value when n is infinite will be made. It will be obvious that these hypothetical distributions could not exist in equilibrium for finite values of n; they are of value only as a means of approach to the limit, and it is shown later that it is not necessary to carry the process very far before the limiting value can be estimated.

The convenience of the numerical process is somewhat dependent on choosing the best points on the axis at which to equate the electric stress to zero, and it was found that to obtain approximation to a limit it was necessary to work with the middle points of the sections of the rod.

V In the case of any of our hypothetical distributions let V be the potential relative to the infinite plane at any point in space due to all the charges in the system, and let V_r be the potential at the same point due to the charges on the rod and its image alone. Then, for any of our chosen points on the axis of the rod,

$$\partial V/\partial y = 0 \quad \text{and} \quad \partial V_r/\partial y = +1.$$

σ_c, σ_d At the upper ends of each of the n sections into which the rod is divided, beginning from the top, we may denote the values of σ thus: Zero, σ_a, σ_b, σ_c, σ_d, σ_e etc. Starting from this we may then express the value of $\partial V_r/\partial y$ for the middle point of each section, and by equating each of them to $+1$ obtain thereby n equations from which to determine σ_a, σ_b, σ_c, σ_d, σ_e, etc. Lastly the potential of the top of the rod can be computed from the known values of σ_a, σ_b, σ_c, σ_d, σ_e etc. The whole process is very easy so long as n is small, but becomes tedious when n exceeds three.

In evaluating $\partial V_r/\partial y$ at any of the proposed points it is more convenient to regard it as a reversed electric stress than as a function of potential. By the aid of a few formulae, which are worked out below, each section of the rod and image can be dealt with in succession, and it is evident that each complete expression must have $2n$ elements.

The formulae required. Suppose a cylindrical shell of external diameter $2a$ having its axis as axis of Y. The shell is supposed to be charged to a surface density σ, where σ obeys the relation $\sigma=s+k.y$, where s and k are constants. s, k

Consider the electric force, P_0, at O the origin of co-ordinates, due to a finite portion of the shell lying between the limits defined by $y=y_1$ and $y=y_2$, where y_2 is algebraically greater than y_1. By symmetry P_0 acts along OY, and its value in the positive direction of y is given by the integral P_0 y_2, y_1

$$P_0=-2\pi a\int_{y_1}^{y_2}\sigma y\,(a^2+y^2)^{-\frac{3}{2}}dy.$$

Since $\sigma=s+ky$ this becomes

$$P_0=-2\pi as\int_{y_1}^{y_2}y\,(a^2+y^2)^{-\frac{3}{2}}dy-2\pi ak\int_{y_1}^{y_2}y^2\,(a^2+y^2)^{-\frac{3}{2}}dy.$$

Writing $\tan\theta=a/y$ and integrating, we have

$$\begin{aligned}P_0&=2\pi s\int_{\theta_1}^{\theta_2}\cos\theta d\theta+2\pi ak\int_{\theta_1}^{\theta_2}\cos\theta\cot\theta\,d\theta\\&=2\pi s\,(\sin\theta_2-\sin\theta_1)+2\pi ak\,(\cos\theta_2-\cos\theta_1+\log(\tan\tfrac{1}{2}\theta_2\cot\tfrac{1}{2}\theta_1)).\end{aligned}$$

If σ_1 and σ_2 be the values of σ corresponding with y_1 and y_2 respectively, we shal have

$$\sigma_1=s+ky_1 \quad\text{and}\quad \sigma_2=s+ky_2,$$

whence

$$s=\frac{\sigma_1y_2-\sigma_2y_1}{y_2-y_1} \quad\text{and}\quad k=\frac{\sigma_2-\sigma_1}{y_2-y_1}.$$

Substituting in the above we have

$$\begin{aligned}P_0=\frac{2\pi}{y_2-y_1}\{&(\sigma_1y_2-\sigma_2y_1)\,(\sin\theta_2-\sin\theta_1)\\&+a\,(\sigma_2-\sigma_1)\,(\cos\theta_2-\cos\theta_1+\log(\tan\tfrac{1}{2}\theta_2\cot\tfrac{1}{2}\theta_1))\}.\end{aligned}$$

If a/y be small so that we may neglect squares and higher powers, and if y_1 and y_2 have the same sign, this reduces to

$$P_0=\frac{2\pi a}{y_2-y_1}\left\{\left(\frac{\sigma_2}{y_2}-\frac{\sigma_1}{y_1}\right)(y_2-y_1)+(\sigma_1-\sigma_2)\log\frac{y_2}{y_1}\right\} \qquad \text{.....(1).}$$

In the special case when $y_1=0$ we have

$$P_0=\frac{2\pi}{y_2}\{\sigma_1y_2\,(\sin\theta_2-1)+a\,(\sigma_2-\sigma_1)\,(\cos\theta_2+\log\tan\tfrac{1}{2}\theta_2)\}.$$

Again, if a/y_2 be small and y_2 be positive, this reduces to

$$P_0=\frac{2\pi a}{y_2}\left\{\sigma_1\left(1-\frac{y_2}{a}\right)+(\sigma_2-\sigma_1)\left(1-\log\frac{2y_2}{a}\right)\right\} \qquad \ldots\ldots(2).$$

If the portion of the shell considered lie on the negative side of the origin, equation (2) must be modified; in that case y_2 is zero and y_1 is negative.

We then have

$$P_0=\frac{2\pi a}{y_1}\left\{\sigma_2\left(1+\frac{y_1}{a}\right)-(\sigma_2-\sigma_1)\left(1-\log\frac{-2y_1}{a}\right)\right\} \qquad \ldots\ldots(3).$$

If the origin be at the centre of a portion of the shell whose total length is $2y_1$, then by a similar process we have, when a/y_1 is small,

$$P_0=\frac{2\pi a}{y_1}(\sigma_1-\sigma_2)\left(\log\frac{2y_1}{a}-1\right) \qquad \ldots\ldots(4).$$

ϕ_0 Again, the potential ϕ_0 at the origin O, due to the portion of the shell lying between the limits y_1 and y_2, is given by the integral

$$\phi_0=2\pi a\int_{y_1}^{y_2}\sigma\,(y^2+a^2)^{-\frac{1}{2}}\,dy.$$

Whence, proceeding as before, we obtain the equation

$$\phi_0=\frac{2\pi a}{y_2-y_1}\left[(\sigma_2-\sigma_1)\left\{(y_2^2+a^2)^{\frac{1}{2}}-(y_1^2+a^2)^{\frac{1}{2}}\right\}-(\sigma_1y_2-\sigma_2y_1)\log(\tan\tfrac{1}{2}\theta_2\cot\tfrac{1}{2}\theta_1)\right].$$

If a/y be small and y_1 and y_2 have the same sign, this reduces to

$$\phi_0=2\pi a\left\{\frac{\sigma_1y_2-\sigma_2y_1}{y_2-y_1}\log\frac{y_2}{y_1}+(\sigma_2-\sigma_1)\right\} \qquad \ldots\ldots(5).$$

Again, in the special case when a, y_2 is small, y_1 is zero and y_2 is positive, we have

$$\phi_0=2\pi a\left\{\sigma_1\log\frac{2y_2}{a}+(\sigma_2-\sigma_1)\left(1-\frac{a}{y_2}\right)\right\} \qquad \ldots\ldots(6).$$

To find the potential due to the shell at an external point T, take axes as before and suppose that the co-ordinates of T are given by $x=x$ and $y=0$. Suppose also that x is large compared with a, so that we may take the surface charge on the shell to be concentrated along the axis, that is we may take a, y to be negligible from the start.

The potential at T due to that part of the rod lying between the limits $y=y_1$ and $y=y_2$ is then given by the expression

ϕ_T
$$\phi_T=2\pi a\int_{y_1}^{y_2}\sigma\,(y^2+x^2)^{-\frac{1}{2}}\,dy.$$

Integrating, we obtain

$$\phi_T=\frac{2\pi a}{y_2-y_1}\left[(\sigma_1y_2-\sigma_2y_1)\log(\tan\tfrac{1}{2}\theta_1\cot\tfrac{1}{2}\theta_2)+(\sigma_2-\sigma_1)\left\{(y_2^2+x^2)^{\frac{1}{2}}-(y_1^2+x^2)^{\frac{1}{2}}\right\}\right]$$

where $\theta_1=\tan^{-1}x/y_1$ and $\theta_2=\tan^{-1}x/y_2$. $\qquad \ldots\ldots(7),$

§ 4. NUMERICAL EXAMPLES

By the aid of the general equations (1) to (7) the numerical equations may be written down in any specific case. As has previously been stated, attention has been confined to the case of a rod 1 m. in height and 4 mm. in diameter. The calculations have been made for values of n from 1 to 5 inclusive. In each case the constants σ_a, σ_b, σ_c, σ_d, etc. have been computed, and thence the potential at the top end of the rod determined. Lack of space prevents the setting out of the work in detail, but a summary of the results is given in table 2. Each row in the table deals with one definite hypothetical case. The last column gives the potential computed for the top end of the rod; this is a somewhat arbitrary proceeding because if the computation had been made for some other point on the rod the figures would not necessarily have been quite the same, though they must approximate to the same limit as n is increased. There are advantages in computing for the top, because that is a region of zero stress at the surface of the rod.

Table 2. Computed values of the density of the surface charge on a rod 1 m. high and 4 mm. in diameter in the five hypothetical cases considered, with the resultant potential at the top of the rod relative to the plane

s-ce m of d n.)	0	20	25	33·33	40	50	60	66·67	75	80	100	Potential of the top of the rod (V)
	(Surface density of charge on rod) $\times 4\pi$											
= 1	0	—	—	—	—	—	—	—	—	—	104·90	106·417
= 2	0	—	—	—	—	47·70	—	—	—	—	123·10	106·090
= 3	0	—	—	32·32	—	—	—	66·25	—	—	136·69	106·134
= 4	0	—	24·71	—	—	48·95	—	—	77·29	—	148·13	106·184
= 5	0	20·13	—	—	39·25	—	59·77	—	—	85·10	158·32	106·224

We see from table 2 that the potential of the rod appears to be somewhat in excess of 106. If the rod were removed the potential at the level of the top would be 100, so that the disturbance produced by the rod is of the order of 6 per cent or more. To determine the limiting value we may plot the potential against $1/n$ and extrapolate the curve. The figures in the last column of table 2 are shown plotted as small circles in figure 2. Such a method is not very satisfactory, and it is better to proceed as follows. There is every reason to suppose that the potential converges to a limit as n is increased indefinitely; call this limit V' and we may assume that the difference between V' and the estimate obtained by using any particular value of n will take the form

$$\alpha/n + \beta/n^2 + \gamma/n^3 + \delta/n^4 + \ldots,$$

V'

, γ, δ

where α, β, γ, δ, etc. are independent of n. From the data of table 2 five equations may now be formed from which to determine V' and the first four coefficients α, β, γ and δ, provided that it may be assumed that the rest of the series is insignificant.

Thus,

$$\begin{aligned}
106{\cdot}417 - V' &= \alpha + \beta + \gamma + \delta,\\
106{\cdot}090 - V' &= \tfrac{1}{2}\alpha + \tfrac{1}{4}\beta + \tfrac{1}{8}\gamma + \tfrac{1}{16}\delta,\\
106{\cdot}134 - V' &= \tfrac{1}{3}\alpha + \tfrac{1}{9}\beta + \tfrac{1}{27}\gamma + \tfrac{1}{81}\delta,\\
106{\cdot}184 - V' &= \tfrac{1}{4}\alpha + \tfrac{1}{16}\beta + \tfrac{1}{64}\gamma + \tfrac{1}{256}\delta,\\
106{\cdot}224 - V' &= \tfrac{1}{5}\alpha + \tfrac{1}{25}\beta + \tfrac{1}{125}\gamma + \tfrac{1}{625}\delta.
\end{aligned}$$

Solving, we find $\alpha = -1{\cdot}653$, $\beta = +2{\cdot}287$, $\gamma = -1{\cdot}358$, $\delta = +0{\cdot}669$ and $V' = 106{\cdot}47$.

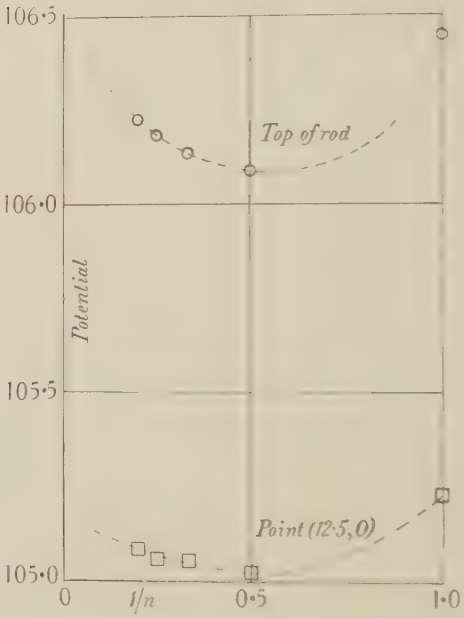

Fig. 2. Estimates of the potential at the top of the rod, and at a point level with the top but 12·5 cm. distant from it, based on various values of $1/n$.

As a check the same process was followed using only the first three terms and the first four equations; in this case the value of V' was found to be 106·45.

As the validity of the limiting value is vital to the investigation it has been examined in another manner. If the hypothetical distributions of charge given in table 2 agree closely with the real distribution, then it must follow that the values of the function $\partial V_r/\partial y$ derived from them must approximate to unity at all points on the axis of the rod. The values when $n = 5$ are shown plotted in figure 3, from which it will be seen that the agreement is reasonably good except at the extreme top and near the bottom. The same procedure was carried out for smaller values of

n, and it was found that both discrepancies decrease as n increases. Discrepancies at the bottom have little influence in any case, while at the top was found to decrease in a manner roughly proportional to $1/n$. Hence there is no reason to doubt that the calculated potential will converge steadily to a limit as n increases, and also that the most important terms in the expression for the difference between the estimate and its limit will be those involving the smaller powers of n.

When the figures obtained above have been rounded off, the best estimate of V' which the present investigation can give is 106·5 for a rod 100 cm. in height and 4 mm. in diameter.

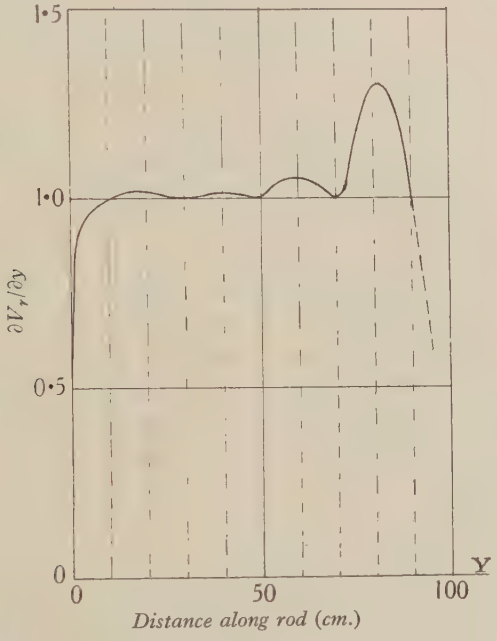

Figure 3. Values of $\partial V_r/\partial y$ along the axis of the rod, computed for the case in which $n=5$.

§ 5. AGREEMENT WITH EXPERIMENT

The value of the potential just obtained may be compared with the experimental result on page 221. The agreement is not perfect, but is good enough to check the general accuracy of both methods. The theoretical investigation suggests that the experimental value must be too low; there is no reason why it should not be so, since it is always difficult to avoid appreciable casual error in observations of potential gradient. The scatter among the seven experimental determinations on page 221 is such that the true mean may be as great as 106·5 for all we can tell.

There is a difference between the practical case and the theoretical one in that in the former the rod passes through a hole in the plane, whereas in the latter it does not. If the hole be small this is immaterial, as the difference in the electric stress in the two cases is entirely negligible except in the immediate neighbourhood of the hole, where it does not affect the calculations.

§ 6. THE SHAPE OF THE EQUIPOTENTIAL SURFACE PASSING THROUGH THE TOP OF THE ROD

It appears from the foregoing calculations that a reasonably good estimate of the potential of the rod can be made even when n is as small as 2 or 3. We may therefore with confidence make use of the hypothetical distributions to determine the shape of the equipotential surfaces near the top of the rod. Since there is no charge at the top of the rod there can be no question of discontinuities in that region. Taking axes as before, consider the potential at a point (x, y) in space near the top of the rod; using equation (7) we may deal with the several portions of the rod and image as before and work out V_r. To find V we remember that $V = V_r - (100 - y)$, where y is measured in centimetres.

The work is tedious but presents no difficulty; it was found convenient to take points at horizontal distances from the rod of $\frac{1}{2}h$ and $\frac{1}{4}h$, i.e. 12·5 and 6·25 cm. The potentials are set out in table 3 for various values of n.

Table 3. Values of V_r and V at points in space at and near the top of the rod in various cases of hypothetical distribution of charge on the rod.

Co-ordinates (x, y) (cm.)		(0, 0)	(6·25, 0)	(6·25, −1·25)	(12·5, 0)	(12·5, −2·5)
$n=1$	V_r	6·417	—	—	5·233	4·880
	V	106·417	—	—	105·233	107·380
$n=2$	V_r	6·090	—	—	5·023	4·670
	V	106·090	—	—	105·023	107·170
$n=3$	V_r	6·133	—	—	5·055	—
	V	106·133	—	—	105·055	—
$n=4$	V_r	6·185	5·602	5·370	5·057	4·685
	V	106·185	105·602	106·620	105·057	107·185
$n=5$	V_r	6·225	—	—	5·085	—
	V	106·225	—	—	105·085	—

Taking the case in which $n = 4$ we can find the points at the same potential as the top of the rod by interpolation on the ordinates $x = 6·25$ and $x = 12·5$. They are found to be (6·25, −0·71) and (12·5, −1·32). These are nearly collinear with the top of the rod. Since the distribution in this case has been shown to be not far from the true one, it may be inferred that the curvature of the equipotential through the top of the rod in the actual case will be very nearly the same as in that just found.

It is next necessary to determine the limiting value of V_r at the point (12·5, 0) when n is infinite. The five estimates in table 3 are plotted as small squares in figure 2. The means of calculation employed (slide-rule and four-figure tables) were not quite accurate enough to give a smooth curve, but as the principles involved are exactly the same as before we may draw a smooth curve through the points, as far as they allow, similar in shape to the curve above. This curve may then

be extrapolated to the ordinate through the origin by exactly the same process as before, save that as we have already smoothed the curve we can only profitably work from four points instead of five. Solving the necessary equations, the limiting value of V is found to be 105·17.

Lastly we require the limiting value of the vertical potential gradient near the point (12·5, 0). Table 3 shows that there is little difference between the computed values whether n be 1, 2 or 4, and therefore we may take the value in the latter case as indicating the actual value sufficiently closely for the purpose, namely a gradient of 2·13 in 2·5 cm.

From the data of the last three paragraphs the equipotential through the top of the rod in the actual case may be determined thus:

The potential at the top of the rod is 106·47.

On the ordinate $x = 12{\cdot}5$ this potential occurs at the point given by the equation $y = -(1{\cdot}30/2{\cdot}13) \times 2{\cdot}50$ cm. That is, $y = -1{\cdot}53$ cm.

Allowing for curvature the intermediate point is

$$x = 6{\cdot}25 \text{ cm.}, \quad y = -0{\cdot}87 \text{ cm.}$$

Since the equipotential surface is symmetrical with regard to the axis of Y, its form near the top of the rod is very nearly that of a cone, having a semi-vertical angle of 83° from the vertical drawn upwards. It follows that if a thin conductor not more than 13 cm. in length be attached to the rod at this angle at the top, it will lie in an equipotential surface, and the collector may be placed at any point on it without altering anything. Hence a fuze fulfilling these conditions will maintain the rod at the same potential independently of the length of the fuze as it burns away.

§ 7. THE ACTUAL DISTRIBUTION OF THE CHARGE ON THE SURFACE OF THE ROD

It remains to discuss the actual distribution of charge on the rod. Five approximations have been worked out for a rod 100 cm. by 4 mm., and in figure 4 three of them are shown plotted corresponding with values of n of 1, 3 and 5; the other two are very similar but have been omitted for the sake of clearness. The question is, what form would the curve take if n were very great?

Since the various approximations have all yielded estimates of the potential which have been shown to be not far from the limiting value, they cannot be very far from the true distribution, except at the bottom end which has not been explored. Taking the case when $n = 5$ as the best, certain refinements suggest themselves which may be applied to it. In the first place, an examination of figure 3 shows that at the extreme top of the rod the gradient of charge must be somewhat steeper than has been postulated. Also at 20 cm. above the plane rather too steep a gradient has been obtained. Furthermore, table 2 shows that at 50 cm. above the plane the density is on the whole tending to increase as n increases from 2 to 5, while the density at the bottom if plotted against $1/n$ suggests an asymptotic curve

when n is large. These several points have been incorporated in the upper curve in figure 4. The noteworthy feature is the close approximation of the curve to a straight line over the upper two-thirds of the length of the rod.

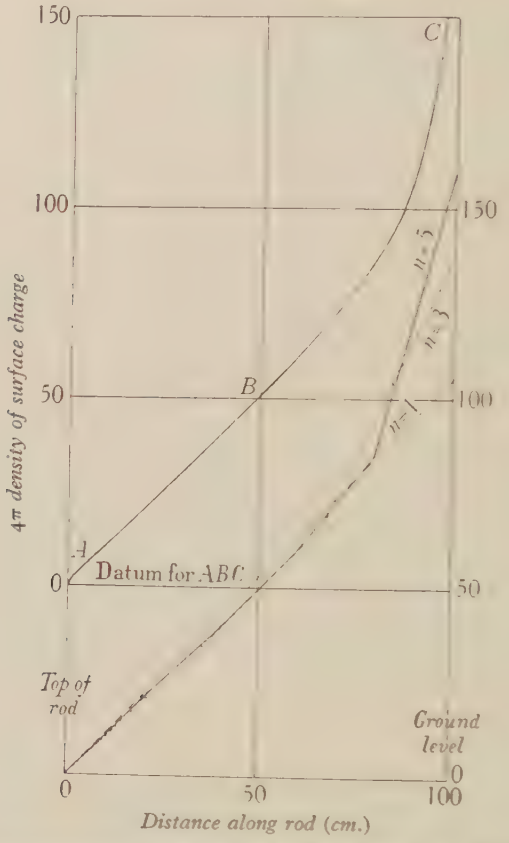

Figure 4. Graph of the product 4π into the density of the surface charge on a rod 100 cm. in height and 4 mm. in diameter, for various values of n. The limiting case is shown above as ABC.

§ 8. EFFECT OF THE DIMENSIONS OF THE ROD

The results so far obtained have been based on a rod of definite dimensions; we have next to consider how far they are generally applicable. It will be seen that in the equations for the determination of P_0 on pages 223, 224 each term is homogeneous and of the first power in σ, but of zero dimensions in the linear factors. Also in the equations for the determination of ϕ_0 the terms are of the first power in both σ and the linear factors. The same conditions apply to the electric stresses and potentials due to the charged plane. It follows that provided the ratio of the diameter to the height of the rod remains the same, identical values of σ_a, σ_b, σ_c, σ_d, etc. will be obtained whatever the height of the rod may be. Equipotential surfaces will remain similar figures as the scale varies, but the absolute magnitude of the potential will be proportional to the linear dimensions. Hence for any rod for which the ratio of

diameter to height is 0·004, all the preceding results are immediately applicable by the application of a simple dimensional factor to all the potentials.

If the ratio of diameter to height be varied, further examination is required. By means of the same methods as before the potentials were worked out for rods 100 cm. in height and 2 and 6 mm. in diameter. They are tabulated in table 4, in which for convenience the results previously obtained for a 4 mm. rod are also included. The limiting values of V_r (0), the value of V_2 at the top of the rod, have been determined from the four cases when $n=1$, 2, 3 and 4, respectively. The limiting value of V_r (0) for a 4-mm. rod is not exactly the same as that previously found by taking five values of n, but we may with little risk of error assume that though the actual values in the fifth row of table 4 are not the best available, yet the proportions between them are very nearly correct. Accordingly in the last row are entered the estimated values of the potential, based on the previously accepted value of 6·47 for the 4-mm. rod.

V_r (0)

Table 4. Potential V_r (0) for rods of various diameters

Diameter of rod	0·2 cm.	0·4 cm.	0·6 cm.
$n=1$	5·612	6·417	7·000
$n=2$	5·372	6·090	6·609
$n=3$	5·395	6·134	6·658
$n=4$	5·436	6·184	6·721
Limiting value of V_r (0) deduced from above	5·704	6·450	7·077
Estimated value of potential	5·72	6·47	7·10

The shape of the equipotential surface through the top of the rod can be worked out in detail as before, but it is not necessary to do so. The potential V_r at any point external to the rod is determined by means of equations similar to (7) on page 224, from which it is seen that V_r is proportional to $2a\sigma$, where σ is used in the general sense. If then in any special case all the σ's are altered in a certain ratio, the external potentials V_r will also alter in the same proportion.

In table 5 the figures are given for the surface distribution on the three rods in the hypothetical case when $n=4$. σ_{25} denotes the surface density at 25 cm. from the top, and so on.

Table 5. Surface density when $n=4$ on rods 100 cm. in height and of various diameters

Diameter of rod	0·2 cm.	0·4 cm.	0·6 cm.
σ_{25}	43·5	24·7	17·9
σ_{50}	86·3	49·0	35·4
σ_{75}	135·7	77·3	56·1
σ_{100}	246·4	148·1	111·9
$2a\,\sigma_{25}$	8·70	9·88	10·74

It will be seen that the distributions in the three cases are very nearly similar; the only appreciable discrepancy is at the bottom of the rod, where the effect on the potential is comparatively small; we may assume that much the same conditions exist in the actual case. The values of $2a\sigma_{25}$ in the bottom row may therefore be taken to represent the proportional magnitudes of the similar distributions of linear charge on the three rods. It follows that the external potentials V_r are proportional to the values of $2a\sigma_{25}$ in the bottom row. Now it will be seen from table 4 that when $n=4$, $V_r(0)$ is also very nearly proportional to $2a\sigma_{25}$, so that the configurations of the isopleths of V_r passing through the tops of the rods are very nearly identical in the three cases. This result has been proved for the case of $n=4$, it can readily be worked out and shown to be true when $n=2$, and we may assume that it is true in the actual case also.

If now we repeat for rods 0·2 and 0·6 cm. in diameter the analysis made on page 228 we find the equipotential surfaces through the tops of the rods to be cones of semivertical angles 83·8° and 81·9° respectively; if fuzes be used with such rods the angle of inclination must be adjusted accordingly.

The results so far obtained may be put in the following general form. A vertical rod of height h and diameter $2a$ is exposed in the manner before described on an infinite charged horizontal plane, having a surface density of q. At the top is fixed a small collector, or a fuze whose length does not exceed $\frac{1}{3}h$, set at an angle of ψ above the horizontal. The potential V' of the rod and the appropriate value of ψ are set out in table 6 for various values of $2a/h$.

Table 6

$2a/h$	0·002	0·004	0·006
$V'/4\pi qh$	−1·0572	−1·0647	−1·0710
ψ	6·2°	7·0°	8·1°

§ 9. THE INFLUENCE OF THE FUZE AS COMMONLY EMPLOYED

When the vertical rod is used as a means of measuring the electric stress it is usual to fix the fuze horizontally, and in such a case the conditions are not quite the same as those which have been discussed above. With a rod 1 m. in height and 4 mm. in diameter the fuze is generally about 12·5 cm. in length and about 5 mm. in diameter, and burns away to nothing in the course of the observation. At the start the active end is situated at the point whose co-ordinates are (12·5, 0), where it will be seen from the results given on page 228 that the potential, apart from the presence of the fuze, is less than that at the tip of the rod by 1·30. It is not possible however to say that the equilibrium potential of the rod and fuze will therefore be less by this amount, because the field of force is altered by the presence of the fuze.

An approximation can be made in the following way. Roughly speaking the fuze lies in a potential-gradient along its axis of 0·104 per cm.; using equation (4) and the same methods as before, and assuming a uniformly increasing surface

density of charge on the fuze from the burning tip to the junction with the top of the rod, we find that a fuze 4 mm. in diameter would have a surface density of $-0{\cdot}53/\pi$ at its junction with the rod, and one of 6 mm. a surface density of $-0{\cdot}40/\pi$. Considering the case of the 4-mm. fuze, since there cannot be a discontinuity as between fuze and rod we may assume that the charges on the rod have been modified in such a way that the surface density at the top is now $-0{\cdot}53/\pi$ instead of zero. As a rough approximation it may be assumed that this modification takes the form of a uniform reduction by $0{\cdot}53/\pi$ of the surface density all over the surface of the rod, which if anything will be an overestimate. Acting on this assumption and using the formulae and methods already given we may calculate by how much the potential of the rod and fuze is less than that of the original rod alone. The result is that for either a 4- or 6-mm. fuze the potential is about 0·65 less than the original potential at the point (12·5, 0).

On this basis the potential of the rod and fuze when the fuze is 12·5 in length will be (106·47 − 1·30 − 0·65), or 104·52, increasing to 106·47 as it just burns away. Taking the mean over the life of the fuze we have 105·5 as the mean potential of the rod and fuze. This result is not greatly dependent on the diameter of the fuze, and may be applied to any between 3 and 6 mm.

§ 10. CONCLUSION

The writer feels a certain amount of diffidence in presenting this approximate solution of a problem hitherto unsolved. Such solutions are liable to leave loose ends here and there, and details are inevitably open to criticism. The method of procedure however seems to have been justified by the agreement between the calculated potential and that found by direct experiment.

An interesting point arose in the course of the work in the choice of the best positions on the axis at which to equate $\partial V_r/\partial y$ with the electric intensity due to the undisturbed plane; the upper ends of each section were tried instead of the middle points, but the result failed to give an approximation to the limit with any reasonable value of n. The reason became apparent when a diagram similar to that of figure 3 was plotted; the curve showed great oscillations, and these became more pronounced as n increased. A few graphs drawn for several values of n on this principle provide an excellent criterion of the validity of the method of approximation employed.

A noteworthy feature of the method which was finally adopted is the comparative closeness of all the several estimates of the potential of the rod to the final limiting value. Even the worst of them, when $n = 2$, departs from it by an amount which is less than the error which nearly always exists in any individual observational measurement of the potential-gradient. The simple case when $n = 1$, the calculations of which only take a few minutes to perform, yields a surprisingly close estimate. Unfortunately this could not be predicted beforehand, but the fact may be useful in other applications of the same process.

§ 11. ACKNOWLEDGMENTS

The writer's thanks are due to Dr L. F. Richardson, F.R.S., and to Dr F. J. W. Whipple, both of whom made valuable suggestions in the course of the work.

REFERENCES

(1) Gordon Dobson. *Geophys. Mem.* **1**, 161 (H.M. Stationery Office, 1914).
(2) L. F. Richardson. *Math. Gaz.* p. 415 (July 1925).
(3) R. E. Watson. *Geophys. Mem.* **5** (H.M. Stationery Office, 1929).

535.338.4:546.481.61

THE BAND SYSTEMS OF CADMIUM FLUORIDE

By R. K. ASUNDI, R. SAMUEL and M. ZAKI-UDDIN,
Muslim University, Aligarh

Received September 21, 1934. *Read in title December* 7, 1934.

ABSTRACT. Two emission band systems attributed to CdF are described and analysed. One, in the orange region, is probably due to a $^2\Pi \rightarrow {}^2\Sigma$ transition, and the other, in the yellow-green, to $^2\Sigma \rightarrow {}^2\Sigma$. The vibrational analyses suggest that the two systems have a common lower state, $^2\Sigma$, which is presumably the ground state. The origins of the two systems are roughly 16558 and 18871 cm^{-1} respectively, and the vibrational coefficients ω_e and $x_e\omega_e$ are of the orders 694·3 and 4·96 for the lower $^2\Sigma$ state, 704·4 and 5·74 for the $^2\Pi$ state, and 672·4 and 5·14 for the excited $^2\Sigma$ state. The heats and products of dissociation and the electronic structures of the three states of CdF are discussed.

§ 1. INTRODUCTION

Little seems to be known about the spectra of cadmium fluoride. The spectrum of CdH is well known and the existence of certain bands supposed to be due to the molecules Cd_2, CdO, $CdCl_2$, $CdBr_2$ and CdI_2 as studied in emission in flame and discharge tube is also quoted in literature[1]. Spectroscopically the CdF molecule should behave similarly to BeF, MgF, CaF, SrF and other similar molecules. The spectra of these molecules are studied and detailed vibrational analyses are available[1]. Data on some of them have also been utilized recently by Lessheim and Samuel[2] in explaining the linkage between the valence electrons of the two constituent atoms. In each of these molecules the metal atom has two valence electrons, both in the *s* state, while the halogen has five *p* electrons in the outermost ring. Following Herzberg[3], these authors show that for the formation of a molecule in such cases the excitation of one of the *s* electrons of the metal atom to a *p* state is necessary before linkage can take place with one of the *p* electrons of the halogen. From the spectra of CaF and SrF etc. they show further that the anomalous terms of the alkaline earth atoms are involved in such of the higher electronic energy levels of these molecules as have a dissociation energy greater than in the ground level. It was thought that CdF may behave in a rather analogous way and an investigation of its spectrum was therefore undertaken.

§ 2. EXPERIMENTAL PROCEDURE

Pure cadmium fluoride was packed in bored copper rods, and also in Hilger's pure graphite rods in some cases, and the arc on 110 volts d.c. was struck between them. It was found that a current of about 5 amperes developed the bands with optimum strength. The bands were found to lie in the range λλ 6000–6300 and

λλ 5300–5530; the entire quartz and glass regions up to 9000 A. were explored with low-dispersion instruments, but no other bands were developed. In their general appearance the bands are very similar to those of CaF.

The region to be explored having been ascertained, the bands were photographed with instruments of higher dispersion. A Zeiss 3-prism glass spectrograph which gives a dispersion of about 35 A./mm. between λλ 6600 and 6000 and about 25 A./mm. between λλ 5500 and 5300 was employed. A small concave grating with a radius of 124 cm. and 30,000 lines to the inch, having a dispersion of about 10 A. mm. in the first order, was also employed.

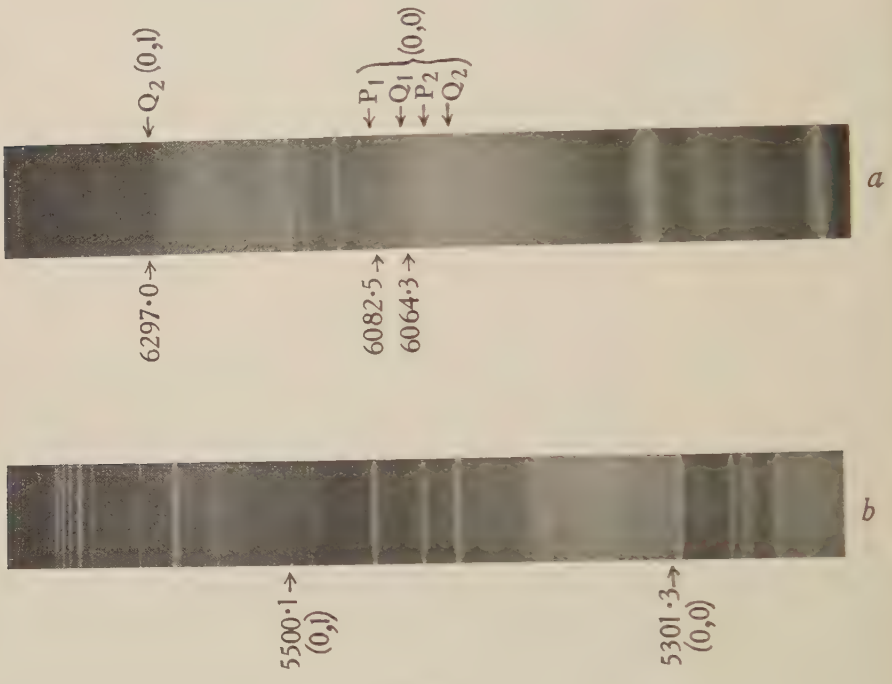

Figure 1.

For the final photographs three plates were taken for the orange and yellow-green bands with the 3-prism spectrograph and two with the grating for the orange. They were measured on a Zeiss-Abbé comparator readable directly to 0·001 mm. and estimable to 0·0001 mm.; in every case the cross-wire was focused on the most intense part of the band-head. The copper lines, the cadmium lines and some iron lines were used as standard wave-lengths. In the case of the prism spectrograms wave-lengths were calculated by means of the usual Hartmann dispersion formula. The mean of three measurements of wave-lengths calculated on three separate plates in the case of the prismatic spectrograms and two of the grating was taken. In most cases the agreement in wave-lengths measured on the different plates was satisfactory, the maximum divergence being 1 A. On account of the rather low dispersion used and the rather diffuse nature of some of the band-heads, very high

accuracy cannot be claimed, the probable error being about 0·3 A. for the prism plates and 0·1 A. for the grating plates. However, in the entire region in which the bands lie, an error of 0·3 A. introduces an error of not more than one unit in wave-number values.

Figure 1 contains the reproductions on an enlarged scale of the various spectrograms taken. A glance at these pictures reveals the close similarity in the physical structure between these bands and those due to CaF; the bands in the orange, figure 1 *a*, are evidently similar to the red bands of CaF, and those in the yellow-green, figure 1 *b*, to the green bands of CaF. Analysis further shows some more similarity to which we shall come later. Tables 1 and 2 give the heads of the two different systems of the CdF bands arranged in the usual $v'\ v''$ notation.

Table 1. CdF yellow-green bands

v', v''	R_2 heads		R_1 heads		v', v''	R_2 heads		R_1 heads	
	λ_{air}	$\nu_{vac.}$	λ_{air}	$\nu_{vac.}$		λ_{air}	$\nu_{vac.}$	λ_{air}	$\nu_{vac.}$
0, 0	2 5301·3	18858	2 5299·3	18865	0, 1	1 5500·2	18176	1 5497·7	18184
1, 1	2 5307·0	18838	2 5305·5	18843	1, 2	1 5504·2	18163	0 5501·1	18173
2, 2	1 5313·2	18816	1 5311·3	18823	2, 3	1 5508·5	18149	1 5506·0	18157
3, 3	1 5319·5	18794	1 5317·8	18800	3, 4	1 5511·7	18138	0 5511·0	18141
4, 4	1 5325·2	18773	1 5323·7	18779	4, 5	1 5516·2	18123	1 6515·7	18125
5, 5	3 5334·3	18741	1 5329·7	18758	5, 6	1 5520·5	18109	0 5518·7	18115
6, 6	3 5340·6	18719	1 5336·2	18735	6, 7	0 5524·8	18095	0 5523·6	18099
7, 7	1 5346·9	18697	5 5342·9	18711	7, 8	0 5529·6	18079	1 5528·1	18084
8, 8	0 5353·8	18673	4 5349·2	18689	8, 9			5532·0	18071
9, 9	1 5360·4	18650	2 5355·6	18667					
10, 10	1 5367·0	18627							

Table 2. CdF orange bands

v', v''	Q_2 heads		P_2 heads		Q_1 heads		P_1 heads	
	λ_{air}	$\nu_{vac.}$	λ_{air}	$\nu_{vac.}$	λ_{air}	$\nu_{vac.}$	λ_{air}	$\nu_{vac.}$
0, 0	4 6036·9	16561	1 6053·3	16515	4 6064·3	16485	5 6082·5	16436
1, 1	3 6034·6	16567	5 6050·6	16523	4 6061·8	16492	2 6079·4	16444
2, 2	3 6032·5	16572	5 6048·6	16528	5 6060·0	16497	1 6077·7	16449
3, 3	2 6031·0	16576	2 6046·7	16533	3 6058·8	16500	1 6076·1	16453
4, 4	1 6029·3	16581	1 6045·0	16538	5 6057·6	16504	1 6074·6	16457
5, 5	1? 6027·9	16585	0 6043·1	16543	3 6056·0	16508	1 6073·5	16460
6, 6					3 6054·7	16512	1 6072·4	16463
0, 1	5 6297·0	15876						
1, 2	(Masked)							
2, 3	4 6285·5	15905						
3, 4	5 6280·9	15917						
4, 5	5 6276·1	15929						
5, 6	4 6272·5	15938						
6, 7	4 6268·3	15949						

§ 3. DESCRIPTION OF THE BANDS

As is well known the wave numbers of the origins of bands belonging to the same electronic band system are expressed by the formula

$$\nu_o = \nu_e + [\omega_e' (v' + \tfrac{1}{2}) - x_e' \omega_e' (v' + \tfrac{1}{2})^2] - [\omega_e'' (v'' + \tfrac{1}{2}) - x_e'' \omega_e'' (v'' + \tfrac{1}{2})^2].$$

If, as in most cases, only the heads of the bands are known, the same equation is satisfactory, provided the wave-number difference between the origin and the heads is constant for all the bands. In many cases however the situation is not very simple, and, according to the nature of the emitter, many characteristic behaviours of the system are met with. In this particular case, as in the case of CaF, SrF, CaCl, SrCl and other similar molecules, we find that only two sequences are developed, namely the 0, 0 and the 0, 1. This points clearly to a case in which the vibrational frequency and the anharmonic constant do not differ greatly in the various electronic levels. Further, the moments of inertia being also about the same, the peculiar physical structure of the bands pointed out by Johnson[4] obtains here. The similarity between these bands and those of the already known molecules of the alkaline earth halides has been of considerable help in arriving at a proper analysis of these bands.

In the yellow-green system we find that the 0, 0 sequence is very clearly developed. Each band-head is accompanied by a nearly equally intense band-head, as in the case CaF. This band system evidently belongs to the transition $^2\Sigma \rightarrow {}^2\Sigma$ in the molecule. The double-headed structure of the bands may be due, as Harvey[5] has pointed out in the case of CaF, to the two R branches (arising from a wide ρ-type doubling) each forming a head of its own. If, on the other hand, we regard one of these as a R head and the other as a Q head, as Johnson[4] does, it is rather difficult to explain how such strong Q branches can be present in a $\Sigma \rightarrow \Sigma$ transition. Quite empirically, therefore, we call the two heads R_1 and R_2. Along the sequence the band-heads go on diverging, and this is a clear indication that we are dealing with an excited level for which, though the frequency of vibration is smaller than the frequency of vibration of the unexcited state, the anharmonic constant is bigger; in this respect also these bands are perfectly analogous to the similar CaF band. The 0, 1 sequence is rather diffuse; but it has been possible to measure R_1 and R_2 heads. Photometric plates of the bands of this sequence were also taken on a Zeiss recording micro-photometer, which helped to identify the position of the bands with more exactness. Figure 2 is a reproduction of the photometric plate taken of this sequence. For the purpose of calculation the values measured on the photometric plates are utilized.

The orange system develops the 0, 0 sequence strongly and its structure clearly indicates that a $\Pi \longleftrightarrow \Sigma$ transition is involved. There are two Q heads and two P heads in the 0, 0 sequence. The 0, 1 sequence however develops only Q heads; this is a handicap for the analysis of the bands, but it seems fairly certain that this is the Q series corresponding to the Q_2 series of the 0, 0 sequence. The other arrangement of putting them with the Q_1 series changes the vibrational frequency by 75 cm.$^{-1}$,

which is highly improbable because we should then have no similarity between the final level of this band system and that of the yellow-green system. The analysis was attempted with a view to correlate, if possible, these two electronic levels, and this we think is perfectly natural because of our knowledge of the behaviour of similar molecules. The appearance of only one Q branch in this sequence is rather surprising but by no means exceptional. We know, for example, that in the analogous bands of CaF[4] the 0, 1 sequence develops only two Q branches ($Q_2+{}^{Q}P_{21}$ and ${}^{P}Q_{12}+P_1$) fairly well, while one of the P-head sequences (P_2) is completely absent, and the other P heads (${}^{O}P_{12}$) are very weak. The 0, 1 sequence on the other hand

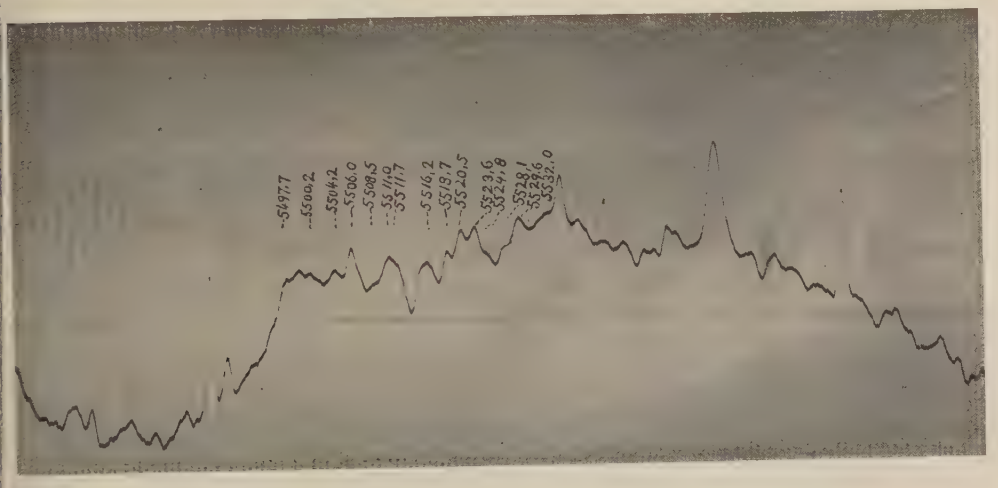

Figure 2.

develops only one Q-head sequence, and this Q-head sequence goes, as in our case, with the Q_2 of the 0, 0 sequence. An interesting explanation of such a situation in CaF is put forward by Harvey[5] and it is clear that the same may be extended to this case also. From all these considerations we believe that we have correctly placed the 0, 1 sequence in the quantum analysis. An isotopic effect would have been an infallible guide in such analysis but unfortunately no such isotopic heads are observed; cadmium possesses several isotopes but the abundance ratio seems to be unfavourable for their detection, at least in the method of excitation of the bands adopted here.

§ 4. ANALYSIS AND DISCUSSION

In a band system in which a fairly large number of sequences are developed, the method of deriving the vibrational equations is not so tedious. Usually many observations are available of the same frequency difference between adjacent vibrational levels, and the weighted mean or arithmetical mean, as the case may be, of all these values is utilized to obtain the frequency differences between successive vibrational levels in the initial and the final states of the molecule. These are then expressed by a suitable quadratic or cubic formula and the vibrational equation is

thence deduced. In cases where, as here, only two sequences are developed, this method is, however, clearly not suitable. We follow Johnson[4] in this case and express each sequence by a polynomial by the rapid least-squares method developed by Birge and Shea[6] and thereby deduce the required vibrational equation by equating the coefficients. Each sequence was first expressed by a polynomial of the third order and so vibrational equations involving cubics were developed, the results being as follows:

Yellow-green system

(i) For R_1 heads:

in 0, 0 sequence, $\nu = 18865{\cdot}05 - 20{\cdot}976v'' - 0{\cdot}124v''^2 + 0{\cdot}0052v''^3$,
in 0, 1 sequence, $\nu = 18198{\cdot}58 - 13{\cdot}23v'' - 0{\cdot}324v''^2 + 0{\cdot}0244v''^3$;
hence, for the whole system,
$\nu_{R_1} = 18865{\cdot}05 + (662{\cdot}62v' - 3{\cdot}78v'^2 - 0{\cdot}067v'^3) - (683{\cdot}60v'' - 3{\cdot}65v''^2 - 0{\cdot}062v''^3)$.

(ii) For R_2 heads:

in 0, 0 sequence, $\nu = 18857{\cdot}68 - 1841v'' - 1{\cdot}104v''^2 + 0{\cdot}064''^3$,
in 0, 1 sequence, $\nu = 18187{\cdot}78 - 11{\cdot}991v'' - 0{\cdot}166v''^2 - 0{\cdot}0035v''^3$;
hence, for the whole system,
$\nu_{R_2} = 18857{\cdot}68 + (666{\cdot}53v' - 3{\cdot}68v'^2 - 0{\cdot}313v'^3) - (684{\cdot}94v'' - 2{\cdot}58v''^2 - 0{\cdot}377v''^3)$.

Orange system

For Q_2 heads:

in 0, 0 sequence, $\nu = 16561{\cdot}05 + 6{\cdot}389v'' - 0{\cdot}591v''^2 + 0{\cdot}055v''^3$,
in 0, 1 sequence, $\nu = 15840{\cdot}65 + 27{\cdot}85v'' - 2{\cdot}82v''^2 + 0{\cdot}15v''^3$;
hence, for the whole system,
$\nu_{Q_2} = 16561{\cdot}05 + (710{\cdot}05v' - 9{\cdot}615v'^2 - 0{\cdot}741v'^3) - (703{\cdot}66v'' - 9{\cdot}024v''^2 - 0{\cdot}686v''^3)$.

In view of the fact already mentioned that the accuracy claimed is not very high, it was also thought advisable to use only a quadratic function; the equations thus obtained are:

Yellow-green system

(i) For R_1 heads:

in 0, 0 sequence, $\nu = 18864{\cdot}75 - 20{\cdot}98v'' - 0{\cdot}1174v''^2$,
in 0, 1 sequence, $\nu = 18200{\cdot}19 - 14{\cdot}722v'' + 0{\cdot}0422v''^2$;
hence, for the whole system,
$\nu_{R_1} = 18864{\cdot}75 + (661{\cdot}75v' - 3{\cdot}11v'^2) - (682{\cdot}43v'' - 3{\cdot}07v''^2)$.

(ii) For R_2 heads:

in 0, 0 sequence, $\nu = 18859{\cdot}99 - 22{\cdot}09v'' - 0{\cdot}140v''^2$,
in 0, 1 sequence, $\nu = 18187{\cdot}61 - 11{\cdot}81v'' - 0{\cdot}214v''^2$;
hence, for the whole system,
$\nu_{R_2} = 18859{\cdot}99 + (667{\cdot}24v' - 5{\cdot}14v'^2) - (689{\cdot}33v'' - 4{\cdot}96v''^2)$.

Orange system

For Q_2 heads:

in 0, 0 sequence, $\nu = 15561{\cdot}21 + 5{\cdot}636v'' - 0{\cdot}1785v''^2$,
in 0, 1 sequence, $\nu = 15856{\cdot}857 + 17{\cdot}114v'' - 0{\cdot}5714v''^2$;
hence, for the whole system,
$\nu_{Q_2} = 16561{\cdot}21 + (689{\cdot}62v' - 5{\cdot}74v'^2) - (692{\cdot}97v'' - 5{\cdot}36v''^2)$.

It is found that the cubic expressions on the whole give smaller O–C values, but

he general equations deduced from them invariably lead to positive values of v^3. This is not a happy situation for they would lead to imaginary values of the heats of dissociation. A similar situation is already met with in the case of the alkaline-earth halides[4]. One way of explaining this is that, in such molecules, Q heads may not represent the origins of the bands[5], and the difference $\nu_h - \nu_o$ is not constant throughout the system. Coupled with this are to be taken into consideration the violent perturbations observed in the present molecule. While some of these may really not be perturbations at all, but only errors of observation, we feel convinced that at least the band in the yellow-green system at ν 18741 is a genuine instance. For these reasons we adopt the quadratic equations to represent the band-heads. Reducing these to the form required by the new quantum theory, we have:

Yellow-green system

For R_1 heads:

$$\nu = 18874{\cdot}04 + [664{\cdot}86\,(v' + \tfrac{1}{2}) - 3{\cdot}11\,(v' + \tfrac{1}{2})^2] - [685{\cdot}50\,(v'' + \tfrac{1}{2}) - 3{\cdot}07\,(v'' + \tfrac{1}{2})^2].$$

For R_2 heads:

$$\nu = 18871{\cdot}1 + [672{\cdot}38\,(v' + \tfrac{1}{2}) - 5{\cdot}14\,(v' + \tfrac{1}{2})^2] - [694{\cdot}29\,(v'' + \tfrac{1}{2}) - 4{\cdot}96\,(v'' + \tfrac{1}{2})^2].$$

Orange system

For Q_2 heads:

$$\nu = 16558{\cdot}31 + [704{\cdot}36\,(v' + \tfrac{1}{2}) - 5{\cdot}74\,(v' + \tfrac{1}{2})^2] - [698{\cdot}34\,(v'' + \tfrac{1}{2}) - 5{\cdot}36\,(v'' + \tfrac{1}{2})^2].$$

In these equations we find again many discrepancies, such as are encountered in the case of similar alkaline earth fluorides. We assume that the final level of these systems is the same. The only justification for this is that the final vibration frequencies for the orange system and the yellow-green R_2 heads are nearly equal though the anharmonic constants widely vary. The yellow-green R_1 heads ought really to give roughly the same equations as R_2 heads, but here again the discrepancy —especially in the anharmonic constant—is very noticeable*. The difference however is not surprisingly large if we remember that the R_1 and R_2 branches of a fully resolved band are usually very different in form. These discrepancies can only

* To satisfy ourselves that this is not a weighty argument against the analysis, we have calculated the equation for the similar bands of the CaF molecule which also shows a wide discrepancy, especially in the anharmonic constant. Thus the R_2 heads of the green bands of CaF are represented by the following equation (*vide* Johnson)[4]:

$$\nu_{\text{head}} = 18888{\cdot}136 + (563{\cdot}388\,v' - 1{\cdot}7160\,v'^2 - 0{\cdot}02245\,v'^3) - (583{\cdot}829\,v'' - 1{\cdot}6339\,v''^2 - \left\{\begin{matrix}0{\cdot}02140\\0{\cdot}02241\end{matrix}\right\} v''^3).$$

The equations for R_1 heads were calculated using Johnson's data in the same way as he has done, with the following result:

$$\nu_{\text{head}} = 18894{\cdot}652 + (559{\cdot}818\,v' - 1{\cdot}265\,v'^2 + 0{\cdot}1983\,v'^3) - (580{\cdot}499\,v'' - 0{\cdot}505\,v''^2 + \left\{\begin{matrix}0{\cdot}1995\\0{\cdot}1991\end{matrix}\right\} v''^3).$$

It is true that these equations are not correct in so far as Johnson's v' v'' numbering is too high by one unit in both v' and v''. But still it is evident that the difference between the coefficients for R_1 and R_2 heads would certainly occur in the corrected equations. Similar discrepancies have also been observed in BeF and other molecules.

be set right by a detailed rotational analysis of the bands, but we believe that the vibrational frequencies derived are of the correct order of magnitude. Under these circumstances, for reasons already mentioned, the data on R_2 heads only were utilized for calculating the heats of dissociation in the case of the yellow-green system. These can be only rough, probably correct to not more than 0·5 V. Before proceeding to discuss this point in detail we should like to draw attention to two more points. (i) The vibrational frequency, which is of the order of 700 cm.$^{-1}$, is higher than for the similar CaF, SrF, and other molecules. That this is of the right magnitude, however, can be seen in table 3 which shows how the frequency of vibration changes as we pass from the hydride to the fluoride in all these cases. The ionization-potential data of the metals concerned also bear this out.

Table 3

Atom	Ionization potential of atom	Hydrides ω_e	Fluorides ω_e	Ratio $\frac{\omega_e \text{ hydride}}{\omega_e \text{ fluoride}}$
Mg	7·61	1493·5	690·8	2·16
Ca	6·09	1316·7	586·7	2·24
Sr	5·67	—	500·1	—
Ba	5·19	—	468·9	—
Cd	8·95	1430·7	692·7	2·07

(ii) The doublet separation for the CdH molecule is about 1000 cm.$^{-1}$ and from analogy we should expect the doublet interval in CdF to be roughly about 900 cm.$^{-1}$; but we find that this is only 75 cm.$^{-1}$. In the 0, 0 sequence of the orange system the P_1 heads are rather diffuse, but the remaining three, Q_1, P_2 and Q_2, are quite sharply developed as can be seen from the enlarged spectrogram, figure 1. Thus there seems to be no doubt about the separation between the Q_1 and Q_2 heads being roughly 75 cm.$^{-1}$. Of course there is the possibility that this is not the deepest $^2\Pi$ state of the molecule, but only a higher excited one. A similar situation was met with in BaH and a lower $^2\Pi$ state was afterwards found with about the right interval. Because of this divergence between the expected and the observed values we have several times tried to see if another arrangement of the heads could be made but without success. The present arrangement is the most straightforward one in such cases and the development of the 0, 0 sequence with its four series cannot be mistaken. We therefore point out this glaring discrepancy and think that very probably this $^2\Pi$ term in the CdF molecule does not arise from the same electronic configuration as the $^2\Pi$ term in CaF and SrF, as will be shown in the discussion on the heats of dissociation. Investigations on the spectrum of the molecule in absorption might throw more light on this point.

§ 5. HEATS OF DISSOCIATION, AND THE STRUCTURE OF CdF

Assuming a linear extrapolation of the vibrational levels one can deduce the heats of dissociation of the CdF molecule in the ground state and the excited states by means of the following well-known formula:

$$D = \frac{\omega_e^2}{4x_e\omega_e \times 8100},$$

where D is the heat of dissociation in volts. The values thus obtained are shown in table 4.

Table 4

Level	D (volts)	Remarks
Ground $^2\Sigma$	3·0	From the yellow-green system (R_2 heads)
	2·8	From the orange system
Excited $^2\Sigma$	2·7	From the yellow-green system (R_2 heads)
Excited $^2\Pi$	2·7	

From these data the potential-energy curves in figures 3 and 4, p. 244, were drawn. The course of these curves is drawn qualitatively but with due regard to the direction of degradation of the bands. The difference between the energies of the dissociation products in the final and the excited states is the same, namely 2·0 V., for both band systems. The only possibility of correlating this energy with the energy of excitation of the constituent atoms is the one shown in the diagrams; i.e. the normal state of the CdF molecule arises thus:

$$\mathrm{Cd}\ (5s,\ 5p)\ ^3P + \mathrm{F}\ (2p)^5\ ^2P \rightarrow \mathrm{CdF},\ ^2\Sigma;$$

and the excited states thus:

$$\mathrm{Cd}\ (5s,\ 6s)\ ^3S + \mathrm{F}\ (2p)^5\ ^2P \rightarrow \mathrm{CdF},\ ^2\Sigma \text{ and } ^2\Pi.$$

The Cd atom in its normal state has, in addition to closed shells, two electrons in the $5s$ group which also is completed, and the fluorine atom five electrons in the $2p$ group. In this state of the Cd atom we have only repulsion on account of the closed group and the linkage starts from the excited level of the configuration (sp).

In the case of the alkaline earths Mulliken[7] assumed that linkage starts with the configuration $(s)^2$ whereas Herzberg[3] showed that the linkage probably starts from the first excited term of the metal atom with the configuration (sp). The helium-like configuration $(s)^2$ should give rise only to a repulsive curve of the two-centre system and this indeed seems to be very probable from the paper of Lessheim and Samuel[2] who have shown that if the ground level of these molecules is considered as arising out of the (sp) configuration, then it is possible to explain why the heat of dissociation in some of the excited states in the alkaline-earth halides and in some other molecules is bigger than in the ground state, and in some cases smaller. The p electron of the metal together with a p electron of the halogen are responsible for the chemical linkage. If the p electron which brings about the linkage is excited, we get

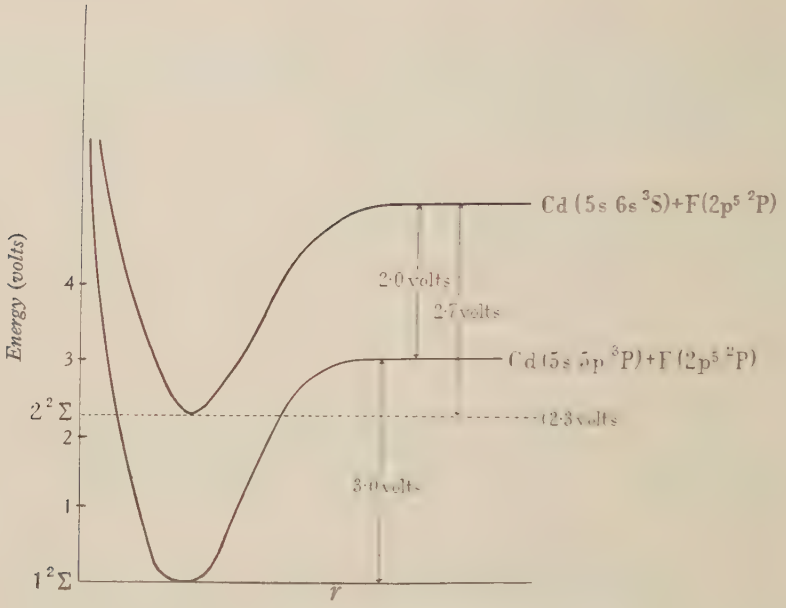

Figure 3. Yellow-green CdF bands (degraded to red).

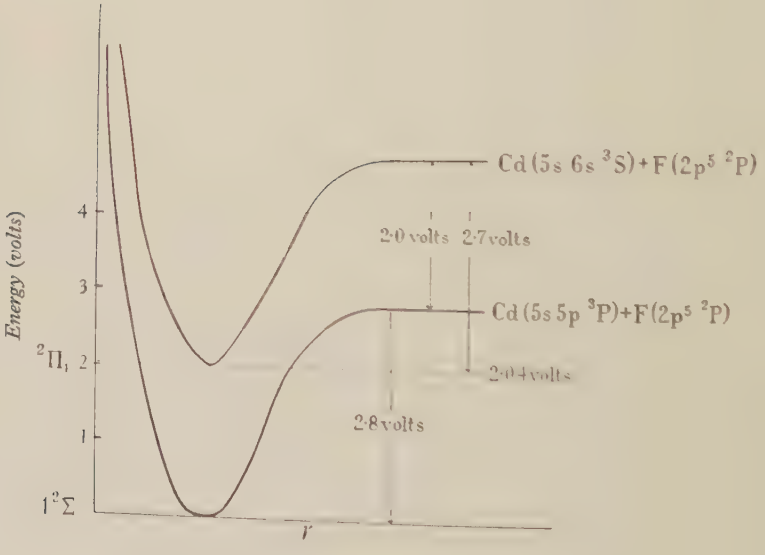

Figure 4. Orange CdF bands (degraded to violet).

a molecular electronic state which has a decreased heat of dissociation and which dissociates adiabatically, yielding a metal in a normal excited state. The s electron of the metal does not take part in the linkage but only disturbs it. Therefore if this s electron in the molecule is now excited, the heat of dissociation increases in the excited level and the term dissociates adiabatically yielding a metal atom in which two electrons are excited, i.e. a metal atom in an anomalous excited state.

For these reasons the ground state of the CdF molecule arises from the configuration Cd $(5s, 5p)\,^3P$, since the configuration Cd $(5s)^2$ gives rise to a repulsive curve only. It can be shown that the spectra of the alkaline-earth oxides, and Hund's theory of their crystal lattice, also lend support to this view[8]. In this case, however, we cannot be certain of the quantum numbers of the united atom and we have recourse to the configuration in the analogous case of BeF. Here we obtain from the configurations of the metal and fluorine the following configuration for the level of the molecule according to Weizel's correlation scheme:

$$^2\Sigma \;:\; 2s\sigma^2\,(2s),\; 2p\pi^4\,(2p),\; 3p\sigma\,(2s),\; 3d\sigma^2\,(2p).$$

Since the dissociation energy decreases in the excited terms observed in CdF, we will consider those configurations of the excited molecule in which the excitation is due to one of the electrons contributing to the linkage; this electron will be either in π^4 or σ^2 group. The excitation will bring it to either the next σ group or the next π group. There are two possible σ groups, $3s\sigma\,(3s)$ and $4p\sigma\,(3s)$, and two possible π groups, $3p\pi\,(3p)$ and $3d\pi\,(2p)$. Since the dissociation energy indicates the electronic configuration $(5s, 6s)$ of Cd, the π group containing p electrons of the separated atoms may be excluded. We therefore derive the following configurations for the excited levels of BeF:

$$^2\Pi \;:\; 2s\sigma^2\,(2s),\; 2p\pi^3\,(2p),\; 3p\sigma\,(2s),\; 3d\sigma^2\,(2p),\; 3s\sigma\,(3s)$$

and

$$^2\Sigma \;:\; 2s\sigma^2\,(2s),\; 2p\pi^4\,(2p),\; 3p\sigma\,(3s),\; 3d\sigma\,(2p),\; 3s\sigma\,(3s);$$

in which the $4p\sigma\,(3s)$ may replace the $3s\sigma\,(3s)$ and the $^2\Pi$ states may be inverted. Both states will have less energy of dissociation. Neglecting now the quantum numbers of the united atom, we suggest therefore the following configurations for the three levels of CdF:

$$^2\Sigma \text{ ground state} \;:\; \sigma^2\,(s),\; \pi^4\,(p),\; \sigma\,(s),\; \sigma^2\,(p).$$

$$^2\Pi \text{ term} \;:\; \sigma^2\,(s),\; \pi^3\,(p),\; \sigma\,(s),\; \sigma^2\,(p),\; \sigma\,(s).$$

$$^2\Sigma \text{ excited state} \;:\; \sigma^2\,(s),\; \pi^4\,(p),\; \sigma\,(s),\; \sigma\,(p),\; \sigma\,(s).$$

Of these, the excited $^2\Sigma$ state is similar to the excited $^2\Sigma$ state observed in the case of CaF and SrF molecules. The difference in the energies of the Cd atom in the $(5s, 6s)\,^3S$ and $(5s, 5p)\,^3P$ states is 2·4 V.[9]. In view of the errors of observation, and for reasons previously explained, we think that the value 2, o obtained from the bands is in fair agreement with this value. The excited $^2\Pi$ state cannot be compared to the $^2\Pi$ state of the alkaline-earth halides. In the case of CaF and other such molecules, the $^2\Pi$ state has a greater dissociation energy than in the ground state and arises out of the anomalous term. In the case of the CdF molecule, the excited $^2\Pi$ has a smaller dissociation energy and arises out of the same terms that give the

excited $^2\Sigma$ state. The reason is that the metals Zn, Cd and Hg of the sub-group of the periodic system have a much higher ionization potential than the alkaline earths. Therefore the anomalous terms of these atoms are also much higher than for the atoms of the main group. The same is already the case in BeF. The anomalous term $(5p^2)\,^3P$ in the Cd atom lies about 5·4 V. above the $(5s, 5p)\,^3P$ term, while in Ca this anomalous term is 2·9 V. above the $(4s, 4p)\,^3P$ term[9]. Since the dissociation energies of the two molecules in their ground states are nearly the same, we assume that the dissociation energy of the CdF molecule which arises out of this configuration in the Cd atom is also about the same as that for the CaF molecule in a similar state, namely 4·8 V. Calculation will show that a transition from such a $^2\Pi$ state to the ground $^2\Sigma$ state should give rise to bands near about $\lambda 3100$. The plates do not show any trace of such a system in this region under the conditions of the present investigation.

REFERENCES

(1) Jevons. *Report on Band-Spectra of Diatomic Molecules* (Phys. Soc. 1932). Also for general reference.
(2) Lessheim and Samuel. *Z. Phys.* **84**, 637 (1933).
(3) Herzberg. *Z. Phys.* **75**, 601 (1930).
(4) Johnson. *Proc. roy. Soc.* A, **122**, 161 (1929).
(5) Harvey. *Proc. roy. Soc.* A, **133**, 336 (1931).
(6) Birge and Shea. *Univ. Calif. Publ. Math.* **2**, 67 (1927).
(7) Mulliken. *Rev. mod. Phys.* **4**, 1–86 (1932).
(8) R. Samuel. "Report on Absorption Spectra." *Proc. Ind. Acad. Sci.* **1** (in press).
(9) Bacher and Goudsmit. *Atomic Energy States* (McGraw-Hill, 1932).

535·338.4:546.182.6

ROTATIONAL ANALYSIS OF THE ULTRA-VIOLET BANDS OF PHOSPHORUS MONOXIDE

By A. K. SEN GUPTA

Communicated by Prof. P. N. Ghosh, October 16, 1934. *Read in title December* 7, 1934.

ABSTRACT. The structure of (0, 0), (0, 1) and (1, 0) bands of the ultra-violet system of the PO molecule has been analysed. The bands are due to a $^2\Sigma \rightarrow {}^2\Pi$ transition. Each band consists of six main branches P_2, Q_2, R_2, and P_1, Q_1, R_1 and two satellite branches $^OP_{12}$ and $^SR_{21}$. The potential-energy curves for both the upper and lower states of the system have been drawn on the basis of the equations given by Morse as well as by Rydberg. From these curves the Condon parabola for the intensity of the bands in the system has been obtained. The relevant molecular constants have been obtained. The products of dissociation in the different states are discussed.

§ 1. INTRODUCTION

A VIBRATIONAL quantum analysis of the ultra-violet bands of phosphorus monoxide has been recently published by Ghosh and Ball[1]. The marked resemblance in appearance which these bands bear to the γ bands of NO led these authors to suggest that they might be due to a $^2\Sigma \rightarrow {}^2\Pi$ transition.

In the present investigation, a rotational analysis of the (0, 0), (0, 1) and (1, 0) bands has been made. The analysis confirms the idea that they are of the $^2\Sigma \rightarrow {}^2\Pi$ type. Each band is found to consist of eight branches, viz., $^OP_{12}$, P_2, Q_2, R_2 and P_1, Q_1, R_1, $^SR_{21}$.

§ 2. SPECTROGRAMS

Using as a source the flame of carbon arc fed from 220-volt d.c. circuit with P_2O_5 placed in the lower (positive) electrode and with a current of 3–4 A., the bands have been photographed in the 1st order of a 21-ft. concave grating recently set up in the laboratory on a Paschen mounting and having a dispersion of about 1·22 A./mm. in the first order in the neighbourhood of λ 2500. The time of exposure was about 15 hours. The usual standard iron arc was used as a comparison spectrum. For measurements a Gaertner precision comparator was used. The wave-numbers given in tables 2, 3 and 4 are correct to $\pm 0{\cdot}2$ cm.$^{-1}$

§ 3. ROTATIONAL ANALYSIS

As the bands were excited at a high temperature, the different series were long and there was considerable overlapping of series lines from one band to another. Many of the observed lines were blends. The bands (0, 0), (0, 1) and (1, 0) were selected for measurement of structure lines in view of their comparatively strong

intensity and minimum overlapping due to the lines of the neighbouring bands. The choice of these bands also enabled us to take full advantage of the combination principle.

Each band is found to consist of eight branches, four of them forming heads. This shows that the band system is due to a $^2\Sigma \rightleftarrows {}^2\Pi$ transition, with negligible spin doubling in the $^2\Sigma$ state. A more definite idea about the nature of transition could not be derived from the criterion of missing lines, for lines of low J values are not sufficiently intense for measurement. The intensity of the different branch lines for moderate J values is, however, in agreement with what one would expect in the case of a $^2\Sigma \rightarrow {}^2\Pi$ transition. In fact, the analysis of each individual band was started on this assumption so that the four heads were attributed to $^oP_{12}$, P_2, P_1 and Q_1 branches. Members of the P, Q, and R series with common values of rotation quantum number of the lower energy state were selected with the aid of the relation

$$R(J)-Q(J)=Q(J+1)-P(J+1),$$

and those of the $^oP_{12}$ and $^sR_{21}$ series from the relations

$$R_1(J)-P_1(J)=R_2(J)-{}^oP_{12}(J)$$

and

$$R_2(J)-P_2(J)={}^sR_{21}(J)-Q_1(J).$$

§ 4. EVALUATION OF THE CONSTANTS

The upper $^2\Sigma$ *state.* The upper-state combinations are defined by

$$R_1(J)-P_1(J)=\Delta_2T_1'(J),\ \ldots\ J=K+\tfrac{1}{2}$$

and

$$R_2(J)-P_2(J)=\Delta_2T_2'(J),\ \ldots\ J=K-\tfrac{1}{2}.$$

Within the limits of experimental error, these differences for (0, 0) and (0, 1) bands are equal in magnitude. This indicates that the two bands have a common upper state and that the spin doubling of the $^2\Sigma$ state is negligible. The values of B' and D_v' for the upper state were calculated by the method of successive approximation from the mean of these differences in accordance with the following relation:

$$\Delta_2T'(K)=B_v'(4K+2)+D_v'(8K^3+12K^2+12K+4).$$

The lower $^2\Pi$ *state.* The lower-state combinations are defined by

$$R_1(J-1)-P_1(J+1)=\Delta_2T_1''(J),\ \text{for the } {}^2\Pi_{\frac{3}{2}} \text{ sub-state,}$$

and

$$R_2(J-1)-P_2(J+1)=\Delta_2T_2''(J),\ \text{for the } {}^2\Pi_{1\frac{1}{2}} \text{ sub-state.}$$

The mutual agreement between these differences in each sub-state for (0, 0) and (1, 0) bands indicates that the two bands have a common lower state. The values of B_v'' and D_v'' were calculated from the relation

$$\Delta_2T''(J)=B_v''(4J+2)+D_v''(8J^3+12J^2+12J+4).$$

The values of the molecular constants are given in table 1.

Table 1. Constants of the PO molecule.

Upper $^2\Sigma$ state	Lower $^2\Pi_{\frac{1}{2}}$ sub-state	Lower $^2\Pi_{1\frac{1}{2}}$ sub-state
$B_e' = 0{\cdot}8121$ cm.$^{-1}$	$B_e'' = 0{\cdot}7613$ cm.$^{-1}$	$B_e'' = 0{\cdot}7645$ cm.$^{-1}$
$B_0' = 0{\cdot}8093$ cm.$^{-1}$	$B_0'' = 0{\cdot}7585$ cm.$^{-1}$	$B_0'' = 0{\cdot}7617$ cm.$^{-1}$
$B_1' = 0{\cdot}8037$ cm.$^{-1}$	$B_1'' = 0{\cdot}7530$ cm.$^{-1}$	$B_1'' = 0{\cdot}7652$ cm.$^{-1}$
$\alpha' = 0{\cdot}0056$ cm.$^{-1}$	$\alpha'' = 0{\cdot}0055$ cm.$^{-1}$	$\alpha'' = 0{\cdot}0055$ cm.$^{-1}$
$D_e' = -1{\cdot}096 \times 10^{-6}$ cm.$^{-1}$	$D_e'' = -1{\cdot}151 \times 10^{-6}$ cm.$^{-1}$	$D_e'' = -1{\cdot}167 \times 10^{-6}$ cm.$^{-1}$
$r_e' = 1{\cdot}402 \times 10^{-8}$ cm.	$r_e'' = 1{\cdot}446 \times 10^{-8}$ cm.	$r_e'' = 1{\cdot}443 \times 10^{-8}$ cm.
$I' = 34{\cdot}109 \times 10^{-40}$ gm. cm^2	$I'' = 36{\cdot}385 \times 10^{-40}$ gm. cm^2	$I'' = 36{\cdot}233 \times 10^{-40}$ gm. cm^2

§ 5. Δ-TYPE DOUBLING

The combination defects in the (0, 1), (0, 0) and (1, 0) bands were computed for each value of J in accordance with the following relation:

$$2\Delta\nu_{dc}\,(J+\tfrac{1}{2}) = \{Q\,(J) - P\,(J+1)\} - \{R\,(J) - Q\,(J+1)\}.$$

The combination defects obtained from R_1, P_1, and Q_1 branches are negative and increase almost linearly with $(J+\frac{1}{2})$ for moderate J values, while those obtained from R_2, P_2 and Q_2 branches are positive and rather smaller in magnitude. This shows that R_1, P_1 and Q_1 branches are to be associated with $^2\Pi_{\frac{1}{2}}$, and R_2, P_2 and Q_2 branches with $^2\Pi_{1\frac{1}{2}}$ sub-states, indicating that $^2\Pi$ state is normal. The nature of the combination defects points further to the fact that the coupling is intermediate between case *a* and case *b* and is nearer to case *a*. This is also supported by the fact that the satellite branches $^OP_{12}$ and $^SR_{21}$ extend to fairly large rotational quantum numbers.

§ 6. POTENTIAL-ENERGY CURVES AND INTENSITY DISTRIBUTION IN THE BAND SYSTEM

Potential-energy curves derived by means of both Morse[2] and Rydberg[3] equations are given in figures 1 and 2. Using the Franck-Condon theory of probability of transition, the Condon parabola for the intensity-distribution in the band system is drawn in figure 3 as deduced from them; M indicates the parabola derived from the Morse curves and R that derived from those of Rydberg. The Condon parabola M seems to be in good agreement with the visual estimation of the intensities of the band-heads, but the parabola R fits still better.

§ 7. PRODUCTS OF DISSOCIATION

An enquiry into the products of dissociation of the PO molecule seems to be of interest in view of the conflicting opinions regarding their identity in the case of the NO molecule. Birge and Sponer and others were of opinion that the latter molecule in its different excited states is dissociated into an excited oxygen atom and a normal nitrogen atom. Hence for the homologous PO molecule one would naturally expect that the value of the atomic excitation energy E_a as calculated from its band system

should be identical with that obtained from the γ bands of NO. From a similar consideration Lessheim and Samuel[4] calculated the values of E_a in the case of NO and PO molecules and found them to be of distinctly different magnitude. This led these authors to conclude that the two oxide molecules in their excited states are

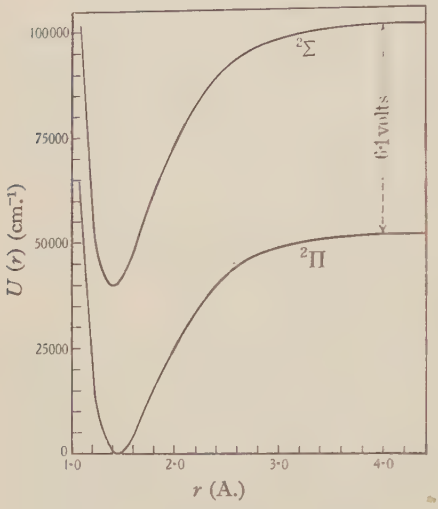

Figure 1. Potential-energy curves by Morse's function.

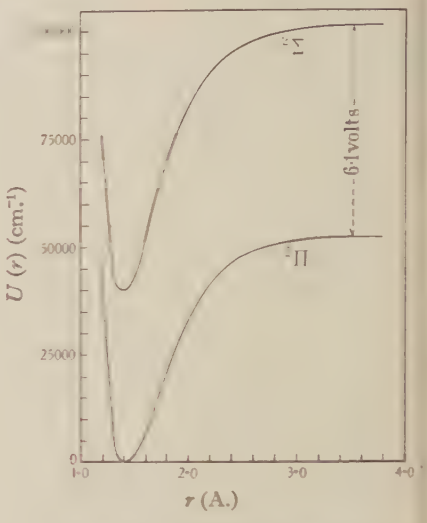

Figure 2. Potential-energy curves by Rydberg's function.

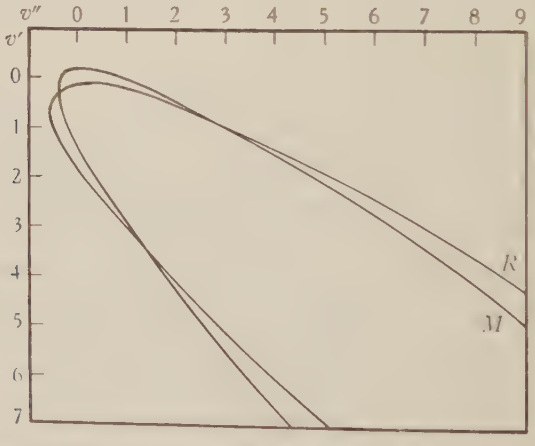

Figure 3. Intensity curves, M from figure 1, R from figure 2.

dissociated into a normal oxygen atom and an excited nitrogen or phosphorus atom. For the PO molecule the heats of dissociation of its different states were calculated by them from the earlier data. In view of the fact that new data are now available from the recent vibrational analysis of Ghosh and Ball, we are now in a position to decide more definitely the identity of the products of dissociation.

From these recent data the value of E_a is calculated to be 6·1 V. and is thus widely different from the atomic excitation energy of the oxygen atom corresponding to the $^5S \rightarrow {}^3P$ transition. It is, however, in fair agreement, within the limits of extrapolation error, with the E_a value of phosphorus, if we assume that the $^2\Pi$ state of the PO molecule is derived from normal P (^4S) and O (^3P) atoms and its upper $^2\Sigma$ state from excited P (^4P) and normal O (^3P) atoms. From the data of energy states published by Bacher and Goudsmit[5] the difference of energy values between a P atom in the normal $(3s^2 3p^3)\ ^4S$ state and that in an excited $(3s^2 3p^2 4s)\ ^4P$ state is 6·9 V. This result, therefore, appears to be in agreement with the view of Lessheim and Samuel.

There is yet another possibility that the products of dissociation of the PO molecule in its normal and excited states may consist respectively of a P atom in $(3s^2 3p^3)\ ^2D$ and $(3s^2 3p^2 4s)\ ^2P$ states, since the difference of energy values between these two atomic states is 5·7 V. This indicates that in the normal state the molecule is dissociated into a normal O atom and a metastable P atom. A similar possibility may be reckoned also in the case of the NO molecule, since the atomic excitation energy derived from the γ bands is 9·4 V., whereas the differences between the energy states of N atom corresponding to $^4P \rightarrow {}^4S$ and $^2P \rightarrow {}^2D$ are 10·3 and 8·3 V. respectively. From the uncertainties involved in the determination of dissociation energies by the method of extrapolation, it is difficult to decide between the two alternatives.

§ 8. DISCUSSION OF RESULTS

A check on the correctness and the analysis was afforded by a rule due to R. T. Birge[6]. According to this rule the quantity $2x_e B_e/\alpha$ is approximately equal to $1{\cdot}4 \pm 0{\cdot}2$. For these bands the substitution of the proper values showed that $2x_e' B_e'/\alpha' = 1{\cdot}59$ and $2x_e'' B_e''/\alpha'' = 1{\cdot}47$.

An additional check is given by the approximate relation that for a molecule composed of two atoms of nearly equal mass, the quantity $\omega_e r_e^3$ is approximately equal to 3000×10^{-24} cm.^{2} This condition is satisfied since we have

$$\omega_e' r_e'^3 = 3800 \times 10^{-24} \text{ cm.}^2 \text{ and } \omega_e'' r_e''^3 = 3700 \times 10^{-24} \text{ cm.}^2$$

It is to be expected that for PO the value of $\omega_e r_e^3$ will be greater than 3000×10^{-24} cm.^{2} since the masses of the two atoms are rather unequal.

§ 9. ACKNOWLEDGMENT

With great pleasure I acknowledge my indebtedness to Prof. Dr P. N. Ghosh for his continual guidance and helpful suggestions during the course of the investigation.

REFERENCES

(1) P. N. Ghosh and G. N. Ball. *Z. Phys.* **71**, 362 (1931).
(2) P. M. Morse. *Phys. Rev.* **34**, 57 (1929).
(3) R. Rydberg. *Z. Phys.* **73**, 376 (1931–2).
(4) H. Lessheim and R. Samuel. *Z. Phys.* **84**, 637 (1933).
(5) R. F. Bacher and S. Goudsmit. *Atomic Energy States* (1932).
(6) R. T. Birge. *Phys. Rev.* **31**, 919 (1927).

Table 2. (0, 0) band at λ 2478

$^2\Sigma \rightarrow {}^2\Pi_{1\frac{1}{2}}$

J''	$^0P_{12}$	P_2	Q_2	R_2	$\Delta_2 T_2'(J)$	$\Delta_2 T_2''(J)$
$1\frac{1}{2}$	—	—	40376·83	—	—	—
$2\frac{1}{2}$	—	—	377·91	—	—	—
$3\frac{1}{2}$	—	—	378·95	—	—	—
$4\frac{1}{2}$	40365·74	—	380·25	—	—	—
$5\frac{1}{2}$	363·95	—	381·62	40392·97	—	18·34
$6\frac{1}{2}$	362·06	40371·61	383·03	395·93	24·32	21·37
$7\frac{1}{2}$	360·36	371·61	384·48	399·10	27·49	24·32
$8\frac{1}{2}$	358·57	371·61	386·29	402·45	30·84	27·49
$9\frac{1}{2}$	357·10	371·61	387·82	405·63	34·02	—
$10\frac{1}{2}$	355·80	—	389·71	408·08	—	33·43
$11\frac{1}{2}$	354·34	372·20	391·60	412·73	40·53	36·49
$12\frac{1}{2}$	353·13	372·59	393·63	416·33	43·74	39·65
$13\frac{1}{2}$	352·10	373·08	395·83	420·99	46·91	42·60
$14\frac{1}{2}$	350·92	373·73	397·87	423·68	49·95	45·71
$15\frac{1}{2}$	349·97	374·28	400·12	427·60	53·32	48·65
$16\frac{1}{2}$	349·12	375·03	402·55	431·69	56·66	51·75
$17\frac{1}{2}$	348·47	375·85	405·06	435·72	59·87	54·86
$18\frac{1}{2}$	347·82	376·83	407·61	439·89	63·06	57·91
$19\frac{1}{2}$	347·23	377·81	410·12	444·12	66·31	60·94
$20\frac{1}{2}$	346·68	378·95	413·06	448·62	69·67	63·87
$21\frac{1}{2}$	346·36	380·25	415·84	453·02	72·77	66·90
$22\frac{1}{2}$	—	381·72	418·78	457·54	75·82	69·99
$23\frac{1}{2}$	345·87	383·03	421·89	462·20	79·17	72·96
$24\frac{1}{2}$	345·87	384·58	424·99	466·96	82·38	75·91
$25\frac{1}{2}$	345·87	386·29	428·35	471·95	85·66	79·04
$26\frac{1}{2}$	345·87	387·92	431·53	476·71	88·79	82·24
$27\frac{1}{2}$	—	389·71	434·96	481·87	92·16	85·12
$28\frac{1}{2}$	346·36	391·59	438·56	486·97	95·38	88·14
$29\frac{1}{2}$	346·88	393·73	442·25	492·12	98·39	91·14
$30\frac{1}{2}$	347·43	395·83	445·86	497·52	101·69	94·08
$31\frac{1}{2}$	347·98	398·04	449·68	502·88	104·84	97·20
$32\frac{1}{2}$	348·68	400·32	453·61	508·46	108·14	100·19
$33\frac{1}{2}$	349·45	402·69	457·59	514·09	111·40	103·23
$34\frac{1}{2}$	350·43	405·23	461·80	519·78	114·55	106·33
$35\frac{1}{2}$	351·30	407·76	465·89	525·60	117·84	109·33
$36\frac{1}{2}$	352·38	410·45	470·15	531·35	120·90	112·37
$37\frac{1}{2}$	353·68	413·23	474·49	537·27	124·04	115·18
$38\frac{1}{2}$	354·92	416·17	479·08	543·51	127·34	118·16
$39\frac{1}{2}$	356·28	419·11	483·59	549·60	130·49	121·30
$40\frac{1}{2}$	357·76	422·21	488·38	555·84	133·63	124·20
$41\frac{1}{2}$	359·38	425·40	493·02	562·35	136·95	127·24
$42\frac{1}{2}$	361·02	428·60	498·06	568·68	140·08	130·33
$43\frac{1}{2}$	362·81	432·02	502·78	575·27	143·25	133·39
$44\frac{1}{2}$	364·68	435·29	507·89	581·86	146·57	136·38
$45\frac{1}{2}$	366·56	438·89	513·06	588·70	149·81	139·21
$46\frac{1}{2}$	368·61	442·65	518·45	595·53	152·88	142·12
$47\frac{1}{2}$	370·79	446·58	523·81	602·46	155·88	145·29
$48\frac{1}{2}$	373·08	450·24	528·95	609·47	159·23	148·36
$49\frac{1}{2}$	375·52	454·10	534·74	616·55	162·45	151·11
$50\frac{1}{2}$	377·91	458·36	540·32	623·74	165·38	154·03
$51\frac{1}{2}$	380·52	462·52	546·05	631·17	168·65	—
$52\frac{1}{2}$	383·13	—	551·74	638·44	—	—
$53\frac{1}{2}$	—	—	557·66	646·04	—	—
$54\frac{1}{2}$	—	—	563·91	653·64	—	—
$55\frac{1}{2}$	—	—	569·83	661·41	—	—
$56\frac{1}{2}$	—	—	576·09	669·03	—	—
$57\frac{1}{2}$	—	—	582·35	677·13	—	—
$58\frac{1}{2}$	—	—	588·70	—	—	—
$59\frac{1}{2}$	—	—	595·37	—	—	—

Table 2 (*cont.*)

$^2\Sigma \rightarrow {}^2\Pi_{\frac{1}{2}}$

J''	P_1	Q_1	R_1	$^sR_{21}$	$\Delta_2T_1'(J)$	$\Delta_2T_1''(J)$
$3\frac{1}{2}$	40590·42	—	40601·63	40609·72	11·21	—
$4\frac{1}{2}$	588·29	—	602·79	612·68	14·50	15·16
$5\frac{1}{2}$	586·47	—	604·27	615·65	17·80	17·97
$6\frac{1}{2}$	584·82	40594·38	605·76	618·79	20·94	21·26
$7\frac{1}{2}$	583·01	594·38	607·41	621·89	24·40	24·41
$8\frac{1}{2}$	581·36	594·38	609·06	625·23	27·70	27·36
$9\frac{1}{2}$	580·05	—	610·70	628·53	30·65	30·33
$10\frac{1}{2}$	578·73	—	612·68	632·00	33·95	33·29
$11\frac{1}{2}$	577·41	595·20	614·66	635·55	37·25	36·43
$12\frac{1}{2}$	576·25	595·63	616·65	639·43	40·40	39·39
$13\frac{1}{2}$	575·27	596·19	618·89	643·07	43·62	42·37
$14\frac{1}{2}$	574·28	596·89	621·16	647·03	46·88	45·43
$15\frac{1}{2}$	573·46	597·64	623·59	651·13	50·13	48·48
$16\frac{1}{2}$	572·68	598·50	626·05	655·13	53·37	51·53
$17\frac{1}{2}$	572·06	599·45	628·63	659·26	56·57	54·57
$18\frac{1}{2}$	571·48	600·54	631·34	663·64	59·86	—
$19\frac{1}{2}$	—	601·70	633·98	668·03	—	60·52
$20\frac{1}{2}$	—	602·92	637·05	672·45	—	63·65
$21\frac{1}{2}$	570·33	604·40	639·93	677·13	69·60	66·72
$22\frac{1}{2}$	570·33	605·76	643·00	681·79	72·67	69·60
$23\frac{1}{2}$	570·33	607·41	646·30	686·56	75·97	72·67
$24\frac{1}{2}$	570·33	609·12	649·57	691·59	79·24	—
$25\frac{1}{2}$	—	610·83	652·98	696·50	—	78·75
$26\frac{1}{2}$	570·82	612·80	656·45	701·67	85·63	81·75
$27\frac{1}{2}$	571·23	614·73	660·09	706·86	88·86	84·80
$28\frac{1}{2}$	571·65	616·87	663·74	712·24	92·09	87·79
$29\frac{1}{2}$	572·30	619·02	667·53	717·55	95·23	90·61
$30\frac{1}{2}$	573·13	621·43	671·44	723·19	98·31	93·66
$31\frac{1}{2}$	573·87	623·74	675·47	728·66	101·60	96·67
$32\frac{1}{2}$	574·77	626·30	679·60	734·47	104·83	99·84
$33\frac{1}{2}$	575·76	628·82	683·84	740·21	108·08	102·92
$34\frac{1}{2}$	576·75	631·57	688·12	746·15	111·37	105·77
$35\frac{1}{2}$	578·07	634·37	692·52	752·24	114·45	108·73
$36\frac{1}{2}$	579·39	637·18	697·10	758·39	117·71	111·82
$37\frac{1}{2}$	580·70	640·30	701·70	764·49	121·00	114·75
$38\frac{1}{2}$	582·35	643·36	706·37	770·92	124·02	117·70
$39\frac{1}{2}$	584·00	646·67	711·25	777·34	127·25	120·73
$40\frac{1}{2}$	585·64	649·87	716·22	783·74	130·58	123·79
$41\frac{1}{2}$	587·46	653·44	721·18	790·48	133·72	126·79
$42\frac{1}{2}$	589·43	657·83	726·40	797·14	136·97	129·75
$43\frac{1}{2}$	591·43	660·55	731·55	804·03	140·12	132·76
$44\frac{1}{2}$	593·64	664·25	736·89	810·94	143·25	135·69
$45\frac{1}{2}$	595·86	668·06	742·38	817·96	146·52	138·62
$46\frac{1}{2}$	598·27	672·05	747·92	825·10	149·75	141·64
$47\frac{1}{2}$	600·74	676·13	753·50	832·23	152·76	144·68
$48\frac{1}{2}$	603·24	680·16	759·28	839·70	156·04	147·64
$49\frac{1}{2}$	605·86	684·56	765·01	846·97	159·15	150·55
$50\frac{1}{2}$	608·73	688·85	771·02	—	162·29	153·48
$51\frac{1}{2}$	611·63	693·38	777·01	—	165·38	156·52
$52\frac{1}{2}$	614·60	697·89	783·26	—	168·66	159·38
$53\frac{1}{2}$	617·63	702·63	789·52	—	171·89	162·33
$54\frac{1}{2}$	620·93	707·34	795·91	—	174·98	165·35
$55\frac{1}{2}$	624·17	712·27	802·30	—	178·13	168·45
$56\frac{1}{2}$	627·46	717·35	808·79	—	181·33	171·13
$57\frac{1}{2}$	631·17	722·33	—	—	—	174·15
$58\frac{1}{2}$	634·64	727·63	—	—	—	—
$59\frac{1}{2}$	638·44	732·90	—	—	—	—
$60\frac{1}{2}$	642·40	738·25	—	—	—	—

Table 3. (0, 1) band at λ 2555

$^2\Sigma \rightarrow {}^2\Pi_{1\frac{1}{2}}$

J''	$^0P_{12}$	P_2	Q_2	R_2	$\Delta_2T_2'(J)$	$\Delta_2T_2''(J)$
$1\frac{1}{2}$	—	—	39154·34	—	—	—
$2\frac{1}{2}$	—	—	154·48	—	—	—
$3\frac{1}{2}$	—	—	156·48	—	—	—
$4\frac{1}{2}$	39143·30	—	157·71	—	—	—
$5\frac{1}{2}$	141·46	—	159·24	39170·60	—	—
$6\frac{1}{2}$	139·78	39149·43	160·78	173·62	24·19	21·07
$7\frac{1}{2}$	138·09	149·43	162·31	176·89	27·46	24·19
$8\frac{1}{2}$	136·56	149·43	164·05	180·19	30·76	—
$9\frac{1}{2}$	135·18	—	165·84	183·72	—	30·15
$10\frac{1}{2}$	133·80	150·04	167·89	187·17	37·13	33·22
$11\frac{1}{2}$	132·73	150·50	169·82	190·84	40·34	36·21
$12\frac{1}{2}$	131·65	150·96	172·00	194·63	43·67	39·26
$13\frac{1}{2}$	130·74	151·58	174·28	198·54	46·96	42·28
$14\frac{1}{2}$	129·74	152·35	176·58	202·55	50·20	45·43
$15\frac{1}{2}$	128·74	153·11	179·04	206·50	53·39	48·37
$16\frac{1}{2}$	128·13	154·18	181·64	210·69	56·51	51·40
$17\frac{1}{2}$	127·72	155·10	184·22	215·00	59·90	54·36
$18\frac{1}{2}$	127·21	156·33	187·07	219·41	63·08	57·44
$19\frac{1}{2}$	126·91	157·56	189·94	223·87	66·31	60·47
$20\frac{1}{2}$	—	158·94	192·93	228·49	69·55	63·40
$21\frac{1}{2}$	126·45	160·47	196·08	233·13	72·66	66·49
$22\frac{1}{2}$	126·45	162·00	199·14	237·93	75·93	69·44
$23\frac{1}{2}$	126·45	163·69	202·55	242·86	79·17	72·40
$24\frac{1}{2}$	—	165·53	205·90	247·89	82·36	75·41
$25\frac{1}{2}$	126·91	167·45	209·46	253·11	85·66	78·50
$26\frac{1}{2}$	127·47	169·39	213·05	258·27	89·88	81·59
$27\frac{1}{2}$	127·98	171·52	216·77	263·55	92·03	84·45
$28\frac{1}{2}$	128·74	173·82	220·61	269·06	95·24	87·50
$29\frac{1}{2}$	129·41	176·05	224·60	274·62	98·57	90·49
$30\frac{1}{2}$	130·17	178·57	228·69	280·28	101·71	93·51
$31\frac{1}{2}$	131·04	181·11	232·77	286·00	104·89	96·46
$32\frac{1}{2}$	132·11	183·82	237·16	291·91	108·09	99·44
$33\frac{1}{2}$	133·34	186·56	241·37	297·77	111·21	102·58
$34\frac{1}{2}$	134·51	189·33	245·88	303·87	114·54	105·30
$35\frac{1}{2}$	135·94	192·47	250·51	310·13	117·66	108·40
$36\frac{1}{2}$	137·32	195·47	255·18	316·37	120·90	111·47
$37\frac{1}{2}$	138·96	198·70	259·97	322·81	124·11	114·44
$38\frac{1}{2}$	140·69	201·93	264·90	329·31	127·38	117·50
$39\frac{1}{2}$	142·53	205·31	269·88	335·81	130·50	120·31
$40\frac{1}{2}$	144·45	209·00	275·00	342·62	133·62	123·43
$41\frac{1}{2}$	146·36	212·58	280·13	349·36	136·98	126·39
$42\frac{1}{2}$	148·66	216·23	285·52	356·25	140·02	129·29
$43\frac{1}{2}$	150·96	220·07	290·92	363·30	143·23	132·17
$44\frac{1}{2}$	153·19	224·08	296·54	370·56	146·48	135·18
$45\frac{1}{2}$	155·77	228·12	302·25	377·74	149·62	138·25
$46\frac{1}{2}$	158·32	232·31	307·97	385·14	152·83	141·19
$47\frac{1}{2}$	161·00	236·55	313·77	392·57	156·02	144·18
$48\frac{1}{2}$	163·69	240·96	319·87	400·14	159·18	147·09
$49\frac{1}{2}$	166·61	245·48	325·90	407·75	162·27	149·96
$50\frac{1}{2}$	169·68	250·08	332·09	415·50	165·42	153·03
$51\frac{1}{2}$	172·82	254·72	338·28	423·37	168·65	155·92
$52\frac{1}{2}$	176·05	259·58	344·84	431·53	171·95	158·87
$53\frac{1}{2}$	179·34	264·54	351·35	439·62	175·12	162·00
$54\frac{1}{2}$	182·88	269·53	358·00	447·71	178·18	164·85
$55\frac{1}{2}$	186·41	274·77	364·66	455·96	181·19	167·69
$56\frac{1}{2}$	190·25	280·02	371·54	464·38	184·36	170·54
$57\frac{1}{2}$	193·94	285·42	378·49	473·02	187·60	173·56
$58\frac{1}{2}$	197·93	290·82	385·57	481·57	190·75	176·48
$59\frac{1}{2}$	201·77	296·54	392·85	—	—	179·57
$60\frac{1}{2}$	—	302·10	—	—	—	—

Table 3 (*cont.*)

$^2\Sigma \rightarrow {}^2\Pi_{\frac{1}{2}}$

J''	P_1	Q_1	R_1	${}^sR_{21}$	$\Delta_2T_1'(J)$	$\Delta_2T_1''(J)$
$3\frac{1}{2}$	39370·35	—	39381·75	39389·82	11·40	—
$4\frac{1}{2}$	368·49	—	383·07	392·75	14·58	15·20
$5\frac{1}{2}$	366·55	—	384·46	396·11	17·91	17·99
$6\frac{1}{2}$	365·08	—	386·06	398·90	20·98	20·93
$7\frac{1}{2}$	363·53	39374·79	387·70	402·24	24·17	24·08
$8\frac{1}{2}$	361·98	374·79	389·51	405·53	27·54	27·11
$9\frac{1}{2}$	360·59	375·24	391·45	409·20	30·86	30·12
$10\frac{1}{2}$	359·39	375·52	393·31	412·73	33·92	33·26
$11\frac{1}{2}$	358·19	375·93	395·43	416·40	37·24	36·13
$12\frac{1}{2}$	357·18	376·60	397·65	420·30	40·47	39·18
$13\frac{1}{2}$	356·25	377·23	399·93	424·23	43·68	42·17
$14\frac{1}{2}$	355·48	378·15	402·40	428·26	46·92	45·08
$15\frac{1}{2}$	354·85	379·04	404·96	432·46	50·11	—
$16\frac{1}{2}$	—	380·14	407·65	436·66	—	51·16
$17\frac{1}{2}$	353·80	381·26	410·40	441·02	56·60	54·11
$18\frac{1}{2}$	353·54	382·53	413·35	445·53	59·81	—
$19\frac{1}{2}$	—	383·85	416·30	450·25	—	60·36
$20\frac{1}{2}$	352·99	385·37	419·41	454·87	66·42	63·31
$21\frac{1}{2}$	352·99	387·06	422·67	459·85	69·68	—
$22\frac{1}{2}$	—	388·81	426·09	464·84	—	69·13
$23\frac{1}{2}$	353·54	390·70	429·51	469·77	75·97	72·29
$24\frac{1}{2}$	353·80	392·54	433·08	475·02	79·28	—
$25\frac{1}{2}$	—	394·61	436·66	480·27	—	78·23
$26\frac{1}{2}$	354·85	396·78	440·50	485·78	85·65	81·18
$27\frac{1}{2}$	355·48	399·11	444·44	491·19	88·96	84·25
$28\frac{1}{2}$	356·25	401·49	448·33	496·80	92·08	87·16
$29\frac{1}{2}$	357·28	403·98	452·54	502·63	95·26	90·14
$30\frac{1}{2}$	358·19	406·65	456·74	508·40	98·55	93·15
$31\frac{1}{2}$	359·39	409·38	461·10	514·44	101·71	96·05
$32\frac{1}{2}$	360·69	412·26	465·54	520·54	104·85	99·02
$33\frac{1}{2}$	362·08	415·21	470·14	526·55	108·06	102·01
$34\frac{1}{2}$	363·53	418·37	474·89	532·88	111·36	104·96
$35\frac{1}{2}$	365·18	421·56	479·69	—	114·51	107·95
$36\frac{1}{2}$	366·94	424·85	484·63	545·86	117·69	110·97
$37\frac{1}{2}$	368·72	428·32	489·70	552·43	120·98	113·97
$38\frac{1}{2}$	370·66	431·84	494·81	559·16	124·15	116·95
$39\frac{1}{2}$	372·75	435·48	500·08	566·12	127·33	119·96
$40\frac{1}{2}$	374·85	439·17	505·39	573·02	130·54	122·91
$41\frac{1}{2}$	377·17	443·15	510·92	580·20	133·75	125·77
$42\frac{1}{2}$	379·62	447·12	516·57	587·35	136·95	128·76
$43\frac{1}{2}$	382·06	451·25	522·25	—	140·19	131·87
$44\frac{1}{2}$	384·70	455·39	528·04	—	143·34	134·78
$45\frac{1}{2}$	385·47	459·75	534·00	—	146·43	137·68
$46\frac{1}{2}$	390·36	464·18	540·03	—	149·67	140·59
$47\frac{1}{2}$	393·31	468·78	546·20	—	153·89	143·57
$48\frac{1}{2}$	396·46	473·49	552·53	—	156·07	146·53
$49\frac{1}{2}$	399·67	478·35	558·84	—	159·17	149·44
$50\frac{1}{2}$	403·09.	483·23	565·38	—	162·29	152·34
$51\frac{1}{2}$	406·51	488·23	571·99	—	165·48	155·35
$52\frac{1}{2}$	410·03	493·33	578·73	—	168·70	158·33
$53\frac{1}{2}$	413·66	498·65	585·58	—	171·92	161·19
$54\frac{1}{2}$	417·54	504·06	—	—	—	164·15
$55\frac{1}{2}$	421·43	509·66	—	—	—	—
$56\frac{1}{2}$	425·47	515·12	—	—	—	—
$57\frac{1}{2}$	429·51	520·90	—	—	—	—
$58\frac{1}{2}$	433·86	526·69	—	—	—	—
$59\frac{1}{2}$	438·25	532·68	—	—	—	—
$60\frac{1}{2}$	442·57	538·72	—	—	—	—

Table 4. (1, 0) band at λ 2396

$^2\Sigma \rightarrow {}^2\Pi_{1\frac{1}{2}}$

J''	$^0P_{12}$	P_2	Q_2	R_2	$\Delta_2T_2'(J)$	$\Delta_2T_2''(J)$
$1\frac{1}{2}$	—	—	41753·66	—	—	—
$2\frac{1}{2}$	—	—	754·70	—	—	—
$3\frac{1}{2}$	41744·59	—	755·75	—	—	—
$4\frac{1}{2}$	742·42	41748·96	757·07	41766·74	17·78	—
$5\frac{1}{2}$	740·58	748·59	758·27	769·53	20·94	—
$6\frac{1}{2}$	738·74	—	759·58	772·49	—	21·45
$7\frac{1}{2}$	736·85	748·08	760·98	775·46	27·38	21·41
$8\frac{1}{2}$	735·27	748·08	762·55	778·60	30·52	27·38
$9\frac{1}{2}$	733·61	748·08	764·12	781·87	33·79	30·52
$10\frac{1}{2}$	732·09	748·08	765·86	785·06	36·98	—
$11\frac{1}{2}$	730·74	—	767·69	788·55	—	36·47
$12\frac{1}{2}$	729·30	748·59	769·46	791·96	43·37	39·59
$13\frac{1}{2}$	728·04	748·96	771·47	795·44	46·48	42·58
$14\frac{1}{2}$	726·90	749·38	773·37	799·12	49·74	45·62
$15\frac{1}{2}$	725·77	749·82	775·60	802·88	53·06	48·69
$16\frac{1}{2}$	724·72	750·43	777·70	806·56	56·13	51·84
$17\frac{1}{2}$	723·77	751·10	780·01	810·48	59·38	54·64
$18\frac{1}{2}$	722·99	751·92	782·42	814·47	62·55	57·87
$19\frac{1}{2}$	722·12	752·61	784·71	818·49	65·88	60·91
$20\frac{1}{2}$	721·46	753·56	787·39	822·65	69·09	63·86
$21\frac{1}{2}$	720·90	754·63	789·93	826·84	72·21	66·90
$22\frac{1}{2}$	720·38	755·75	792·67	831·05	75·30	69·97
$23\frac{1}{2}$	720·03	756·87	795·27	835·51	78·64	73·04
$24\frac{1}{2}$	719·68	758·01	798·34	839·97	81·96	75·93
$25\frac{1}{2}$	—	759·58	801·24	844·53	84·95	78·99
$26\frac{1}{2}$	719·16	760·98	804·18	849·08	88·10	82·18
$27\frac{1}{2}$	719·16	762·35	807·35	853·81	91·46	84·96
$28\frac{1}{2}$	719·16	764·12	810·53	858·54	94·42	88·12
$29\frac{1}{2}$	719·16	765·69	813·78	863·45	97·76	90·93
$30\frac{1}{2}$	—	767·61	817·30	868·53	100·92	94·09
$31\frac{1}{2}$	719·68	769·36	820·67	873·54	104·18	97·26
$32\frac{1}{2}$	720·03	771·27	824·23	878·58	107·31	100·17
$33\frac{1}{2}$	720·38	773·37	827·79	883·79	110·42	103·12
$34\frac{1}{2}$	720·90	775·46	831·59	889·10	113·64	106·15
$35\frac{1}{2}$	721·46	777·64	835·25	894·50	116·86	109·19
$36\frac{1}{2}$	722·12	779·91	839·27	900·02	120·11	112·23
$37\frac{1}{2}$	722·99	782·27	843·15	905·47	123·20	115·31
$38\frac{1}{2}$	723·77	784·71	847·25	911·14	126·43	118·18
$39\frac{1}{2}$	724·72	787·29	851·28	916·98	129·69	121·36
$40\frac{1}{2}$	725·77	789·78	855·62	922·61	132·83	124·41
$41\frac{1}{2}$	726·90	792·57	859·96	928·62	136·05	127·24
$42\frac{1}{2}$	728·21	795·37	864·15	934·39	139·02	130·28
$43\frac{1}{2}$	729·60	798·34	868·82	940·59	142·25	133·08
$44\frac{1}{2}$	730·82	801·31	873·26	946·70	145·39	136·31
$45\frac{1}{2}$	732·39	804·28	878·01	953·04	148·76	139·27
$46\frac{1}{2}$	733·96	807·43	882·56	959·20	151·77	142·29
$47\frac{1}{2}$	735·53	810·75	887·57	965·54	154·79	145·13
$48\frac{1}{2}$	737·27	814·07	892·25	972·06	157·99	148·14
$49\frac{1}{2}$	739·10	817·40	897·43	978·58	161·18	151·17
$50\frac{1}{2}$	741·11	820·89	902·20	985·20	164·31	154·18
$51\frac{1}{2}$	743·02	824·40	907·67	992·07	167·67	157·05
$52\frac{1}{2}$	745·20	828·15	912·65	998·86	170·71	160·28
$53\frac{1}{2}$	747·38	831·75	918·21	42005·74	173·95	163·09
$54\frac{1}{2}$	749·64	835·77	923·48	012·63	176·86	166·12
$55\frac{1}{2}$	751·92	839·62	928·93	019·69	180·07	169·02
$56\frac{1}{2}$	754·53	843·61	934·59	026·93	183·32	171·96
$57\frac{1}{2}$	—	847·73	940·28	034·00	186·27	174·96
$58\frac{1}{2}$	—	851·97	945·91	041·42	189·45	177·76
$59\frac{1}{2}$	—	856·26	951·98	—	—	180·78
$60\frac{1}{2}$	—	860·64	—	—	—	—

Table 4 (*cont.*)

$^2\Sigma \rightarrow {}^2\Pi_{\frac{1}{2}}$

J''	P_1	Q_1	R_1	$^sR_{21}$	$\Delta_2T_1'(J)$	$\Delta_2T_1''(J)$
$2\frac{1}{2}$	—	—	—	41981·58	—	—
$3\frac{1}{2}$	41965·01	—	41976·25	984·22	11·24	—
$4\frac{1}{2}$	962·99	—	977·44	987·05	14·45	15·25
$5\frac{1}{2}$	961·00	—	978·76	989·96	17·76	18·24
$6\frac{1}{2}$	959·20	—	980·18	992·95	20·97	21·27
$7\frac{1}{2}$	957·49	41968·71	981·58	996·11	24·09	24·31
$8\frac{1}{2}$	955·86	968·71	983·18	999·23	27·32	27·31
$9\frac{1}{2}$	954·27	968·71	984·83	42002·57	30·56	30·32
$10\frac{1}{2}$	952·86	—	986·59	005·74	33·73	33·37
$11\frac{1}{2}$	951·46	—	988·45	009·45	36·99	36·37
$12\frac{1}{2}$	950·22	—	990·39	012·98	40·17	39·46
$13\frac{1}{2}$	948·99	—	992·33	016·51	43·34	42·45
$14\frac{1}{2}$	947·94	970·40	994·54	020·31	46·60	45·45
$15\frac{1}{2}$	946·98	971·00	996·74	024·06	49·86	48·54
$16\frac{1}{2}$	946·00	971·65	999·03	027·81	53·03	51·52
$17\frac{1}{2}$	945·22	972·49	42001·34	031·79	56·12	54·51
$18\frac{1}{2}$	944·52	973·25	003·85	036·02	59·33	57·63
$19\frac{1}{2}$	943·81	974·30	006·46	040·11	62·65	60·53
$20\frac{1}{2}$	943·27	975·31	009·08	044·51	65·81	63·63
$21\frac{1}{2}$	942·83	976·47	011·82	048·76	68·99	66·60
$22\frac{1}{2}$	942·48	977·70	014·74	053·09	72·26	—
$23\frac{1}{2}$	—	979·01	017·57	057·69	—	—
$24\frac{1}{2}$	—	980·42	020·65	062·37	—	75·70
$25\frac{1}{2}$	941·87	981·95	023·75	067·13	81·88	78·78
$26\frac{1}{2}$	941·87	983·51	026·93	071·85	85·06	—
$27\frac{1}{2}$	—	985·20	030·20	076·81	—	—
$28\frac{1}{2}$	—	987·05	033·57	081·61	—	87·72
$29\frac{1}{2}$	942·48	988·85	030·10	086·73	94·62	90·74
$30\frac{1}{2}$	942·83	990·92	040·64	091·87	97·81	93·83
$31\frac{1}{2}$	943·27	992·84	044·25	097·19	100·98	96·83
$32\frac{1}{2}$	943·81	995·10	048·05	102·50	104·34	99·73
$33\frac{1}{2}$	944·52	997·28	051·85	107·95	107·33	102·83
$34\frac{1}{2}$	945·22	999·60	055·75	113·50	110·53	105·85
$35\frac{1}{2}$	946·00	42001·94	059·73	119·10	113·73	108·77
$36\frac{1}{2}$	946·98	004·51	063·91	124·68	116·93	111·79
$37\frac{1}{2}$	947·94	007·05	068·13	130·53	120·19	114·92
$38\frac{1}{2}$	948·99	009·78	072·41	136·48	123·22	117·81
$39\frac{1}{2}$	950·32	012·63	076·81	142·34	126·49	120·58
$40\frac{1}{2}$	951·63	015·45	081·24	148·43	129·61	123·77
$41\frac{1}{2}$	953·04	018·49	085·84	154·60	132·80	126·79
$42\frac{1}{2}$	954·45	021·43	090·37	160·65	135·92	129·81
$43\frac{1}{2}$	956·03	024·62	095·23	—	139·20	132·75
$44\frac{1}{2}$	957·72	027·86	100·02	—	142·30	135·59
$45\frac{1}{2}$	959·44	031·25	104·98	—	145·34	138·62
$46\frac{1}{2}$	961·40	034·60	109·95	—	148·55	141·67
$47\frac{1}{2}$	963·31	038·17	115·05	—	151·74	144·58
$48\frac{1}{2}$	965·37	041·80	120·20	—	154·83	147·57
$49\frac{1}{2}$	967·48	045·47	125·56	—	158·08	150·60
$50\frac{1}{2}$	969·60	049·36	130·89	—	161·29	153·50
$51\frac{1}{2}$	972·06	053·25	136·39	—	164·33	156·53
$52\frac{1}{2}$	974·36	057·14	141·90	—	167·54	159·47
$53\frac{1}{2}$	976·92	061·21	147·58	—	170·66	162·44
$54\frac{1}{2}$	979·46	065·45	153·31	—	173·85	165·38
$55\frac{1}{2}$	982·30	069·70	—	—	—	168·38
$56\frac{1}{2}$	984·93	074·33	—	—	—	—
$57\frac{1}{2}$	987·93	078·76	—	—	—	—
$58\frac{1}{2}$	990·92	083·19	—	—	—	—
$59\frac{1}{2}$	994·01	087·97	—	—	—	—
$60\frac{1}{2}$	997·10	092·58	—	—	—	—

621.317.755

TIME-MARKING A CATHODE-RAY OSCILLOGRAPH BY HARMONICS

By L. F. RICHARDSON, M.A., D.Sc., F.Inst.P., F.R.S.

Received September 6, 1934. *Read in title December* 7, 1934.

ABSTRACT. A docile time-marker was arranged in which the oscillograph acted also as a triode giving retroaction in a tuned circuit where one of the harmonics of the trace-frequency was selected and applied to the Wehnelt cylinder so as to modulate the focus of the trace.

§ 1. GENERAL DESCRIPTION

A former paper[1] described time-marks made by periodically unfocusing the electron beam by applying an oscillating potential to the cylindrical shield which surrounds the filament of the oscillograph. The time-marking potential was produced by a triode oscillator of an ordinary kind. It subsequently occurred to me that the oscillograph might itself serve as a triode. The circuit shown in figure 1 proved to be extremely convenient, after various difficulties had been overcome in the way that will be described.

The Wehnelt shield G of the oscillograph behaved like the grid of a triode, controlling the anode current, so as to produce retroaction; but of course its potential to the filament is of the opposite sign to that in a triode. No special coupling was introduced between the phenomenon and time-marking circuit. There is however inevitably a small capacitance-coupling inside the oscillograph and at its base.

In the previous method, where a quite independent oscillator was used to interrupt the trace, the ratio of the two frequencies, that of the time-marker and that of the phenomenon, had to be very accurately adjusted in order to hold the time-marks steady enough for photography. A change in the ratio of frequencies changed the speed of the marks and they were apt to race so fast as to become invisible. That is to say, the previous arrangement behaved like a stroboscope.

The present apparatus has several types of actual or possible behaviour. *Type I.* If retroaction could be made sufficient to maintain free oscillation of the circuit NK, we should presumably have again the headstrong stroboscopic behaviour of the independent oscillator. *Type II.* Actually retroaction has been just not enough for steady free oscillations, and the behaviour of the apparatus was correspondingly docile. The time-marks never moved too fast to be seen. When the frequency of either the light-spot or the time-marker has been slightly changed, and left so, the marks have not acquired a new speed, they have acquired a new stationary position and sometimes a new distinctness. This steadiness is a great advantage for photography.

The advantage however is not all in favour of a time-marker with a decrement; for the greatest attainable number of time-marks on the trace has been much smaller,

only 15; whereas with steady free oscillation 196 were attained. The greatest number of marks obtainable with the circuit of figure 1 appeared to be dependent on the highest harmonic in the voltages applied to the deflector plates; for when these

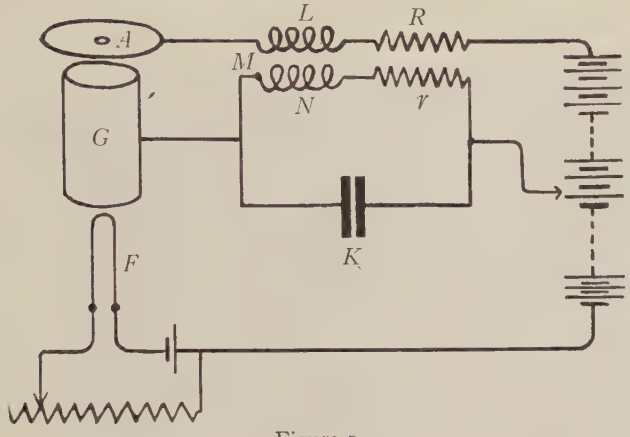

Figure 1.

voltages were pure sine waves only one blur could be obtained on the trace. The finest attainable subdivision of time is thus automatically almost sufficient to analyse the finest detail in the phenomenon.

There are two varieties of type II depending on whether there is a jerk at one part of the trace or not. A jerk in a periodic phenomenon can of course be analysed by Fourier methods into harmonics. Nevertheless there is something in the relations between the phases and amplitudes of the successive harmonics which distinguishes a jerk from a ripple.

Variety II A. The free oscillation of the time-marker was damped, but it was started once in every period of the phenomenon by a jerk, and decreased during the rest of the period. This is shown in plate I, figure 1 which consists of three oscillograms superposed, the time-marker frequency being 11 times that of the trace for one oscillogram, $11\frac{1}{2}$ for the next, and 12 times for the last. The light-spot travelled in the sense $\alpha\beta\gamma\delta\epsilon$ completing the circuit 1821 times per sec. The exposure was about 15 sec. The thinness of the trace between α and β shows that the spot was moving at its fastest there. A time-mark, a blur, stands near γ; and however the capacitance K was varied there always was a time-mark near γ. As the capacitance K was increased the marks spread along the trace $\gamma\delta\epsilon$, the mark near γ remaining almost stationary, the others being more displaced as they were farther along the trace. The conspicuousness of the marks decreased from δ to ϵ and from ϵ to α. This indicates that the rapid portion $\alpha\beta$ acted like an electrical jerk in starting the oscillation in the circuit NK; and that the circuit NK was oscillating with a decrement.

On reversal of the sign of the mutual inductance M by turning over of one coil, the marks became much feebler on $\delta\epsilon$ though still plain on $\gamma\delta$. This showed that the oscillograph had indeed been giving retroaction, which had tended to maintain the oscillations started by the jerk. As the capacitance K in the time-marker was con-

tinuously varied, the blurs not only moved along the trace but periodically waxed and waned in distinctness. The values of K producing maxima of distinctness were found to be those for which the time-marker-frequency was an integral multiple of the trace-frequency.

Variety II B. The free oscillation of the time-marker was damped; the oscillation applied to the deflector plates contained harmonics, but no conspicuous jerk. Figure 2 of the plate shows, superposed, three oscillograms in which the light-spot travelled in the clockwise sense 9800 times per sec. The frequency of the time-marker was severally 5, $5\frac{1}{2}$ and 6 times that of the trace.

When the frequency of the time-mark has been changed, all the marks have taken up new positions. Unlike variety II A, variety II B gave no stationary mark. Certain tuning-capacitances K gave marks which were specially conspicuous, and these values of K corresponded to harmonics of the trace-frequency. This was shown by plotting G. W. O. Howe's well-known diagram[2] of K against n^{-2} where n is the number of blurs on the trace. The points lay nearly on a straight line.

The frequency of the time-marks was thus obtained as a whole multiple of the known frequency of the trace. In this way the condenser K was calibrated for frequency. On account of self-capacitance, and of the coupling M L-N, the values of K and N determined at low frequencies had to be regarded as giving merely a rough check on the time-marking frequency.

To produce satisfactory marks, the shield voltage was first adjusted by battery so that the trace was slightly blurred. When the oscillatory voltage of the circuit K-N was superposed some parts of the trace went into focus, other parts became more blurred. The amplitude of the time-marking voltage was estimated by altering the superposed steady voltage of the focusing battery until the time-marks alternately appeared and disappeared; and was thus found to be about 1 V. As this is a small fraction of the range of good focus, it is certain that there was one blur, not two, in each complete oscillation of the time-marking voltage.

To avoid any appreciable deflection of the cathode-rays by the stray field from the time-marking coils it was found to be quite sufficient to remove the coils to a distance of 1 m. from the tube and to orient them so that the electrons moved along the lines of magnetic force, for the central ray. The particulars thus far given may suffice to justify the results obtained by this method and set out in another memoir.

§ 2. FURTHER PARTICULARS

This section is appended for those who wish to use the method in the laboratory.

Coils. Some guidance as to the kind of coils required for L and N was provided by the well-known theory[2] of the maintenance of oscillations in the similar circuit having a triode instead of an oscillograph. For maintenance or growth,

$$M \geqslant \frac{rK}{g} \text{ approximately} \qquad \ldots\ldots(1),$$

where M is the mutual inductance and r is the resistance of the condenser plus that of the coil N both at the resonant frequency and $g = \hat{c}u_a / \hat{c}e_g$ in which u_a is the anode

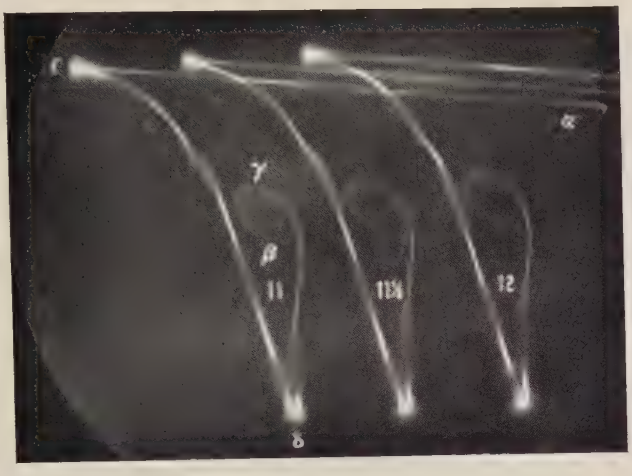

Figure 1.

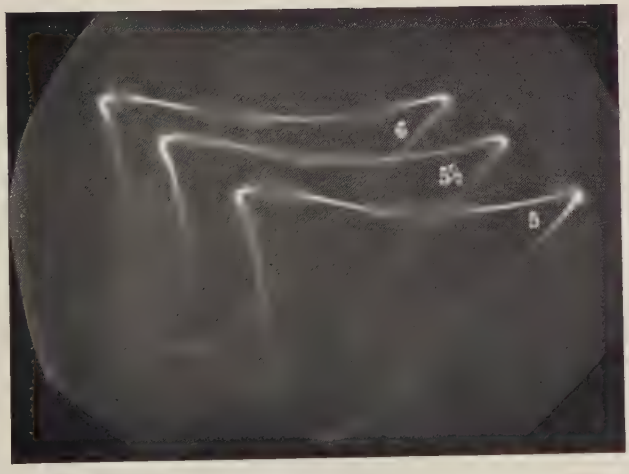

Figure 2.

[*To face p.* 260

current and e_g the potential between grid and filament. In order to increase g it was found beneficial to increase the filament current to 0·93 A. and to decrease the anode voltage e_a to 265 V. This done, g was found to be 7×10^{-5} ampere volt^{-1} for an oscillograph supplied by Standard Telephones and Cables, Ltd. and marked type 4018-A.

Thus g for the oscillograph was of the order of $\frac{1}{30}$ of the g customary in small triodes. Consequently the coils had to have small decrements if the oscillations were to be maintained.

We have by the theory of the tuned circuit at frequency ν,

$$K = \frac{1}{(2\pi\nu)^2 N} \text{ approximately} \qquad \ldots\ldots(2).$$

On elimination of K between (1) and (2),

$$M \geqslant \frac{r}{(2\pi\nu)^2 Ng} \qquad \ldots\ldots(3).$$

If M is unknown we have anyway the restriction

$$\sqrt{(LN)} > M \qquad \ldots\ldots(4).$$

Eliminating M between (3) and (4),

$$\frac{L^{\frac{1}{2}} N^{\frac{3}{2}}}{r} \geqslant \frac{1}{g(2\pi\nu)^2} \qquad \ldots\ldots(5).$$

On substitution of numerical values it was seen that this condition was not easy to satisfy. Suitable coils were either costly to buy or troublesome to make; but unlike triodes and batteries they should last a lifetime.

Several coils were tried for L and N. The frequency required was of the order of 10^4 c./sec. or 10^5 c./sec. Secondaries of old induction coils or slices thereof were useless; they had too low an open-circuit frequency, about 2×10^3 c./sec. and 3×10^3 c./sec. Radio coils, sold for broadcast reception at 2×10^5 c./sec., had too small a time-constant N/r. Best wave-meter coils should do; but actually some coils were made for the purpose, after studying information about self-capacitance and high-frequency resistance given in writings by G. W. O. Howe[5], D. W. Dye[4] and E. B. Moullin[7].

Three particular coils formed serviceable combinations when arranged as explained in the table.

Reference mark	Self inductance at 50 c./sec. (henries)	Open-circuit frequency (c./sec.)	Coil resistance at 10° C.		Resistance r at 9800 c./sec. (Ω.)
			at 0 c./sec. (Ω.)	at 9800 c./sec. (Ω.)	
A = R 33/2	0·124	$4{\cdot}5 \times 10^4$	102	130 ± 5	< 170
B = R 33/3	0·00857	$1{\cdot}5 \times 10^5$	2·4	2·9	3·4
C = Igranic Honeycomb	0·0100	4×10^5 (Makers' value)	23·6		

The inductances were measured by the aid of a Campbell variable mutual inductance. The high-frequency resistances were measured both by distuning and by the added resistance method; as described by Moullin[7]. The dielectric in the condensers was mica or air.

Combination for time-marker frequencies between 10^4 *and* 3×10^4 *c./sec.* Tuning-coil *A*, anode-coil *B*. At the lowest frequency in this range

$$\frac{r}{(2\pi\nu)^2 Ng} < 0{\cdot}0052 \text{ H.},$$

whereas $M = 0{\cdot}0095_5$ H., so that the condition for growth was satisfied at 9800 c. sec., and probably throughout the range of frequency.

Combination for time-marker frequencies between 2×10^4 *and* 10^5 *c./sec.* Tuning-coil *B*, anode-coil *C*. At the lowest frequency in this range, r being estimated as less than 6 ohms,

$$\frac{r}{(2\pi\nu)^2 Ng} < 0{\cdot}000{,}65 \text{ H.},$$

whereas $M = 0{\cdot}001_4$ H. or more. Again the condition for growth was satisfied.

Yet actually, for both combinations, the time-marker oscillated with a decrement. So there must be in the oscillograph some dissipation of energy not occurring in a triode. The high resistance of the return path from the fluorescent screen is conceivably the cause of the dissipation.

Order of connections. A minor difficulty was that when the anode connections were altered while the filament was lit, the anode fuse melted, at 0·1 A. The energy presumably came from the magnetic field of the coil *L*. It was necessary to make the connections in the order opposite to that recommended by the makers[3], putting on the anode volts permanently while the filament was cold and then slowly increasing the filament current. The reverse procedure was adopted for disconnecting.

Focussing battery. For adjusting the battery-voltage on the Wehnelt shield, steps of 1·5 V. were rather large, but 0·5 V. steps were small enough. The latter were provided by placing small accumulators in opposition to dry Leclanché cells.

Intermittent vision. Faint time-marks, which might pass unnoticed if persisting steadily, became clearly visible when the time-marker capacitance *K* was switched repeatedly in and out of resonance.

§ 3. ACKNOWLEDGMENT

This paper is a bye-product of a research for which apparatus was provided by the Government Grant Committee. This loan is gratefully acknowledged.

REFERENCES

(1) L. F. Richardson. *Proc. phys. Soc.* **45**, 135–41 (1933).
(2) L. B. Turner. *Wireless*, pp. 265, 266 (Camb. Univ. Press, 1931).
(3) Standard Telephones and Cables, Ltd. Bulletin G 577/3 "Improved Cathode Ray Oscillograph," Type 4018-A.
(4) D. W. Dye. *Dict. App. Physics*, 2, "Radio Frequency Measurements."
(5) G. W. O. Howe. *J. Instn elect. Engrs*, **60**, 67–72 (1921).
(6) G. W. O. Howe. *Proc. phys. Soc.* (1912) quoted in E. B. Moullin's *Radio Frequency Measurements*, p. 338 (Griffin, 1931).
(7) E. B. Moullin. *Radio Frequency Measurements* (Griffin, 2nd ed., 1931).

551.594.11

IONIZATION CHARTS OF THE UPPER ATMOSPHERE, PART II

By G. MILLINGTON, Marconi's Wireless Telegraph Co., Ltd.

Communicated by Prof. S. Chapman, August 30, 1934. *Read December* 21, 1934.

ABSTRACT. This paper discusses an envelope correction to some ionization charts previously published, and in addition presents the new charts on a circular projection to help in the study of conditions in the polar regions.

§ 1. INTRODUCTION

This paper is in the nature of an appendix to a previous paper, here referred to as "part I," which was published some time ago[1], and is mainly concerned with a small correction to the charts contained therein. It was pointed out that in order to reduce the amount of work to reasonable dimensions the simplifying assumption was made that the density, time (ν, ϕ) curve for the height z_0 at which the noon rate of ionization was a maximum could be taken as the envelope of the system of (ν, ϕ) curves for varying values of the height z. It was realized that the error involved would be greatest in the sunrise region, but it was thought that for the values of the σ_0 chosen, namely 0·5 and 1, the error would not be serious. Detailed comparison of the theoretical charts with experimental data has shown, however, that there is a consistent discrepancy in this critical region, the charts always yielding density-values which are too low. The error introduced by the assumption may thus be greater than was anticipated, and it is important to know whether it is responsible for the whole of the discrepancy or whether there is a residual effect to be accounted for in some other way.

ν, ϕ, z_0

z

It was therefore decided to investigate the problem at least for one set of conditions, e.g. for latitude 60° in winter, where the effect would be most noticeable. Accordingly a number of (ν, ϕ) curves were worked out for different values of z. Now in figure 3 of part I the rate-of-ionization function $F(z, \chi)$ is plotted for a number of values of z, where χ is the zenithal angle of the sun.

F

χ

Actually z is there called z_0 and is expressed in terms of χ_0 by the relation $z_0 = \log_e f(R, \chi_0)$, the curves being drawn for a series of values of χ_0, the noon zenithal angle of the sun. The curves are only drawn for values of χ beyond their respective χ_0 values, and it will be seen that each curve lies entirely outside all the curves for smaller values of χ_0. If, however, the curves are continued backwards it will be found that each curve crosses all the curves before it. For the chosen latitude and season the minimum value of χ is the appropriate value of χ_0, and beyond χ_0 the F curves for values of z smaller than z_0 will all lie inside the z_0

R, χ_0

curve and need not be considered in determining the envelope of the (ν, ϕ) curves; for it is obvious that if the F curves for two values of z do not intersect then the corresponding (ν, ϕ) curves will not intersect either, and we can ignore the inner curve.

Fortunately a little work soon suggested an easy method of making a close approximation to the required envelope, by means of which it was possible to work out the complete modified charts with less labour than the original charts required. The fact already mentioned, that the curves of figure 3 in part I if continued back intersect, suggests that the set of curves has an envelope which passes through the initial points of each of the curves. From equation (1) of part I we have for the form of the function F

$$F = \exp\,[1 - z - \exp\,(-z).f\,(R, \chi)],$$

and the equation $\partial F/\partial z = 0$ for eliminating z to obtain the equation of the envelope gives

$$-1 + \exp\,(-z).f\,(R, \chi) = 0,$$

and on substitution in F for the equation of the envelope,

$$F = \exp\,(-z) = \frac{1}{f\,(R, \chi)}.$$

From equation (7) of part I it follows at once that when $\chi = \chi_0$,

$$F\,(z_0 \chi) = 1/f\,(R, \chi_0),$$

so that the envelope passes through the initial points of the curves of figure 3 of part I, as was anticipated. Now since the function $f\,(R, \chi)$ increases upwards from unity with increasing values of χ, the solution for the envelope is only valid for positive values of z (it being remembered that z is not the actual height h but is referred to a height h_0 as datum level). This corresponds to the easily verified fact that as z increases negatively the F curves lie wholly inside one another, but as they are all inside the curve for $z = 0$ they can be neglected as far as our problem is concerned.

Now if the fundamental differential equation, given in (4) of part I,

$$\sigma_0 \frac{d\nu}{d\phi} + \nu^2 = F,$$

is solved not for a given height z but for the envelope function F or $1/f\,(R, \chi)$, then the (ν, ϕ) curve obtained must lie outside all the possible (ν, ϕ) curves for various values of z. Calculation shows moreover that if it is not the true envelope it is at any rate a very close approximation for widely different conditions of season and latitude, especially in the critical region where the correction is of most importance. Although the mathematical process involved may have no physical justification, it can be seen that the method suggests what in a general way must be true, that as time progresses the position where the maximum density occurs will tend to follow the variation in height at which the rate of ionization is a maximum. Moreover the method suggests a possible interaction between neighbouring regions which may occur as a process of diffusion of ions, and we are

probably not justified in seeking to approximate closer to the envelope of the (ν, ϕ) curves. The modified charts have therefore been worked out on this basis, and thus the labour required is actually reduced owing to the use of a single F curve instead of having to interpolate from a set of $F(z_0\chi)$ curves. In any case the charts now set an upper limit to the theoretical ν values.

§ 2. CALCULATION OF THE CORRECTED CHARTS

Much of the material already obtained and outlined in § 5 of part I can be used, but a graph of the envelope function F or $1/f(R, \chi)$ is needed and is given in figure 1. In the calculations for solving the differential equation, F can be neglected when it is less than 0·001, i.e. when χ is greater than about 102°, but the region between $\chi = 90°$ and 102° is very important, especially in high latitudes in winter when χ_0 itself is large. Now as the curve for F does not take account of the fact that as χ increases above 90° the curvature of the earth cuts off the sun's radiation from the lower regions of the atmosphere, we must verify that in practice the F function does exist at least as far as $\chi = 102°$. If we write $\chi = 90 + \epsilon$ then at a height h the sun's radiation is cut off when ϵ exceeds the limiting value $\epsilon_{max.}$ given by sec $\epsilon_{max.} = 1 + h/R$*, and in figure 2 $\chi_{max.}$ is plotted as a function of h. Although the curve soon settles down to very small increases of $\chi_{max.}$ for large increases of h, χ can be greater than 102° provided that h is greater than 145 km. Since in the construction of the charts we are mainly concerned with the upper or F region of the Heaviside layer, h is actually greater than this value, so that in practice the increased attenuation of the sun's radiation due to the longer path through the earth's atmosphere reduces the F function to a negligible value before the radiation is actually cut off by the curve of the earth.

The solution of the differential equation follows along the lines given in part I and the resulting set of (ν, ϕ) curves is given in figures 3 to 5 where for convenience ϕ has been converted from radians to Greenwich mean time. They are only given for the value $\sigma_0 = 0{\cdot}5$, as experience has shown that this value corresponds with present conditions rather than $\sigma_0 = 1$ as suggested in part I, while it may be useful later to construct charts for $\sigma_0 = 0{\cdot}25$. From these curves ν was plotted as a function of the latitude for a series of values of ϕ as this was found useful for interpolating to obtain the (ν, ϕ) curve for any other latitude and was an aid towards the accurate construction of the charts from the curves. The new charts for $\sigma_0 = 0{\cdot}5$ are given in figures 6 and 7.

Comparison between the new and old charts shows that while the positions of the contour lines of equal density are scarcely changed round mid-day, the region after sunrise where the lines are crowded together and represent the rapid early-morning increase of density is moved noticeably towards the sunrise line. But although in other parts the charts agree well with experimental data there is still some discrepancy in the sunrise region sufficient to suggest that there is an effect not accounted for by the theory.

* R here is of course not Chapman's parameter in $f(R, \chi)$ but the radius of the earth.

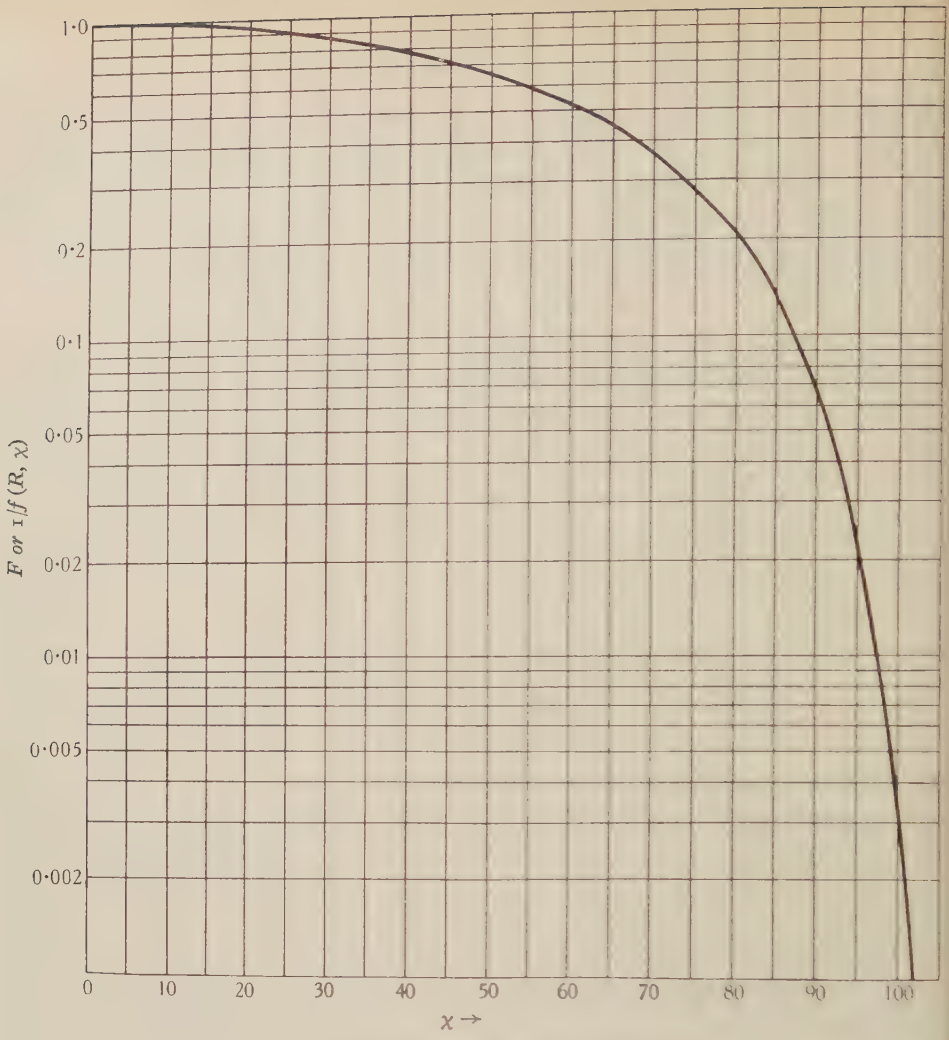

Figure 1. The envelope function F or $1/f(R, \chi)$.

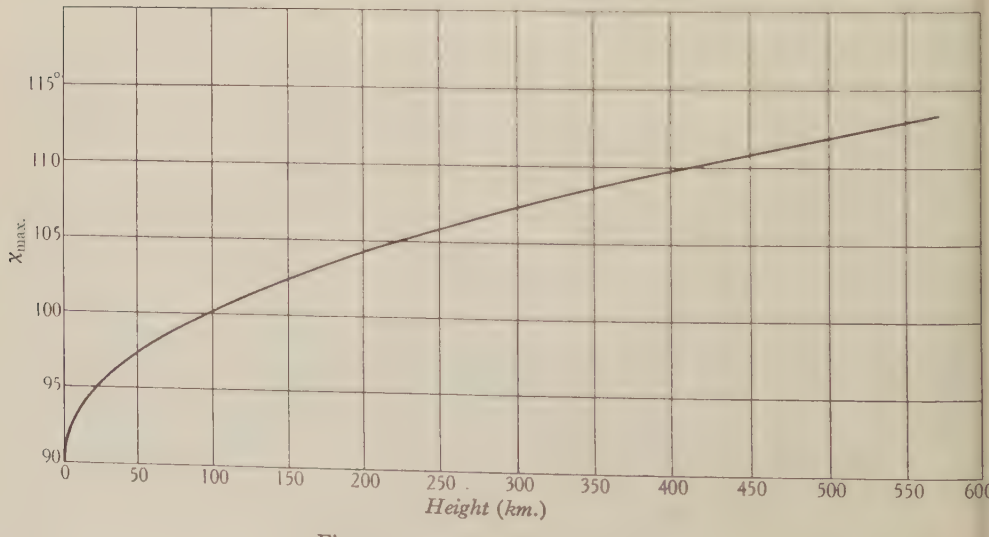

Figure 2. $\chi_{max.}$ as a function of h.

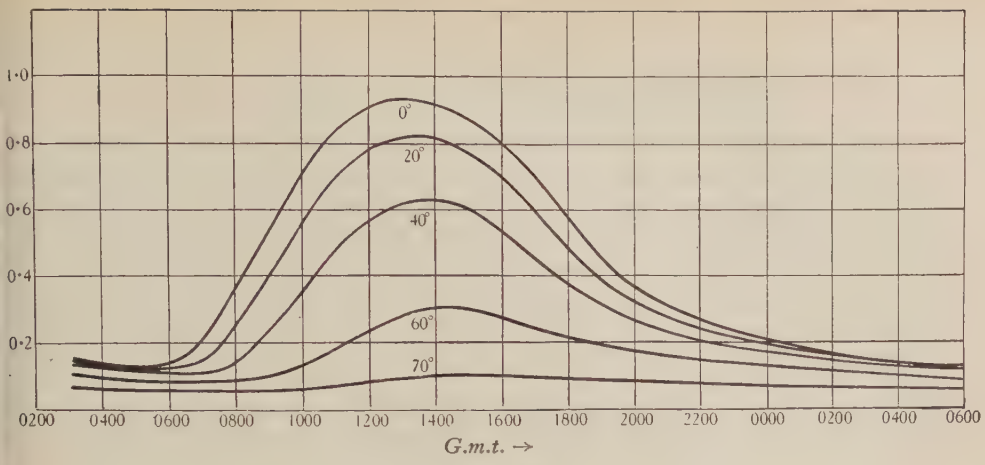

Figure 3. Winter, $\sigma_0 = 0{\cdot}5$. Latitudes 0, 20, 40, 60, 70°.

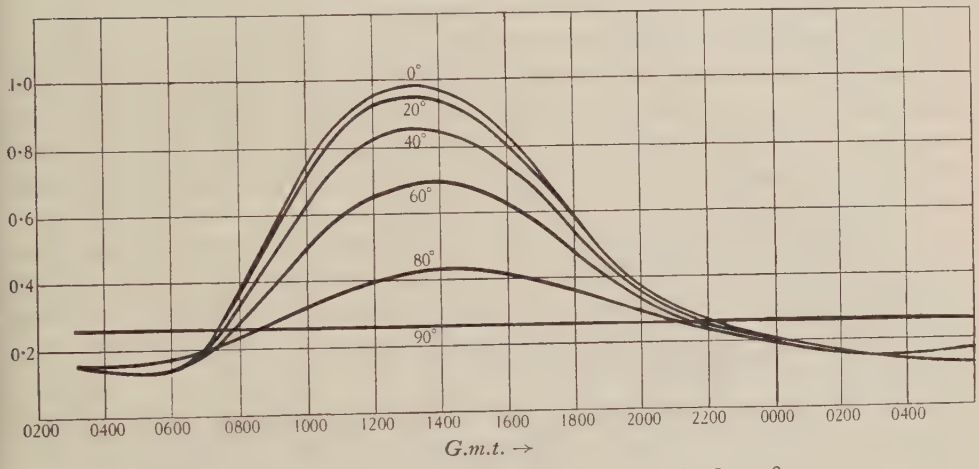

Figure 4. Equinox, $\sigma_0 = 0{\cdot}5$. Latitudes 0, 20, 40, 60, 80, 90°.

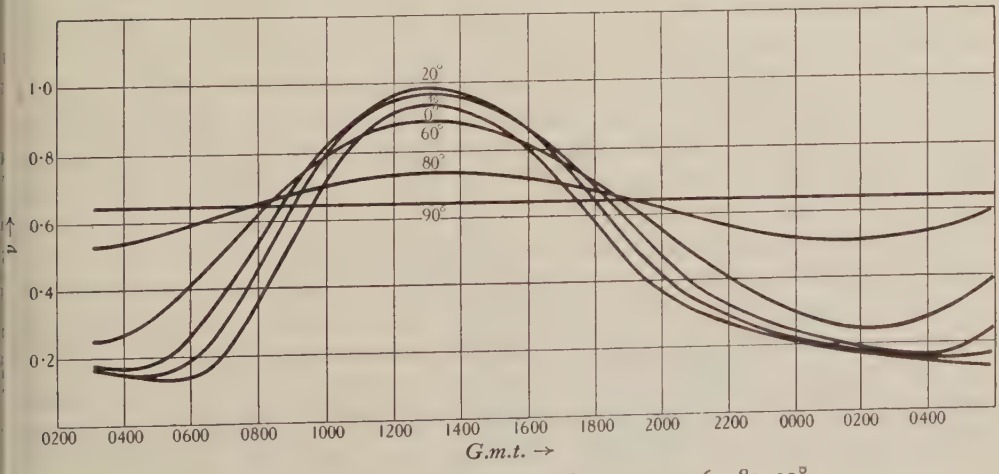

Figure 5. Summer, $\sigma_0 = 0{\cdot}5$. Latitudes 0, 20, 40, 60, 80, 90°.

§ 3. A POLAR PROJECTION OF THE CHARTS

The charts so far have been constructed in conjunction with a Mercator projection of the world, and there are two great advantages in using this projection to study short-wave long-distance transmission problems with the aid of such charts. Firstly the projection is conformal, i.e. small areas are shown undistorted and true bearings are indicated, and secondly it lends itself to a very convenient method of studying the change in ionization along any given route with change of local time at some fixed place by merely moving the chart parallel to its length from east to west. There are, however, two serious drawbacks to the Mercator projection. Firstly there is the linear distortion which increases rapidly as one proceeds to high latitudes and gives quite a false impression of the relative lengths in the various grades of density of the chart for any route running more or less from north to south. Arising from this we have secondly the complete break-down of the projection in the polar regions, where the charts fail to give any true idea of what happens to the contour lines of equal density over the polar cap. In order therefore to study the conditions along great-circle routes which pass near to the poles, e.g. round-the-world echoes on the London-to-Capetown route, and in view of the present interest in experimental work carried out in the polar regions, it seemed advisable to supplement the existing charts with others constructed according to some form of circular projection with the pole as centre.

In any such projection the process of moving the chart across the map transforms into a rotation about the pole, but obviously we shall need a separate map for each hemisphere. Adopting the usual convention and drawing the maps so that a journey eastward along a line of latitude in the southern hemisphere is represented by a clockwise direction, as opposed to a counter clockwise direction in the northern hemisphere, it will be seen that the equinox chart for the southern hemisphere is the mirror image of the equinox chart for the northern hemisphere, while the southern chart for the December solstice is the mirror image of the northern chart for the June solstice and vice versa. The rotation of the earth is represented by rotating the maps in opposite directions as if they were geared together so that they always touch at corresponding places on the equator. To study the conditions along any north-to-south route the maps are fixed so that they touch at the point where the route crosses the equator and the route appears unbroken as it passes from one map to the other. The charts are then rotated in opposite directions over the maps, and if necessary some simple mechanism could be devised to gear them together.

The projection which has been chosen for the purpose is the one in which the radius of the circle representing any line of latitude is proportional to $\tan \frac{1}{2}\theta$ where θ is the colatitude, since this is the only circular projection which is conformal. It is the stereographic projection used largely in crystallography, and as is well known it has the most useful property that great circles on the sphere which do not pass through the poles project as arcs of circles which terminate on diameters. In addition it is the only projection in which all small circles on the sphere project

as circles. (Of course if the small circle cuts the equator this property only holds if we project the southern hemisphere with respect to the north pole on the same map as the northern hemisphere or vice versa.) This property is useful if we wish to study the ionization at places in relation to their distances from some fixed point other than the pole, e.g. in discussing effects in the neighbourhood of the magnetic pole or the skip-distance phenomena observed at any particular place. The linear distortion with this projection is never more than 2 to 1 and owing to the conformal property is independent of direction. Actually, when referred to the equator as standard, distances in colatitude θ must be multiplied by $1+\cos\theta$, so that it is fairly easy to estimate the true lengths of any route which lie in the various grades of the chart. In practice the size of the map is chosen so that the polar regions where areas are reduced fourfold are represented on a reasonably large scale.

As the projection is well known it is not thought necessary to give here any detailed methods of drawing in circles on it, but the following suggestions may be helpful. If we wish to draw the projection of a small circle of radius δ degrees round the point whose longitude is ϕ and colatitude is θ, the points $(\phi, \theta-\delta)$ and $(\phi, \theta+\delta)$ which can be put on the projection at once by the tan $\frac{1}{2}\theta$ rule will define a diameter of the required circle which can then be constructed from geometrical principles. This holds even if the small circle cuts the equator, but in this case we have in addition the fact that where it cuts the longitude is $(\phi \pm \psi)$ where $\cos\psi = \cos\delta/\sin\theta$. If we wish to draw the great circle joining two points whose longitudes are ϕ_1 and ϕ_2 respectively and whose colatitudes both measured from the north pole are θ_1 and θ_2 respectively, then the great circle cuts the equator at longitudes ϕ and $(\phi+\pi)$ where $\tan\phi = a_2/a_1$

δ

ψ

and $$a_1 = \sin\theta_1 \cos\theta_2 \cos\phi_1 - \sin\theta_2 \cos\theta_1 \cos\phi_2, \qquad a_1$$

while $$a_2 = \sin\theta_1 \cos\theta_2 \sin\phi_1 - \sin\theta_2 \cos\theta_1 \sin\phi_2 \qquad a_2$$

and the nearest points of approach to the poles will be given by $(\phi \pm \frac{1}{2}\pi, \theta_{\text{min.}})$,

where $$\tan\theta_{\text{min.}} = a^{-1} \sin\theta_1 \sin\theta_2 \sin(\phi_2 - \phi_1)$$

and $$a^2 = a_1^2 + a_2^2. \qquad a$$

From these points the circle can be constructed.

Lastly it can be shown that the great circle through any point (θ, ϕ) which makes an angle δ with the great circle passing through the point and the poles cuts the equator at longitude $(\phi \pm \psi)$ where $\tan\psi = \cos\theta \tan\delta$, the sign depending upon the direction in which δ is taken. ψ

The charts for the northern hemisphere for $\sigma_0 = 0{\cdot}5$ are shown in figures 8 to 10 and are based on the corrected charts of figures 6 and 7 with extra contour lines for $\nu = 0{\cdot}13$, $0{\cdot}05$ and $0{\cdot}02$ to give more detail in the polar regions in winter. In figures 11 and 12 are given outline maps of the two hemispheres for use with the charts. The charts show well how little seasonal variation there is on the equator. In summer the minimum density over the hemisphere occurs on the equator about twenty minutes before sunrise and corresponds to $\nu = 0{\cdot}13$. At the

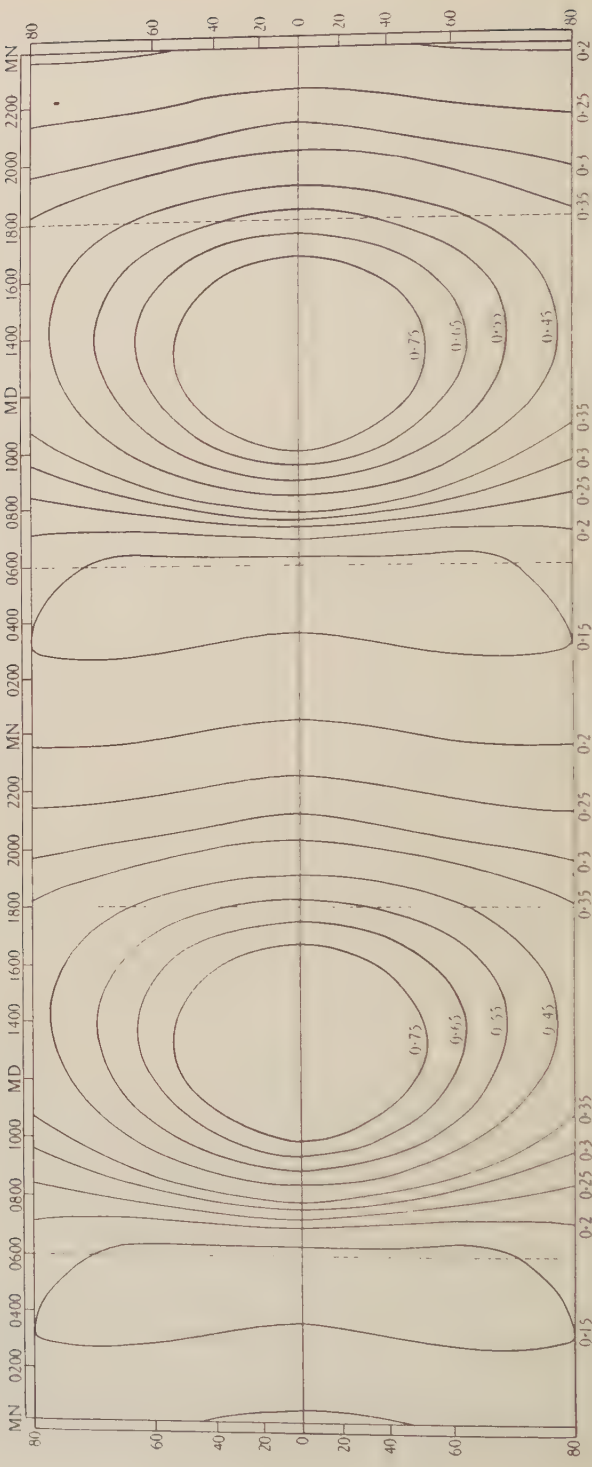

Figure 6. Equinox chart, $\sigma_0 = 0{\cdot}5$.

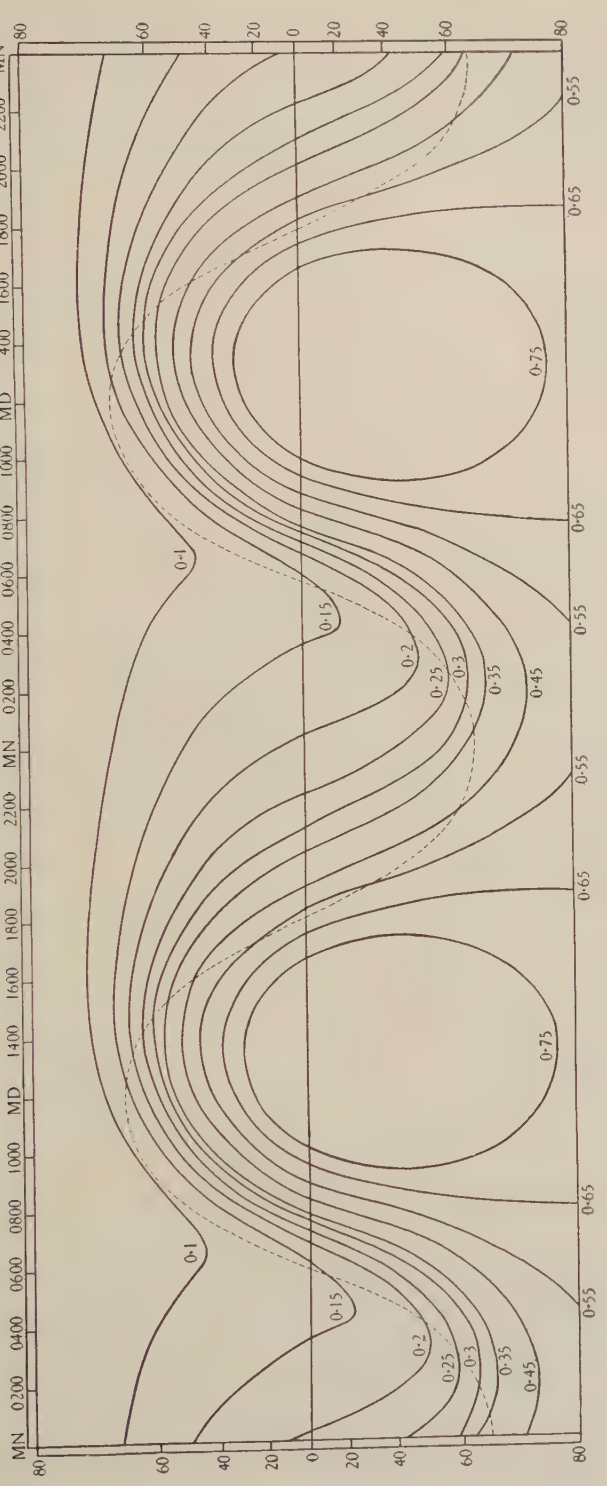

Figure 7. Winter chart, $\sigma_0 = 0{\cdot}5$.

equinox the minimum density is still about 0·13 but it now extends from the equator up to latitude 60°, and is represented in the chart by a single thick line. In winter this line has opened out into a contour which just reaches the equator (corresponding to the summer minimum) and encloses all the polar regions within latitude 68°. The $\nu = 0{\cdot}10$ contour just touches latitude 70° but does not extend

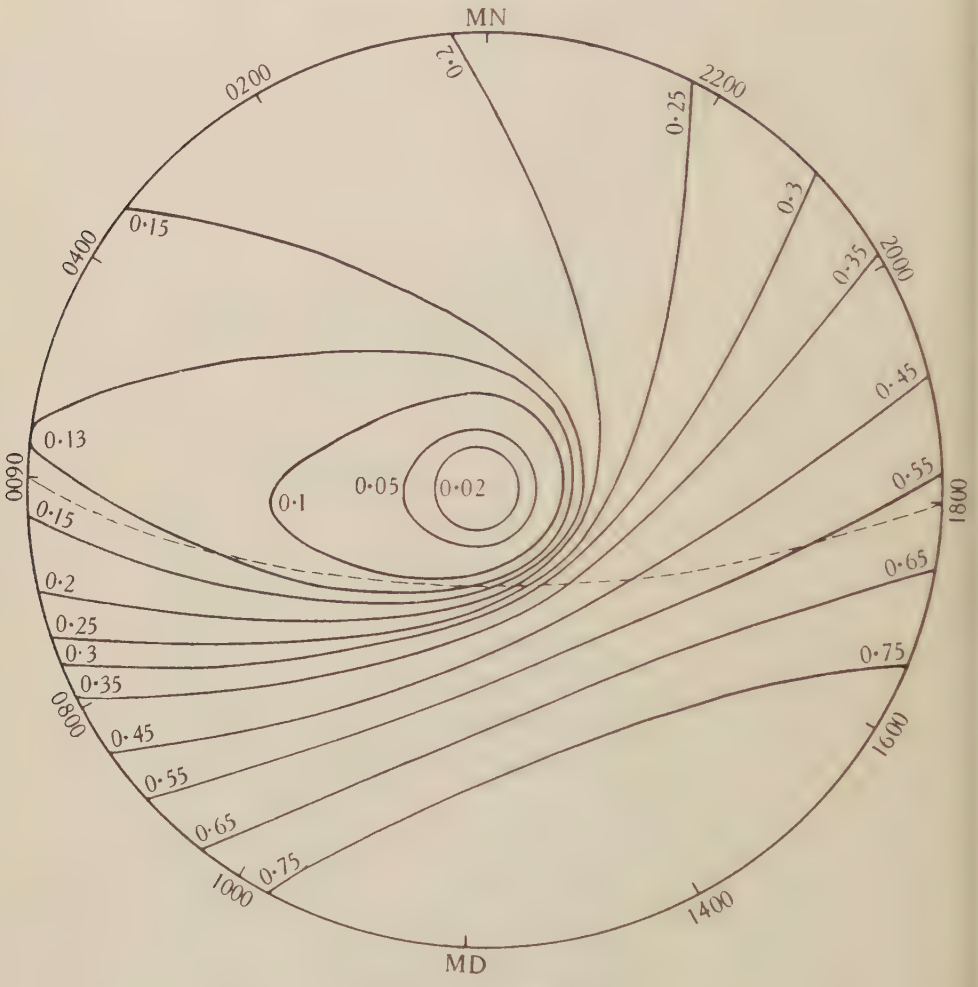

Figure 8. Winter chart, $\sigma_0 = 0{\cdot}5$.

below latitude 40°, while the $\nu = 0{\cdot}05$ contour lies wholly between latitudes 70° and 80°. The $\nu = 0{\cdot}02$ contour is very nearly a circle corresponding to latitude 80°. That the contour lines should approximate to circles for small values of ν can be seen by writing the equation connecting ν_s and ν_r the sunset and sunrise values in the form

$$\frac{\nu_s}{\nu_r} = 1 + \frac{\phi_r - \phi_s}{\sigma_0} \cdot \nu_s,$$

so that even in the long winter night when $\phi_r - \phi_s$ approaches 2π, ν_s/ν_r differs from unity by less than 0·25 when $\nu = 0{\cdot}02$.

The extra contour lines show how rapidly the maximum density decreases in the region of the pole at mid-winter. At the pole itself the ionization is negligible and it is a matter of some importance to know the extent of the polar cap over

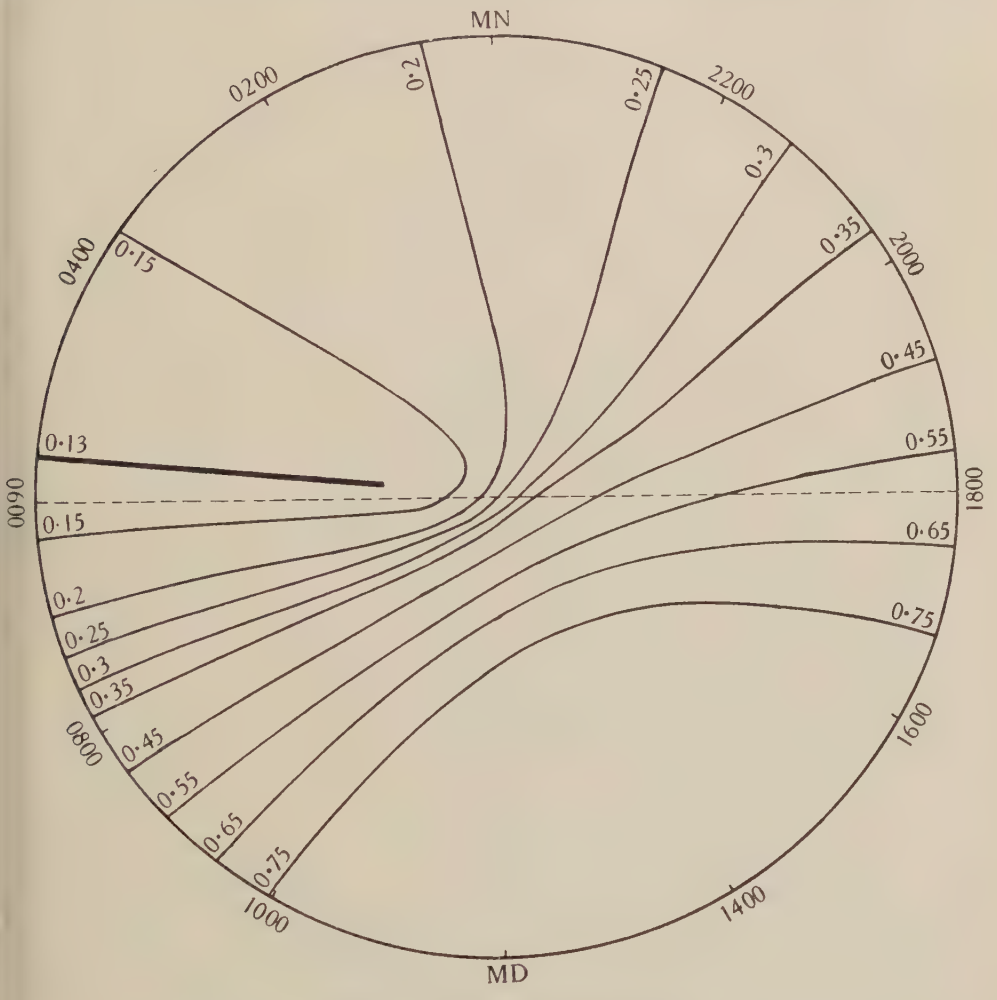

Figure 9. Equinox chart, $\sigma_0 = 0{\cdot}5$.

which there is effectively no ionization and how the area diminishes on either side of the winter solstice. There is no easy way of determining what are the maximum and minimum densities for any given latitude and season, but we can get an approximate solution to the problem by using the fact already mentioned that for small density values the contour lines become nearly circular about the pole, together with the knowledge that at any place where the noon zenithal angle is χ_0 the maximum value of ν must be less than $\sqrt{\{1/f(R, \chi_0)\}}$ except at the pole where

l it is equal to this quantity. Knowing that for a latitude l when the declination of the sun is δ the value of χ_0 is $|\, l-\delta \,|$, we can find at once the upper limit of ν. Thus, as we have seen, ν is about 0·02 at latitude 80° in mid-winter when $\delta = -23{\cdot}5°$, and extrapolation from a graph of $\nu\{1/f(R,\chi)\}$ shows that ν is probably less than 0·01 at latitude 81·5°, less than 0·005 at 83°, and possibly less than 0·001 at

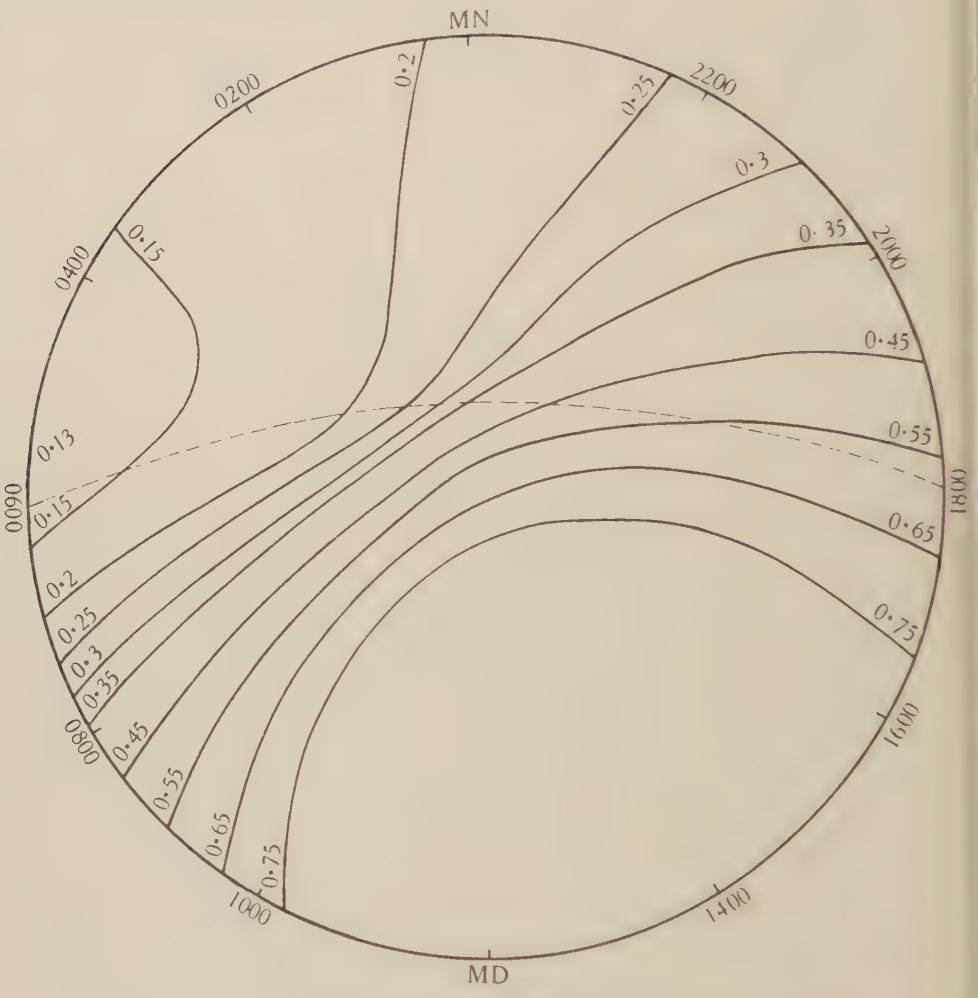

Figure 10. Summer chart, $\sigma_0 = 0{\cdot}5$.

latitude 86°. In considering the effect of the change of season we have to remember that as we move away from mid winter the minimum density does not remain at the pole. The equinox chart shows the way in which the contour lines spread out across the pole until nowhere over the earth's surface does the density fall below $\nu = 0{\cdot}13$. But at first the major effect is the shrinking of the contours of small density into the pole with the contraction and final disappearance of the area of negligible ionization. Now the relation $\chi_0 = |\, l-\delta \,|$ gives an approximate rule that as δ changes from the mid-winter value of $-23{\cdot}5°$ the contours for $\nu < 0{\cdot}02$ close

n to a latitude nearer the pole by the amount of change in δ. Thus when $\delta = -13{\cdot}5^\circ$ he density has everywhere risen above $\nu = 0{\cdot}02$, and this corresponds to a period of about eight weeks on either side of the winter solstice. The density is probably everywhere above $\nu = 0{\cdot}05$ when δ is about -10° since ν becomes $0{\cdot}05$ at the pole when $\delta = -10{\cdot}5^\circ$. In this way the extent and duration of this polar dark area, as we may call it, can be fairly well defined.

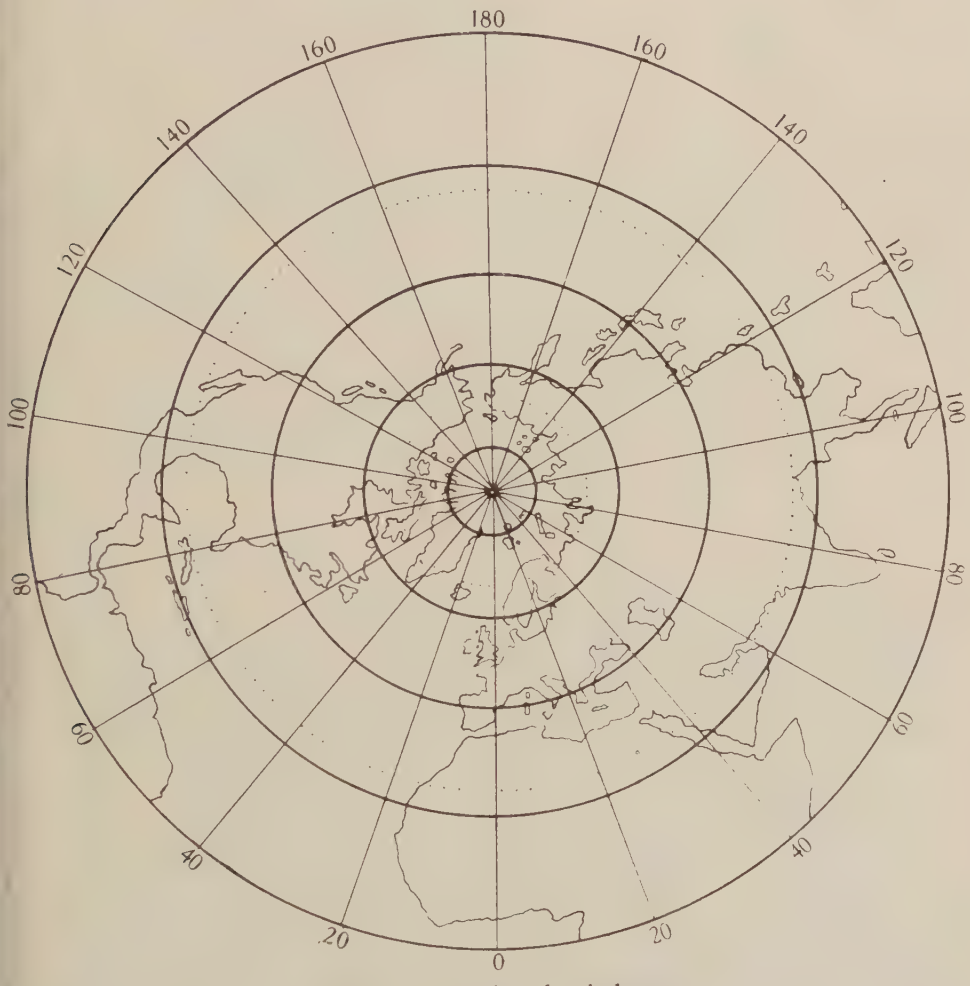

Figure 11. Northern hemisphere.

The significance of this dark area is that it has been worked out on the assumption of ideal theoretical conditions in which it is assumed that there will be no tendency of outside ions to diffuse in towards the pole, and that it implies that at mid-winter short waves could not be transmitted at all on any route crossing this polar area. The theory takes no account of the existence of the earth's magnetic poles and of the large effects which are thereby produced, especially in the northern latitudes into which the electrons from the sun tend to be deflected. Unfortunately the difficulties in the way of making direct observations across the polar cap,

especially in winter, are very great, and it also happens that there are very few long-distance commercial routes which pass near to the pole, but it is useful to have the ideal theoretical conditions as a basis for analysing any available experimental data.

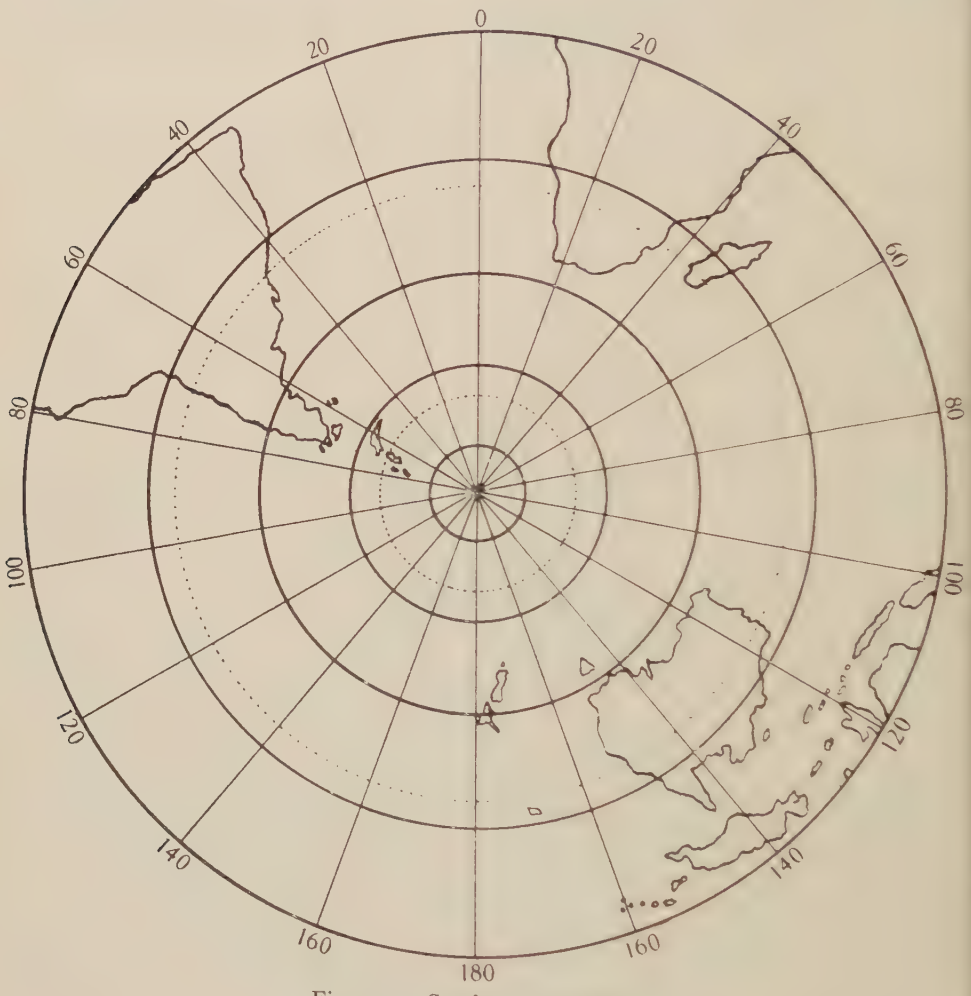

Figure 12. Southern hemisphere.

In conclusion it will be seen that the polar charts give a much better idea of the density conditions over the polar caps than can be obtained from the Mercator projection, and although they are not so convenient they can be used by the method indicated above to study routes which cross the equator. They also give a better idea of the overall daylight attenuation for a route lying in more than one grade and should have a special application in the study of magnetic-storm effects.

REFERENCE

(1) G. Millington. *Proc. phys. Soc.* **44**, 580 (1932).

621.396.615.1

SOME EXPERIMENTS ON ELECTRONIC OSCILLATIONS

By W. A. LEYSHON, Ph.D., F.Inst.P.

Received October 23, 1934. *Read with demonstration December* 21, 1934.

ABSTRACT. The paper gives results of measurements made on the wave-length of the oscillations generated by small triodes using the positive-grid (Barkhausen-Kurz[1]) method, in a fixed oscillatory circuit which, in most of the cases studied, was formed by the valve electrodes and leads. It was found possible, with the grid current emission limited, to express the relation between the generated wave-length λ, the grid voltage v_g, and the plate voltage v_p, by a straight-line graph connecting $(v_g - \mu v_p)$ with λ, where $\mu\left[\left(\frac{dv_g}{dv_p}\right)_{\lambda \text{ const.}}\right]$ was a constant for a particular valve. The results show that μ is constant whatever the value of λ generated by the triode and associated circuit. It is suggested that triodes connected in the manner described might be used as oscillation wave-meters working over a limited range.

§ 1. INTRODUCTION

In some preliminary experiments on electronic oscillations generated by small receiving triodes of the bright-emitter type the effect of joining the electrode leads through a condenser of capacity 0·0005 μF. was noted. The effect was greatest when the condenser was connected to the plate and filament leads, close to the valve. In a particular experiment it was found that the galvanometer deflection when resonance occurred in the wave-meter was increased ten times by connecting the condenser in this way. A large, but not proportionate, increase in the plate current of the valve was noted at the same time. With the condenser in position, oscillations could be obtained with lower filament current than was sufficient without it, other circuit conditions remaining unchanged. A second condenser between the plate and the other end of the filament was found to be a further improvement.

The increased strength of oscillation due to these condensers was illustrated in an experiment made with a Mullard *R* valve. A small flash-lamp bulb was inserted as a resistance in the condenser circuit, figure 1. The conditions were as follows: $V_g = 104$ V., $i_g = 39$ mA., $v_p = 2$ V. With the bulb in, $D = 20$ divisions and $i_p = 120$ divisions. With the bulb removed, $D = 700$ divisions and $i_p = 280$ divisions. These results show that considerable current was flowing in the condenser circuit. With this method of connexion, observations were made of the variation of the generated wave-length with alteration of grid voltage, plate voltage, and filament emission.

For convenience, the various quantities referred to in the paper are represented by symbols as shown below:

v_g v_g is grid voltage and
v_p v_p plate voltage } measured from the negative end of the filament;
v_f v_f is the filament voltage;
i_g i_g the grid current;
Δi_g Δi_g the change in mean grid current due to oscillations;
i_p i_p the plate current;
i_f i_f the filament current;
D D the deflection of the galvanometer at resonance in the wave-meter circuit, and
λ λ the wave-length of the oscillations, while
μ $\mu = \left(\frac{dv_g}{dv_p}\right)_{\lambda \text{ const.}}$

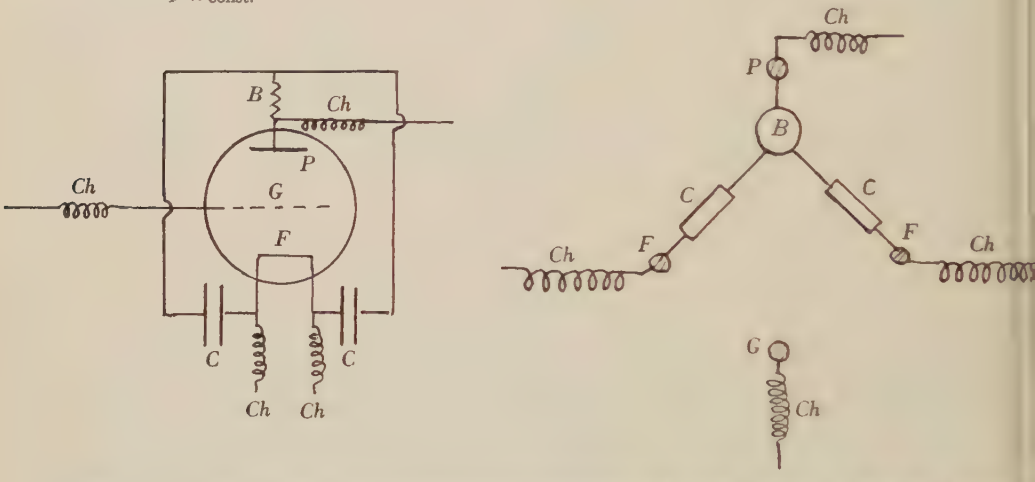

Figure 1. P, plate; G, grid; F, filament; C, C, condensers; Ch, Ch, chokes; B, flash-lamp bulb.

§ 2. DESCRIPTION OF APPARATUS AND EXPERIMENTAL RESULTS

The triodes used were two B.T.H. R valves, one, R_1, having had the pins removed; two Mullard R triodes, of different sizes; a Q valve, an L.S.I. valve, a valve X of R type of unknown manufacture, and a T.M.C. valve with a fixed Lecher-wire circuit attached to grid and anode, and bridged at the end remote from the valve by a condenser of large capacity. Thus experiments were made with triodes differing considerably from each other both in construction and in electrode-spacing.

The wave-meter used was like that described by Chapman[2]. The coupling between the valve circuit and the wave-meter was loose enough for the plate current to be independent of the wave-meter bridge position.

It was found that the relation between grid voltage and wave-length for a particular value of plate voltage was a linear one, and that when the lines were drawn for different values of plate voltage they were parallel. Further, the relation between grid voltage, plate voltage and wave-length could be shown by a single straight line connecting $(v_g - \mu v_p)$ with λ, where μ had a different value for each valve tested.

Some curves showing the straight-line relationship between $(v_g - \mu v_p)$ and λ are shown in figures 2 and 3. The marked values of v_g and v_p indicated on the graph show the wide range of these quantities over which the relationship held in the case of the small Mullard valve, figure 3.

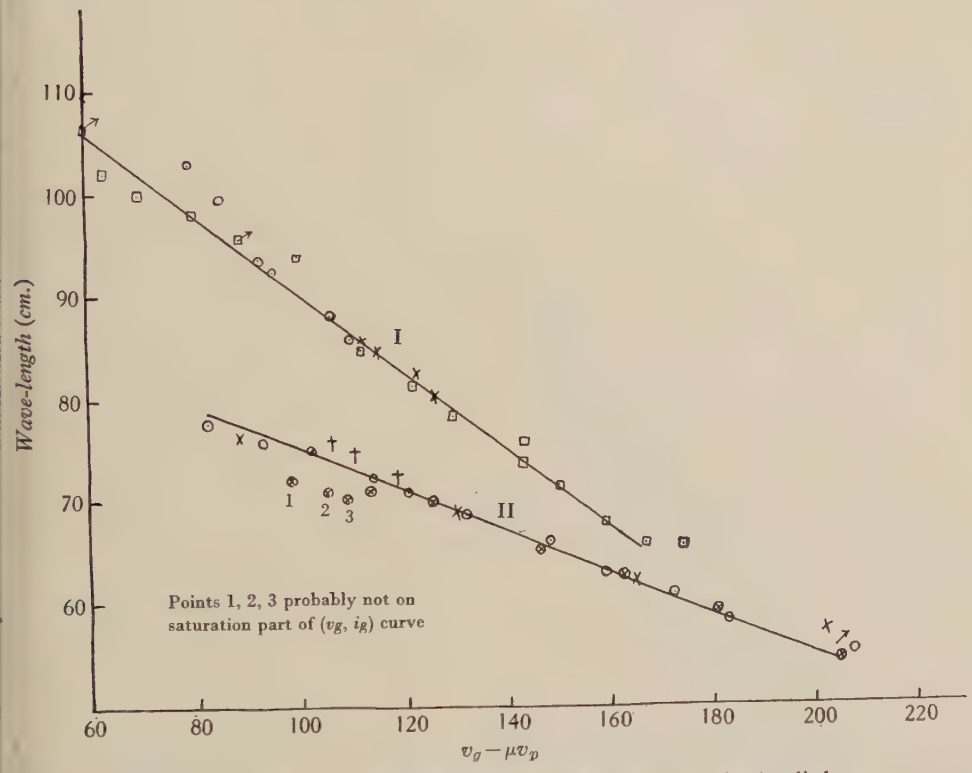

Figure 2. I, B.T.H. *R* valve (R_1) with pins removed, this valve contained a little gas, $\mu = 3{\cdot}33$; ⊡ $v_p = -3$, $i_g = 17$–20 mA.; × $v_g = 100$, $v_p = -2 \rightarrow -8$, $i_g = 20$ mA.; ⊙ $v_g = 80$, $v_p = 0 \rightarrow -9$, $i_g = 20$ mA.; ⊡ $v_p = -3$, $i_g = 10$ mA. II, B.T.H. *R* valve (R_2) with pins left on, $\mu = 2{\cdot}5$; ⊙ $v_p = -3$, $i_g = 20 \rightarrow 34$ mA., blocking condensers 0·0003 mF.; †, × $v_p = -6$, $i_g = 15 \rightarrow 34$ mA., blocking condensers 0·001 mF.; ⊘ $v_p = -11$, $i_g = 16 \rightarrow 30$ mA., blocking condensers 0·0003 mF.; ↗ $v_p = -20$, $i_g = 40$ mA., blocking condensers 0·0003 mF.

A further experiment was made with the valve *X* by means of the circuit of figure 1 without the flash-lamp bulb resistance and with rather long choke coils, on which it was found that there were standing waves of quite considerable amplitude. The circuit was then set up again, the choke coils being omitted completely. The grid lead to the milliammeter was made as short and straight as possible,

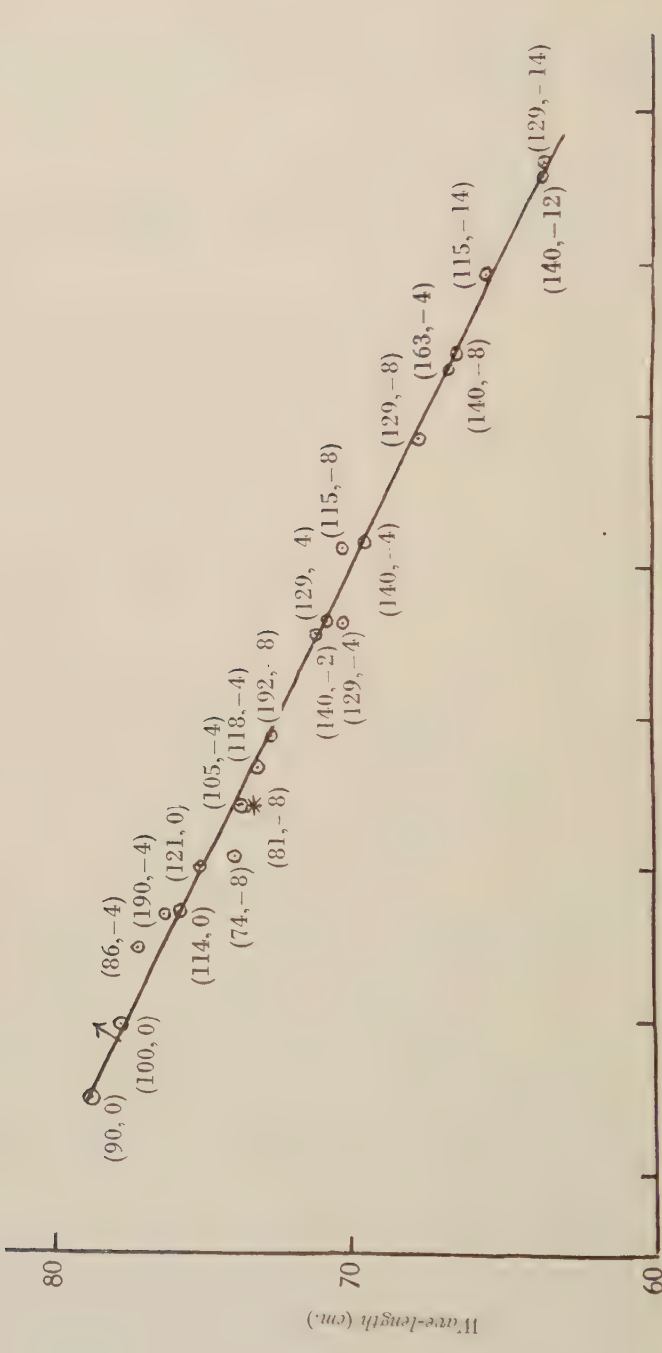

Figure 3. Mullard *R* valve working on saturation part of (τ_0, i_p) curve. Blocking condensers 0·0003 mF. except at * (0·0001 mF.) and ↗ (0·001 mF.).

as also was the anode lead. The latter was run parallel and close to the filament leads. The valve oscillated over about the same range of voltages, but the slope of the $(v_g, \lambda)_{v_p \text{ const.}}$ curve was less. In figure 4 are shown curves connecting $(v_g - \mu v_p)$ with λ for these conditions. The value of $\mu \left[\left(\frac{dv_g}{dv_p}\right)_{\lambda \text{ const.}}\right]$ was, as would be

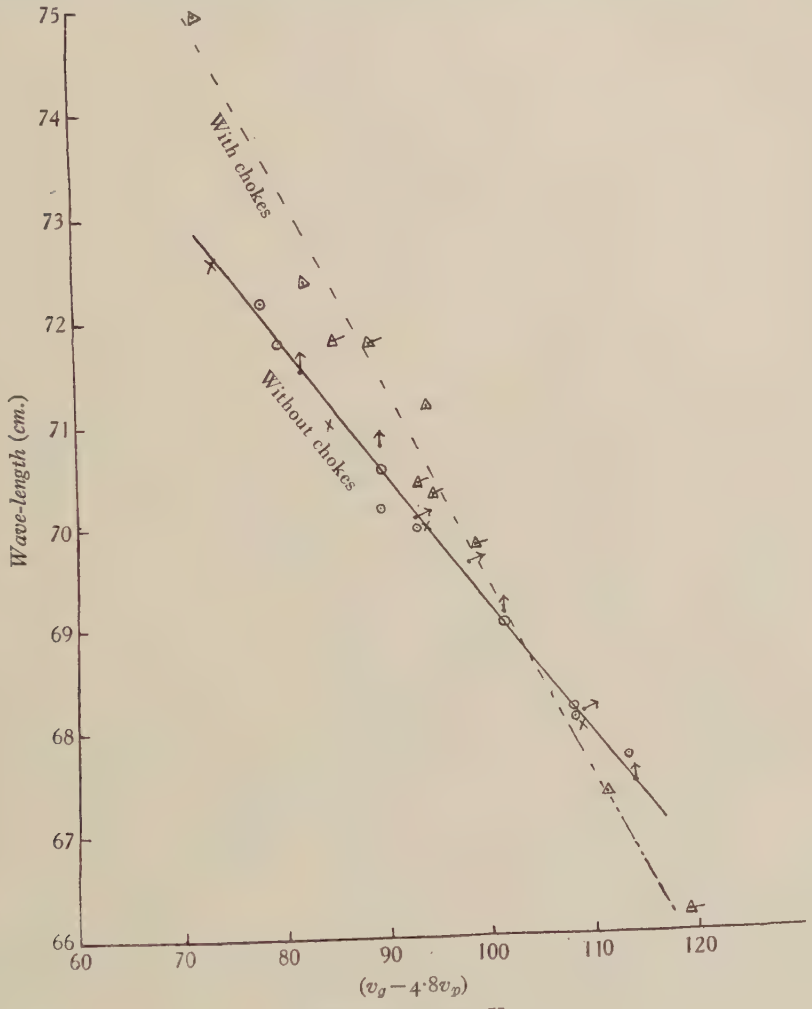

Figure 4. Valve *X*.

× $v_p = 0$; ⊙ $v_p = -2$; ↑ $v_p = -4{\cdot}5$; ↗ $v_p = -6{\cdot}5$, no chokes.

△ $v_p = 0$; ◁ $v_p = -6$, with long chokes.

expected, unaltered by changing the external circuit. This experiment shows how the change in wave-length resulting from a given alteration of electrode potential is diminished by reducing the effective resistance of the attached oscillatory circuit.

The straight-line relationship between v_g and λ was still found to hold, and the slope of the line was found to alter at a particular value of v_g dependent on the filament emission for a T.M.C. valve, with fixed Lecher-wire circuit attached to

the plate and grid terminals (see figure 5). It was further noted that the condenser at the end of the fixed Lecher-wire system was definitely a potential node for smaller values of v_g, but as the value of v_g was raised it ceased to be so. In figure 5 is also shown a (v_g, λ) curve obtained with the circuit of figure 1, except that one condenser only connected plate and filament and B was omitted. The difference between the two curves shows the effect of the attached oscillatory circuit on the generated wave-length.

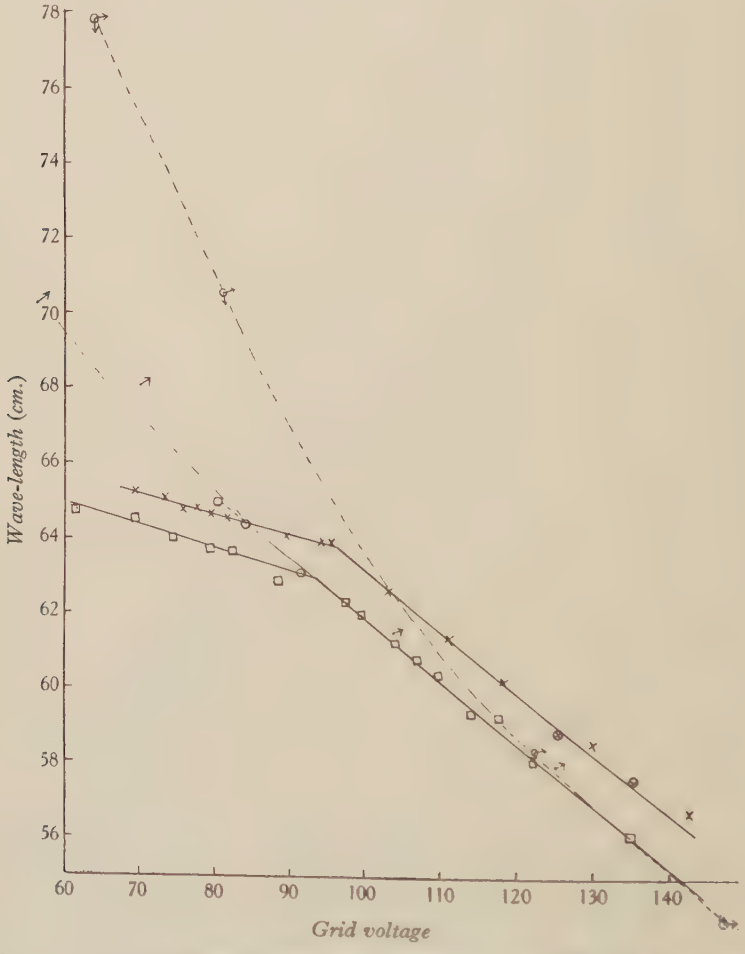

Figure 5. T.M.C. valve with fixed Lecher-wire circuit between grid and plate; ⊡ $v_p = -2{\cdot}05$, $i_g = 27$ mA.; ⊙ $v_p = -2{\cdot}6$, $i_g = 12{\cdot}75$ mA.; × $v_p = 0$, $i_g = 27$ mA.; · from graphs of v_g and position of λ meter bridge for max. deflection; ⊕ calculated by Scheibe's method ($v_p = -2{\cdot}05$); ↗ $v_p = -2$, condenser between plate and F – (August 1933 and August 1934).

In obtaining results with the circuit of figure 1 but with B omitted, i_p and D (for resonance in the wave-meter circuit) were noted, the position of the valve with reference to the wave-meter wires being left unaltered. Curves connecting v_g with i_p and v_g with D for a particular value of v_p are given in figure 6 for four different triodes.

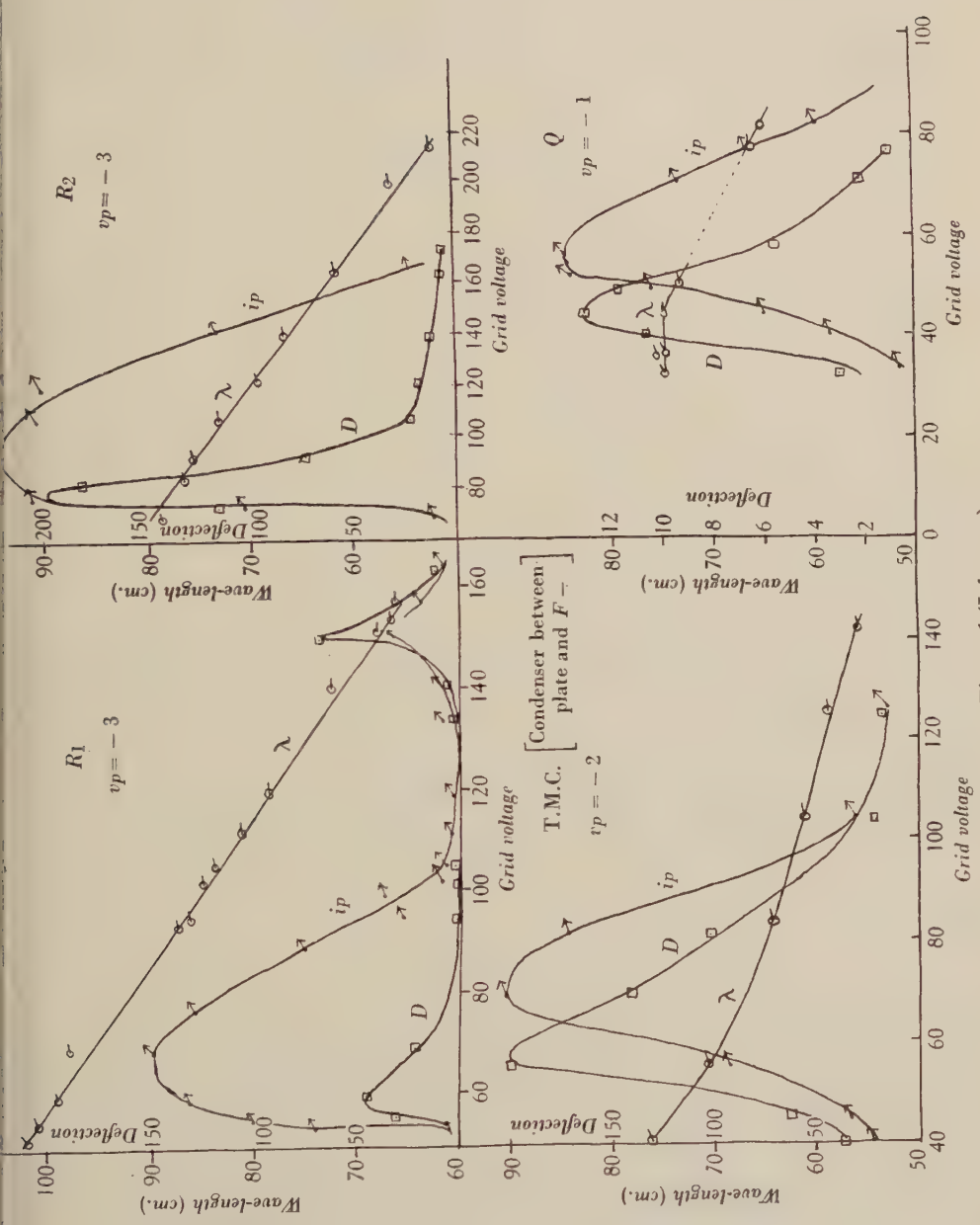

Figure 6 (July 1933).

The form of these curves suggests very strongly that some kind of tuning is taking place as the grid voltage is altered. They may be compared with the curve recently given by Gill and Donaldson[4] for a triode used as a receiver of ultra-short waves. In the present case it is to be supposed that the potential differences impressed on the electrodes are due to oscillations maintained in an oscillatory circuit consisting of the valve electrodes and leads.

It will be noted that $D_{\max.}$ and $i_{p\max.}$ do not in general occur for the same value of grid voltage. This corresponds with the observations made by other workers to the effect that maximum amplitude of oscillation and maximum plate current

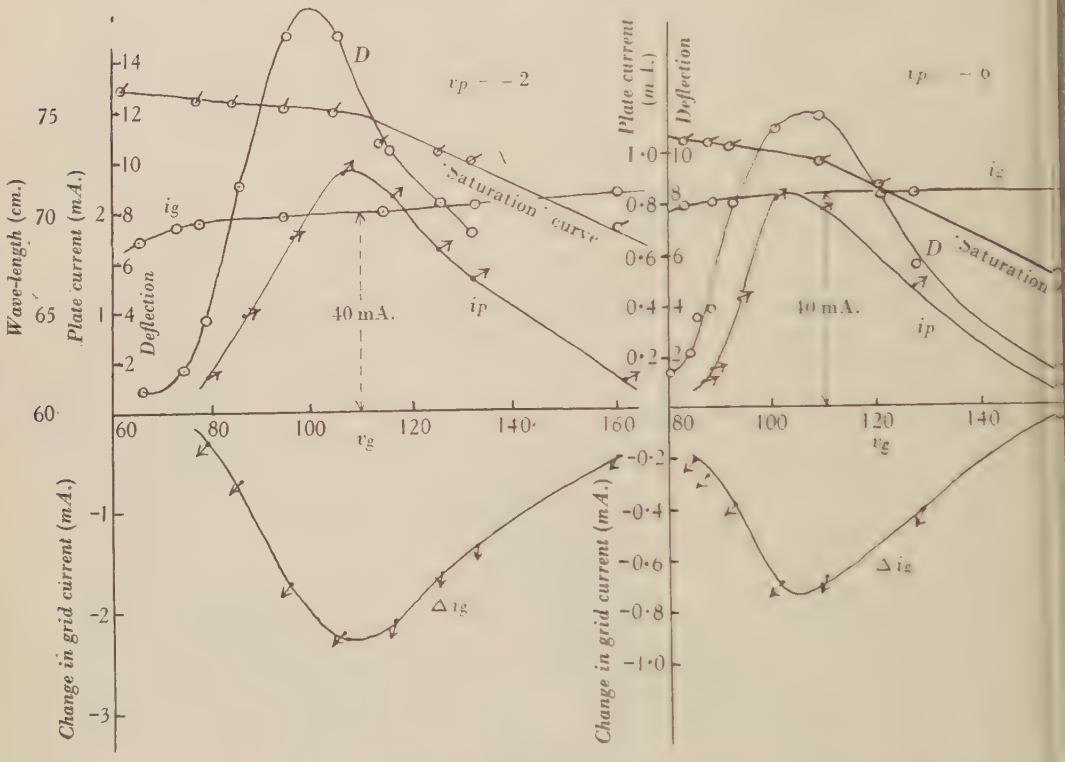

Figure 7.

do not coincide as the length of a Lecher-wire circuit attached to the generating triode is altered while the static potentials applied to the electrodes remain unchanged. In figure 7 is shown the variation with v_g of D, i_p and Δi_g for two values of v_p for the Mullard valve; i_p and Δi_g are proportional to each other and of the same order of magnitude. Evidently in this case a certain fraction of the constant total emission current was alternately taken by the plate and by the grid. The variations in i_g were measured by means of a balanced galvanometer in the grid circuit.

In almost all cases in which i_g was recorded simultaneously with λ, a change in slope of the $(v_g, \lambda)_{v_p\text{const.}}$ curve was observed in the neighbourhood of the top

bend of the (v_g, i_g) curve, and therefore usually in the neighbourhood of the maximum amplitude of oscillation. The abrupt changes in slope of the (v_g, λ) curves shown in figure 5 for the T.M.C. valve coincided with the points of maximum oscillation, which in this case occurred for values of v_g considerably greater than that required to draw the saturation current from the filament. This triode contained a certain amount of gas.

§ 3. NOTES ON THE RESULTS

After the relationship between $(v_g - \mu v_p)$ and λ had been established, a paper appeared by Clavier[3] in which it was stated that for the frequency most strongly maintained by the micro-ray valves used in the Lympne-St. Inglevert 17 cm.-wave service, a linear relation between grid and plate voltages held over a wide range of values. The results given in the present paper show that this linear relationship holds for the very different oscillation arrangements described here, and furthermore that it holds not only for the frequency most strongly maintained but for *any* frequency generated by the system comprising the tube and associated circuit.

A linear relation between grid voltage and wave-length was also found by Grechowa[6] for a double-tube arrangement with fixed oscillatory circuit attached, but the effect of alteration of plate voltage was not shown as in the present experiments. The effect of an alteration of grid or plate voltage on the generated wave-length may be considered as twofold. Firstly, by alteration of the quantity and static distribution of space charge within the tube, the effective capacity of the electrodes may be altered. Secondly, the time of transit of the electrons between the electrodes is altered so that the phase of the current at the electrode under consideration is altered with respect to the oscillating voltage there. The change of phase is, of course, accompanied by a change in amplitude of the generated oscillations. If neither the filament-grid space nor the grid-plate space is carrying its saturation current the first effect would not be marked, and the second effect would be predominant.

In order to see how experimentally determined wave-lengths compared with those calculated on the assumption that $\lambda = 2cT$, where T is the time of transit of an electron between the electrodes in the absence of oscillation, and $c = 3 \times 10^{10}$ cm./sec., the dimensions of the valves used were measured as accurately as possible (i) by using a cathetometer and (ii) by projecting enlarged images on a screen by means of a projecting lantern. The electrodes of commercial valves of the type used are not likely to be of exact cylindrical symmetry, but the particular valves chosen approximated to this condition.

In the case of the triode R_2 the experimental results for the shortest values of λ fitted almost exactly the (v_g, λ) curves obtained by calculation of the electron transit time between filament and turning-point on the assumption that neither space charge nor oscillations influenced this time.

In the case of the other valves such exact coincidence was not found. However, in all cases, except that of the Mullard valve, the experimental values of λ were

shorter than those calculated from $\lambda = 2cT$ according to the method given by Scheibe[7].

Various authors have noted that the effect of increasing space charge as well as of increasing amplitude of oscillation is to shorten the wave-length of the electronic oscillations generated by a triode.

It may be concluded that the straight-line relationship between $(v_g - \mu v_p)$ and λ, for oscillations generated in a suitable fixed circuit by a positive-grid triode, has been established experimentally. A quantitative explanation of the relationship has not been found. However, lack of agreement between the measured wave-lengths and those found from calculated transit times must be ascribed to the disturbing factors not allowed for in the wave-length calculations, such as (i) the quantity of space charge and its distribution; (ii) the amplitude of oscillation of the electrode potentials; and (iii) the phase differences between these potentials and the currents to the electrodes.

The definiteness and repeatability of the results of the wave-length determinations with fixed circuit conditions and the linear dependence of λ on the applied potentials suggest that a triode connected in the simple way described might be used as an oscillation wave-meter over a limited range; moreover, the amplitude of oscillation could be altered by adjustment of the filament current without appreciable change in the wave-length, provided that v_g was sufficiently great.

§ 4. ACKNOWLEDGMENTS

The experimental work described in this paper was carried out mainly in the Physics Department of the London (R.F.H.) School of Medicine for Women; it was completed in the Electrical Laboratory at Oxford, with the kind permission of Prof. J. S. Townsend.

I should like to express my thanks to Dr W. H. Eccles for the interest he has taken in the work, and to Mr E. W. B. Gill for helpful suggestions made while I was working in the Electrical Laboratory.

REFERENCES

(1) Barkhausen H. and Kurz, K. *Phys. Z.* **21**, 1 (1920); E. W. B. Gill and J. H. Morrell. *Phil. Mag.* **44**, 161 (1922).
(2) Chapman, F. W. *Exp. Wireless*, **9**, No. 108, 500 (1932).
(3) Clavier, A. *L'Onde élect.* **13**, No. 147, 101 (1934).
(4) Gill, E. W. B. and Donaldson, R. H. *Phil. Mag.* **15**, 1177 (1933).
(6) Grechowa, M. T. *Z. Phys.* **35**, 50 and 59 (1925); **38**, 621 (1926).
(7) Scheibe, A. *Ann. Phys.*, Lpz., **73**, 54 (1924).

541.183.26

MODELS OF THE SUPERPOSITION AND INTERPENETRATION OF COMPONENTS IN GAS MIXTURES ADSORBED UPON THERMIONIC, PHOTOELECTRIC, AND CATALYTIC SURFACES: PART I, PRINCIPLES

By M. C. JOHNSON, M.A., D.Sc., Physics Department, Birmingham University

Received October 16, 1934, *and in revised form November* 14, 1934.
Read in title December 21, 1934.

ABSTRACT. Models of intermolecular attraction and repulsion are developed to represent the penetration of one adsorbed substance through another. Such interchanges between two or more components are important in view of the complex surface structures required for control of thermionic or photoelectric emission, and for the many physical and chemical experiments in which a metal is covered with a thin deposit of another metal over an intermediate gas layer; the latter may reach its final equilibrium between the metals after migration from above or below. Other relationships between successive adsorbed materials range from the protection of a layer by inert gas, to the disruption of a catalyst by penetration of reacting vapour. The concepts of bulk diffusion and electrolysis, applied successfully to comparatively thick oxides, etc., require supplementing when the exchanges take place between two layers each of single atomic thickness. Accordingly we adopt simplified models to enquire what properties a molecule must possess if it is either to penetrate and replace, or to remain superposed upon and stabilize, a previously adsorbed group of molecules. The range of models is chosen to cover certain main features of oxygen, hydrogen, caesium, and inert gases, adsorbed in dissociated, ionic, and other states upon a tungsten surface. The enquiry yields some of the conditions whereby any given metal-gas sequence is able to rearrange its layers into a stable equilibrium independent of the order in which the components were originally deposited. In successive approximations we consider first the adhesion of given molecular models to a clean surface, and to the same surface when screened by a previous deposit in the form of a complete sheet. Distribution of the previous deposit is next taken into account as giving access to the solid through interstices between inert or repelling atoms and ions. The restriction to immobility of the first deposit is then removed; the energy required for lateral migration is also considered for a second layer upon a first layer, and for the first layer loaded by the second layer. The work done in penetration of one layer by another then becomes determinate for the given models. Finally the modifications needed for fissures and edges on the solid lattice are briefly discussed, for application to the catalytic activity of isolated areas and grains.

§ 1. INTRODUCTION

THE production of thermionic filaments capable of large and lasting emission at low temperatures[1], and of photocells capable of a required sensitivity and spectral range[2], depends essentially on the formation of surface layers which are often very complex; they may include one or more gases and metallic vapours deposited, modified by discharge, and required to remain stable during long life exposed to the residuals of a high vacuum or to the impurities of an inert atmosphere. The attainment of equilibrium ensuring such stability may involve one or more exchanges of position by interpenetration between one layer and another.

The mechanics of adsorption[3] presented by such assemblages is not susceptible of exact treatment. We suggest, however, that by constructing very simple models, i.e. by assuming certain laws of force and dimensions of spheres of molecular influence, it is possible to determine within specified limits the extent to which two components bearing at least some of the properties of known gases may be expected to interpenetrate; this distinguishes ultimately between mixtures which must be deposited on a surface in the order finally required, and mixtures which may be left to arrange themselves.

The present paper is concerned with outlining the method for all likely substances rather than pursuing detail of any one of them; the terms "caesium," "oxygen," etc., are only used to describe highly conventionalized constructions chosen as caesium-like, oxygen-like, etc., from one or two representative tendencies.

§ 2. ATTRACTION OF A MOLECULE OUTSIDE AN ALREADY ADSORBED LAYER

Method. The chance of a molecule from the gaseous phase penetrating or displacing any outer layer on which it impinges depends on (*a*) the time during which it can remain attached before re-evaporation, (*b*) the interstices of the outer layer, and (*c*) the lateral movements of which the atoms of the outer layers are capable during that attachment. Since (*a*) is known to vary exponentially with temperature and with the potential energy of the attachment, its range of variation is obtainable by determining the difference between energy of adhesion to a clean surface and energy of adhesion to the same surface if the latter is already covered by a screening layer of adsorbed gas or vapour. Before discussing in § 3 the structure of such a screen, we consider the simpler case in which it is regarded as a locally plane and complete sheet, whose thickness d' is equal to the supposed diameter of the adsorbed particle.

In the simplest case the attraction of impinging gas to the solid is unaltered in character by the interposed screen, but merely diminished in magnitude owing to the gas being prevented from closest approach to the solid. In more complex cases the screen itself adds its own attraction to that transmitted through it from the solid, as in the cementing of an alkali to tungsten by a gas layer. In extreme cases the

screen or even the surface layers of the solid become detached by attraction to incoming gas, as in the formation of WO_3, the action of CO on Ni, etc. A further complexity is introduced if the screen modifies qualitatively and not only quantitatively the forces between solid and gas. For Van der Waals's forces this modification is probably slight. It may become important, however, if the screen is held by a valency bond to the surface, as in the so-called chemisorption of O_1 and H_1; if this bond is saturated by the first layer, similar particles approaching from the gas may no longer feel even the weakened residual attraction appropriate to their greater distance from the solid. For instance if Ni has caused the formation of a layer of H_1 by surface dissociation, subsequently impinging H_2 forms a second but probably undissociated layer by Van der Waals's attraction only, and any H_1 generated in the gas, e.g. by discharges, will also have to adsorb by Van der Waals's attraction. A second layer of mobile oxygen upon a first layer of rigid oxygen covering a metal filament is probably also to be explained in this way.

Starting with the simplest case of the plane, inert, non-modifying layer, if the laws of variation of attraction and repulsion with distance can be reliably assumed, the action of this interposed screen can be represented by simply displacing outwards the repulsions and retaining the same attractions as were felt at corresponding distances from a clean surface. We combine the attraction appropriate to a distance d from the solid with the repulsion appropriate to a distance $d-d'$, when d' is the thickness of the screen. This type of model is only strictly valid if the atoms of the first adsorbed layer are similar in hardness to the solid itself. d, d'

Let the potential energy E_1 of an impinging particle at a distance d from the bare solid be given by E_1

$$E_1=\lambda d^{-n}-\mu d^{-m} \qquad \text{.....(1),}$$

where n and m represent laws of decrease of repulsive and attractive energy with respect to the solid, and λ and μ are constants which must be chosen, for any n and m, to enable the position of equilibrium under all the forces to occur at a correct distance from the surface. Then for the potential energy E_2 of attraction of the same atom to an already gas-covered surface, this approximation gives n, m λ, μ E_2

$$E_2=\lambda\,(d-d')^{-n}-\mu d^{-m} \qquad \text{.....(2).}$$

Graphs of E_1 and E_2 plotted against d illustrate the effect of the screening layer in causing the potential minimum, representing position of equilibrium in adsorption, to become rapidly shallower as it is displaced outwards, figures 1, 2 and 3.

Values of the constants. The effects of d', and the distance at which the first potential minimum occurs, and also the distribution of adsorbed atoms to be considered later, require some convention to be adopted as to atomic dimensions in gases, vapours, and solids.

The size of any atom varies greatly according as it is defined through (*a*) gas-collision target, (*b*) X-ray crystallographic packing, (*c*) maximum density in charge distribution of an outer electron shell. Since O_1 and H_1 are inaccessible by (*a*), and (*b*) yields mainly ionic states, a complete set of radii is only obtainable through (*c*) and will appear excessive or deficient, according to the nature of the surrounding

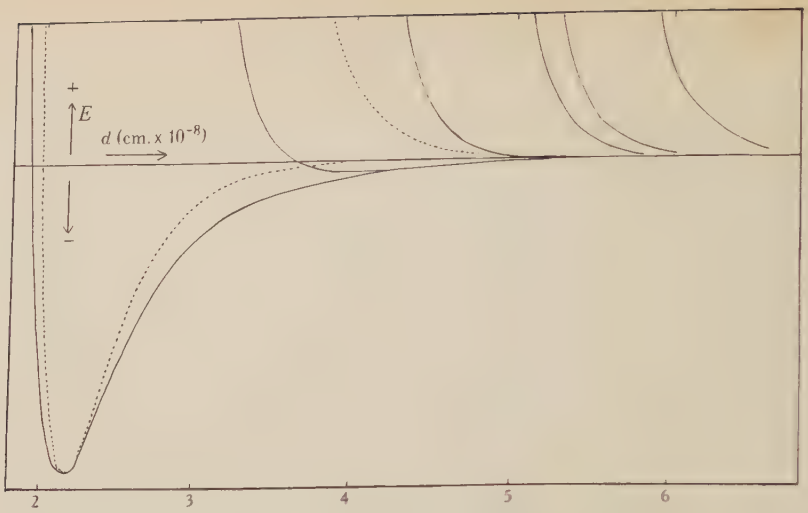

Figure 1. Model 1, $n=12$, $m=6$ ————. Model 3, $n=12$, $m=11$ ————.

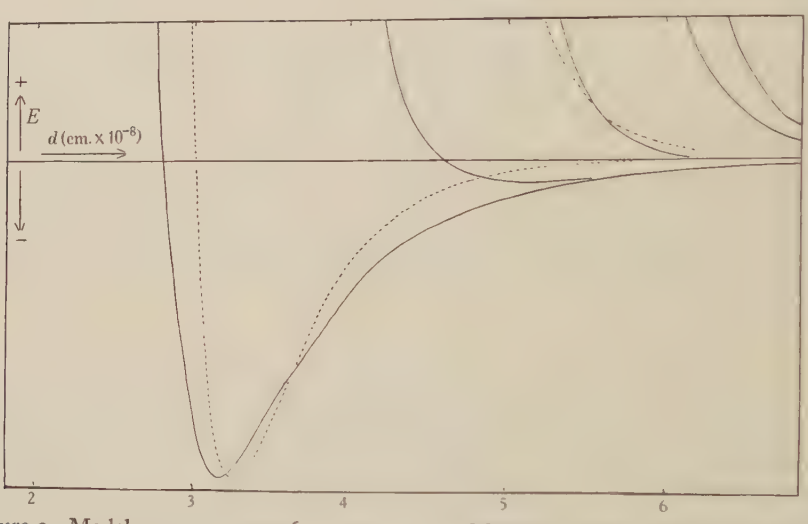

Figure 2. Model 2, $n=12$, $m=6$ ————. Model 4, $n=12$, $m=11$ ·····.

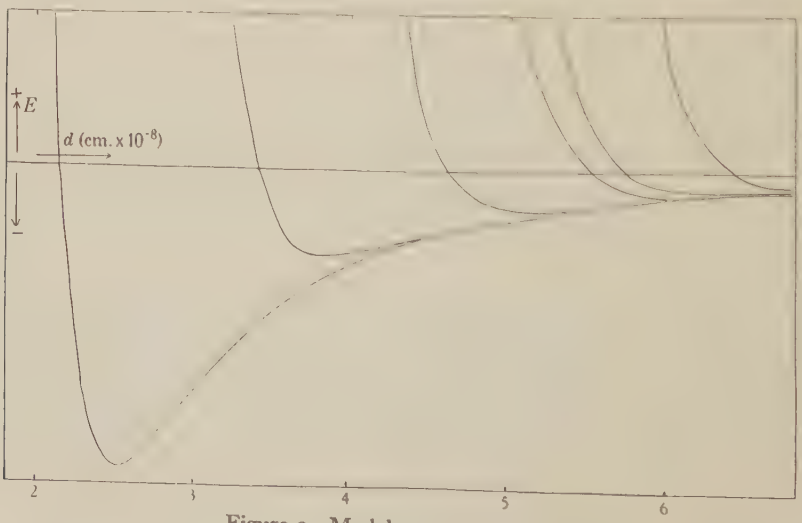

Figure 3. Model 5, $n=12$, $m=3$.

fields, when comparison with (*a*) or (*b*) arises. The definition of radii through atomic wave functions has been developed by Slater, Hartree, Pauling, and others; although Slater's comprehensive table[4] has been superseded for certain atoms, it fulfils best our need of exhibiting all atoms on a single comparable basis: accordingly we adopt the mean of his O_1 and H_1 as smallest possible model, and his Cs as largest possible model. These exaggerate both upper and lower limits, and his tungsten constitutes a too overlapping lattice. But for our purpose of emphasizing consequences of differences in size these exaggerations are an advantage rather than otherwise in this general survey. Our diagrams differ radically from those employed in crystal analysis, where overlapping and separation are both avoided by confining definitions of radii to (*b*) alone, and where the structure is in equilibrium, under forces not necessarily those of a monomolecular adsorbed layer, so that the problem of penetrability does not arise.

Table 1

H_1	O_1	He	H_2	A	O_2	Cs	W	Cs^+	$O^{-(-)}$	
$\frac{1}{2}d'=0{\cdot}5$	0·5	1·0	1·4	1·5	1·8	4·25	2·7	1·75	1·35	$\times 10^{-8}$ cm.

In any model of an interface the distance between centres of adsorbed and adsorbing particles might be approximately the sum of these structural radii, or if the adsorbate packs as if taking part in certain types of chemical reaction the distances might be compressed to the order of $\frac{2}{3}$ the sum of the radii. To compare such alternatives we choose values of λ and μ which will give minima in the potential curve at $(d'/2+\bar{d}'/2)$, models 2 and 4, and also at $\frac{2}{3}(d'/2+\bar{d}'/2)$, models 1 and 3, where $\bar{d}'$ is the diameter of the atom in the solid. The repulsive index n we take as always 12, and it is not likely to be smaller except possibly for the soft alkalis. m is known to be about 6 for Van der Waals's forces, models 2 and 1; 3 for dipole forces, model 5; and much higher for the homopolar bond. Since this latter can be imitated by an induced polarization involving the square of a dipole moment, and the dipole moment may itself vary with distance up to a fourth power, the greatest steepness in attractive potential can be represented suitably by giving to m the value 11, models 4 and 3. Actually these forces may decrease exponentially with distance, but to a considerable approximation and with greater computational facility a power model suffices. $\bar{d}'$

Figures 1, 2 and 3 show the equilibrium of a second adsorbed layer in comparison with that of a first, calculated from the above values inserted in equations (1) and (2). Each group of shallow curves represents the combined attractive and repulsive energy of an impinging atom when the surface is covered with the several inert-model screening layers; the single deep curve of each group represents the corresponding values of the quantities if the surface were bare. Thus for these simple models it it possible to see at once how much less work has to be done by the solid in evaporating a second layer than in evaporating the first layer, as measured by the decreasing depth of the minima; we also see the dependence of this decrease upon the type of attraction exercised, as represented by its particular laws of force. While sufficient range of variation with distance is covered by the several models,

the scale of ordinates will differ in different cases served possibly by similar models; e.g. the depth of the trough in the curve for O_1 and H_1 is of the order of 10^5 calories per gram-molecule, but for He at the other extreme it is of the order of 10^2.

E_1' E_2' *Results.* Let E_1' be the energy of adsorption of the first layer on the bare surface, i.e. the work to be done in evaporating the first gas. Let E_2' be the corresponding value for the second layer on the gas-screened surface. The values of E_2' E_1' are tabulated in table 2 from the several graphs, showing the reduction of adsorptive power by the inert screens.

Table 2

d' (cm. $\times 10^{-8}$)	1·0	2·0	2·8	3·0	3·6	Adsorption model
E_2'/E_1'	0·29	0·13	0·08	0·06	0·04	5
	0·07	0·01	0·005			2
	0·03	0·005				1
	<0·005					4
	<0·005					3

We proceed to indicate briefly the application of this table.

(*a*) One of the largest known values of E_1' is that for O_1 on W, estimated by Langmuir[5] to be about 160,000 calories per gram-atom. The models 4 and 3 are the most appropriate for such an adsorption which has the strength of a chemical attraction of extremely short range; from the above table it is seen that only 800 cal. could remain as the maximum possible energy of adsorption outside a close screen whose thickness is that of the smallest possible atom. Independently of whether such screen does itself saturate the available valency of the metal, we have from this figure a reason why no second layer of O_1 is found by surface dissociation, and also a reason for expecting O_1 or H_1 present in a gaseous discharge to be only weakly adsorbed, if the W is already covered by a packed layer similar to this model.

(*b*) The next largest values of E_1' belong to metallic vapours, e.g. 65,000 cal., is estimated in Langmuir's [6] experiments with Cs on W. The forces involved are not necessarily of the shortest range, and models 2 and 1 are allowable, giving the maximum energy of binding of a second layer as 4500 cal. through a model screen corresponding to O_1 or H_1, 650 through He, and 300 through diatomic gases.

(*c*) Van der Waals's forces provide heats of adsorption up to the order of 600 cal. only, and these will be reduced on the same scale to 400, and to less than 100 cal., through H_1, He, and diatomic layers.

(*d*) The longer range forces of model 5 are less drastically diminished by the gas screens, but in their case the value of E_1' is less initially. A strong dipolar molecule provides energy of surface adhesion of the order of 3000 cal., which will be reduced by the H_1, He, and diatomic layers to 900, 400, and 300 cal. per gm.-mol. respectively.

(*e*) With the forces of longest range, E_1' may be large if due to the attraction of an opposite ion in a polar crystal; at a metal surface an ion or a molecule of dipolar structure will experience the similar attraction to its image at a corresponding

distance behind the surface. A screen of monomolecular thickness may double the distance of a layer while the energy of image attraction of gaseous ions falls only to half value; at the smallest atomic distances the mirror plane is an inadequate model, but the decrease of potential with distance will be closely linear outside the regions of chemical attraction.

Two standards of comparison must be used in applying these and similarly derived estimates of the diminished energy with which a second substance, or a second layer of the same substance, adheres outside a first adsorbed layer. Firstly take the attraction of the screen itself, which should be added to that which it transmits from the solid. For screens of inert gas, or of active gas whose valency is saturated, this attraction will be very small; in other important cases the attraction to the screen is of the same order as that of the screen itself to the solid, as when a diatomic molecule is formed from H_1 striking adsorbed H_1, or when CO_2 is formed at a Pt surface, or when multimolecular layers are formed from most vapours. The extreme case when atoms of the solid become detached has been mentioned. Qualitatively such processes may be represented as transitions from the troughs of figures 1, 2 and 3, to other troughs of potential energy with respect to isolated centres in the adjacent gaseous phase, as depicted by Gurney and by Fowler in the study of electrolysis. Since the energy in the final trough is often that of some well-known gaseous compound, comparison may be effected between this known energy and the energy of adsorption, the latter being less than the former if the reaction proceeds irreversibly.

The second standard of comparison is that of the vibrational energy levels in the adsorbed state; the energy of thermal equilibrium is of the order of 300 cal. per gm.-mol. at 100° K., 900 cal. at 300°, and 3000 cal. at 1000°. Hence comparison of these with the data derived above will decide, for any given model at a given temperature, the chance of a second layer adhering to a first layer long enough for completion of the gradual mutual penetrations which we discuss later.

In addition, the graphs indicate the distinction between rates of change of energy with distance for nearer and further layers; these determine the work done during any small normal displacement involved in lateral migration of adsorbed particles, and will be used below in estimating the penetration of layers by their mobilities.

§ 3. PENETRATION THROUGH INTERSTICES OF A RIGID LAYER

Distribution of an immobile inert adsorbate. We next remove the restriction by which the first adsorbed gas was regarded as a plane sheet completely withholding further gases from the solid. Let saturation of any layer be defined, for the present needs, as the state in which the maximum number of particles is present, consistent with their equilibrium, at a given temperature, in the fields due to neighbours and to the solid below. When a steady state has been reached, the surface density at saturation may either fall short of close packing or may exceed close packing, if the latter be defined as the number of particles which can be arranged with their diameters in contact. Figure 4 illustrates models in which this excess or deficiency

affects a layer's penetrability towards later arrivals from the gas phase. In this diagram the outer electron shells of the metal are represented by the dotted circles, and the atoms adsorbed on face or edges are represented by the full circles.

In using the values of d' from table 1 both neutral and negatively charged oxygen atoms must be taken into account as well as the diatomic molecule. The accepted diameter in crystal compounds, $2{\cdot}7 \times 10^{-8}$ cm., refers to an ionic state, but although some writers have suggested this state for adsorbed oxygen, the proof by detection of evaporating ions would be exceedingly difficult; such evidence as exists indicates that the evaporated adsorbate is neutral, both in the case of O_1 and H_1. On the other hand the alkalis evaporate as positive ions, according to a well-known law, from a surface of large enough electronic work function, while some at least of their atoms behave as neutral when still adsorbed. It is not possible to distinguish sharply between stable existence as a charged ion in an adsorbed state and mere loss or gain of an electron in separating from the surface; development of the new theory of molecular orbitals will probably remodel such states as are incapable of permanent association with a fixed number of electrons, and distinction between ions and neutrals is merely an approach from two extremes between which any actual facts must lie.

Neutral atomic oxygen and hydrogen. If the number of gas atoms in a saturated layer on tungsten is limited chemically to a final proportion of one to each exposed atom of the metal, we must suppose that the components of a diatomic gas molecule, dissociating under surface forces, experience initial attraction to several neighbouring metal centres. Round each of the latter a spherical shell will represent the locus of a potential energy minimum such as was studied in § 2, and the position of an adsorbed atom in equilibrium on the crystal lattice will be the nearest point to the intersection of as many as possible of such shells. This position is marked with shaded circles on the face and top edge in figure 4, in contrast to the positions marked – which would satisfy similar valency considerations but would be unstable for small displacements unless the gas-tungsten complex possessed a moment resisting rotation. Since the heat of adsorption of O_1 on W, attributable to a very intimate bond, is so enormous, the models of figure 1 are appropriate, so that the radius of the sphere of equilibrium is even smaller than the bounding radius of the W atom, if the adsorbed particle is a normal neutral atom. Considerations not very different apply to H_1.

An important feature of any such small atomic model is that tungsten covered by the neutral gas screen will present, even at saturation, a surface with the greater part of the metal still exposed, though with its free valencies no longer fully available. Similar impinging gases can therefore penetrate in most places unimpeded to the W; but if the valency of the metal is already saturated, this will limit subsequent adsorption to a Van der Waals's mechanism which, though weak, does not restrict their final density of packing. Such additional O_2 and O_1 will not follow any lattice structure, and are shown on the lower edge of figure 4. Hence even when the screen considered in § 2 becomes locally of vanishing thickness, so that the results given in table 2 are only applicable at separated points, it is still necessary to regard the second oxygen particle in Langmuir's OOW as a diatomic

molecule, penetrating easily between the large interstices of a strongly held layer of atoms but unable to dissociate. By similar mechanism we may explain the inhibition of hydrogen dissociation at an oxygen-covered surface.

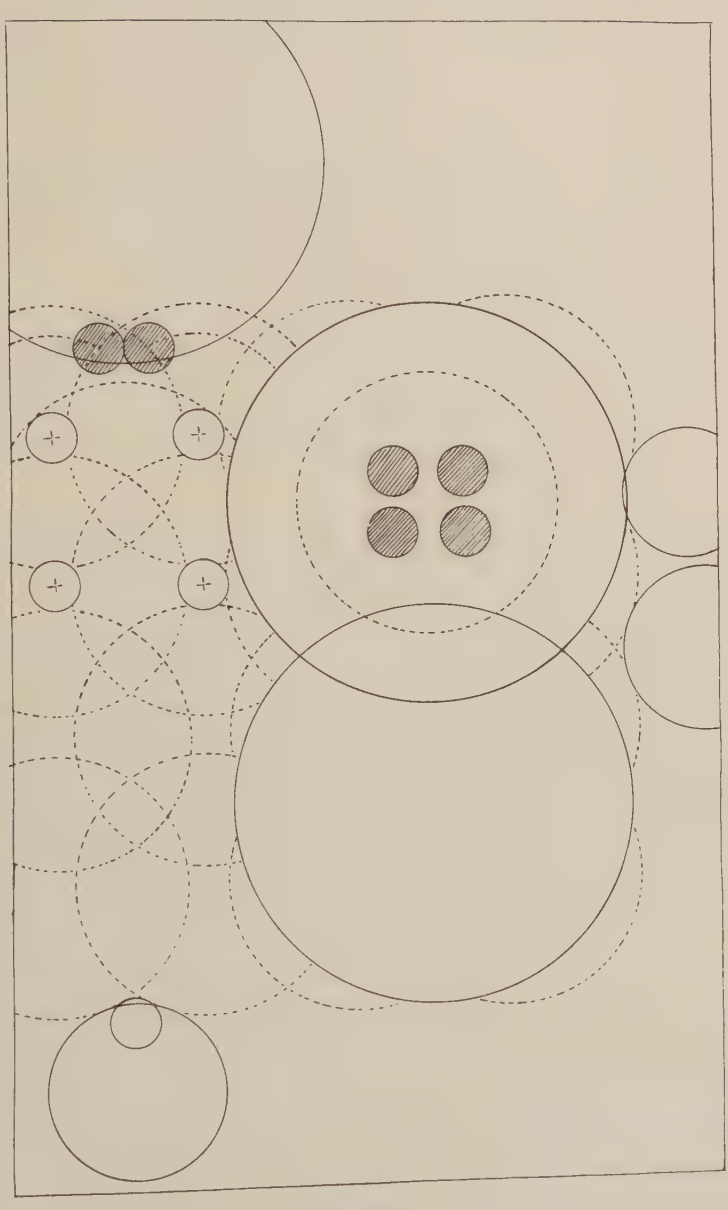

Figure 4.

The presence of O_2 or O_1 on W cannot be regarded as in stable equilibrium; the formation of volatile WO_3 when excess oxygen is admitted shows that further transition to a new grouping occurs, with a loosening of the bond from tungsten to tungsten.

Caesium. In contrast, the model representing extreme alkaline properties has a saturation density actually in excess of close packing if the neutral state is assumed; for any model approaching this extreme, penetrability to outside gases becomes unlikely except by the lateral displacements discussed later. If the adsorbed atoms crowd as closely into the W as into each other the Cs will take up the position shown at the top edge of figure 4; in this the central atom of the body-centred W lattice has the four oxygens above it clustered as near to the intersection of their minimum equipotential surfaces as their mutual repulsions allow, with one Cs atom above the group. Here again the oxygen-screen thickness of § 2 becomes vanishingly small, explaining the well-known fact that the Cs is more strongly held to OW than to W; since in our model the attraction of the O_1 atoms is added to that of the metal without the latter itself being seriously weakened by distance.

Van der Waals's adsorption of inert and diatomic particles is illustrated along the lower edge of figure 4. Not being subject to valency restriction, these and many metallic vapour layers when saturated do not present permanent interstices for penetration by external gases, and have to depend for such upon the displacements which we consider in § 4. In these cases the effective thickness of screen does not fall short of that considered in the models discussed in § 2.

Ions of oxygen and alkali. The sizes of these oppositely charged ions are not so unlike as those of their neutrals, and are shown on the right-hand edge in figure 4. The distribution of any one sign is limited by mutual repulsion.

The penetrability of any layer depends on the fields of force existing between its constituent particles, and it is only with neutral and spherically symmetrical atoms that this field can be considered negligible outside their boundary.

Distribution of immobile mutally repelling adsorbate: ions. The energy of mutual repulsion scatters any assemblage of like ions if they are not enclosed, and in a closed space would cause an appearance of enormous internal pressure on any boundary. Three consequences for the theory of penetration are to be noted: (i) The constituents of even a very unsaturated layer experiencing such mutual repulsion will tend to escape into the gas phase. The alkalis possess an inert core, therefore ions of Cs will be unrestrictedly driven apart, while ions of oxygen and hydrogen may be prevented from scattering by valency bonds to individual atoms of the solid. (ii) The electrostatic field surrounding an ion decreases so slowly with distance that it nowhere approaches zero in its lateral fluctuations over even a very sparse sheet of charged particles. Penetration by outside gases will involve passage through whatever potential barrier is presented by this fluctuating field, and cannot rely on interstices such as existed between neutrals of similar size and packing. (iii) Adsorbed ions can only remain in a stationary pattern when strongly held to individual atoms of the solid; otherwise they will show a gas-like mobility.

Distribution of dipoles. If the work function of a metal is not such as to alter the net charge of the adsorbed atoms, they may nevertheless suffer considerable distortion in the field of the surface, resulting in behaviour as dipoles towards neighbours. The mutual repulsive energy E between two like dipoles of moment μ reaches a maximum, under favourable orientation, given by

E, μ

$$E = \mu^2/d^3.$$

An estimate of μ is available since Langmuir considered the heat of adsorption of isolated Cs atoms on W was about 65,000 calories per gram-molecule, but for Cs in a saturated layer about 41,000 cal. The deficiency represents approximately 17×10^{-13} ergs per atom. If this is accounted for by mutual repulsions at the mean distance of 6×10^{-8} cm. used in figure 4, the repulsion of one particle by four similar neighbours implies that

$$\mu = 9{\cdot}6 \times 10^{-18} \text{ e.s.u.}$$

Conclusion of § 3. The dimensions and force laws of the models appropriate to neutral O_1 and H_1 allow gas molecules to penetrate freely through wide interstices in the first adsorbed layer; but as these models are also associated with saturation of the valency of the metal with respect to those gases, any second layer, though reaching the solid, is only weakly held there. The models corresponding to large alkali atoms and to diatomic molecules allow no such interstices in a saturated layer. Ions cannot be packed as densely as neutrals, but their scattering is greater for an inert than for an active core. Even a sparse ionic layer covers the whole surface with its potential barrier. The repulsion of distorted neutrals exerts a calculable but slighter effect on their spacing, and hence on the penetrability of a layer.

§ 4. PENETRATION BY DIFFERENTIAL MOBILITY OF LAYERS

Migration on clean surface. It is well known from experiment that the state of aggregation of adsorbed gases and vapours ranges from an almost complete freedom of migration over the surface, giving a two-dimensional gas, in some cases, to a rigid binding with either a characteristic spacing or the spacing of the underlying solid, giving a two-dimensional lattice, in others. Lennard-Jones[7] has initiated methods for calculating the energy which an adsorbed particle in a first layer must acquire in order to migrate from one cell to another on the surface of certain types of lattice. When a second layer is adsorbed upon the first layer in the manner we have discussed, the chance of the former penetrating the latter will obviously depend on its ability to migrate along the screen until it finds any of the interstices mentioned in § 3. Similarly, any migration of atoms in the screening layer itself will contribute towards opening such interstices.

Figures 5 and 6 show the components, in the plane of the surface and normal to it respectively, of such a change in position. In figure 5 the largest and smallest circles represent the boundaries of models used in § 3 for Cs and O_1; the dotted circles are sections of spheres whose radius is equal to the distance of the potential minimum in figure 1 from its attracting W centres. The length and direction of the horizontal arrow indicates the smallest movement by which an adsorbed atom, in equilibrium above the central W atom of the body-centred cube, can migrate to the top of a pass without actual evaporation; once the energy for this movement is obtained the atom can wander over an infinite network of such paths without needing further gain except to counteract losses by collision. An oblique movement, ending at the head of the vertical arrow, would require the surmounting of a higher pass and allow a wider choice of subsequent migration routes. The main lateral component of migration is derivable graphically or algebraically from the change in distance

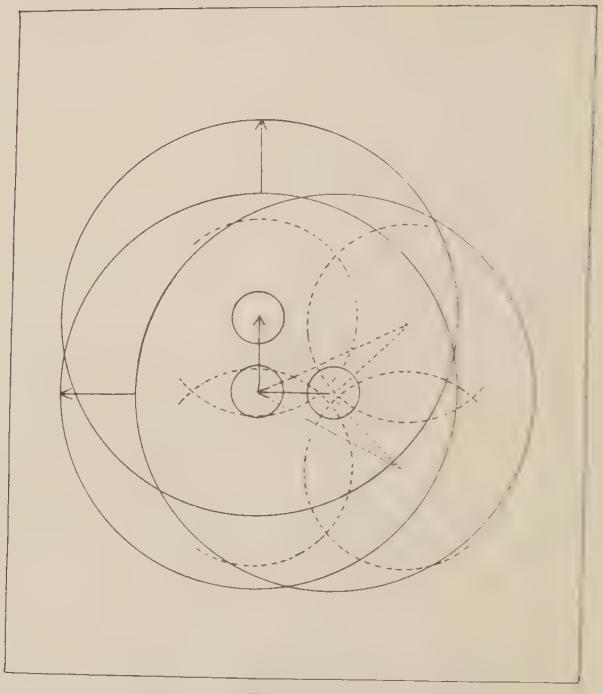

Figure 5.

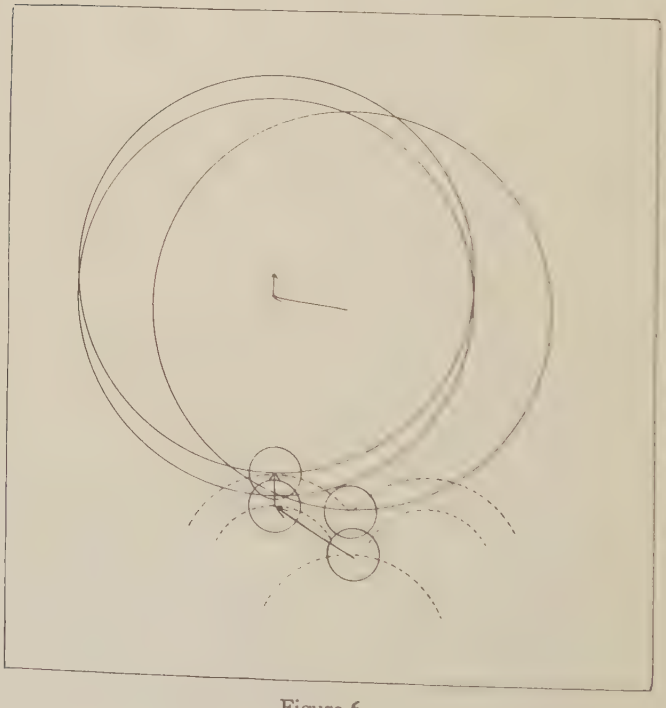

Figure 6.

relative to central and right-hand W atoms, indicated by the dotted straight lines.

In the plotting of the normal components, figure 6, the dotted circles around the W atoms are supplemented by smaller circles which trace the intersection of pairs of the equipotential spheres represented by the former; the innermost pair of O_1 positions show migration over these smaller circles, corresponding to the horizontal arrow of figure 5, and the outermost pair show the further migration at right angles, along the vertical arrow of figure 5. Three-dimensional components of displacement are taken from these diagrams, and the distance from each W atom at the top of the pass between lattice cells is compared with that at the trough in the centre of a cell. Referring then to the appropriate model in § 2, the work done in removal from trough to pass is calculated to the accuracy needed.

We find thus that if the energy of binding of the O_1 is 160,000 cal., the energy needed to mount the nearest pass, and hence to migrate over the surface, is nearly 90,000 cal., or more than 50 per cent. For Cs, 12,500 out of 65,000 cal. are needed. It is not unexpected that the smallest adsorbed particle, capable of penetrating almost through the solid lattice, should be so much less mobile than the large Cs; the estimate for the latter is close to that found in Langmuir's thermionic experiment with Cs on W, where the energy of migration is 21 per cent of the heat of adsorption, compared with the 19 per cent calculated from our model. Particles held by the much smaller Van der Waals's forces will have a much greater mobility.

Adsorbed ions are attracted to images in a plane surface; at such close distances the ideal plane is not an accurate localization, but an approximation from figure 4 places the work of migration of an ion between 5 per cent and 10 per cent of its work of evaporation.

Migration on gas-covered surface. Combining the results of the preceding section with those of § 2, it becomes evident that the great decrease of attraction which we found outside a screening layer must render all above that layer extremely mobile with respect to the underlying solid; not only is the residual attraction weak, but the graphs of § 2 show that the work done in migrating is further decreased by the flattening of the potential curves at great distances, until the path from trough to pass in a second layer becomes almost an equipotential. Only when the screening atoms themselves act as attracting centres will the second layer approach rigidity, and then only such measure of rigidity as was also possessed by the first layer.

Penetration due to migration of upper layer. The model of greatest rigidity, corresponding to neutral O_1, was also in § 3 that of sparsest distribution; hence, apart from inhibition of penetration by lateral repulsion as described below, any atom striking any part of the oxygenated surface needs only the slightest displacement to reach the underlying metal.

Penetration due to migration of lower layer. At the other extreme the very large and overlapping Cs atoms will not allow any penetration from outside unless they are pushed apart, which action we found to require the large energy of 12,500 calories per gram-molecule, greater than the total adsorption energy of any substance held by Van der Waals's forces alone, and greater than the diminished energy (§ 2) of even

the strongest adsorption outside the Cs. It is experimentally known that oxygen adsorbed upon an alkaline-earth metal on tungsten succeeds slowly in penetrating and reversing the order, e.g. from WBaO to WOBa at about 1300° K. If these particles are neutral and have any likeness to the models we have used, our investigation suggests that the outer layer migrates easily over the lower one, but that until the lower is forced by the heating of the tungsten to migrate, mutual interpenetration cannot set in. A similar effect probably underlies the diffusion outwards of a layer of alkali from a bulk alkali already covered with a gas layer. Observation of the temperature variation of these exchanges would provide, on our theory, information as to the mobility of the lower rather than of the upper layer.

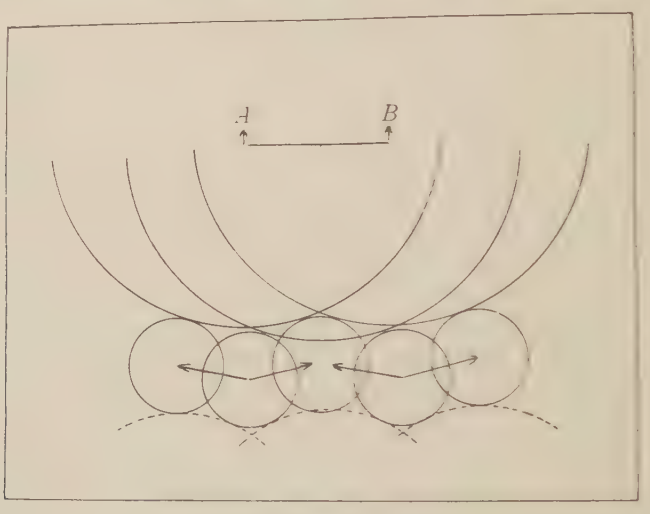

Figure 7.

Inhibition of mobility of lower layer by comparative rigidity of upper layer. This is illustrated in figure 7, with respect to the extreme example of a layer of helium models adsorbed on the metal at low temperature, with Cs deposited subsequently. An unprotected layer of He would only remain unevaporated at a very low temperature, and its lateral mobility would be very complete. But to achieve the migration shown by the arrows in figure 7 the protected or loaded He will have also to gain the energy needed to displace the Cs atom normally through the distance *A*, *B*. The large energy of migration of Cs found at the beginning of the present section is greatly reduced outside the He screen, but may still exceed the small migration energy of the He or even the energy required for the latter's evaporation. Such an immobilizing of an inner by an outer layer occurs in the trapping of molecules during deposit of sputtered and evaporated metal in the presence of gas, and is responsible for many of the electrical and optical properties of films so formed.

In contrast to the penetration due to migration of the lower layer, interpenetration of this double layer will depend mainly upon mobility being attained by the upper atoms, and temperature coefficients must be interpreted accordingly.

Inhibition of penetration by lateral repulsion. If the first layer or screen is no longer inert towards impinging gas, the initial requirement (§ 2) for penetration has the greater chance of fulfilment, through the lengthened interval before re-evaporation of the second layer; but an opposing tendency is also introduced if screen and gas molecule form together a complex which possesses preferential orientation with respect to (*a*) neighbours, or (*b*) the underlying solid. In some strong bindings of gas to screen, access of the former to the solid would be opposed as involving work of rotation of the combined structure. In case (*a*), this work is needed to overcome the lateral repulsion considered in § 3, if the layer is closely packed. In case (*b*), even without close packing, work has to be done in interpenetration of the two layers if attraction of the gas is exclusively to the screen, since distortion may then repel the outer atom from the solid. Such a system approaches the strictly oriented organic adsorption on liquids, studied by Adam and others, the nearer and further portions of a long chain molecule corresponding to the lower and upper atoms of our double layer. The directional properties of some types of valency bond may also appear in certain adsorptions, reinforcing the tendency for the second layer to remain outside the first and not penetrate to the solid.

Two-phase single layer of two components. When penetration has been achieved, there may have occurred a complete exchange of position between upper and lower layers, or, if one component is not much more strongly bound to the surface than the other, the two may form a mixed layer but still one of monomolecular thickness. In many cases, owing to discrepancy in size of atoms, etc., two such coplanar components will not be of the same mobility; thus arises the phenomenon of a two-phase adsorbed layer, conforming neither to the homogeneous two-dimensional gas nor to the two-dimensional lattice.

It is possible to illustrate (figure 8) the restriction which an immobile component may exercise on the migration of a companion. The closed contours round the summit of each lattice atom limit the regions over which a certain adsorbed particle can wander at a given temperature; the solid has also adsorbed a few isolated Cs and O_1 particles, whose rigidity was found to be considerable at moderate temperatures. The path of the migrating particle in the absence of any second component is restricted only to the shaded area between these equipotential contours; but where this area is covered by comparatively immobile Cs or O_1, freedom of movement in their directions is curtailed. A very sparse distribution may even block several adjacent channels and keep any one migrating atom to a small region of surface. Wherever any irregularity of distribution in the underlying solid allows a local opening of path, otherwise closed by the interspersed O_1 or Cs, a sudden increase in migration takes place; the picture thus adapts itself to the phenomena of lattice edges and fissures to be discussed in § 5.

Conclusion of § 4. We have shown, by analysing the components of displacement of given models, that the probability of an adsorbed atom being laterally mobile or rigidly attached will depend on its size and on the force laws of its adsorption bond. Selected examples of each of these dependencies range from rigid oxygen through semi-rigid alkalis to very mobile diatomic and inert gases and ions and the greatest

mobility of all substances on gas-covered surfaces. Penetration of a second layer through a first layer is in certain cases determined by mobility of the outer component, in others by that of the inner, but may be inhibited by the loading of one atom by another and by the lateral repulsion between complex molecular structures. If a penetration is effected, a single layer of more than one component exhibits the state of aggregation of a fluid whose movement is restricted to definite channels.

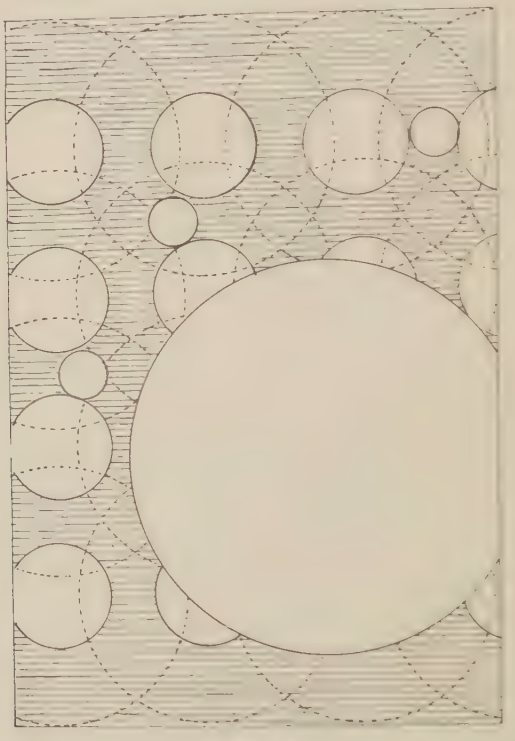

Figure 8.

§ 5. PENETRATION AT EDGES AND FISSURES IN A SOLID SURFACE

It is well known that irregularities in the microcrystalline structure of solids play a large part in the catalytic activity of their surfaces, and also in the extent to which impurities from both inside and outside a metal become enabled to modify its thermionic and photoelectric emission. If a group of surface atoms becomes partially isolated by the non-uniform distribution of its neighbours, its valencies must be less saturated than if it were completely surrounded, so that a denser clustering of any single adsorbate will be liable to occur in the neighbourhood; further, if two components are present in the gas phase, the increased probability of their adsorption in juxtaposition to each other at such points, edges, and corners, will increase locally the catalytic activity of the metal for reactions between those two gases. Beyond these general effects, we enquire whether any local modifications

of catalytic activity can be ascribed to irregularities which modify our previous conclusions regarding penetrability of layers on a plane lattice.

As previously, the behaviour of front and rear portions of a long chain molecule, adhering perpendicularly to an interface, throws light on the behaviour of the two superposed components of a double layer. If the surface contains an isolated projection, the head of the chain can reach the mean plane while the tail lies alongside the raised excrescence, and similarly a fissure allows the head to go below the mean surface while the tail is level with the plane. In both cases the outer portion of the molecule has access to atoms of the solid from which it is otherwise withheld. Since decomposition of organic molecules forms the main experimental basis of the projecting-patch theory of catalysis (and indeed the applicability of that theory to reactions other than the decomposition in question has been challenged), the explanation may partly be attributable to such penetration by an outer portion of an orientated molecule which would, at a perfectly plane surface, never reach the metal.

Extending the term "penetration" from the behaviour of the rear portion of a long single molecule to that of the outer component of a double layer, let us take three conventionalized types of irregularity, of which any actual surface region will present instances similar in principle to but more complex in detail than the proposed models.

Projection above plane lattice. Consider an idealized lattice on which projects a single row of additional atoms. On the solid is adsorbed a saturated layer of larger atoms, and on this layer impinge smaller atoms. So long as the projecting atoms and the two gas components differ considerably in size, the former introduce gaps in the regular packing of the otherwise saturated layer, allowing the second component of smaller size to enter between the projection and the first component. Access to the solid will occur at temperatures too low for normal interpenetration of the two gases to be attained by the mechanism discussed in connexion with migration of the lower layer, and a number of the smaller atoms will accumulate in any such hollows of atomic size caused by the presence of the projection. Reactions in which these small atoms take part will tend to be accelerated along such linear projections, since this trap greatly extends the duration of their life in the unevaporated state. Such an effect will be greatest for the greatest discrepancy in size between the gaseous components, and for the greatest mobility of the smaller atom. Since the latter condition will be best fulfilled if the projecting row of atoms are not themselves too strongly attracting, the effect of the projection may be greater if it consists of partly inert foreign particles than if it consists of the underlying metal itself: thus we approach the conception of a non-reacting promoter facilitating the catalytic powers of a more active solid.

Parallel-sided fissure of atomic width. Consider a fissure whose width is not greater than that of the larger atoms of the first gas component. In this case the second component has not the additional mode of access which, in the case of a projection above a plane lattice, allowed it to undermine a saturated layer. But when once any ordinary penetration at the top of the fissure sets in, accumulation of the second and smaller component in the vacant space below can proceed, draining

the gas phase into the metal by decreasing continuously the chance of re-evaporation of the dissolved gas. All consequences of penetration of the first layer by the second will thus be accelerated from such point sources or line sources.

Narrowing fissure. In most practical cases the open end of a fissure is wider than the largest atom: the principal difference between this case and the last is in the chance of escape of reactants and of products of reaction; this decides whether the reactions initiated at a fissure proceed indefinitely or are terminated. In general, if the fissure is wide enough for the larger atoms also to accumulate in it, their presence will accelerate reactions in which they take part but will retard reactions involving only the other components and the solid, by blocking the way to evaporation.

In addition to the above types of mechanism, by which surface irregularities anticipate and accelerate the plane penetrations discussed in previous sections, all fissures and projections cause local suspension of the inhibitions of interpenetration of layers by lateral repulsion.

By introducing third and fourth components of varied properties, the models can be extended, in principle, to allow discussion of catalytic poisons as well as of promoters. Another extension is indicated where lattice irregularities cause transmission and accumulation of material which was initially in the interior of the metal instead of in the gas phase. A molecular mechanism of penetrability is required for the phenomena of release from solid solution, e.g. the renewal of surface layers from within a thoriated filament, and the effect thereon of existing deposits from outside.

The very much simplified structures to which we have confined attention are sufficient to indicate that the common preparation of a solid for chemical activity by heating and by alternate oxidation and reduction must cover a very complex sequence of physical processes, which will rarely be either reversible or repeatable; a single treatment may succeed in mobilizing each component to take advantage of fissure growth, but its repetition at excess temperature may lead to inhibition of activity by sintering or closure of fissures. Up to a certain point, increase of subdivision of a solid facilitates most of the mechanisms we have described, to a limit based on the following considerations. Let A be the activity of a surface, defined by the velocity of reaction of given components striking unit area under given conditions of temperature and pressure. Then if unit activity is that of which the perfect lattice is capable and A' the added activity at grain-boundaries or fissure-edges,

$$A = 1 + A',$$

$$A' = f\left(\frac{n_1}{n_2}\right),$$

where n_1 is the number of particles striking an edge and n_2 the number striking the plane area, and f is some function.

In the simplest case where square grains are separated by cracks of the kind first studied by Smekal and by Zwicky, $n_1 n_2$ will increase a hundredfold during any subdivision of the surface which reduces average grain-length from 10^{-3} cm. to 10^{-5} cm., for atoms about 3×10^{-8} cm. in diameter. Where f is a constant, and made

arge by favourable development of some of the irregular penetrations which we have uggested, A will be increased by any treatment which tends to break up the solid, p to a limiting ratio of n_1/n_2 set by the size of the gas particles.

§ 6. CONCLUSION

It has been shown that only in certain restricted circumstances can two substances adsorbed from the gaseous phase maintain stable existence as superposed trata, even if the one is completely condensed before the other is admitted to the urface. In general the two substances will interpenetrate with greater or lesser apidity, in certain cases sharing a single layer of monomolecular thickness, and in thers reversing their order of proximity to the underlying solid. The occurrence f these interpenetrations has been related to regular and irregular structure of the olid, to dimensions and force laws of any two adsorbed components, and to their mobilities and the several inhibitions controlling the latter. All the results have been btained by very much simplified models and conventionalized force laws; only to he extent that actual oxygen, hydrogen, inert gases, alkali vapours, etc., have roperties describable in terms of these simple models, will the conclusions apply to hese substances.

It is hoped next to deal quantitatively with certain of the problems treated here nly in general outline.

REFERENCES

(1) General reference, Reimann, *Thermionic Emission* (1934).
(2) General reference, Hughes and DuBridge, *Photoelectric Phenomena* (1932).
(3) General reference, *Faraday Society Discussion on Gas Adsorption* (1932).
(4) Slater. *Phys. Rev.* **36**, 57 (1930).
(5) Langmuir and Villars. *J. Amer. chem. Soc.* **53**, 486 (1931).
(6) Taylor and Langmuir. *Phys. Rev.* **44**, 423 (1933).
(7) Lennard-Jones. *Trans. Faraday Soc.* **28**, 333 (1932).

535·52

CONVERGENT POLARIZED LIGHT AND HERTZ'S PROBLEM FOR A UNIAXIAL MATERIAL

By F. F. P. BISACRE, O.B.E., M.A., B.Sc.

Received November 1, 1934. *Read in title December* 21, 1934.

ABSTRACT. The paper gives a mathematical treatment of the behaviour of convergent polarized light passing through a uniaxial crystal, together with some practical details relating to the production of rings and brushes. The Fresnel wave surface is shown to be the isophasic for a system of waves diverging from a point source in the crystal. Explicit expressions are given, in terms of elementary functions, for the electric and magnetic fields and the energy-stream, both far from and close to the source; and the validity of Fresnel's construction is discussed.

§ 1. INTRODUCTION

On account of purely technical mathematical difficulties the classical theory of the optics of crystals is usually based almost entirely upon plane waves; the Fresnel wave surface is deduced as the envelope of a system of plane waves passing through the crystal in all directions.

In making instruments to exhibit the well-known rings and brushes, opticians have carefully reproduced the conditions that have had to be assumed in the mathematical theory. But the usual rings and brushes can be produced as easily and as brilliantly with truly divergent polarized light as with the artificial system of plane waves that is usually described as "convergent polarized light," much to the mystification of the student.

An attempt is made in this paper to show that in the case of a uniaxial crystal the Fresnel wave surface is not merely the envelope of a system of plane waves passing through the material, but the actual isophasic for a system of waves diverging from a point-source in the crystal. No attempt is made here to deal with the much more difficult mathematical problem of a biaxial crystal*. The problem is, of course, to solve Hertz's problem for a uniaxial material.

* One of the earliest treatments of this problem (from the elastic solid standpoint) was given, nearly a century ago, by Lamé, and can be found in his treatise *Leçons sur la Théorie mathématique de l'Élasticité des Corps solides* (Paris, 1852, 2nd ed., 1866). Certain general solutions have been discussed by Herglotz, who used mathematical methods of extreme difficulty. His papers are: "Ueber die Integration linearer partieller Differentialgleichungen mit Konstanten Koefficienten, Teile I, II, III." *Ber. sächs. Ges.* (*Akad.*) *Wiss.* 78 (1926) (I, II), 80 (1928) (III); "Ueber die Integration linearer partieller Differential-gleichungen mit Konstanten Koefficienten," *Abh. math. Sem. hamburg. Univ.* 6, Heft 7 (1928). See also S. Kowalewski, "Über die Brechung des Lichtes in kristallinischen Mitteln", *Acta Math.* (1885); V. Volterra, "Sur les vibrations dans les milieux biréfringents", *Acta Math.* (1892); J. Grünwald, "Ausbreitung der Wellenbewegungen in optisch zweiachsigen elastichen Medien", *Boltzmann-Festschrift* (Leipzig, 1904).

§ 2. CALCULATION OF THE MAGNETIC AND ELECTRIC FIELDS

We begin with Lorentz's equations for a set of principal axes,

$$\left.\begin{aligned} c\left(\frac{\partial H_z}{\partial y}-\frac{\partial H_y}{\partial z}\right)&=4\pi\rho v_x+K_1\dot{E}_x\\ c\left(\frac{\partial H_x}{\partial z}-\frac{\partial H_z}{\partial x}\right)&=4\pi\rho v_y+K_1\dot{E}_y\\ c\left(\frac{\partial H_y}{\partial x}-\frac{\partial H_x}{\partial y}\right)&=4\pi\rho v_z+K_3 E_z\end{aligned}\right\} \quad \ldots\ldots(1),$$

H, E

c, ρ
v, K
x, y, z

so that Oz is the axis of symmetry of the material.

$$-c\ \text{curl}\ \mathbf{E}=\dot{\mathbf{H}} \quad \ldots\ldots(2),$$

$$\text{div}\ \mathbf{H}=0 \quad \ldots\ldots(3),$$

$$\text{div}\ \mathbf{D}=\rho \quad \ldots\ldots(4),$$

where
$$D_x=K_1E_x/4\pi, \text{ etc.} \quad \ldots\ldots(5),$$

D

and by (4)
$$K_1\frac{\partial E_x}{\partial x}+K_1\frac{\partial E_y}{\partial y}+K_3\frac{\partial E_z}{\partial z}=4\pi\rho \quad \ldots\ldots(6).$$

We assume that ρ and $\mathbf{v}$ are given as functions of position and time, where $\mathbf{v}$ is the velocity of electric charge. Assume, as usual, that $\mathbf{A}$ is a vector potential such that

$\mathbf{v}$
$\mathbf{A}$

$$\mathbf{H}=\text{curl}\ \mathbf{A},$$

then
$$\dot{\mathbf{H}}=\text{curl}\ \dot{\mathbf{A}},$$

and, by (2),
$$-c\ \text{curl}\ \mathbf{E}=\text{curl}\ \dot{\mathbf{A}},$$

i.e.
$$\text{curl}\ (\dot{\mathbf{A}}+c\mathbf{E})=0,$$

or, since curl grad $\phi=0$,

$$\mathbf{E}=-\dot{\mathbf{A}}/c-\text{grad}\ \phi \quad \ldots\ldots(7),$$

ϕ

where ϕ is an arbitrary scalar function of x, y, z and t.

Thus (1) becomes

$$\left.\begin{aligned} c\left(\frac{\partial H_z}{\partial y}-\frac{\partial H_y}{\partial z}\right)&=4\pi\rho v_x+K_1\left(-\frac{\ddot{A}_x}{c}-\frac{\partial\dot{\phi}}{\partial x}\right)\\ c\left(\frac{\partial H_x}{\partial z}-\frac{\partial H_z}{\partial x}\right)&=4\pi\rho v_y+K_1\left(-\frac{\ddot{A}_y}{c}-\frac{\partial\dot{\phi}}{\partial y}\right)\\ c\left(\frac{\partial H_y}{\partial x}-\frac{\partial H_x}{\partial y}\right)&=4\pi\rho v_z+K_3\left(-\frac{\ddot{A}_z}{c}-\frac{\partial\dot{\phi}}{\partial z}\right)\end{aligned}\right\} \quad \ldots\ldots(8),$$

for, since
$$\begin{aligned}\text{curl}\ \mathbf{H}&=\text{curl curl}\ \mathbf{A}\\ &=\text{grad div}\ \mathbf{A}-\Delta\mathbf{A},\end{aligned}$$

Δ

$$\left.\begin{aligned} 4\pi\rho v_x-\frac{K_1}{c}\ddot{A}_x+c\Delta A_x&=\frac{\partial}{\partial x}(c\ \text{div}\ \mathbf{A}+K_1\phi)\\ 4\pi\rho v_y-\frac{K_1}{c}\ddot{A}_y+c\Delta A_y&=\frac{\partial}{\partial y}(c\ \text{div}\ \mathbf{A}+K_1\phi)\\ 4\pi\rho v_z-\frac{K_3}{c}\ddot{A}_z+c\Delta A_z&=\frac{\partial}{\partial z}(c\ \text{div}\ \mathbf{A}+K_3\phi)\end{aligned}\right\} \quad \ldots\ldots(9).$$

A has, so far, been incompletely defined; its curl only is specified so far. We complete its specification by defining its divergence and this we do by putting

$$c \operatorname{div} \mathbf{A} + K_1 \dot{\phi} = 0 \qquad \text{.....(10),}$$

hence the first two equations of (9) become

$$\left.\begin{aligned} c\Delta A_x - \frac{K_1}{c}\ddot{A}_x &= -4\pi\rho v_x \\ c\Delta A_y - \frac{K_1}{c}\ddot{A}_y &= -4\pi\rho v_y \end{aligned}\right\} \qquad \text{.....(11),}$$

and the third $$c\Delta A_z - \frac{K_3}{c}\ddot{A}_z = -4\pi\rho v_z + c\,\frac{K_1 - K_3}{K_1}\,\frac{\partial}{\partial z}\operatorname{div}\mathbf{A} \qquad \text{.....(12),}$$

or, somewhat more conveniently,

$$\left.\begin{aligned} &\left(-\frac{K_1}{c^2}\frac{\partial^2}{\partial t^2} + \frac{\partial^2}{\partial x^2} + \frac{\partial^2}{\partial y^2} + \frac{\partial^2}{\partial z^2}\right) A_x = -\frac{4\pi\rho v_x}{c} && (a) \\ &\left(-\frac{K_1}{c^2}\frac{\partial^2}{\partial t^2} + \frac{\partial^2}{\partial x^2} + \frac{\partial^2}{\partial y^2} + \frac{\partial^2}{\partial z^2}\right) A_y = -\frac{4\pi\rho v_y}{c} && (b) \\ &\left[-\frac{K_1}{c^2}\frac{\partial^2}{\partial t^2} + \frac{\partial^2}{\partial z^2} + \frac{K_1}{K_3}\left(\frac{\partial^2}{\partial x^2} + \frac{\partial^2}{\partial y^2}\right)\right] A_z = -\frac{4\pi\rho v_z}{c} \times \frac{K_1}{K_3} \\ &\qquad + \frac{K_1 - K_3}{K_3}\frac{\partial}{\partial z}\left(\frac{\partial A_x}{\partial x} + \frac{\partial A_y}{\partial y}\right) && (c) \end{aligned}\right\} \qquad \text{...(13).}$$

We shall suppose a Hertzian electric dipole [1] at the origin with its axis pointing in any direction. We can choose the axes so that $v_y = 0$, i.e. so that the axis of the dipole lies in the xz plane. Equation 13 (b) now disappears as well as the last term in the last bracket on the right of equation 13 (c). Equation 13 (a) in A_x is a standard wave equation and has a well-known solution having a suitable singularity at the origin and vanishing at infinity to the proper order. It is

$$A_x = \frac{\dot{M}_x}{cr}\, e^{ip(t - r/a)} \qquad \text{.....(14),}$$

$\dot{M}$, M where by $\dot{M}_x$ we mean $ip M_x$, M_x being the maximum value of the x component of the electric moment of the dipole, and

$$\left.\begin{aligned} \frac{c^2}{K_1} &= a^2 \\ r^2 &= x^2 + y^2 + z^2 \end{aligned}\right\} \qquad \text{.....(14a).}$$

r and

We are left with equation 13 (c) to solve. Since a solution having the required singularity at the origin and vanishing at infinity in the proper way is unique, we only need a particular integral of equation 13 (c). We can obtain it in the following $A_{z,0}$ way. A_z can be considered as made up of two parts, $A_{z,0}$ coming from the *first* $A_{z,1}$ term on the right of equation 13 (c) and $A_{z,1}$ from the second term. We have then

$$\left[-\frac{1}{a^2}\frac{\partial^2}{\partial t^2} + \frac{\partial^2}{\partial z^2} + \frac{K_1}{K_3}\left(\frac{\partial^2}{\partial x^2} + \frac{\partial^2}{\partial y^2}\right)\right] A_{z,0} = -\frac{K_1}{K_3}\frac{4\pi\rho v_z}{c},$$

or, putting $x, y = \sqrt{\left(\frac{K_1}{K_3}\xi\right)},\ \sqrt{\left(\frac{K_1}{K_3}\eta\right)}$, ξ, η

$$= \frac{1}{\beta}\xi,\ \frac{1}{\beta}\eta, \qquad \beta$$

we have $$\left(\Delta' - \frac{1}{a^2}\frac{\partial^2}{\partial t^2}\right) A_{z,0} = -\frac{K_1}{K_3}\frac{4\pi\rho v_z}{c} \qquad \text{.....(15),}$$

where $$\Delta' \equiv \frac{\partial^2}{\partial\xi^2} + \frac{\partial^2}{\partial\eta^2} + \frac{\partial^2}{\partial z^2}.$$

This is a standard case like the last, so

$$A_{z,0} = \frac{1}{\beta^2}\frac{\dot{M}_z}{cP}\, e^{ip(t-P/a)} \qquad \text{.....(16),}$$

where $$P^2 = \xi^2 + \eta^2 + z^2 \qquad P$$
$$= \beta^2(x^2+y^2) + z^2.$$

This wave is a point-source spherical wave in ξ, η, z space and so a spheroidal wave in x, y, z space. We are now left to find $A_{z,1}$, where

$$\left[-\frac{1}{a^2}\frac{\partial^2}{\partial t^2} + \frac{\partial^2}{\partial z^2} + \frac{1}{\beta^2}\left(\frac{\partial^2}{\partial x^2} + \frac{\partial^2}{\partial y^2}\right)\right] A_{z,1} = \left(\frac{1-\beta^2}{\beta^2}\right)\frac{\partial^2}{\partial z\,\partial x}\left\{\frac{\dot{M}_x}{cr}\, e^{ip(t-r/a)}\right\} \quad \text{...(17).}$$

Put $$\frac{1-\beta^2}{\beta^2}\frac{\partial B}{\partial z} = A_{z,1} \qquad B$$

and $$B' = Bc/\dot{M}_x \qquad B'$$
$$= \partial g/\partial x \qquad g$$

} .....(18),

then $$\left[-\frac{1}{a^2}\frac{\partial^2}{\partial t^2} + \frac{\partial^2}{\partial z^2} + \frac{1}{\beta^2}\left(\frac{\partial^2}{\partial x^2} + \frac{\partial^2}{\partial y^2}\right)\right] g = \frac{1}{r}\, e^{ip(t-r/a)}$$

or $$\left[-\frac{1}{a^2}\frac{\partial^2}{\partial t^2} + \frac{\partial^2}{\partial z^2} + \frac{1}{\beta^2}\left(\frac{\partial^2}{\partial\rho^2} + \frac{1}{\rho}\frac{\partial}{\partial\rho}\right)\right] g = \frac{1}{\sqrt{(\rho^2+z^2)}}\, e^{ip(t-(\rho^2+z^2)^{\frac{1}{2}}/a)} \quad \text{...(19),}$$

where $$r^2 = x^2+y^2+z^2 = \rho^2+z^2. \qquad \rho$$

Now it is possible that, if

$$\left(\frac{\partial^2}{\partial\rho^2} + \frac{1}{\rho}\frac{\partial}{\partial\rho}\right) g' = \frac{1}{\sqrt{(\rho^2+z^2)}}\, e^{ip(t-(\rho^2+z^2)^{\frac{1}{2}}/a)},$$

then $$\left(-\frac{1}{a^2}\frac{\partial^2}{\partial t^2} + \frac{\partial^2}{\partial z^2}\right) g' = \frac{G}{\sqrt{(\rho^2+z^2)}}\, e^{ip(t-(\rho^2+z^2)^{\frac{1}{2}}/a)} \qquad \text{.....(19 a),}$$

where G is some *constant**; and this supposition proves to be true, as we shall now show. We can easily solve

$$\rho\frac{\partial^2 g'}{\partial\rho^2} + \frac{\partial g'}{\partial\rho} = \frac{\rho}{\sqrt{(\rho^2+z^2)}}\, e^{ip(t-(\rho^2+z^2)^{\frac{1}{2}}/a)},$$

i.e. $$\frac{\partial}{\partial\rho}\left(\rho\frac{\partial g'}{\partial\rho}\right) = \frac{\partial}{\partial\rho}\left\{-\frac{a}{ip}\, e^{ip(t-(\rho^2+z^2)^{\frac{1}{2}}/a)}\right\},$$

i.e. $$\rho\frac{\partial g'}{\partial\rho} = -\frac{a}{ip}\, e^{ip(t-(\rho^2+z^2)^{\frac{1}{2}}/a)},$$

i.e. $$g' = -\frac{a}{ip}\int_\infty^\rho \frac{1}{\rho}\, e^{ip(t-(\rho^2+z^2)^{\frac{1}{2}}/a)}\, d\rho \qquad \text{.....(20).}$$

* Dr John Dougall suggested this to me.

Differentiating twice with respect to z, we get

$$\frac{\partial^2 g'}{\partial z^2} = \int_\infty^\rho \frac{\rho}{r^3} e^{ip(t-r/a)}\, d\rho - \frac{ip}{a}\int_\infty^\rho \frac{z^2}{\rho r^2} e^{ip(t-r/a)}\, d\rho \qquad \text{.....(21),}$$

and differentiating twice with respect to t and dividing by $-a^2$ we get

$$-\frac{1}{a^2}\frac{\partial^2 g'}{\partial t^2} = \frac{ip}{a}\int_\infty^\rho \frac{1}{\rho} e^{ip(t-r/a)}\, d\rho \qquad \text{.....(22).}$$

Adding equations (21) and (22), we get

$$\left(-\frac{1}{a^2}\frac{\partial^2}{\partial t^2} + \frac{\partial^2}{\partial z^2}\right) g' = \int_\infty^\rho \left(\frac{\rho}{r^3} + \frac{ip}{a}\cdot\frac{\rho}{r^2}\right) e^{ip(t-r/a)}\, d\rho$$

$$= \int_\infty^\rho \frac{\partial}{\partial \rho}\left\{-\frac{1}{r} e^{ip(t-r/a)}\right\} d\rho$$

$$= -\frac{1}{r} e^{ip(t-r/a)};$$

hence G of equation 19 (a) is given by

$$G = -1 \qquad \text{.....(23),}$$

so the hypothesis is proved.

We can now easily get a solution of equation (19).

λ, g' Let $g = \lambda g'$, where g' is the function given by equation (20); then, substituting in equation (19), we get

$$\left[-\lambda\left(\frac{1}{r} e^{ip(t-r/a)}\right) + \frac{\lambda}{\beta^2}\left(\frac{1}{r} e^{ip(t-r/a)}\right)\right] = \frac{1}{r} e^{ip(t-r/a)},$$

i.e.

$$\lambda\left(\frac{1}{\beta^2} - 1\right) = 1,$$

$$\therefore \lambda = \frac{\beta^2}{1-\beta^2} \qquad \text{.....(24),}$$

and

$$g = \frac{\beta^2}{1-\beta^2} g'$$

solves equation (19), where

$$g' = -\frac{a}{ip}\int_\infty^\rho \frac{1}{\rho} e^{ip(t-\sqrt{(\rho^2+z^2)}/a)}\, d\rho \qquad \text{.....(25),}$$

and, by equation (18),

$$B' = \frac{\beta^2}{1-\beta^2}\cdot\frac{\partial g'}{\partial x} = \frac{Bc}{\dot{M}_x} \qquad \text{.....(26);}$$

$$\therefore B = \frac{\dot{M}_x}{c}\cdot\frac{\beta^2}{1-\beta^2}\cdot\frac{\partial g'}{\partial x},$$

$A_{z,1}$ and

$$A_{z,1} = \frac{\dot{M}_x}{c}\cdot\frac{\partial^2 g'}{\partial z\,\partial x} = \frac{\dot{M}_x}{c}\cdot\frac{\partial}{\partial z}\cdot\left(\frac{\partial g'}{\partial \rho}\cdot\frac{\partial \rho}{\partial x}\right)$$

$$= \frac{\dot{M}_x}{c}\cdot\frac{xz}{\rho^2}\cdot\frac{1}{r}\cdot e^{ip(t-r/a)} \qquad \text{.....(27).}$$

This function has a singularity along the whole z-axis. We can remove it in the following way:

Since $\xi=\beta x$, $\eta=\beta y$, we get

$$\left[-\frac{1}{a^2}\frac{\partial^2}{\partial t^2}+\frac{\partial^2}{\partial z^2}+\frac{1}{\beta^2}\left(\frac{\partial^2}{\partial x^2}+\frac{\partial^2}{\partial y^2}\right)\right]u\equiv\left(-\frac{1}{a^2}\frac{\partial^2}{\partial t^2}+\frac{\partial^2}{\partial z^2}+\frac{\partial^2}{\partial \xi^2}+\frac{\partial^2}{\partial \eta^2}\right)u\,(\xi,\eta,z).$$

We know from equations (20) and (23) that

$$u=-\frac{a}{ip}\int_\infty^R\frac{1}{R}e^{ip(t-P/a)}\,dR \qquad \text{.....(28),} \qquad u$$

where $R^2=\xi^2+\eta^2=\beta^2(x^2+y^2)$ R

and $P^2=R^2+z^2$ P .....(29)

lead to the equation $$\left(\frac{\partial^2}{\partial\xi^2}+\frac{\partial^2}{\partial\eta^2}\right)u=-\left(-\frac{1}{a^2}\frac{\partial^2}{\partial t^2}+\frac{\partial^2}{\partial z^2}\right)u,$$

i.e. $$\left(-\frac{1}{a^2}\frac{\partial^2}{\partial t^2}+\Delta'\right)u=0,$$

i.e. $$\left[-\frac{1}{a^2}\frac{\partial^2}{\partial t^2}+\frac{\partial^2}{\partial z^2}+\frac{1}{\beta^2}\left(\frac{\partial^2}{\partial x^2}+\frac{\partial^2}{\partial y^2}\right)\right]u=0.$$

We can consequently add any multiple we please of

$$\frac{\dot{M}_x}{c}\cdot\frac{\xi z}{R^2}\cdot\frac{1}{P}e^{ip(t-P/a)}$$

to the solution already obtained; compare equation (27). Let us add $-\beta$ times this expression, where

$$-\beta\xi z/R^2=-xz/\rho^2.$$

The complete solution is then

$$A_{z,1}=\frac{\dot{M}_x}{c}\cdot\frac{xz}{\rho^2}\left(\frac{1}{r}e^{ip(t-r/a)}-\frac{1}{P}e^{ip(t-P/a)}\right) \qquad \text{.....(30),}$$

which has a singularity at the origin only. Our vector potential is then

$$A_x=\frac{\dot{M}_x}{cr}\cdot e^{ip(t-r/a)},$$

$$A_z=\frac{1}{\beta^2}\cdot\frac{\dot{M}_z}{cP}\,e^{ip(t-P/a)}$$

$$+\frac{\dot{M}_x}{c}\cdot\frac{xz}{\rho^2}\left(\frac{1}{r}e^{ip(t-r/a)}-\frac{1}{P}e^{ip(t-P/a)}\right) \qquad (31),$$

where $\beta^2=K_3/K_1$

and $P^2=\beta^2(x^2+y^2)+z^2.$

The electromagnetic field is at once given from this vector potential, since

$$\left.\begin{aligned}&\mathbf{H}=\operatorname{curl}\mathbf{A}\\&\mathbf{E}=-\dot{\mathbf{A}}/c-\operatorname{grad}\phi\\&c\operatorname{div}\mathbf{A}+K_1\phi=0\end{aligned}\right\} \qquad \text{.....(32).}$$

and

where

The first of these equations gives the readiest means of calculating **H** from **A**; but, once **H** is known, **E**, for points at a distance, can be more simply found directly from Lorentz's equations observing that the first three become

$$c \operatorname{curl} \mathbf{H} = (K_1, K_1, K_3)\, \dot{\mathbf{E}}$$

except at the origin, giving $\dot{\mathbf{E}}$ and hence **E** immediately. Since A_z alone involves purely spherical waves, it is immediately clear that H_z, alone of all the six components of the field, proceeds exclusively on a spherical isophasic. We propose to examine the fields due to these vector potentials, at a considerable distance from the origin, bearing in mind that for this purpose we need only differentiate the exponential functions, treating the rest of the expressions for the A's as constant.

§ 3. THE SPHERICAL WAVE

F Put $$A_x' = F.e^{-i\alpha r}.e^{ipt}, \text{ where } F.e^{ipt} = \frac{\dot{M}_x}{cr}\, e^{ipt},$$

G $$A_z' = G.e^{-i\alpha r}.e^{ipt}, \text{ where } G.e^{ipt} = \frac{xz}{\rho^2}.\frac{\dot{M}_x}{cr} e^{ipt}$$

α and $$\alpha = p/a.$$

Then, the common factor e^{ipt} being omitted,

$$\left.\begin{aligned} H_x &= (-i\alpha).\frac{xyz}{r\rho^2}.Fe^{-i\alpha r} \\ H_y &= (-i\alpha).\frac{y^2 z}{r\rho^2}.Fe^{-i\alpha r} \\ H_z &= (-i\alpha).\left(-\frac{y(x^2+y^2)}{r\rho^2}\right).Fe^{-i\alpha r} \end{aligned}\right\} \quad \ldots\ldots(33).$$

This result shows that, if $$\mathbf{R} = (x, y, z),$$

$$(\mathbf{RH}) = 0,$$

i.e. **H** is perpendicular to the radius vector, **R**.

From equation (33) we get at once the real forms of H:

$$\left.\begin{aligned} H_x &= \frac{p^2}{a}.\frac{M_x}{cr}.\frac{xyz}{\rho^2 r}.\cos p\left(t-\frac{r}{a}\right) \\ H_y &= \frac{p^2}{a}.\frac{M_x}{cr}.\frac{y^2 z}{\rho^2 r}.\cos p\left(t-\frac{r}{a}\right) \\ H_z &= -\frac{p^2}{a}.\frac{M_x}{cr}.\frac{y(x^2+y^2)}{\rho^2 r}.\cos p\left(t-\frac{r}{a}\right) \end{aligned}\right\} \quad \ldots\ldots(34).$$

The amplitude of H is therefore

$$|H| = \frac{p^2}{a}.\frac{y}{\rho}.\frac{M_x}{cr} \quad \ldots\ldots(35)$$

and

$$h = \frac{p^2}{a}.\frac{y}{\rho}.\frac{M_x}{cr}\cos p\left(t-\frac{r}{a}\right) \quad \ldots\ldots(35a),$$

where h is the numerical value of the whole magnetic vector at any time and place.

To calculate the electric vector, we have

$$c \operatorname{curl} \mathbf{H} = (K_1, K_1, K_3)\, ip\mathbf{E},$$

i.e.

$$\left.\begin{aligned} E_x &= \frac{c}{ipK_1} (\operatorname{curl} \mathbf{H})_x \\ E_y &= \frac{c}{ipK_1} (\operatorname{curl} \mathbf{H})_y \\ E_z &= \frac{c}{ipK_3} (\operatorname{curl} \mathbf{H})_z \end{aligned}\right\} \quad \ldots\ldots(36),$$

whence

$$\left.\begin{aligned} E_x &= -\frac{ip}{c} \cdot \frac{y^2 r^2}{\rho^2 r^2} \cdot F e^{-i\alpha r} \\ E_y &= +\frac{ip}{c} \cdot \frac{xyr^2}{\rho^2 r^2} \cdot F e^{-i\alpha r} \\ E_z &= 0 \end{aligned}\right\} \quad \ldots\ldots(37);$$

so the real forms are:

$$\left.\begin{aligned} E_x &= \frac{p^2}{c} \cdot \frac{M_x}{cr} \cdot \frac{y^2 r^2}{\rho^2 r^2} \cdot \cos p\left(t - \frac{r}{a}\right) \\ E_y &= -\frac{p^2}{c} \cdot \frac{M_x}{cr} \cdot \frac{xyr^2}{\rho^2 r^2} \cos p\left(t - \frac{r}{a}\right) \\ E_z &= 0 \end{aligned}\right\} \quad \ldots\ldots(38).$$

The scalar product $(\mathbf{RE})$ is again zero, so $\mathbf{E}$ is perpendicular to the radius vector. Also $(\mathbf{EH}) = 0$; therefore $\mathbf{E}$ and $\mathbf{H}$ are perpendicular. Also, since $E_z = 0$, $\mathbf{E}$ lies wholly in the plane parallel to xy, i.e. $\mathbf{E}$ lies along the parallel of latitude and $\mathbf{H}$ lies along the meridian through the point. The amplitude of $\mathbf{E}$ is

$$\frac{p^2}{c} \cdot \frac{M_x}{cr} \cdot \frac{y}{\rho} \quad \ldots\ldots(39)$$

and

$$e = \frac{p^2}{c} \cdot \frac{M_x}{cr} \cdot \frac{y}{\rho} \cdot \cos p\left(t - \frac{r}{a}\right) \quad \ldots\ldots(40),$$

where e is the numerical value of the whole electric vector. The vector product is

$$|[\mathbf{EH}]| = \mathbf{eh} = \frac{p^4}{ca} \cdot \left(\frac{M_x}{cr}\right)^2 \cdot \frac{y^2}{\rho^2} \cdot \cos^2 p\left(t - \frac{r}{a}\right) \quad \ldots\ldots(41)$$

and, if

$$\begin{aligned} x &= r \sin\theta \cos\phi, \\ y &= r \sin\theta \sin\phi, \\ z &= r \cos\theta, \\ y/\rho &= \sin\phi; \end{aligned}$$

hence, since the Poynting vector $\mathbf{S}$ is given by

$$\mathbf{S} = \frac{c}{4\pi} [\mathbf{EH}],$$

energy radiates outwards on the spherical wave at a mean rate $S_{m,1}$, where

$S_{m,1}$

$$S_{m,1}=\frac{c}{8\pi}\cdot\frac{p^4}{ca}\cdot\left(\frac{M_x}{cr}\right)^2\sin^2\phi$$

$$=\frac{1}{8\pi}\cdot\frac{p^4}{c^2a}\cdot\frac{M_x^2}{r^2}\cdot\sin^2\phi \qquad \text{.....(42).}$$

It is evident that $S_{m,1}$ is constant all over any meridian; on a given isophasic it varies with the longitude only.

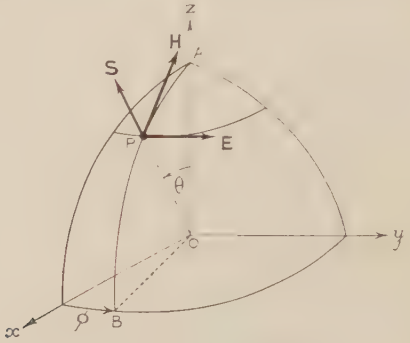

Figure 1. Spherical field.

§ 4. THE SPHEROIDAL WAVE

We now want a similar calculation for the spheroidal wave.

Put
$$A_z''=\left(\frac{1}{\beta^2}\cdot\frac{\dot{M}_z}{cP}-\frac{xz}{\rho^2}\cdot\frac{\dot{M}_x}{cP}\right)e^{-i\alpha P}\cdot e^{ipt} \qquad \text{.....(43)}$$

$$=ipBe^{-i\alpha P}\cdot e^{ipt},$$

where
$$Be^{ipt}=\left(\frac{1}{\beta^2}\cdot\frac{M_z}{cP}-\frac{xz}{\rho^2}\cdot\frac{M_x}{cP}\right)e^{ipt} \qquad \text{.....(44),}$$

and observe that
$$\frac{\partial P}{\partial x}=\beta^2\frac{x}{P},\quad\text{where}\quad\beta^2=K_3/K_1,$$

β
$$\frac{\partial P}{\partial y}=\beta^2\frac{y}{P},$$

$$\frac{\partial P}{\partial z}=\frac{z}{P},$$

since
$$P^2=\beta^2(x^2+y^2)+z^2.$$

Then, the common factor e^{ipt} being omitted,

$$\left.\begin{aligned}H_x&=\frac{\partial A_z}{\partial y}=(-i\alpha)\cdot\beta^2\cdot\frac{y}{P}\cdot ipBe^{-i\alpha P}\\ H_y&=-\frac{\partial A_z}{\partial x}=-(-i\alpha)\beta^2\frac{x}{P}\cdot ipBe^{-i\alpha P}\\ H_z&=0\end{aligned}\right\} \qquad \text{.....(45).}$$

This shows that $(\mathbf{RH})=0$, i.e. $\mathbf{H}$ is perpendicular to the radius vector, $\mathbf{R}$.

The real form of **H** is

$$H_x=\frac{p^2}{a}.\beta^2.\frac{y}{P}.B.\cos p\left(t-\frac{P}{a}\right),$$

$$H_y=-\frac{p^2}{a}.\beta^2.\frac{x}{P}.B.\cos p\left(t-\frac{P}{a}\right),$$

$$H_z=0.$$

The amplitude of **H** is $\frac{p^2}{a}.\beta^2.\frac{\rho}{P}.B,$

so that $$h=\frac{p^2}{a}.\beta^2.\frac{\rho}{P}.B.\cos p\left(t-\frac{P}{a}\right) \qquad \text{.....(46),}$$

where B is defined by equation (44).

We can calculate the electric vector by the formula (36).

$$\left.\begin{aligned} E_x&=+\frac{ip}{c}.\beta^2.\frac{xz}{P^2}.ipB.e^{-i\alpha P}\\ E_y&=+\frac{ip}{c}.\beta^2.\frac{yz}{P^2}.ipB.e^{-i\alpha P}\\ E_z&=-\frac{ip}{c}.\beta^2.\frac{\rho^2}{P^2}.ipB.e^{-i\alpha P}\end{aligned}\right\} \qquad \text{.....(47).}$$

Consequently the real values are:

$$\left.\begin{aligned} E_x&=-\frac{p^2}{c}.\beta^2.\frac{xz}{P^2}.B.\cos p\left(t-\frac{P}{a}\right)\\ E_y&=-\frac{p^2}{c}.\beta^2.\frac{yz}{P^2}.B.\cos p\left(t-\frac{P}{a}\right)\\ E_z&=+\frac{p^2}{c}.\beta^2.\frac{\rho^2}{P^2}.B.\cos p\left(t-\frac{P}{a}\right)\end{aligned}\right\} \qquad \text{.....(48).}$$

The amplitude of **E** is $\frac{p^2}{c}.\beta^2.\frac{\rho r}{P^2}.B;$

$$\therefore\ e=\frac{p^2}{c}.\beta^2.\frac{\rho r}{P^2}.B\cos p\left(t-\frac{P}{a}\right).$$

Equation (47) shows that **E** is perpendicular to **R**; also, by equations (45) and (47),

$$(\mathbf{EH})=0,$$

so that **E** is perpendicular to **H**.

The vector product of **E** and **H** is

$$\frac{p^4}{ac}.\beta^4.\frac{\rho^2 r}{P^3}.B^2.\cos^2 p\left(t-\frac{P}{a}\right)$$

and consequently the mean rate, $S_{m,2}$, of radiation of energy is $S_{m,2}$

$$S_{m,2}=\frac{1}{8\pi}.\frac{p^4}{c^2aP^2}.\left(\frac{r}{P}\right)^3\sin^2\theta\,\{M_z-\beta^2M_x\cos\phi\cot\theta\}^2 \qquad \text{.....(49),}$$

where $$P^2=\beta^2(x^2+y^2)+z^2 \qquad \text{.....(50).}$$

Since $H_z = 0$, the **H** vector lies along a parallel of latitude of the spheroid and **E** in the meridian plane, perpendicular to **R**. **D**, however, is along the meridian, as can be easily shown, so that **D** and **H** lie in the tangent plane at P.

The Poynting vectors of each system are radial. Since the **E** of one field is parallel to the **H** of the other, the radiation of energy is given by the sum of $S_{m.1}$ due to the spherical field and $S_{m.2}$ due to the spheroidal field. This follows from the fact that

$$[\mathbf{A}+\mathbf{B}, \mathbf{C}+\mathbf{D}] = [\mathbf{AC}]+[\mathbf{BD}]$$

if **B**, **C** are parallel and **A**, **D** are parallel. It is also clear that if we draw the tangent plane to the spheroid at P, the projection of the radius vector from O on to this tangent plane lies in the plane containing the meridian through P. This

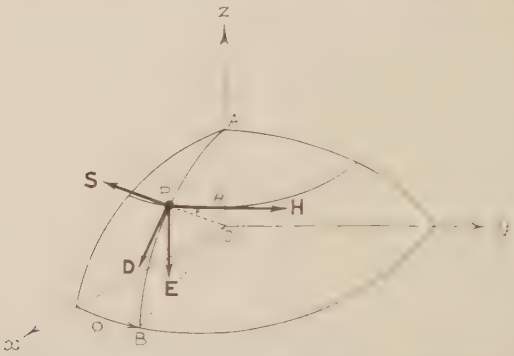

Figure 2. Spheroidal field. **S** is along OP and perpendicular to **E** and **H**; **D** and **H** lie in tangent plane at P; **D** and **E** lie in plane OAB.

projection therefore gives the plane in which **E** and **D** lie, as it should by Fresnel's rule. It will be seen from equation (31) that if we make M_1 equal to 0 the spherical field vanishes entirely, leaving only the spheroidal field due to M_2. If we now let $K_3 \to K_1$ (the isotropic case), this spheroidal field becomes spherical. Thus the spherical field of the isotropic case of an electric dipole is the degenerate spheroidal field—it is not the spherical field of the electric dipole in an aelotropic medium. Hence the **E** and **H** vectors are directed in accordance with the well-known results for the isotropic case. The directions of **E** and **H** for the aelotropic spherical field are perpendicular to these directions. If we start with an isotropic material and a dipole along Oz a spherical wave is generated. If we now introduce aelotropy by letting K_3 differ from K_1 while $K_1 = K_2$, this spherical wave becomes spheroidal. If we now let the dipole become oblique so that M_2 exists, then a new spherical wave makes its appearance.

§ 5. FIELD VERY CLOSE TO THE ORIGIN

Suppose $r \ll \lambda$, say $r = \lambda/100$. The most complicated form we have to differentiate, spatially, is

$$\frac{xz}{\rho^2}\cdot\frac{1}{r}\cdot e^{-i\alpha r} = \frac{xz}{\rho^2}\cdot\frac{1}{r}\left(1 - i\alpha r - \frac{\alpha^2 r^2}{2} \cdots\right)$$

$$= \frac{xz}{\rho^2}\cdot\frac{1}{r} - i\alpha\frac{xz}{\rho^2} - \text{positive powers of } r,$$

so that, when r and $\rho \to 0$ every quantity that matters comes from the first term; i.e. the retardation of phase becomes insignificant. It is therefore of little useful purpose to distinguish the two wave fields; it is more convenient to consider separately the field due to M_x and that due to M_z.

Field due to M_x. The vector potential is now given by

$$\left.\begin{aligned} A_x &= \frac{1}{r} \\ A_z &= \frac{xz}{\rho^2}\left(\frac{1}{r}-\frac{1}{P}\right) = \frac{(\beta^2-1)\,xz}{Pr\,(P+r)} \end{aligned}\right\} \qquad \text{.....(51),}$$

each multiplied by $ipM_x/c \,.\, e^{ipt}$.

These functions have singularities at the origin only.

To calculate $\mathbf{E}$ it is best to use the formula

$$\left.\begin{aligned} \mathbf{E} &= -\frac{\dot{\mathbf{A}}}{c} - \text{grad}\,\phi \\ \dot{\phi} &= -\frac{c}{K_1}\,\text{div}\,\mathbf{A} \end{aligned}\right\} \qquad \text{.....(52).}$$

where

Here grad ϕ is the important term, for it is two orders lower in r than $\dot{\mathbf{A}}$. Hence

$$\mathbf{E} \approx -\text{grad}\,\phi,$$

where

$$\dot{\phi} = -\frac{c}{K_1}\,\text{div}\,\mathbf{A},$$

and

$$\begin{aligned} \text{div}\,\mathbf{A} &= \frac{\partial A_x}{\partial x} + \frac{\partial A_z}{\partial z} \\ &= -\beta^2 \cdot \frac{x}{P^3} \times \frac{ipM_x}{c} \cdot e^{ipt}. \end{aligned}$$

If we put

$$\dot{\phi} = ip\Phi e^{ipt}$$

we get

$$\Phi = \frac{K_3}{K_1^2} \cdot M_x \cdot \frac{x}{P^3} \qquad \text{.....(53),}$$

and

$$\left.\begin{aligned} E_x &= -\frac{K_3}{K_1^2} \cdot M_x \cdot \frac{\partial}{\partial x}\left(\frac{x}{P^3}\right) e^{ipt} \\ E_y &= -\frac{K_3}{K_1^2} \cdot M_x \cdot \frac{\partial}{\partial y}\left(\frac{x}{P^3}\right) e^{ipt} \\ E_z &= -\frac{K_3}{K_1^2} \cdot M_x \cdot \frac{\partial}{\partial z}\left(\frac{x}{P^3}\right) e^{ipt} \end{aligned}\right\} \qquad \text{.....(54).}$$

When $K_3 = K_1$ equation (53) reduces to

$$\Phi = \frac{1}{K_1} \cdot M_x \cdot \frac{x}{r^3} = -\frac{\partial}{\partial x}\left(\frac{M_x}{K_1 r}\right),$$

which is the correct potential for an electrostatic doublet of moment M_x in an isotropic medium of dielectric constant K_1. The vector defined by equation (54) is not perpendicular to the radius vector. The H field can be calculated immediately from equation (51), if it is wanted.

If we put $p=0$ in equation (54), we get the electrostatic field due to the doublet at rest.

Field due to M_z. In this case

$$A_x=0,$$
$$A_y=0,$$
$$A_z=\frac{1}{P}\cdot\frac{ipM_z}{\beta^2 c}\cdot e^{ipt}$$

and

$$\Phi=\frac{1}{K_3}\cdot M_z\cdot\frac{z}{P^3}$$
$$=-\frac{\partial}{\partial z}\left(\frac{M_z}{K_3 P}\right) \qquad \text{.....(55),}$$

and therefore

$$\left.\begin{aligned} E_x&=-\frac{1}{K_3}\cdot M_z\cdot\frac{\partial}{\partial x}\left(\frac{z}{P^3}\right)e^{ipt}\\ E_y&=-\frac{1}{K_3}\cdot M_z\cdot\frac{\partial}{\partial y}\left(\frac{z}{P^3}\right)e^{ipt}\\ E_z&=-\frac{1}{K_3}\cdot M_z\cdot\frac{\partial}{\partial z}\left(\frac{z}{P^3}\right)e^{ipt}\end{aligned}\right\} \qquad \text{.....(56).}$$

If $p=0$ in equation (56) we get the electrostatic field for this dipole, at rest. Since $A_x=0=A_y$, the magnetic lines of force corresponding to this field are circles lying in planes perpendicular to Oz and having their centres on the Oz axis.

It is evident from these solutions that an electric dipole always generates a spheroidal wave. It will not generate the spherical wave if M_z is zero, i.e. if the dipole lies wholly along the Oz axis, so that such a dipole generates a purely spheroidal field. One surmises that a purely spherical field would be generated by a magnetic dipole lying wholly along Oz, and this proves to be the case.

Equation (13c) is consistent with $A_z=0$ if

$$v_z=0$$

and

$$\frac{\partial A_x}{\partial x}+\frac{\partial A_y}{\partial y}=0,$$

i.e.

$$A_x=-\frac{\partial F}{\partial y}$$
$$A_y=+\frac{\partial F}{\partial x},$$

F where

$$F=F(x, y, z, t).$$

Also, by equation (13b), $\quad -\frac{1}{a^2}\ddot{A}_y+\Delta A_y=0, \quad$ since $v_y=0,$

hence

$$-\frac{1}{a^2}\ddot{F}+\Delta F=0,$$

giving

$$A_x=-\frac{\partial}{\partial y}\left\{\frac{1}{r}u\left(t-\frac{r}{a}\right)\right\}$$

and
$$A_y = +\frac{\partial}{\partial x}\left\{\frac{1}{r}u\left(t-\frac{r}{a}\right)\right\},$$

i.e.
$$H_x = -\frac{\partial^2}{\partial z\,\partial x}\left\{\frac{1}{r}u\left(t-\frac{r}{a}\right)\right\},$$
$$H_y = -\frac{\partial^2}{\partial z\,\partial y}\left\{\frac{1}{r}u\left(t-\frac{r}{a}\right)\right\},$$
$$H_z = +\left(\frac{\partial^2}{\partial x^2}+\frac{\partial^2}{\partial y^2}\right)\left\{\frac{1}{r}u\left(t-\frac{r}{a}\right)\right\},$$

which is easily shown to be the field due to a magnetic dipole along Oz at the origin*. A field due to electric and magnetic dipoles along the axis of symmetry Oz consists of physically distinct fields, a radial spheroidal field due to the electric dipoles and a radial spherical field due to the magnetic dipoles. The field due to an isolated oblique dipole cannot be generated by a combination of electric and magnetic dipoles along Oz, for the compensating waves do not appear in either of these special cases.

The spheroidal isophasic is given by

$$t-\sqrt{(\xi^2+\eta^2+z^2)}/a = \text{a constant, say zero,}$$

where
$$\xi=\beta x,\ \eta=\beta y,\ \beta^2=K_3/K_1;$$

so that
$$K_3(x^2+y^2)+K_1z^2=C^2t^2 \qquad (57),$$

where C is the velocity of light in vacuo, or, alternatively, C

$$\frac{x^2}{c^2}+\frac{y^2}{c^2}+\frac{z^2}{a^2}=t^2 \qquad \text{.....(58),} \qquad a, c$$

i.e.
$$\frac{x^2}{c^2}+\frac{y^2}{c^2}+\frac{z^2}{a^2}=1, \text{ for } t=1 \qquad \text{.....(59),}$$

which is precisely Fresnel's form.

The Fresnel spheroid is, then, a genuine isophasic for a divergent wave, even close to the origin. The isophasics of the spherical field are obviously the spheres

$$r=a \qquad (60),$$

so that the Fresnel surface

$$(r^2-a^2)(a^2x^2+a^2y^2+c^2z^2-a^2c^2)=0$$

is a true isophasic for a wave diverging from a point source in a uniaxial crystal. The spheroids (58) are such that, if two are drawn for values of t, say t' and t'', t', t'' then the lengths of the radii r' and r'' drawn in the same direction are given by r', r''

$$\frac{r''}{r'}=\frac{t''}{t'} \qquad \text{.....(61),}$$

a relation true for any direction. Consequently the velocity of the spheroid in any fixed radial direction is constant, but of course it is different for different directions. The radii of

$$\frac{x^2}{c^2}+\frac{y^2}{c^2}+\frac{z^2}{a^2}=1=F(x,y,z) \qquad \text{.....(62)}$$

* Cf. the standard Hertz problem in an isotropic medium.

$\mathcal{V}$ consequently give the ray speed $\mathcal{V}$ for point-source spheroidal fields, at points
V sufficiently far from the origin, for we have shown that the Poynting vector is then radial. The sheet itself advances everywhere normally to itself at a speed V which varies from point to point in the sheet. Equation (58) is

$$F(x, y, z, t) = 0,$$

so that the speed is given by

$$|V| = -\frac{\partial F/\partial t}{\{\Sigma(\partial F/\partial x)^2\}^{\frac{1}{2}}}$$

$$= \frac{1}{\{(x_0^2+y_0^2)/c^4 + z_0^2/a^4\}^{\frac{1}{2}}},$$

P when $t=1$, at the point $P(x_0, y_0, z_0)$.

The tangent plane at P is

$$\frac{x_0 X}{c^2} + \frac{y_0 Y}{c^2} + \frac{z_0 Z}{a^2} - 1 = 0 \qquad \ldots\ldots(63),$$

and the perpendicular distance from O to this plane is

$$\frac{1}{\{(x_0^2+y_0^2)/c^4 + z_0^2/a^4\}^{\frac{1}{2}}},$$

i.e. the phase speed at P (defined as the speed at which the isophasic advances normally to itself) is equal to the perpendicular distance from O on to the tangent plane at P, i.e. the usual Fresnel rule holds good, and

$$\mathcal{V}\cos\widehat{rn} = V.$$

§ 6. CONCLUSIONS

(i) The Fresnel surface

$$(r^2-a^2)(a^2x^2+a^2y^2+c^2z^2-a^2c^2) = 0$$

is the true isophasic system ($t=1$) for divergent light radiating from an electric dipole with its axis in any direction, in a uniaxial crystal.

(ii) Provided we are far enough from the origin for the space derivatives of $e^{i\alpha r}$ to swamp the space derivatives of such quantities as $\frac{xz}{\rho^2}\cdot\frac{1}{r}$ or $\frac{1}{r}$, then the direction of the Poynting vector for each wave system is radial and the **E** and **H** of each wave system lie in the plane perpendicular to the radius vector and are perpendicular to each other, i.e., $\mathbf{E}_1 \perp \mathbf{H}_1$ and $\mathbf{E}_2 \perp \mathbf{H}_2$; but $\mathbf{E}_1$ is also perpendicular to $\mathbf{E}_2$. For the spherical wave, **H** lies in a meridian; for the spheroidal wave, **E** lies in the meridian plane. For the spheroidal wave, $\mathbf{E} \perp \mathbf{R}$ the radius vector, and therefore does not lie in the tangent plane, in which both **H** and **D** lie. Since the two systems of vectors are cross-perpendicular, i.e. $\mathbf{E}_1 \perp \mathbf{E}_2$ and $\mathbf{H}_1 \perp \mathbf{H}_2$, the resultant Poynting vector is merely the sum of the Poynting vectors for each system.

(iii) The well-known Fresnel construction for finding the direction of **D**, and hence the plane containing **E**, for the spheroidal field, and also the relation between

the ray speed $\mathcal{V}$ and the phase speed V apply at points sufficiently far from the origin.

(iv) Fresnel's rules do not apply quite close to the origin, $r \leqslant \lambda$, for the wave system is not really established in this region. Here the electric field is the electrostatic field due to the dipole, varying sinusoidally with time without appreciable phase lag due to distance.

(v) If the spherical and spheroidal waves are to be considered separately we must exclude points on the z axis, for each of these waves separately gives indeterminate fields on the z axis; for example, H_x by formula (33) contains the factor $\cos\theta . \cos\phi . \sin\phi$, and if we let $\theta \to 0$ the value of H_z is not unique because it depends on the meridian along which we have approached the point on the z axis. The whole field due to both waves is, however, perfectly determinate at all points except the origin. This is an interesting instance of a case where the actual field cannot be completely resolved, everywhere, into two waves, a spherical one and a spheroidal one. The formulae (53) and (55) show that, when these equations are taken jointly, the whole electric field given by them is precisely what it should be close to the origin.

§ 7. PRACTICAL DETAILS

In order to produce the rings and brushes as simply as possible the writer has found the following modifications in a Reichart microscope to be sufficient.

(i) A brass ring was turned which fitted into the sub-stage in place of the ordinary condenser fitting. Into one end of this ring the polarizing prism was fitted, and into the other screwed end the usual condenser lens was screwed. This condenser illuminated the bottom surface of a specimen of crystal with a spot of highly convergent polarized light. Such a source is, of course, not the same as an ideal electric dipole source.

(ii) A lens was fitted into an adapter carrying an analysing prism and this adapter was screwed into the end of the draw-tube in place of the usual stop. This arrangement merely converted the draw-tube into a weak microscope for viewing the back of the objective and passing only polarized light; see figure 3. With this arrangement the usual rings and brushes are seen brilliantly both with uniaxial material (quartz and calcite) and biaxial material (arragonite). The most convenient objective was the No. 3 Reichart ($\frac{2}{3}$ in.).

If the draw-tube is withdrawn altogether, the rings and brushes are visible quite clearly to the naked eye if a nicol prism is held in front of the eye and crossed. They appear on the back of the object glass. In the specimens examined, the uniaxial material was cut perpendicular to the optical axis and the biaxial material, perpendicular to the bisector of the axes. The detailed theory of the ring-formation would be difficult for these conditions of illumination, since the isophasic emerging from the crystal into air is not even spherical for the ordinary wave and is still less so for the extraordinary wave. These surfaces, outside the crystal, are not congruent, whereas with plane waves, they are. But symmetry alone is sufficient

to secure the formation of the rings. It follows that if the wave-retardation is sufficient to cause blackness with crossed nicols at the point r, ϕ it will do so, whatever ϕ is, in the case of a uniaxial material cut perpendicular to the optical axis, and at $-r, \phi$ in the case of a biaxial material cut perpendicular to the bisector of the optical axes.

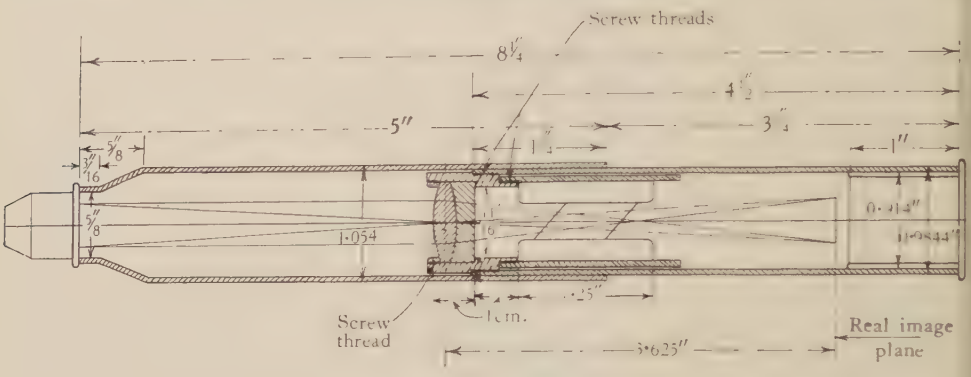

Figure 3.

§ 8. ACKNOWLEDGMENT

In conclusion, it is a pleasant duty to express my gratitude to Dr John Dougall. He has not only undertaken the tedious work of checking the calculations but has made many very helpful criticisms and suggestions.

REFERENCE

(1) Riemann-Weber. *Differentialgleichungen der Physik*, **2**, 421, § 4.

621.396.11 : 551.51.053.5

THE PROPAGATION OF MEDIUM RADIO WAVES IN THE IONOSPHERE

By D. F. MARTYN, Ph.D., A.R.C.Sc., F.Inst.P., Research Physicist,
Australian Radio Research Board

Communicated by Prof. O. U. Vonwiller, July 9, 1934. *Read in title November* 2, 1934.

ABSTRACT. All the available measurements of sky-wave intensities at medium frequencies are collated and expressed as field-strength, distance curves for six typical wavelengths and for distances from 25 to 1000 km. It is shown how this material may be used for the determination of the non-fading radii of broadcasting emitters over country of any effective conductivity. From the observational material an empirical expression for the reflection coefficient of the lower E layer of the ionosphere is derived. It is shown that the observations are incompatible with the existence of a linear or parabolic gradient of ionization in this layer. This incompatibility is not removed by the assumption of an absorbing or D region below the E layer, or by consideration of the variation with height of the collision frequency ν of an electron with the air molecules in the E layer. It is found that the observations can be fully explained if the gradient of ionization is given by the exponential form $N = \epsilon^h$, where h is the height in km. above the region where ionization first becomes appreciable. This gradient also gives rise to equivalent heights which are in agreement with experience. It is found that ν has a value of 10^6 collisions per second at a height of 90 km., in close agreement with Chapman's recent estimate. It is shown that the conclusions reached are not affected by use of the ray methods of geometrical optics, or by neglect of the influence of the earth's magnetic field.

§ 1. INTRODUCTION

A large number of measurements have been made in recent years of the field-intensities due to stations emitting on broadcasting frequencies. In general this field is composed of two parts, that due to the ground-propagated wave and that due to the downcoming wave produced by reflection or refraction in the ionosphere. The propagation of the former wave is reasonably well understood, principally owing to the work of Watson[27], Sommerfeld[26] and T. L. Eckersley[12]. The applicability of the analyses of these authors has been confirmed by a large number of measurements accumulated in all parts of the world during the last few years.

Until quite recently few data had been published which would permit a full analysis of sky-wave-propagation at these frequencies. The early work of Appleton and Ratcliffe[5] has now been supplemented by the measurements of the Union Internationale de Radio-Diffusion[11] in Europe, the Federal Radio Commission[23] in America, and the Radio Research Board in Australia[8, 17].

In this paper it is proposed first to review these measurements and to set out

curves depicting the variation of field-intensity of the sky wave at distances up to 1000 km. over a frequency spectrum ranging from 1500 to 150 kc./sec. Secondly, this material will be utilized to derive information regarding certain aspects of the structure of the *E* layer of the ionosphere, notably the ionization gradient, the value of the collision frequency of an electron with the air molecules, and the possibility of the existence of an absorbing region at a level below the *E* layer.

§ 2. DISCUSSION OF FIELD-INTENSITY DATA

Examination of the large number of measurements cited above reveals good agreement between the field-intensities of the sky wave obtained in Europe, America and Australia during 1930 and 1931, years of slightly less than average sunspot activity. There is evidence[22] that field-intensities at these frequencies decrease with increasing sunspot activity, so that we may expect sky-wave intensities to reach their maximum values this year. There is not sufficient evidence, however, to indicate whether there will be a differential influence over the radio-frequency spectrum under consideration. On the whole, it seems probable that variation of sunspot activity will only affect the absolute values of the sky-wave intensities, and will not influence appreciably the variation of intensities with frequency and distance from the emitter.

On all frequencies there is evidence of a steady increase of intensity with distance from the emitter, extending up to distances of about 600 km. Thereafter the field decreases steadily, and beyond 2000 km. it appears to fall off according to an inverse-distance law.

For distances less than about 1200 km. there is evidence that the higher frequencies are rather less attenuated than the lower. In this region, however, the ratio of the field-intensities at the extreme ends of the frequency spectrum is seldom greater than 2 : 1, and at greater distances than 1200 km. the attenuation appears to be independent of frequency.

The sky wave fluctuates rapidly from minute to minute and from night to night, so that it is obviously a matter of some difficulty to select from the measurements a quantity which will be truly representative of the sky-wave field-intensity. It has been suggested by a committee at the Lucerne conference that quasi-maximum intensities be employed for this purpose[24].

The quasi-maximum intensities are defined as those values of field-intensity which are exceeded during only 5 per cent of the time of observation. With this definition the sky wave reaches an intensity of 0·35 mV. m. at a distance of 500 km. on a frequency of 1500 kc./sec. for 1 kW. of radiated power, while all frequencies give a value of about 0·04 mV./m. at a distance of 2000 km.

§ 3. AN EMPIRICAL FORMULA FOR SKY-WAVE FIELD-INTENSITIES

As a preliminary to theoretical investigation an attempt has been made to develop a single empirical formula which would express adequately the variations of the observed intensities over the range of observation. If we assume that the

ERRATA

"A new precision colorimeter", by JOHN J. MANLEY, M.A., D.Sc. Oxon., *Proc. phys. Soc.* **47**, 70 (1935), line 1:

for 0·1 mm. *read* 1·0 mm.

"The propagation of medium radio waves in the ionosphere", by D. F. MARTYN, Ph.D., A.R.C.Sc., F.Inst.P., *Proc. phys. Soc.* **47**, 325–334 (1935):

for ¶ *read* π

radiating properties of the emitting aerial in the vertical plane may be expressed by a cosine law, i.e. that the energy radiated at an angle θ with the horizontal is proportional to $\cos\theta$, then the sky-wave field-intensity E at a distance R km. in the horizontal plane is given by[12]

θ

E, R

$$E=\frac{3\sqrt{(10\,W)}.r\cos\theta}{\sqrt{(R^2+4H_0^2)}}\ \text{mV./m.} \qquad \ldots\ldots(1),$$

where W watts is the total power radiated, H_0 is the height of the reflecting layer in kilometres, and r is the reflection coefficient of the layer.

W, H_0

r

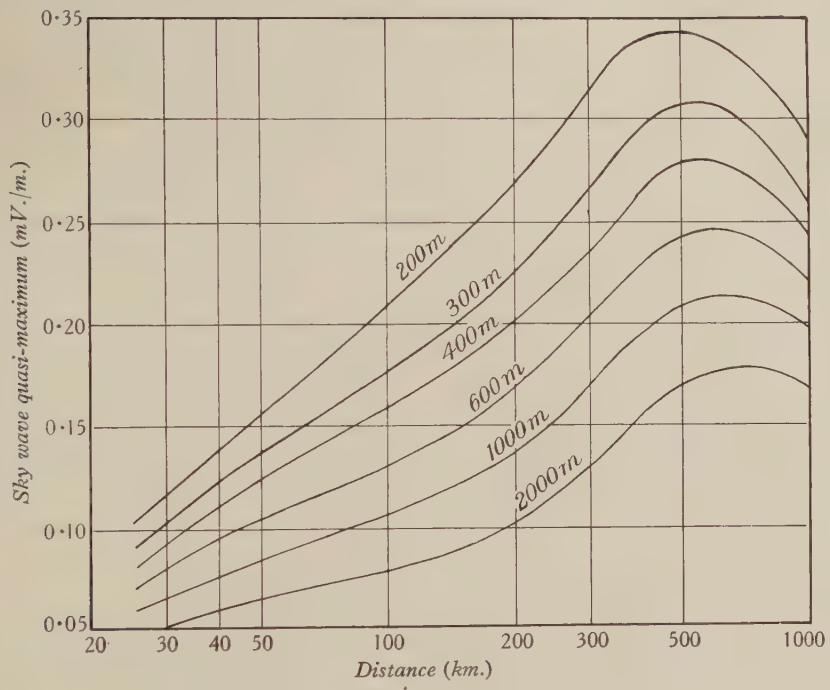

Figure 1.

If the power radiated be 1 kW. then

$$E=\frac{0{\cdot}3rR}{R^2+4H_0^2}\ \text{V./m.} \qquad \ldots\ldots(2).$$

Practically all evening transmission of the sky wave at these frequencies is due to the E layer of the ionosphere, so that without incurring much error we may assign to H_0 an average value of 100 km., and then the only unknown quantity in this equation is r. If now we write for r the empirical expression

$$r=3{\cdot}3\epsilon^{-\cos^2(i_0-35^\circ)\log_{10}\lambda} \qquad \ldots\ldots(3),$$

where

$$i_0=\frac{\P}{2}-\theta,$$

i_0

and λ is the wave-length in metres, then it is found that equation (2) gives a very close approximation to the observed field-intensities. The intensities calculated from equations (2) and (3) are shown in figure 1 for six typical wave-lengths and for

λ

distances ranging from 25 km. to 1000 km. Beyond about 1000 km., radio transmission at these frequencies must occur chiefly by multiple reflections between the earth and the ground, so that the equations cannot be expected to apply without modification.

The curves in figure 1 may be used to determine the distance from a broadcasting station at which fading first becomes serious. This happens when the quasi-maximum sky-wave intensity is equal to one-half the ground-wave intensity. It follows that if ground-wave field-intensity, distance curves be superposed on figure 1, and if an average ground conductivity of 10^{-13} e.m.u. be assumed, with

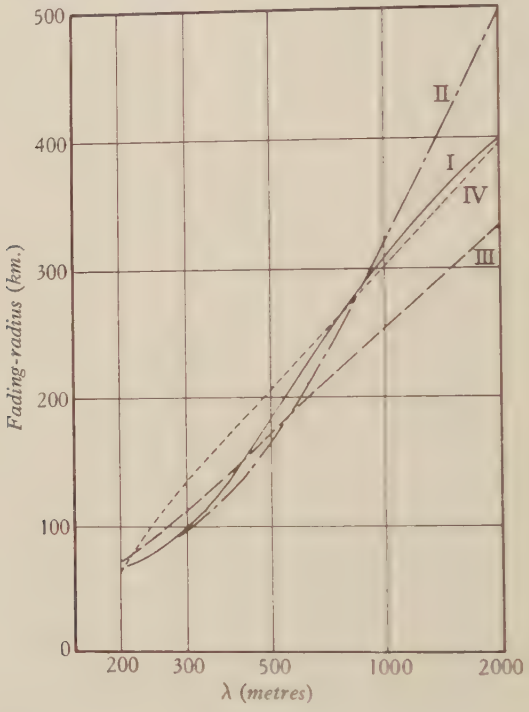

Figure 2.

a scale of field-intensities double that shown for the sky wave in figure 1, then the fading-radius is given by the intersection of the ground-wave and sky-wave curves for the desired wave-length λ. For ground of conductivity other than 10^{-13} e.m.u., it is only necessary to substitute for the ground-wave curve of wave-length λ the curve of equivalent[3] wave-length λ', and to utilize the intersection of this curve with the sky-wave curve of wave-length λ. In this way a curve has been derived showing the variation of fading-radius with frequency, for country of average conductivity. It is shown in figure 2 as curve I. In the same figure, for comparison purposes, there are given curves which summarize the experience of broadcasting authorities. Curve II is due to the Union Internationale de Radio-Diffusion, curve III to the Federal Radio Commission, and curve IV to the Van der Pol committee.

It will be observed that curve I, which is derived from the above empirical formula for the sky-wave intensities, is in good agreement with the combined experience of these authorities.

Reverting to equation (3), it will be observed that the apparent reflection coefficient of the E layer attains a minimum value when the rays are incident at an angle of 35°. It is important to enquire whether this is a true indication of the variation of reflection from the layer with changing angle. Now in any formula of the type (3), if the angle 35° be omitted it is found that (2) gives a maximum of signal-strength at distances considerably less than the observed value of 500 km. The main object of the introduction of this angle is therefore to retard the increase of reflection coefficient with distance. Now in deriving equation (2) we have assumed that the polar radiation diagram of the emitting aerial in the vertical plane is given by a cosine law. There is little doubt that the majority of the aerials used in the actual measurements do not conform to this condition, since most aerials used for broadcasting are designed to radiate as strongly as practicable in the horizontal direction. They will therefore be expected to give a maximum sky wave at a greater distance from the emitter than would an aerial conforming to the cosine law. We therefore attribute the presence of the angle 35° in the formula to this circumstance of aerial design, and consider that it is not necessarily significant in respect of the reflection coefficient of the layer.

In applying these observations to the investigation of the structure of the ionosphere, care has therefore been taken to utilize only measurements made at the longer distances, where uncertainty regarding the high-angle radiation of the aerial becomes unimportant.

§ 4. THEORIES OF SKY-WAVE PROPAGATION

Appleton[2] has made a theoretical investigation of the variation of equivalent height with frequency and angle of incidence, and Appleton and Ratcliffe[5] have examined the dependence of the reflection coefficient of the E layer on the same quantities.

They have considered the two cases of a linear and parabolic gradient of ionization in the layer. In both cases it appears that h', the contribution to the equivalent height made by the path in the layer, should vary as some power of $\cos i_0$ and of p, the angular frequency of the wave. The same remarks apply to the theoretically deduced attenuation coefficients of the layer. The same workers have examined these problems experimentally, although over a somewhat limited range of variation of $\cos i_0$ and p. They found, contrary to expectation, that the attenuation coefficient of the layer was nearly constant for different angles of incidence of the wave, while the equivalent height appeared either to be constant or to increase slightly with increasing angles of incidence. In order to explain their results these authors have postulated the existence of a D region of ionization below the E region. They point out that a ray approaching the layer at a large angle of incidence will have travelled further in the D region and experienced greater absorption than one approaching

h'
p

at vertical incidence. In this way the theoretical decrease of attenuation in the E layer with increasing angle of incidence is offset.

Now it is easy to show that the balancing of these opposing tendencies can only be effective at a particular value of i_0, and moreover that this balance will be somewhat critical since it involves the third or fourth power of $\cos i_0$. Moreover for values of i_0 greater than the critical balancing value we should have an increase of attenuation with increasing i_0, a condition which is opposed to the facts revealed in § 3 above.

Again, these authors have suggested that the effect of the D region would be to increase the equivalent height of the E layer for increasing angles of incidence, owing to the "longer path in the D region." But if the equivalent path in the D region is $2D'$ for vertical incidence, then the contribution to the equivalent height of the E region is D', while in the same way, for angle of incidence i_0, the contribution of the D region to the equivalent path is $2D' \cos i_0$, and to the equivalent height is $2D' \cos i_0/2 \cos i_0$ or D'. It seems therefore that the D region cannot cause a variation of E-layer heights for varying angles of incidence in the manner suggested by Appleton and Ratcliffe.

D'

There is, however, another possible way in which the supposed D region could affect the E-layer equivalent heights. In its passage through the D region any ray must be diverted from its original line of travel. Simple optical considerations show that in such an event we have approximately

$$H' = H_0' + D\delta\mu/\cos^2 i_0,$$

where H' is the observed equivalent height,

H'

H_0' the equivalent height which would be observed in the absence of the D region,

H_0'

D the thickness of the D region, and

D

$(1-\delta\mu)$ the refractive index of the D region.

μ

It will be observed that the influence of the D region is to cause an increase of H' for increasing values of i_0. Now in Appleton and Ratcliffe's experiments $\cos^2 i_0$ varied from 1 to 0·75 and there was some evidence of an increase of H' with i_0. On the other hand, in some experiments conducted by the Radio Research Board in Australia and shortly to be published, it has been possible to extend the range of variation of $\cos^2 i_0$ from 1 to 0·25, and no marked variation of H' has been found. Now if the D region is responsible for the small variation of H' observed by Appleton and Ratcliffe, then we should expect the variation in the latter experiments to be three times as great, and consequently to be quite marked.

Summing up the above considerations, with regard to both the apparent absorption coefficients and equivalent heights of the E layer, it appears that the hypothesis of a D region is inadequate to explain the results. In what follows an attempt will be made to interpret the results, taking into account possible gradients of ionization in a single E layer and the probable variation of the collision frequency ν with height.

ν

§ 5. THE STRUCTURE OF THE *E* LAYER

It appears that the maximum ionization-density $N_{max.}$ in the *E* layer is attained around noon, typical values being of the order 2×10^5 electrons per cm.^{3}[4]. This value decreases steadily until about two hours after sunset, when the rate of decrease falls off considerably, leaving an almost steady ionization of the order of 10^4 electrons per cm.^{3} The latter figure is in good agreement with values obtained in Australia[21]. It appears that the height at which this maximum value exists is about 100 km. at noon, and somewhat higher during the night.

Our knowledge of the ionization-gradient is much less definite. For values of N approaching $N_{max.}$ from below there is some experimental[1] and theoretical[9] evidence to show that the gradient is approximately parabolic. There appears to be no reliable experimental evidence yet available concerning the gradient for small values of N. During night hours the position is even more obscure, there being evidence that the theory of Chapman is then invalid for the lower part of the *E* layer[29].

We shall therefore endeavour to make use of the observations quoted in §§ 2 and 4 above in order to derive information about the ionization-gradient in the lower part of the layer, since it is just this region that is responsible for the propagation of waves of medium radio frequencies. There is considerable evidence that the thickness of the *E* layer is large compared with the wave-lengths we are considering. Now it is not usual for these waves to penetrate the *E* layer, so that in general we shall be justified in neglecting the effect of electron-limitation on the intensity of the waves, and can confine ourselves to the consideration of absorption.

At present our knowledge of the value of ν at the level of the *E* layer is derived from three sources. These are (i) the kinetic theory of gases as applied to the earth's atmosphere, (ii) the observations of Lindeman and Dobson[18] on meteors, and (iii) the theory of Bailey and Martyn[6] on the interaction of radio waves. All three sources give a value for ν of $n \times 10^5$ per second, where n is a small integer. It is one of the objects of the present investigation to attempt to evaluate n more accurately. The variation of ν with height is given by the law

n

$$\nu = \nu_1 \epsilon^{-h/H},$$

where ν_1 is the value of ν at the beginning of the *E* layer,

ν_1

h the height above this level, and

h

H the height of the homogeneous atmosphere.

H

The quantity H is a slowly varying function of h but may safely be assumed to be constant over the region we shall consider. Its absolute value depends on the temperature and constitutes of the atmosphere in the *E* layer. It is probable that convection[20] exists at these levels, so that the composition of the atmosphere is not very different from that at the ground. The experiments of Whipple[28] on the refraction of sound-waves in the upper atmosphere, and the calculations of Gowan[14] taking account of absorption in the ozone layer, are in agreement with a temperature

of 300° K. Taking these considerations into account, H cannot differ greatly from 10 km. at the level of the E layer.

Evidence has been obtained by Green[15] that two layers of ionization may exist simultaneously at heights near to 100 km. This stratification of the E layer has also been observed recently by Ratcliffe and White[25] on wave-lengths of 75 m. and 150 m. For the wave-lengths and the angles of incidence which we are considering here, there is little doubt that reflection normally occurs from the lower of these two layers. It will be understood therefore that the conclusions reached below apply to this lower layer.

§ 6. STATEMENT OF THE PROBLEM

All the available evidence[5, 21] shows that long-distance transmission up to about 1000 km. is mainly due, at medium frequencies, to a wave which has undergone a single reflection from the E layer. The empirical formula developed in § 3 above therefore gives the actual reflection coefficient of the layer for the ranges of frequencies and angles of incidence specified. Appleton and Ratcliffe[5] have examined this reflection coefficient for the two cases of a linear and a parabolic gradient of ionization in the layer. They obtained a reflection coefficient equal to $\exp(-A\nu\cos^3 i_0/\lambda^2)$ in the first case, and to $\exp(-B\nu\cos^2 i_0\lambda)$ in the second, where A and B are constants. In each case a ray theory of refraction was used, and the influence of the earth's magnetic field and the variation of ν with height were neglected. It will be observed that both of these expressions for the reflection coefficient of the layer are in serious disagreement with the experimental results quoted in § 3, which show a small *decrease* in reflecting power with increasing wave-length. This discrepancy has been noted by Appleton and Ratcliffe in examining their own experimental results, and they have attributed it to the presence of an absorbing D region below the E layer, and or to the fact that ν varies with height.

It has been shown in § 4 that the existence of a D region during the night is incompatible with the evidence. The remaining alternative is examined in the following sections, where account is taken of the variation of ν with height.

In what follows we shall use a ray treatment, and neglect the influence of the earth's magnetic field, two approximations which require justification. It is well known that the methods of geometrical optics are only applicable when the change of optical properties of the medium in the course of a wave-length is small. This condition, which is of fundamental importance in the theory of wave mechanics, has been expressed by de Broglie[10] in the form

$$\mu\cos i\,\frac{d\left(\frac{1}{\mu}\right)}{dh}.\lambda \ll 1 \qquad \text{.....(4),}$$

where μ is the refractive index of the medium and h is the direction of maximum gradient in the layer. It will be observed that, for a given wave-length, this condition is most likely to be satisfied for long-distance transmission, where $\cos i$ is necessarily small. We shall then be justified in employing a ray treatment so long as the relation (4) is satisfied.

Turning now to the second proposed approximation we note that for long-distance propagation such as we are considering, in moderately high latitudes, transmission occurs approximately at right angles to the earth's magnetic field. Now in such event the magneto-ionic[3] theory shows that, in the now doubly-refracting layer, the ordinary ray will be propagated as if no magnetic field were present. For the lower wave-lengths the extraordinary ray will then be strongly absorbed and need not be considered further. On the other hand, for the longer wave-lengths in the broadcasting spectrum, the extraordinary ray may have a much smaller absorption coefficient than the ordinary ray, and at first sight it might seem that it could not be neglected. Closer analysis reveals however that the extraordinary wave must penetrate more deeply into the layer, and for likely conditions of ionization-gradient will be absorbed to much the same extent as the ordinary wave. Again, the polarization of the extraordinary wave is such that the magnetic vector is nearly vertical, so that it will produce but a small effect in an aerial at the surface of the ground.

Summing up these considerations we find that we shall be justified in neglecting the influence of the extraordinary ray in long-distance reception, and that we shall obtain a close approximation to the intensity of the ordinary wave by neglecting the earth's field entirely.

§ 7. A THEOREM

We shall be concerned below with the general case of a ray incident on the E layer at any angle of incidence. It is convenient to show that the results for any angle may be deduced from those for vertical incidence by a simple substitution.

Lorentz[19] has shown that the absorption by a dispersive medium of a wave of angular frequency p can be expressed by the coefficient

p

$$K=\frac{\nu}{2c\mu}\cdot\frac{4\P Ne^2}{m(p^2+\nu^2)} \qquad \text{.....(5),}$$

K

where the ratio of the intensity of the emergent wave to that of the incident wave is given by

$$\frac{E}{E_0}=\epsilon^{-\int\kappa ds} \qquad \text{.....(6),}$$

and μ, the refractive index of the medium, is given by

$$\mu^2=1-\frac{4\P Ne^2}{m(p^2+\nu^2)} \qquad \text{.....(7),}$$

and where c is the velocity of light in free space, and e, m are the charge and mass of an electron in e.s.u.

c, e, m

Let us further write

$$\rho^2=4\P e^2/m$$

ρ

and

$$N=\psi(h).$$

ψ

Then the absorption experienced by a wave at vertical incidence is given by

$$2\int_0^{h(\mu=0)}\kappa ds=\int_0^{h_0}\frac{\nu\,(1-\mu^2)}{c\mu}\,ds$$
$$=\int_0^{\psi^{-1}(p^2/\rho^2)}\frac{\nu_1\epsilon^{-h/H}\rho^2\psi\,(h)\,dh}{pc\sqrt{\{p^2-\rho^2\psi\,(h)\}}} \qquad \ldots\ldots(8).$$

provided $\nu^2\ll p^2$.

In the same way, for an angle of incidence i_0, the absorption is given by

$$2\int^{h\,(\mu=\sin i_0)}\kappa ds=\cos i_0\int_0^{\psi^{-1}(p^2\cos^2 i_0/\rho^2)}\frac{\nu_1\epsilon^{-h/H}\rho^2\psi\,(h)\,dh}{cp\cos i_0\sqrt{\{p^2\cos^2 i_0-\rho^2\psi\,(h)\}}} \qquad \ldots\ldots(9).$$

It follows that

$$\left(2\int_0^{h\sin i_0}\kappa ds\right)_{p,\,i_0}=\cos i_0\left(2\int_0^{h_0}\kappa ds\right)_{p\cos i_0,\,0} \qquad \ldots\ldots(10),$$

so that we need only investigate the absorption for vertical incidence, that at incidence i_0 being immediately deducible therefrom.

By similar reasoning it may be shown that the equivalent path P' in the layer for any angle of incidence may be deduced from that at vertical incidence by the relation

$$(P')_{p,\,i_0}=\frac{1}{\cos i_0}(P')_{p\cos i_0,\,0} \qquad \ldots\ldots(11).$$

§ 8. ANALYSIS OF LINEAR IONIZATION-GRADIENT

α Let us write $N=\alpha^2 h$

a and $a=p/\rho\alpha$.

η_0 Then for vertical incidence the attenuation η_0 is given by

$$\eta_0=2\int_0^{h_0}\kappa ds=\frac{\nu_1}{ac}\int_0^{a^2}\frac{h\epsilon^{-h/H}\,dh}{\sqrt{(a^2-h)}} \qquad \ldots\ldots(12).$$

Writing $h^{\frac{1}{2}}=a\cos\theta$, we have

$$\eta_0=\frac{2a^2\nu_1}{c}\epsilon^{-a^2/2H}\int_0^{\frac{\pi}{2}}\epsilon^{-a^2\cos 2\theta/2H}.\cos^3\theta d\theta \qquad \ldots\ldots(13).$$

To effect this integration we make use of Sonine's expansion,

$$\epsilon^{z\cos\theta}=I_0(z)+2\sum_{n=1}^{\infty}I_n(z)\cos n\theta,$$

where $I_n(z)$ is the modified Bessel coefficient given by

$$I_n(z)=\sum_{k=0}^{\infty}\frac{1}{\Pi(k)\,\Pi(n+k)}\left(\frac{z}{2}\right)^{n+2k},$$

and $\Pi(k)$ is Gauss's function having the values unity for $k=0$, and $k!$ for positive integral values of k.

Upon performing this integration, we have to a close approximation

$$\eta_0 = \frac{4a^2\nu_1}{3c}\epsilon^{-a^2/2H}\left(1-\frac{3a^2}{10H}+\frac{19a^4}{280H^2}-\frac{47a^6}{5040H^3}+\frac{a^8}{8870H^4}\right) \quad \ldots\ldots(14),$$

and hence for angle of incidence i_0, by (10),

$$\eta_{i0} = \frac{4a^2\nu_1\cos^3 i_0}{3c}\epsilon^{-a^2\cos^2 i_0/2H}\left(1-\frac{3a^2\cos^2 i_0}{10H}+\frac{19a^4\cos^4 i_0}{280H^2}-\frac{47a^6\cos^6 i_0}{5040H^3}+\frac{a^8\cos^8 i_0}{8870H^4}\right) \quad \ldots\ldots(15).$$

If we neglect the variation of ν with height, then $H=\infty$ and the expression reduces to

$$\eta_{i0} = \frac{4a^2\nu_1\cos^3 i_0}{3c},$$

which is the form obtained by Appleton and Ratcliffe in this simple case, and is in disagreement with the observations. We proceed to examine whether the terms introduced by consideration of the variation of ν with height are adequate to explain the discrepancies.

To investigate the dependence of attenuation on frequency we differentiate equation (15) with respect to a, which is proportional to p. Then if the experimental observations are to be satisfied, we must have

$$\frac{d\eta_{i0}}{da} = 1-\frac{11a^2\cos^2 i_0}{10H}+\frac{99a^4\cos^4 i_0}{280H^2}-\frac{359a^6\cos^6 i_0}{5040H^3}+\frac{a^8\cos^8 i_0}{200H^4}\leqslant 0 \quad \ldots(16),$$

so that

$$\frac{a^2\cos^2 i_0}{H}\geqslant 1{\cdot}35.$$

But $a^2\cos^2 i_0 = h_{i0}$ is the depth of penetration of the ray into the layer, and it may readily be shown that h', the contribution to the equivalent height of the layer made by the path in the layer, is equal to $2h_{i_0}$ when the gradient of ionization is linear. It follows that $h'\geqslant 27$ km.

This condition must be satisfied over the whole frequency spectrum, so that for wave-lengths near 200 m. we must have $h'\geqslant 2000$ km. So large a value for h' cannot exist in practice, since the total equivalent height of the layer is only about 100 km.

We conclude that the ionization-gradient at the under surface of the E layer is not of linear form.

§9. ANALYSIS OF PARABOLIC IONIZATION-GRADIENT

Let us write

$$N=\alpha^2h^2,$$

then for vertical incidence we have

$$\eta_0 = 2\int_0^{h_0}\kappa ds = \frac{\nu_1}{ac}\int_0^a \frac{\epsilon^{-h/H}h^2}{\sqrt{(a^2-h^2)}}.dh = \frac{a\nu_1}{c}\int_0^{\pi/2}\cos^2\theta\,\epsilon^{-a\cos\theta/H}\,d\theta \quad \ldots\ldots(17),$$

where $h=a\cos\theta$.

Making further use of Sonine's expansion, we find

$$\eta_0 = \frac{a\nu_1}{4c}\left(\P - \frac{8a}{3H} + \frac{3\P a^2}{8H^2} - \frac{16a^3}{45H^3} + \frac{5\P a^4}{192H^4} - \frac{8a^5}{525\P H^5}\right) \quad \ldots\ldots(18),$$

so that

$$\eta_{i0} = \frac{a\P \nu_1 \cos^2 i_0}{4c}\left(1 - \frac{8h_{i0}}{3\P H} + \frac{3h_{i0}^2}{8H^2} - \frac{16h_{i0}^3}{45\P H^3} + \frac{5h_{i0}^4}{192H^4} - \frac{8h_{i0}^5}{525\P H^5}\right) \quad \ldots\ldots(19),$$

where, as before, $h_{i0} = a\cos i$ and is the depth of penetration of the ray. Differentiating with respect to a, we have, if the attenuation does not decrease with increasing wave-length,

$$1 - \frac{16h_{i0}}{3\P H} + \frac{9h_{i0}^2}{8H^2} - \frac{64h_{i0}^3}{45\P H^3} + \frac{25\P h_{i0}^4}{192H^4} - \frac{48h_{i0}^5}{525\P H^5} \leqslant 0 \quad \ldots\ldots(20),$$

so that

$$h_{i0} \geqslant 12 \text{ km.},$$

while

$$h_{i0}' = \tfrac{1}{2}\P h_{i0} = 19 \text{ km.}$$

By the same reasoning as was employed in § 8 above we find that so large a value for h_{i0}' would give rise to much larger variations of the equivalent height of the E layer than are observed in practice, and we conclude that the gradient of ionization in the layer is not parabolic. It is to be observed however that this gradient gives rise to results which are less divergent from the observed results than those obtained with the linear gradient. Moreover, there would appear to be a greater chance of the observations being satisfied by a layer in which the gradient of ionization varies with the depth of penetration of the incident ray. Accordingly, we proceed in the next section to examine the properties of a layer in which the ionization-gradient is exponential in form.

§ 10. ANALYSIS OF EXPONENTIAL GRADIENT

Let us write

$$N = \gamma e^{\beta h}$$

and

$$k = \rho^2\gamma/p^2.$$

Then for vertical incidence

$$\eta_0 = \frac{k\nu_1}{c}\int_0^{h_0} \frac{\epsilon^{(\beta - 1/H)h}\, dh}{\sqrt{(1 - ke^{\beta h})}} \quad \ldots\ldots(21),$$

where

$$h_0 = \beta^{-1}\log_e k^{-1}.$$

Substituting

$$ke^{\beta h} = \cos^2\theta$$

we have

$$\eta_0 = \frac{2\nu_1 k^{1/\beta H}}{c\beta}\int_0^{\cos^{-1} k^{\frac{1}{2}}} \cos^{(1 - 2/\beta H)}\theta\, d\theta = \frac{2\nu_1 k^{1/\beta H}}{c\beta} \quad \ldots\ldots(22),$$

provided that

$$\left|\frac{2}{\beta H}\right| \ll 1$$

and

$$k \ll 1.$$

Hence for angle of incidence i_0 we have

$$\eta_{i0} = \frac{2\nu_1}{c\beta} k^{1/\beta H}\cos^{(1 - 2\beta H)} i_0 = \frac{2\nu_1 \cos i_0}{c\beta}\left(\frac{\rho\gamma^{\frac{1}{2}}}{p\cos i_0}\right)^{2\beta H} \quad \ldots\ldots(23).$$

It is seen that the attenuation decreases slowly with increasing frequency, and aries approximately as $\cos i_0$. The dependence of attenuation on these factors is herefore just of the type indicated by experiment. We proceed to examine the agnitude of the quantities involved.

It is clearly necessary first of all to determine the value of γ, which is the ioniza-on-density postulated at the foot of the layer. Now the theory of Lorentz, on hich we have based our analysis, becomes invalid when the number of electrons s small in a cube whose side is equal to 1 vacuum wave-length, so that a lower mit exists to the permissible value of γ. At the same time an upper limit is set by he fact that if γ is too great, appreciable absorption will occur below the region efined as the foot of the layer. For the frequencies under consideration we can afely assume a value of unity for γ, so that we consider the layer to commence at he point where one electron per cm^3 is found.

The gradient of ionization is determined by the value of β. Let us take β equal o 1 and examine the magnitudes of the quantities involved. Consider the value ^{7}, for which $\lambda = 190$ m. of the frequency p, and the angle of incidence 70°, for which $R = 550$ km.

Then by equation (23),

$$\eta_{70} = 0{\cdot}97 \times 10^{-6}\, \nu_1.$$

But by measurement we have from equation (3), for the average* value of η_{70},

$$\eta_{70} = \cos^2 35^\circ \log_{10} 190 - \log_e 3{\cdot}3/2 = 1{\cdot}05,$$

ence the theoretical value of the attenuation is in agreement with the measured alue if $\nu_1 = 1{\cdot}1 \times 10^6$. Taking this value for ν_1 we proceed to examine the variation of the reflection coefficient with p. A comparison between the observed and cal-culated values of η over the complete range of broadcasting frequencies is shown in figure 3. It is seen that the calculated values are in close agreement with the ob-served values over the entire range.

It will be observed that this comparison has been made for a large value of i_0, where uncertainty regarding the radiation characteristics of the aerials employed is of little importance. The variation of η with i_0 is set out in figure 4, where a com-parison is made between the observed and calculated values of the attenuation, for values of R ranging from 350 to 1150 km. The comparison is made for a wave-length of 190 m., and once again it is seen that close agreement exists between the observed and calculated values.

It appears therefore that the facts of long-distance transmission on broad-casting frequencies can be accounted for, to a very close approximation, by re-fraction in a layer in which the ionization-gradient is given by $N = e^{h(km)}$. The agree-ment with experience is so good that we proceed to examine this model of the E layer more closely. In the first place it appears desirable to test the applicability of

* The average value of the reflection coefficient of the layer is found to be approximately one-half of the quasi-maximum value. The larger value of the latter coefficient is probably due mainly to the presence of multiply reflected rays from the E layer. The effect of these rays will be largely eliminated by taking the average value of the reflection coefficient.

the ray theory to such a layer. Writing

$$\mu^2 = 1 - \delta\mu$$
$$= 1 - k\epsilon^h,$$

we find that (4) becomes

$$\tfrac{1}{2}\mu \cos i \, d\mu \,.\, \lambda \ll 1,$$

where λ is measured in km.

Now $\delta\mu$ has a maximum value of $\cos^2 i_0$ and $\cos i$ varies from $\cos i_0$ to zero along the trajectory of the ray, so that we may safely say that the ray theory is applicable for the ranges of wave-length and distance which we have considered above.

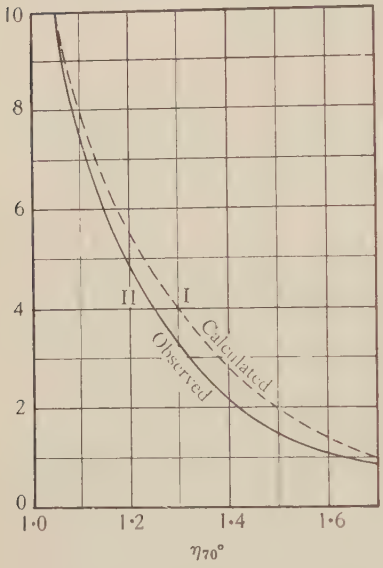

Figure 3.

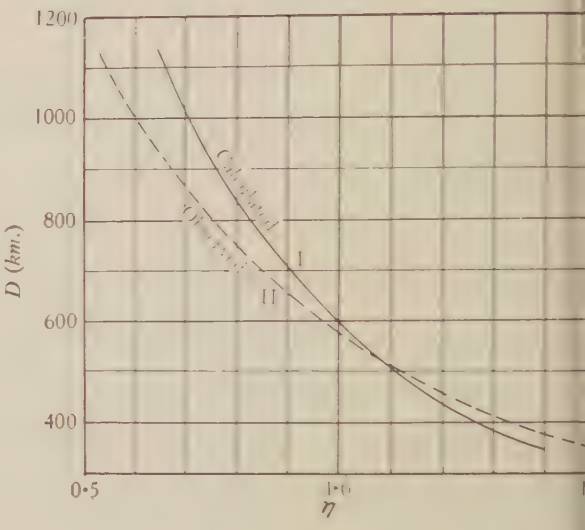

Figure 4.

Secondly, it will be remembered that in § 7 we have assumed that $\nu^2 \ll p^2$. Now we have seen above that ν_1 has the value $1{\cdot}1 \times 10^6$ collisions per second, so it would seem that the above assumption is invalid. It must be pointed out, however, that little absorption occurs in the regions where ν is of the order 10^6, since the ionization there is small. The greater part of the absorption occurs near the top of the ray's trajectory, where ν may be but $\frac{1}{3}$ of this value, so that the condition $\nu^2 \ll p^2$ may be satisfied even for the longest wave-lengths. It is to be noted, however, that even were this assumption to prove invalid for the longest wave-lengths it would lead to but little alteration in our conclusions, while for the shorter wave-lengths no doubt as to its validity exists.

Finally, it is necessary to examine the equivalent heights which would be measured for this layer. For vertical incidence we have

$$h_0' = \int_0^{h_0} \frac{dh}{\sqrt{(1 - k\epsilon^{\beta h})}},$$

nd writing $k\epsilon^{\beta h} = \cos^2\theta$, we have

$$h_0' = \frac{2}{\beta}\int_0^{\cos^{-1}k^{\frac{1}{2}}} \frac{d\theta}{\cos\theta} = \frac{1}{\beta}\log_e\frac{4}{k},$$

here $k^{\frac{1}{2}} \ll 1$.

Hence for incidence i_0,

$$h'_{i0} = \frac{1}{\beta}\log_e\frac{4\cos^2 i_0}{k},$$

o that, if $\beta = \gamma = 1$,

nen $$h'_{i0} = \log_e(1{\cdot}3\times 10^{-9}\, p^2\cos^2 i_0);$$

hen $p = 10^7$ and incidence is vertical, $h_0' = 12$ km., while when $p = 10^6$ and incidence is vertical $h_0' = 7$ km. These values appear entirely reasonable, although o simultaneous height-measurements with which they could be compared have een made over this range of wave-lengths.

Since the total equivalent height of the layer measured on these wave-lengths s normally near to 100 km. it follows that the value of $\nu_1 = 10^6$ occurs at a height f about 90 km. This result is in very close agreement with Chapman's estimate, as uoted by T. L. Eckersley[13].

The variation of equivalent height with angle of incidence is very small, in greement with the observations[5, 21].

§ 11. DISCUSSION AND CONCLUSIONS

It has been shown that on medium radio frequencies the intensities of the sky waves, and their variation with frequency and distance, are inconsistent with the presence of a linear or parabolic gradient of ionization in the *E* layer. The assumption of an absorbing *D* region of ionization does not remove the inconsistencies.

On the other hand, the facts of long-distance transmission, where the angle of incidence of the sky wave on the *E* layer is greater than 60°, can be accounted for to a close approximation if the gradient of ionization be of exponential form. It has been explained that the observations at short distances become unreliable owing to the uncertainty regarding the vertical polar diagram of the emitting aerials. Nevertheless it may be shown from equations (2) and (3) that the field-intensities observed very close to the emitter are only a few times greater than those deduced from equation (23). This result seems entirely reasonable in view of the important influence of even a small horizontal portion of the emitting antennae when θ approaches 90°, and the consequent serious departure from the assumed polar radiation diagram which must occur at such short distances. Our inability to use the short-distance observations does not however limit seriously the amount of material with which the theory can be compared. Between 60° and 80°, $\cos(i_0)$ varies from 0·5 to 0·17, while the distances covered, from 350 km. to 1100 km., ensure that the results of the great majority of the observing stations are utilized. The range of variation of p is some tenfold.

Again, it should be pointed out that in utilizing the measurements for the deduction of the reflection coefficient of the ionized layer no account has been taken of the imperfect conductivity of the ground and its influence on the measured fields. It may be shown[7] that this effect becomes of importance for the shorter wave-lengths and the longer distances, when it may reduce the observed field-intensities by some 20 per cent. It follows that the reflection coefficient of the layer for the shorter wave-lengths is slightly greater than is indicated by equation (3). It appears therefore that a value of ν slightly less than $1{\cdot}1 \times 10^6$ collisions per second might give an even better fit to the observations. In view, however, of the statistical nature of the observations, and of the necessary variabilities of emitting aerials and observing personnel, as well as the naturally occurring variations in the ionized layer, it does not seem profitable at this stage to attempt a more accurate determination of the values of ν or of the ionization-gradient.

Summing up the discussion and analysis of the wide range of observations available, it appears difficult to escape the conclusion that the gradient of ionization in the layer is very sharp and closely approaches exponential form, that the collision frequency ν has the value 10^6 at a height of about 90 km., and that the D region, if it exists, must have a very low ionization content.

As a corollary to these conclusions it follows that the equivalent height of the E layer measured at long wave-lengths should not differ by more than a few km. from those measured at the lower end of the broadcasting band of wave-lengths. Experimental evidence on this point appears to be lacking. The measurements of Hollingworth[16] on a wave-length of 14,350 m. show heights of 90 km. during the day in winter, although there is necessarily some doubt as to the accuracy of height-measurements on these very long wave-lengths.

It is, however, a necessary consequence of the conclusions reached in this paper that the equivalent height of the layer for the longer wave-lengths in the medium-frequency spectrum (2000 m.) should not differ greatly from 95 km.

§ 12. ACKNOWLEDGMENTS

The work described has been carried out as part of the programme of the Australian Radio Research Board. The author wishes to express his indebtedness to Mr W. J. Wark, M.Sc., for considerable assistance in the compilation of the field-intensity data; to Dr A. L. Green, who has carefully checked all the calculations and made some valuable suggestions; to Prof. V. A. Bailey for the benefit of some helpful discussion; and finally to the Chairman of the Board, Prof. J. P. V. Madsen, for his continued encouragement and advice throughout the progress of the investigation.

REFERENCES

(1) Appleton. *Proc. phys. Soc.* **42**, 321 (1930).
(2) Appleton. *Proc. phys. Soc.* **41**, 43 (1928); **42**, 321 (1930).
(3) Appleton. *J. Instn elect. Engrs*, **71**, 642 (1932).
(4) Appleton and Naismith. *Proc. roy. Soc.* A, **137**, 36 (1932).
(5) Appleton and Ratcliffe. *Proc. roy. Soc.* A, **128**, 133 (1930).
(6) Bailey and Martyn. *Phil. Mag.* **18**, 369 (1934).
(7) Bouthillon. *J. Éc. Polyt.*, Paris, **25**, 151 (1925).
(8) *Bull. Counc. sci. industr. Res. Austr.* No. 63 (1932).
(9) Chapman. *Proc. phys. Soc.* **43**, 26 (1931).
(10) de Broglie. *J. Phys. Radium*, **7**, 321 (1926).
(11) Documents du C.C.I.R. Deuxième Réunion, Mai–Juin, 1931.
(12) Eckersley. *Proc. Inst. Radio Engrs*, N.Y., **20**, 1555 (1932).
(13) Eckersley. *Proc. roy. Soc.* A, **137**, 169 (1932).
(14) Gowan. *Proc. roy. Soc.* A, **128**, 531 (1930).
(15) Green. *Bull. Counc. sci. industr. Res. Austr.* No. 59 (1932).
(16) Hollingworth. *J. Instn elect. Engrs*, **64**, 579 (1926).
(17) *J. Instn Engrs Aust.* **5**, 193 (1933).
(18) Lindeman and Dobson. *Proc. roy. Soc.* A, **103**, 339 (1923).
(19) Lorentz. *Theory of Electrons*, p. 132.
(20) Maris. *Terrestrial Magnetic and Atmospheric Electricity*, p. 233 (1928).
(21) Martyn, Cherry and Green. *Proc. phys. Soc.* **47**, 340 (1935).
(22) Pickard. *Proc. Inst. Radio Engrs*, N.Y., **15**, 749 (1927).
(23) *Proc. Inst. Radio Engrs*, N.Y., **20**, 611 (1932).
(24) Rapport du Dr Van der Pol. *Conférence Européenne des Radiocommunications*, Document No. 1, p. 41 (Lucerne, 1933).
(25) Ratcliffe and White. *Proc. phys. Soc.* **46**, 107 (1934).
(26) Sommerfeld. *Ann. Phys.*, Lpz., **81**, 1135 (1926).
(27) Watson. *Proc. roy. Soc.* A, **95**, 83 (1919).
(28) Whipple. *Quart. J. R. met. Soc.* p. 331 (1931).
(29) White. *Proc. phys. Soc.* **46**, 91 (1934).

621.396.11 : 551.51.053.5

LONG-DISTANCE OBSERVATIONS OF RADIO WAVES OF MEDIUM FREQUENCIES

By D. F. MARTYN, Ph.D., A.R.C.Sc., R. O. CHERRY, M.Sc.
AND
A. L. GREEN, Ph.D., Research Physicists,
Australian Radio Research Board

Communicated by Prof. O. U. Vonwiller, July 9, 1934. *Read in title November* 2, 1934.

ABSTRACT. The frequency-change technique of Appleton and Barnett has been applied to the analysis of the downcoming waves from a distant transmitter. The observations were carried out simultaneously at distances of 25 and 700 km. from the emitter, which operated on a frequency of 1415 kc. sec. It was found that several downcoming waves were present at the more distant receiving station. Each of these waves was identified by using the path-length of the singly reflected wave from the *E* layer as a reference. In this way it was found that the equivalent heights of both the *E* and the *F* layers are relatively stable over the 700-km. transmission path, and do not vary appreciably with the angle of incidence of the wave. The equivalent height of the *F* layer showed a pronounced minimum at about 3 a.m. each morning. The rate of propagation of the minimum height in the horizontal direction appears to be slower than the rate of sunset propagation in the same direction. The ionization-density in the *E* layer in the early morning was always greater than $2{\cdot}4 \times 10^3$ electrons per cm^3, and during half the period of the observations was less than $8{\cdot}3 \times 10^3$ electrons per cm^3. The intermediate layer was observed regularly at sunrise. From the measurements of equivalent heights at different angles of incidence it is concluded that the gradient of ionization at the lower boundary of the *E* layer is sharp.

§ 1. INTRODUCTION

In general the field-intensity due to an emitting station is made up of two parts, that due to the ground wave which has been propagated over the earth's surface and that due to downcoming waves which have experienced one or more reflections from the ionosphere. Numerous investigations[2] have been made of the characteristics of the downcoming waves at comparatively short distances, of the order 100 km., from the emitter. The particular advantage of this procedure is that the ground wave is then comparable in intensity with the downcoming wave, so that it may be used as a reference wave, of known and stable characteristics, with which the much more variable downcoming wave may be compared. In this way much valuable information has been obtained about the equivalent or virtual heights of the layers of the ionosphere and of the ionization-densities in these layers.

On the other hand it is not possible for such conditions to examine effectively the variation, with changing angles of incidence, of the equivalent heights of the layers and of their reflection coefficients. A knowledge of these variations would be

of considerable value in the elucidation of the structure of the ionosphere, and in particular of the gradient of ionization therein. Now, in general, if i be the angle of incidence of the wave on the layer, then the theoretical dependence of the equivalent height and reflection coefficient on i is given by some low power of $\cos i$. For the experimental conditions outlined above the maximum possible change in $\cos i$ is about 15 per cent, so that great refinement of technique would be required to examine the small variations involved.

In the experiments described in this paper two receiving centres were used, at distances of 700 and 25 km. from the emitter, so that the range of variation of $\cos i$ was from 0·3 to 1 or some 200 per cent.

Preliminary observations by one of us[5] indicated that over the greater distance mentioned more than one downcoming wave was receivable. The present series of experiments has established the fact that one of these waves, that which has undergone a single reflection at the surface of the E layer, is invariably present. Moreover, simple geometrical considerations show that the length of the equivalent path of this wave is almost independent of the precise height of the E layer, normally occurring changes in which produce a change of only 1 per cent in the total path. It is possible then to make use of this wave as a reference wave of known path-length and to measure therefrom the equivalent paths of other waves which may be present.

Again, it might be anticipated that a complication would exist in such long-distance experiments in that the constitution of the ionosphere might not be uniform over the entire path. Evidence to the effect that at times this non-uniformity exists has been found in the experiments, but it has been possible to interpret the measurements even in such conditions, and indeed it has been possible to utilize them in order to study the height of the layer at several points above the great-circle path between emitter and receiver, and so to study the horizontal propagation of changes in the layer.

Finally, it has been possible to obtain measurements of the maximum ionization-density in the E layer by noting the presence or absence of the multiply reflected waves from that region. For the frequency employed (1415 kc./sec.) this layer is usually penetrable at vertical incidence during the night, but is seldom penetrated for the larger angles of incidence. In this way it has been possible to study the night-to-night variation of the maximum ionization-density in the layer during the period of the observations.

§ 2. EXPERIMENTAL PROCEDURE

The emitter was located in the P. N. Russell School of Engineering in the University of Sydney. It radiated approximately 1 kW. on a frequency of 1415 kc./sec. The receiving sites were located at Liverpool, N.S.W., and Melbourne, Victoria, distant 25 and 700 km. respectively from the emitter. Throughout the investigation the frequency-change method of equivalent-path determination due to Appleton and Barnett[3] was employed. The frequency-change was normally about 7·5 kc./sec.

For recording purposes an Einthoven galvanometer and camera were used at Liverpool. In Melbourne a Moll galvanometer having a period of 0·2 sec. was used in conjunction with a photographic drum recorder of a type previously employed[15]. The frequency-changes, which are automatically produced at the transmitter, occupied about three seconds each. Since the number of interference fringes obtained in Melbourne ranged from 2 to 16 there appeared to be a possibility that the fringes might be distorted owing to the relatively great period of the galvanometer. A calibration of the galvanometer response at low frequencies was made, and a correction factor was found which would enable the true amplitude of any given set of fringes to be deduced. As had been anticipated, this correction factor is larger for the larger fringe numbers. The present paper is concerned only with equivalent-path determinations, which depend only on the number of fringes present, and this correction factor has not been used in it. Indeed, for this work certain advantages accrue from the use of a galvanometer having a comparatively low period, since the fringes due to the higher orders of reflection are relatively suppressed, the interpretation of the records for the lower orders of reflection being thus facilitated. Moreover there is a tendency for the reception of low-amplitude atmospherics to be suppressed, and this again facilitates the interpretation of the records. The galvanometer was shunted with a resistance of 29 Ω., a value which was found to give a satisfactory balance between the undesirable features of over- and under-damping.

The receiver used in Melbourne had three stages of high-frequency amplification employing variable-mu valves. The necessary flatness of the frequency, amplitude response curve was obtained by slightly detuning each stage of amplification. With the screen grid of the detector valve connected to the negative terminal of the high-tension supply the plate current was 2 or 3 μA. when no signal was being received. The rectified current varied linearly with the intensity of the incoming signal, reaching a value of 75 μA. for the maximum signals received, which had a field intensity of the order 0·5 mV./m.

At Liverpool, owing to the strong ground-wave signal, it was found better to use a square-law detector in which the steady plate current had been balanced out. The two stages of radio-frequency amplification were coupled by a band pass unit to ensure flatness of tuning.

The experiments were carried out from midnight to sunrise on eleven mornings between the 5th and 28th October, 1932. At intervals of ten minutes a set of six complete frequency-changes lasting one minute was sent out from the emitter. During the pre-sunrise period, when conditions were changing rapidly, the interval between each set of observations was shortened to five minutes.

§ 3. EXPERIMENTAL RESULTS

General discussion. The results obtained at Liverpool were typical of those obtained for such frequencies over short distances, and call for no special comment here. It need only be remarked that the most frequently observed wave was one which had been reflected once from the *F* layer. On two days out of the eleven the

layer was observed during the greater part of the morning. On most mornings the intermediate layer was observed during the transfer from the F to the E region which is associated with the sunrise period.

The results obtained in Melbourne were considerably more complex. On all occasions interference fringes were obtained, showing that at least two down-coming waves were invariably present. A typical set of fringes is reproduced in figure 1, where it is seen that the primary number of fringes is 4·2 while there is evidence of a secondary set of 12·5 fringes. During the series of experiments almost every possible number of fringes between 2 and 18 has been counted, and at first sight the analysis would appear to be difficult. If the fringe-counts be plotted against time, however, it is soon seen that each count lies on one of several continuous curves, and it only becomes necessary to identify the rays corresponding to each curve. The identification was facilitated by the curves set out in figure 2, which show the path-lengths and angles of incidence of the singly, doubly and triply reflected rays plotted as a function of layer-height. We shall denote the singly, doubly, triply,

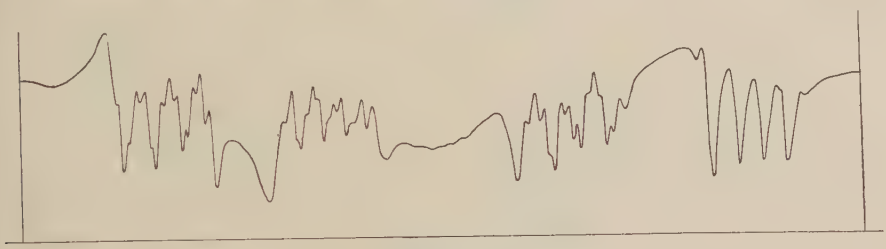

Figure 1.

etc. reflected waves from the E region by E_1, E_2, E_3, etc. and from the F and intermediate regions by F_1, I_1, etc. Then the curve showing the path difference between E_1 and F_1 say, will be denoted by (F_1-E_1).

On plotting the curves it is found that the most commonly observable fringe-counts are produced by (F_1-E_1), (F_2-E_1), (E_2-E_1), (F_2-E_2) in that order of frequency of occurrence. It is seen, therefore, that the principal part of the received signal is due to E_1, the singly-reflected wave from the E region. The rays E_2 and F_1 have never been observed simultaneously, but it is frequently noticed that one ray may give place to the other for a brief time. Now reference to figure 2 shows that for normally occurring F-layer heights these two rays approach the E layer at almost the same angle of incidence. It is clear, therefore, that the transit from the E_2 to the F_1 ray is due to electron-limitation in the E layer. The size of the fringes produced by the E_2 and the F_1 rays are usually comparable.

Temporal path variations. When the F-layer heights are steady the values measured at Liverpool and Melbourne are remarkably equal. In such circumstances the heights measured in both places do not differ by more than 10 km., which is about the limit of accuracy of the measurements for this layer. The E-layer heights vary by not more than two or three km. in similar circumstances.

One of the most striking features of the results is the pronounced minimum which occurs in the F-layer equivalent heights at approximately 3 a.m. (Eastern

Australian standard time). This effect, which has been noticed by other workers[8], was found on seven out of nine mornings when the F layer was observable. The layer usually commences to fall at about 1.30 a.m. and after passing through a minimum value attains its normal value again at about 4 a.m. The total fall is usually about 40 km. It is found that the equivalent height of the F layer measured at Liverpool attains this minimum value some time before that measured in Melbourne. If the height in the latter case be deduced from the $(F_1 - E_1)$ curve then the difference in

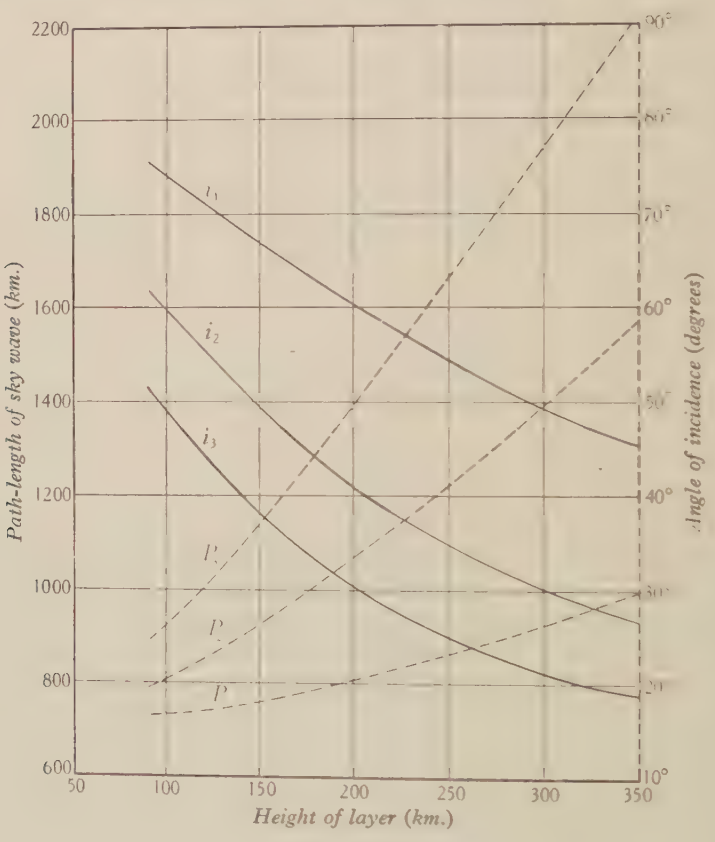

Figure 2.

Δt time Δt between the attainment of the minimum heights is about 30 minutes. Now the difference between the times of sunset in Sydney and Melbourne is 24 minutes, so that if the minimum in the F-layer heights is directly associated with solar influences, then we should expect Δt to have a value of about 12 minutes. It appears, therefore, that the rate of propagation of the F-layer minimum height in the direction Sydney–Melbourne (49° 11′ W. of S.) is slower than the rate of sunset propagation in the same direction.

Shortly before sunrise the F-layer heights recorded at both Liverpool and Melbourne rise to abnormally great values, and eventually E-layer reflection sets in.

There is no doubt that this phenomenon is due to the reduced group-velocity caused by increasing ionization below the F layer.

It is noticeable that the apparent rise in the F layer observed at Melbourne takes place much more slowly than that recorded at Liverpool. This is attributed to the fact that the sun's rays must take considerably longer to irradiate the path of the F_1 ray received in Melbourne than that of the F_1 ray received at almost vertical incidence in Liverpool.

Ionization-densities of the E layer. For the case of propagation between Sydney and Melbourne the angle between the direction of the earth's magnetic field and the direction of propagation of the rays at the apices of their paths in the E layer is such that propagation approximates to the transverse type of the magneto-ionic theory[4]. From the theory it may be shown that in this case the ordinary ray* will be much less attenuated than the extraordinary ray, and the refractive index of the layer for the ordinary ray will be given very nearly by

$$\mu^2 = 1 - 4\pi Ne^2/mp^2,$$

where μ is the refractive index of the medium, μ

N is the density of ionization, N

p is the popular frequency of the wave, and p

e, m are the charge and mass of an electron (e.s.u.). e

By Snell's law the refractive index at the apex of the path of the refracted ray is given by

$$\mu = \sin i,$$

where i is the angle of incidence of the ray on the medium. Hence penetration of i the medium occurs when the maximum ionization-density in the medium is less than N_0, where

$$N_0 = \frac{mp^2 \cos^2 i}{4\pi e^2}.$$

The critical ionization-densities for which penetration of the E layer occurs are set out in table 1 for the various rays observed.

Table 1

Ray and wave-length (km.)	i (degrees)	N_0 ($10^3 \times$ electrons per cm^3)
E_1	72	2·4
E_2	57	7·4
F_1 (250)	55	8·3
F_1 (300)	49	11
F_2 (250)	35	17
F_2 (300)	30	19
I_2	48	11

Throughout the course of the experiments the ray E_1 was always present. It follows that the ionization-density in the E layer was always greater than $2{\cdot}4 \times 10^3$ electrons

* We have here neglected the controversial Hartree polarization term (*Nature*, **132**, 929 (1933)).

per cm³. The F_1 ray was present during 55 per cent of the time of observation, so that the ionization-density in the E layer was less than $8{\cdot}3 \times 10^3$ electrons per cm³ during that time. On two nights the ionization-density was seldom less than 10^4 electrons per cm³, as evidenced by the almost complete absence of F rays. It is to be remarked that if the Hartree polarization term be proved valid then the densities given above must be increased by 50 per cent.

§ 4. ANALYSIS OF TYPICAL RESULTS

Test of October 6, 1932. *Sunrise at Sydney*, 5.27 *a.m.* The results obtained on this morning are shown in figure 3 in which the uppermost curve gives the layer-heights measured at Liverpool, while the lower curves give the path-differences

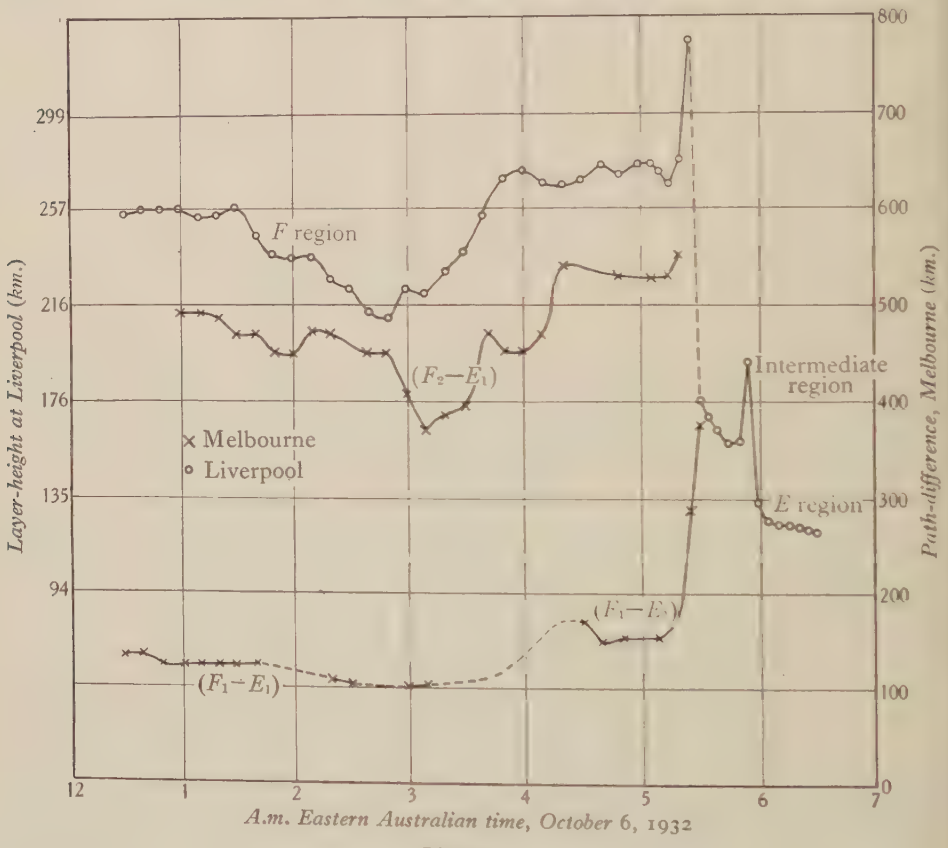

Figure 3.

measured in Melbourne. The left-hand scale of ordinates refers to the Liverpool measurements and the right-hand one to those made in Melbourne. It will be seen that the (F_2-E_1) curve is practically unbroken, indicating the almost continuous presence of the F_2 ray. The minimum path-difference occurs about 27 minutes after the minimum height recorded at Liverpool.

The (F_1-E_1) curve is more irregular, breaks occurring at 1.40, 2.30, and .10 a.m. We interpret these breaks as due to nocturnal increases of the ionization n the E region.

The close agreement of the F-layer heights measured at Liverpool and Melbourne is readily apparent at 1 a.m. and 5 a.m., times when the F layer is relatively stationary. Making use of figure 2, we find the F-layer height* at 1 a.m. to be (*a*) 256 km., (*b*) 252 km., and (*c*) 245 km. as deduced from (*a*) Liverpool observations, (*b*) the difference (F_2-E_1), and (*c*) the difference (F_1-E_1). In the same way we find at 5 a.m. heights of (*a*) 275 km., (*b*) 262 km., and (*c*) 268 km. deduced in the same way. At 5.25 and 5.30 a.m. there is evidence of considerable group-retardation in the F_1 ray, showing that the ionization below the F layer has increased considerably.

Test of October 21, 1932. *Sunrise at Sydney*, 5.07 *a.m.* The results obtained on this morning are shown in figure 4. This test gave perhaps the most interesting results of the present series. During the early hours of the morning the F_1 ray was not received, showing that the ionization in the E layer was greater at that time than in the test described in (*a*) above.

At 1.30 a.m. the E layer is detectable at Liverpool, while from 1.20 a.m. onwards the F_2 ray is received in Melbourne. Now the results obtained in Melbourne fall into two continuous curves, and consideration of figure 2 shows that it is very probable that these two curves are due to (*a*) the difference (F_2 – a singly reflected ray from the E region) and (*b*) the difference (F_2 - a doubly reflected ray from the E region). Now, if such be the case, then at any time the difference in the ordinates of these two curves should give the value of (E_2-E_1). Between 1 and 2 a.m. the average value of this quantity is 73 km., so that the height of the E region must be near to 100 km. At 2 a.m. however the upper curve starts to rise, while the lower curve starts to fall, and at 2.20 a.m. the difference in the ordinates is 160 km., corresponding to an E-layer height of 150 km., which is a height considerably greater than normal for this layer. There is however another possibility. It has been suggested by Ratcliffe and White[7] that the E layer has a stratified formation, one layer, which they term the e layer, existing at a height of about 105 km., while the other has a height of about 135 km. Now in our experiments an e_2 ray must penetrate the e layer before an e_1 ray, owing to the smaller angle of incidence of the former ray. We consider therefore that up till 2 a.m. both the singly and doubly reflected rays from the lower region come from the e layer, while at 2 a.m. the e_2 ray penetrates to the E layer at about 130 km. At 2.30 a.m. the difference between the ordinates has fallen to a steady value of 100 km., showing that the e_1 ray has now penetrated to the E layer proper.

e
e_2
e_1

This interpretation of the results is supported by the observation of fringes corresponding directly to (E_2-e_1) at the end of the 2 a.m. record, and again by the observation of a fringe count giving (E_2-E_1) at the end of the 2.20 a.m. record.

Again, Ratcliffe and White have given reasons for believing that the presence of

* All height-measurements have been corrected in order to allow for the effect of the curvature of the earth.

the *e* region is associated with magnetic storms. Reference to the *Cosmic Data Ursigrams* for October 21 shows that this day was marked by moderate disturbance consisting of irregular oscillations. It is worthy of remark that all other days on which tests were conducted were magnetically quiet, and in none of them was there evidence of spasmodic appearance of the *e* layer.

The *F* layer measured at Liverpool rose sharply in height between 3.10 and 3.30 a.m.* This increase is reflected some 30 minutes later in the Melbourne curves.

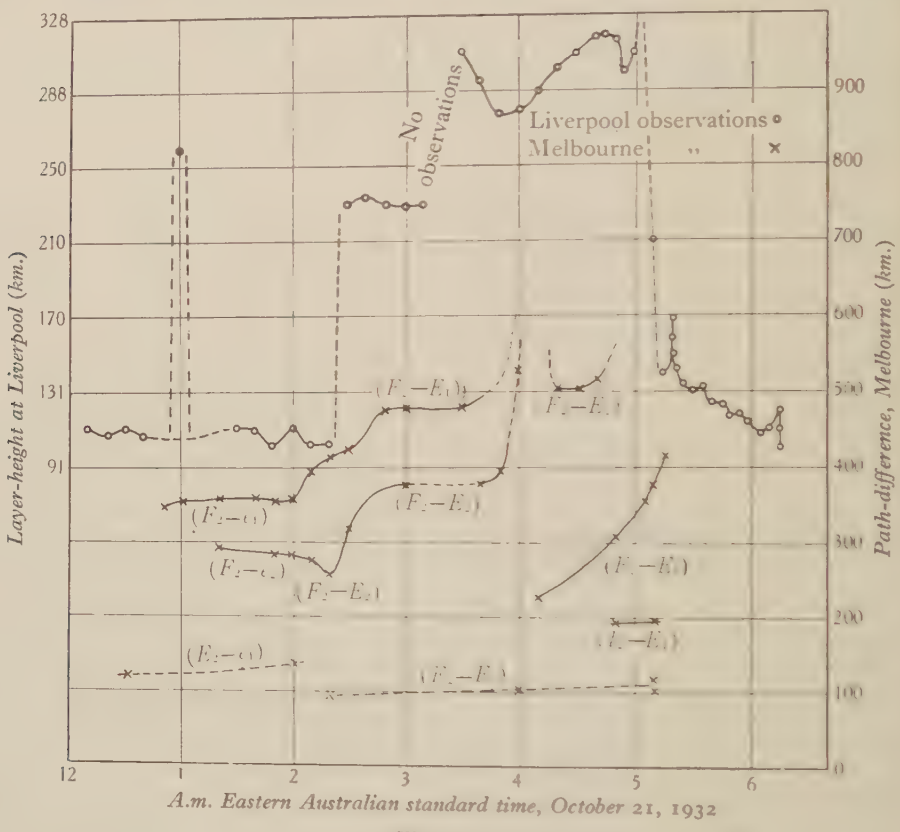

Figure 4.

After 4 a.m. the fringes become so numerous, and consequently so small, that they could not be counted. Between 3.20 and 3.50 a.m. the *F* layer fell at Liverpool, and this is shown at 4.20 a.m. in Melbourne by the reappearance of the (F_2-E_2) curve.

At 4.10 the F_1 ray made its first appearance in Melbourne and the (F_1-E_1) curve rises steadily until 5.15 a.m. when the *E* layer becomes impenetrable. At 4.50 and 5.10 a.m. there is evidence of a doubly reflected ray from the intermediate region.

Test of October 28, 1932. Sunrise at Sydney, 5.00 a.m. On this morning, figure 5, the ionization-density was so great that the *E* layer was only penetrable for

* Unfortunately no observations were made during this interval.

few minutes, even for the vertically incident rays at Liverpool. It will be seen that the e layer was responsible for the reflection of the rays received in Melbourne till 3.30 a.m., when the e_2 ray penetrated to the E region. Almost simultaneously penetration of the e layer occurred at Liverpool. At 4.30 a.m. the F_1 ray appeared in Melbourne, and group-retardation set in, causing a rapid increase in the path difference $(F_1 - e_1)$.

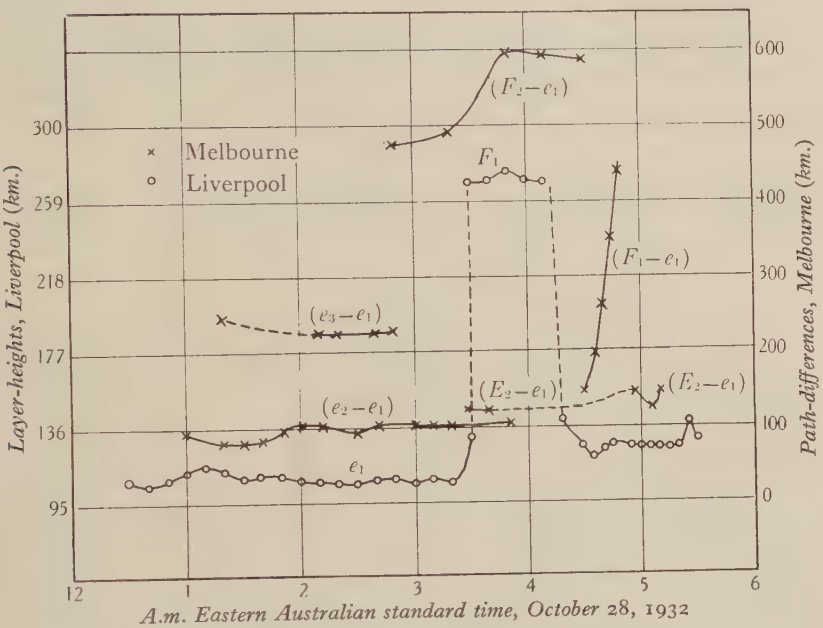

Figure 5.

The agreement between the equivalent heights of both the F and E regions measured at Melbourne and Liverpool is very close. Thus between 1 a.m. and 3 a.m. the average heights of the e layer deduced from (*a*) Liverpool observation, (*b*) the difference $(e_3 - e_1)$ and (*c*) the difference $(e_2 - e_1)$ are (*a*) 108 km., (*b*) 109 km., and (*c*) 109 km. respectively.

At 4.20 a.m. reflection at Liverpool occurs from the E region, but evidence of the presence of the e region is obtained for the shallow-range e_1 ray in Melbourne until 5.10 a.m., when the absorption of the waves became too great to permit of further observations.

§ 5. CONCLUSIONS

It has been remarked that interference fringes are always observable in Melbourne. The presence of fringes has previously been noted by one of us[5] on a longer wave-length (351 m.).

It is concluded that on broadcasting frequencies, at distances of the order 700 km., there are normally present at least two sky waves. The two principal sky waves are usually of comparable intensity, so that a large part of the fading experienced in such circumstances must be due to interference between these waves.

One of the most striking features of the results is the general uniformity of both the *E*-layer and the *F*-layer equivalent heights over the 700 km. between Melbourne and Sydney, at times when these layers are comparatively steady. Now the equivalent height of that part of the path of a ray which lies in an ionized layer depends on $\cos i$, so that if the path in the layer is appreciable in comparison with the total path of the ray, we should observe appreciable differences between the layer-heights recorded simultaneously in Melbourne and Liverpool. For example, if the gradient of ionization be given by $N = \alpha h$, where h is the height above the beginning of the layer[1], and h' is the contribution to the equivalent layer-height made by the path in the layer, then

h
h'

$$h' = \frac{mp^2 \cos^2 i}{2\pi\alpha e^2},$$

so that h' would vary some tenfold in our experiments as $\cos i$ ranged from 1 to 0·3.

Again, if the gradient of ionization be parabolic, of the form

$$N = \beta^2 h^2,$$

then

$$h' = \frac{\sqrt{(\pi m)} . p \cos i}{4\beta e},$$

and h' would vary some threefold.

For constant gradients of either of these forms it follows that h' cannot be greater than one or two kilometres. Now it can be shown that such small values for h' would be accompanied by lower values of attenuation than are observed in practice[6], so that we may conclude that the ionization gradient on the under side of the layer is sharper than is indicated by either of the above forms. It appears however that an exponential gradient[7] will explain the small variation of h' with i.

It may be concluded that, whatever be the ionization gradient, the *E* and *F* layers are both normally comparatively uniform in characteristics over the 700 km. path between Sydney and Melbourne.

During the occurrence of the dip in the *F* layer equivalent height which occurs about 3 a.m., however, it appears that there is a definite difference between the time of occurrence of the minimum heights over Sydney and Melbourne. The time lag in Melbourne is greater than could be accounted for directly by solar rotation.

Finally there is clear evidence that the average ionization density in the *E* layer over the whole 700 km. path of observation varies considerably from night to night. The significance of these variations will be discussed in another paper.

§ 6. ACKNOWLEDGMENTS

This work has been carried out as part of the programme of the Australian Radio Research Board. The authors wish to express their thanks to Mr W. J. Wark, M.Sc., for assistance in the experimental work, to Prof. T. H. Laby, F.R.S., for the provision of facilities in the Natural Philosophy Department of the University of Melbourne, to Mr A. H. Mutton, B.E., who was responsible for the operation of the emitter, and finally to Prof. J. P. V. Madsen for his continued encouragement and advice throughout the progress of the investigation.

REFERENCES

(1) Appleton. *Proc. phys. Soc.* **41**, 43 (1928).
(2) Appleton. *J. Instn elect. Engrs*, **71**, 642 (1932) (for bibliography).
(3) Appleton and Barnett. *Proc. roy. Soc.* A, **109**, 621 (1925).
(4) Appleton and Builder. *Proc. phys. Soc.* **45**, 208 (1933).
(5) Cherry. *Bull. Counc. sci. industr. Res. Austr.* No. 63 (1932).
(6) Martyn. *Proc. phys. Soc.*, p. 323 of this volume.
(7) Ratcliffe and White. *Proc. phys. Soc.* **46**, 107 (1934).
(8) Schafer and Goodall. *Proc. Inst. Radio Engrs*, N.Y., **19**, 1434 (1931).

620.152.272 546.815 : 620.172

AN INTERFERENCE EXTENSOMETER AND SOME OBSERVATIONS ON THE ELASTICITY OF LEAD

By BRUCE CHALMERS, B.Sc., Ph.D., Lecturer in Mathematics and Physics, The Sir John Cass Technical Institute.

Received October 19, 1934. *Read December* 7, 1934.

ABSTRACT. A description is given of an extensometer in which interference fringes are used to measure elastic and plastic extensions of specimens of length about 3 cm. to an accuracy of about 3×10^{-7} cm. Experiments on specimens of lead are described, and the following are the principal results obtained. (i) A specimen that has not recently been severely strained has a definite range in which Hooke's law is obeyed within experimental limits, and a definite elastic limit. (ii) When the specimen has recently been severely strained, a new type of closed elastic-hysteresis loop is obtained. (iii) The elastic after-effect was investigated, and it was found that when the stress is below the elastic limit, the whole of the observed effect can be accounted for thermodynamically. (iv) The true plastic after-effect (creep) was found to commence when the elastic limit is exceeded.

§ 1. INTRODUCTION

It is the object of the experimental study of elasticity to express the amount of a strain as a function of the stress producing it. To a first approximation, such a relationship is supplied by Hooke's law, the law of linear variation of strain with stress. More refined investigations have not only shown that deviations from Hooke's law occur, but have indicated that the stress is not the only variable on which the strain depends. More explicitly, it is found that the strain may vary with time as well as with stress, and that even when this time-variation has been allowed to reach completion, the strain is not necessarily a single-valued function of the stress, but may depend upon previous values of it. The stress-and-strain relations for a single specimen of a particular material are thus of great complexity; and when the material is a metal a further complication is introduced by the fact that the elastic properties of a metal depend upon the thermal and mechanical treatment to which the metal has been subjected, as well as on the purity of the metal.

It is evident, therefore, that in order to arrive at fundamental knowledge of the mechanism underlying the real elastic properties of metals, investigations must be made on specimens in some standard state of mechanical and thermal treatment. Now the effect of such treatment is to modify the size and disposition of the constituent crystals of the specimen. The standard state is therefore the state in which the specimen consists of a single crystal. The experimental difficulty of preparing very large single metal crystals sets a limit to the size of specimen readily obtainable, and the experimental method designed for the investigation of the elastic properties of single metal crystals should therefore be suitable for small specimens.

The experimental study of elasticity has been severely handicapped in the past by the fact that torsional and flexural strains are easier to measure than extensional strains. In both the former types of strain, the stress, and therefore also the strain, varies throughout the cross-section of the specimen. This, however, is not the case with extensional stresses which give homogeneous strains.

The requirement of an appropriate apparatus designed for investigations on the elastic properties of single crystals of metals is, therefore, the measurement of the extensions produced by known tensions acting on short specimens of the metal. The apparatus described below fulfils this requirement, and although experiments on single crystals have not yet been made, the results obtained in experiments on polycrystalline lead seem to be of sufficient interest to justify separate publication.

In particular, a type of elastic hysteresis loop which has not previously been noticed has been observed to occur in certain conditions, while in other circumstances lead has a definite elastic range in which Hooke's law is obeyed.

§ 2. EXPERIMENTAL METHOD

The apparatus consists essentially of two parts, of which the respective functions are to apply a known stress to the specimen and to measure the strain produced. The main frame of the apparatus consists of two vertical brass plates, each about 25 cm. square, held parallel to each other at a distance apart of about 8 cm. by horizontal brass bars screwed to the plates. The disposition of the cross-bars is shown in section in figure 1 (*A*, *F*, *Z*, *Z*).

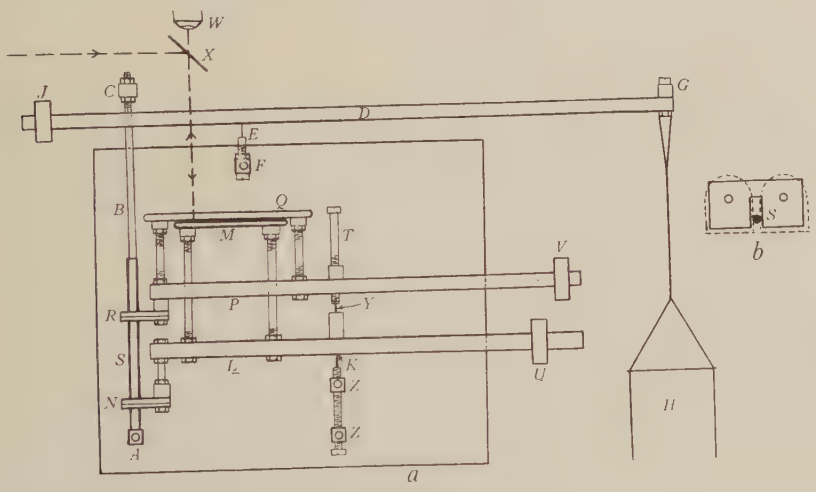

Figure 1.

Application and measurement of the stress. The specimen *S*, figure 1 *a*, is soldered at its lower end to the centre of the cross-bar *A*, and its upper end is soldered to the end of the brass rod *B*, so that *S* and *B* are collinear. The upper end of *B* is fixed to a cross bar *C* through which an upward force is applied to *B* and *S*. Near each end of *C*, $2\frac{1}{2}$ cm. from *B*, is a screw held vertically by a screw thread in *C* and a lock nut,

and from the lower end of each of these screws a steel gramophone needle point projects. These points rest in punch marks on the two bars *D*, which are rigidly connected to form the lever through which the stress is applied. The bars *D* pivot on the points of two gramophone needles *E* carried by screws passing through the cross bar *F* of the main frame.

The ends *G* of the bars *D* are connected by a cross-bar, and this cross-bar supports a glass tube *H* of length 25 cm. and diameter 6 cm., closed at its lower end and open at the top. Water can be introduced into or removed from the tube *H* by means of a two-way syphon (not shown in diagram).

The stress applied to the specimen is directly proportional to the amount of water in the tube *H* in excess of that required to balance the counterpoise weight *J* which is supported by the other end of the lever *DD*. Since the syphon tube dips into the water, allowance must be made for the downward force which it applies; this force is equal to the weight of the water displaced by the tube. Hence the level of the water-surface in *H* indicates the stress applied. The water-level is determined by means of a pointer which is moved vertically so as just to touch the water-surface. The pointer is supported by a glass rod which moves along a scale. The tube *H* is calibrated by introducing known amounts of water and observing the change of water-level.

Measurement of the strain. In order to determine the strain of the specimen corresponding to any stress, it is necessary to measure changes in the distance between two points on the specimen. These measurements were made by an optical interference method as follows. Two screws *K*, 4 cm. apart as measured along the bars *Z*, *Z*, each carry a gramophone needle, point upwards. On these points is supported a brass frame *L*, to which are rigidly attached a flat piece of glass *M*, and an arrangement *N* through which contact is made with the specimen *S*. *N* consists of two similar brass plates, shown in figure 1, between which are held two halves of a razor-blade of the three-hole type. The position of the razor-blades, which lie in a horizontal plane, is indicated by the dotted lines in figure 1 *b*. The distance apart of the razor-blades is adjusted so that they just cut the surface of the specimen when it is inserted in the position *S*.

The second frame *P* of the interferometer, figure 1 *a*, holds a second glass plate *Q* and a second arrangement *R* similar to that shown in figure 1 *b*. The frame *P* is supported on *L* at two points by means of two screws *T*, the actual points of support being gramophone needle points projecting downwards from the screws *T*. The distance and angle between the glass plates *Q* and *M* can be adjusted by means of the screws *T*.

The frames *L* and *P* are each counterbalanced by the adjustable weights *U* and *V*, so that no stress is applied to the specimen *S* through *R* or *N*. The interferometer is illuminated from above by means of light from a mercury arc passing through a water cell and a monochromatic green filter, and reflected downwards from the glass slip *X*. The fringes produced by the interference between the light reflected upwards from the lower surface of *Q* and from the upper surface of *M* are viewed through the microscope *W*. The direction and spacing of the fringes, which are the

pci of points of equal separation of the plates M and Q, can be adjusted by means of he screws T. This adjustment is made so that the fringes form a series of parallel nes whose direction is perpendicular to the plane of figure 1*a*, i.e., parallel to the ne TT of the fulcrum of the interferometer unit. When the distance RN alters, the ringes move in a direction perpendicular to their length. The plates Q and M were ieces of good plate glass mirror, and it was found that the fringes obtained when here was no silvering on either plate were sufficiently sharp and sufficiently straight or satisfactory measurements to be made.

Precautions taken to avoid disturbances. In order to avoid disturbances due to ibrations of the bench on which the apparatus stood, the two frames P and L of the nterferometer were held together by two steel springs in the plane of the two crews T. The springs, being in the plane of the fulcrum about which the upper rame moves on the lower one, exert no force on the specimen through the interferometer. A second precaution to avoid vibrations was to fix the syphon arrangements nd the apparatus for measuring the water-level in H on a different bench from the ne on which the apparatus was placed. The apparatus itself was supported in a ater bath on pads of rubber sponge which almost entirely prevented any effect rom slight vibrations of the bench. In spite of these precautions it was occasionally ound that vibrations occurred which altered the position of the fringes. This did ot occur often, and did not cause serious difficulty in the experiments. Smaller ibrations made the fringes appear to broaden for the duration of the vibrations, ut did not permanently alter the position of the fringes.

The surface of the water in the water bath was just below the level of the ower interferometer mirror, the specimen, contact pieces and supporting screws eing under water.

Design of apparatus. A certain degree of compromise has been necessary in esigning the apparatus, since the conditions necessary for the elimination of ibration appear to be incompatible with strict geometrical considerations. It must e realized, however, that the components of the instrument only turn through very mall angles, seldom exceeding 10^{-4} radian.

The particular instance in which this applies is that of the lower interferometer rame L. The point of support K should be in the same horizontal plane as the point of contact N, as the point N must move in a direction perpendicular to the line NK. The reason why this condition was not observed was that it was considered essential that the upper frame P should rest directly on the lower frame L and not on a second cross-bar, in order to obtain consistent readings and to avoid vibrations. The point Y should therefore not be allowed to move horizontally when L rotates, so Y must not be far above the point of support K. Since the upper frame P moves considerably more than the lower frame L, it is desirable that Y and R should be in the same horizontal plane. Thus K must be higher than N. Since N is near the lower end of the specimen, its movement during an experiment is very small; hence the frame L turns through a very small angle (not exceeding 2×10^{-5} radian). It follows that the horizontal reaction on N during an experiment is very small, and that the horizontal movement of N will be small compared with the relative

vertical motion of R and N. It follows that the error in the results due to non-observance of the strict geometrical considerations of design will be negligible. The results obtained indicate that this is the case; see § 3.

Experimental procedure. The experimental procedure depended upon the nature of the variation under investigation, and in general consisted in first adjusting the screws T so that the spacing of the fringes seen in the microscope was suitable, then allowing the temperature of the apparatus to become steady or, more usually, uniformly rising. The movement of the fringes caused by thermal expansion of the specimen and apparatus owing to this slow rise of temperature was allowed for in the results.

Movements of the fringes due to changes of water-level in H were investigated by changing this water-level by equal steps and observing the movement of the fringes during and after the change of stress. The movements of the fringes were measured and expressed in terms of the fringe-spacing as a unit.

Accuracy of the method. The length of the specimen between R and N was about 3 cm., and the change of this length which will cause a displacement of the fringe system by one fringe space can be estimated as follows. When the fringe system is displaced by one unit, the change in the distance between Q and M at the point of observation is one-half wave-length of the light used. The mercury green line 5460 A. was used in all the experiments, so that the change of distance between Q and M for one fringe shift is $\frac{1}{2} \times 5460$ A. or $2{\cdot}73 \times 10^{-5}$ cm. This is the change of separation of Q and M at the point on which the microscope is focused. The increase Δl of the length l of the specimen is greater than this because the specimen is farther than the point of observation from the fulcrum; hence the change in separation of QM must be multiplied by a factor, which was found to be 1·35. The change of length of the specimen corresponding to a shift of one fringe is $2{\cdot}73 \times 1{\cdot}35 \times 10^{-5}$ cm. or $3{\cdot}68 \times 10^{-5}$ cm., so that $\Delta l/l$, the extension per unit length per fringe $= 3{\cdot}68/3{\cdot}00 \times 10^{5} = 1{\cdot}23 \times 10^{-5}$ approximately.

The microscope used for observing the fringes contained an eye-piece scale. By adjusting the fringes to be about ten scale-divisions apart, and reading the position of a fringe and the distance between two fringes to one-tenth of a scale division, movements of the fringes could be determined to 0·01 of a fringe. It was usually found advantageous to observe two or three fringes. A movement of 0·01 fringe represents a value of $\Delta l/l$ equal to $1{\cdot}23 \times 10^{-7}$.

In the experiments described below, the position of the fulcrum E was such that a movement of one fringe was obtained when the water-level in H was changed by about 1 cm. The position of the water-level could be read to about 0·1 mm., so that the stress was measured to about the same accuracy as the strain. The tube H was calibrated by introducing known volumes of water from a burette, and observing the corresponding rise in water-level.

When observations of $\Delta l/l$ are made to an accuracy of the order of 10^{-7} cm. cm., the temperature of the specimen assumes considerable importance. The coefficient of expansion of lead is $2{\cdot}76 \times 10^{-5}$ cm. cm.$^{-1}$ C., so that an increase of length of 10^{-7} cm./cm. is produced by a rise of temperature of about 0·003° C. A correction

or change of temperature during the course of a series of observations was made when necessary from a calibration curve giving the movement of the fringes which occurred with change of temperature, when other things were equal. The water bath was kept vigorously stirred and its temperature was measured to 0·01° C. The rate of change of temperature of the water bath was always small and steady, and never exceeded 0·5° C. per hour. The results quoted in § 3 show that the accuracy obtained was of the order anticipated.

§ 3. EXPERIMENTAL RESULTS

The experimental work has consisted in the investigation of the variation of the distance between two points on a particular specimen of lead with the applied tension and with time. The specimen was a lead wire, 3 mm. in diameter, containing less than 0·001 per cent impurity, to which no special heat treatment had been applied. The results obtained can be described in general as follows. The variation of the length of the specimen with tension and time depends upon the history of the specimen, and in particular on whether the specimen has recently been subjected to a stress above a certain critical value. The results will therefore be considered in two sections, namely those obtained on an unstrained specimen, and those obtained after the specimen has been strained.

The results obtained with the unstrained specimen are comparatively simple, Hooke's law being obeyed within a small but definite stress-range. When this range is exceeded, the behaviour of the specimen deviates from Hooke's law in the usual way. These results are described in detail in the next paragraph. If, however, the specimen has previously been subjected to a stress much larger than the stress at which deviation from Hooke's law occurs, and if it has been allowed sufficient time for its length to become constant, then a type of elastic hysteresis manifests itself. The formation of the hysteresis loop, which is of a type not previously described, is discussed at the end of this section. The experimental study of these effects is complicated by the presence of elastic after-effects.

Elasticity of the unstrained specimen. Two typical stress-and-strain curves obtained with an unstrained specimen are shown in figure 2, in which graph (*a*) shows a case in which the elastic limit has not been exceeded, while graph (*b*) shows a case in which it has. The points on (*a*) lie on a straight line, their greatest deviation not exceeding 5×10^{-7} cm./cm. The points for increasing stress are represented as crosses, while those corresponding to decreasing stress are shown as circles. The two sets of points lie on the same line, and there is no observable permanent set of the specimen. The points shown were obtained by increasing or decreasing the stress by measured amounts, and waiting for three minutes after each change of stress before taking the reading of the fringes. This was necessary because the specimen does not attain the final length corresponding to any stress for a few minutes, eventually reaching a definite length. This elastic after-effect was observed whenever the stress was changed, and will be further described below.

The curve (*b*), figure 2, shows that there is a limit to the region in which Hooke's law is obeyed. This limit occurs when the strain is just above 3×10^{-5} cm./cm. The critical stress is 9·0 kgm. cm.^{2} This point is also the lower limit of strains which result in permanent set observable by the present method. A third characteristic of this critical strain is that when it is exceeded a change takes place in the type of elastic after-effect obtained.

The method of investigation of the after-effect was to change the tension on the specimen by definite steps, usually either about 1500 gm. cm.^{2} or 3000 gm. cm.^{2} corresponding to changes of water-level in the tube *H*, figure 1 (*a*), of 1 cm. and 2 cm. respectively. These changes of tension were made in the direction of either

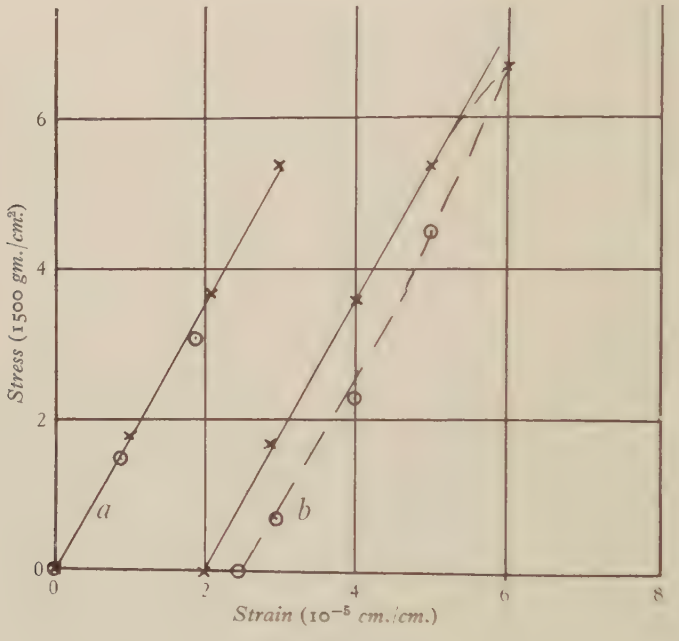

Figure 2.

increasing or decreasing stress, and after each change the movement of the fringes was observed until it was less than 0·01 fringe per minute, which corresponds to a change of length of the specimen of about 10^{-7} cm. cm. per minute.

The type of curve obtained when the tension did not exceed the elastic limit was always that shown in figure 3 (*a*) in which several curves, selected at random, for these changes of stress are shown. It is found that similar curves are obtained with increasing and decreasing stresses, and that so long as the elastic limit is not exceeded the curve depends only on the change of tension and not on the tension itself.

Some uncertainty as to the time zero of these curves is inevitable, for the stress cannot be increased or decreased suddenly without causing vibrations that prevent measurements from being made. With the method of changing the stress adopted,

.e. syphoning water into and out of the tube, the change of stress takes at least ; seconds and usually considerably more, and in general the zero of the curves could hot be fixed to within about 10 seconds. This uncertainty will be referred to again n the discussion of results.

Curves of the type shown were always obtained unless the elastic limit was exceeded. When the stress applied was above the elastic limit, the after-effect no onger ceased after a few minutes, but continued for a much longer time in a manner similar to that described in the next section.

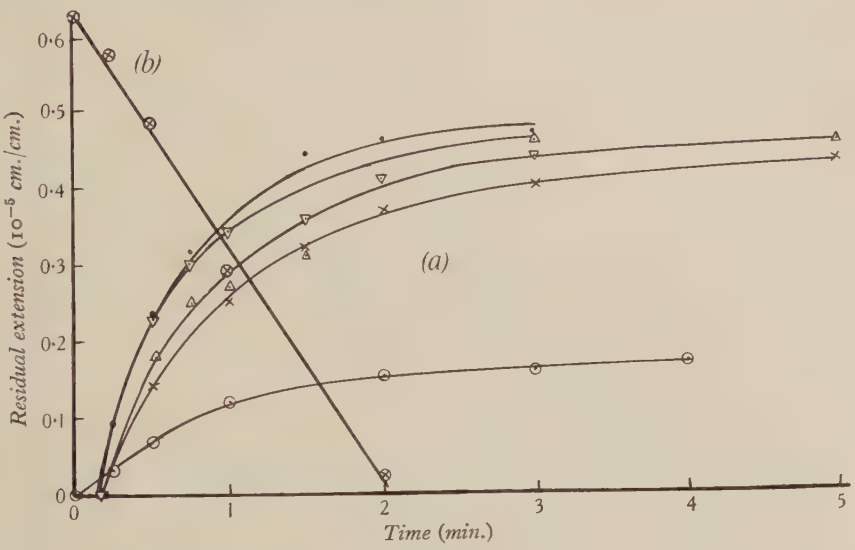

(a) × = +3000 gm./cm²
● = −3000 gm./cm² (Ordinates negative).
⊙ = +1500 gm./cm²

(b) ⊗ = log (extension), on a different scale.

Figure 3.

Elastic hysteresis of the strained specimen. If the stress is increased by steps from zero up to a maximum and then reduced to zero, and if a reading of the length is taken for each stress after sufficient time has elapsed for the lengths to have become constant, a closed loop denoting the existence of hysteresis is obtained. A series of such curves corresponding to different maximum stresses is shown in figure 4 (*a*).

Each loop consists of two curved parts and two straight lines. The curved parts are similar for all the loops of the series, and the same two parallel straight lines form the straight parts of all the loops. It follows that the width of the loop, i.e. the difference in the lengths which the specimen has when the stress is increasing and when it is decreasing, is independent of the maximum stress reached, provided that the latter is less than the elastic limit. The width of the loop and the slope of the straight lines vary with temperature and with the crystalline state of the metal; for instance they depend on whether the elastic limit has recently been exceeded. The

width of the loop obtained with the same specimen varied, in the experiments described, between $0{\cdot}5 \times 10^{-5}$ cm./cm. and $2{\cdot}5 \times 10^{-5}$ cm./cm. according to the amount of strain to which the specimen had been subjected.

A further observation regarding the hysteresis loop is that the lower extremity of the loop can be produced at any stress-value by increasing the tension from that point. A typical example demonstrating this observation is given in figure 4 (*b*). The stress was increased from *A* to *B*, then decreased from *B* to *C*, increased from *C* to *D* and finally reduced from *D* to *A*. The point *C* behaved in a manner similar to

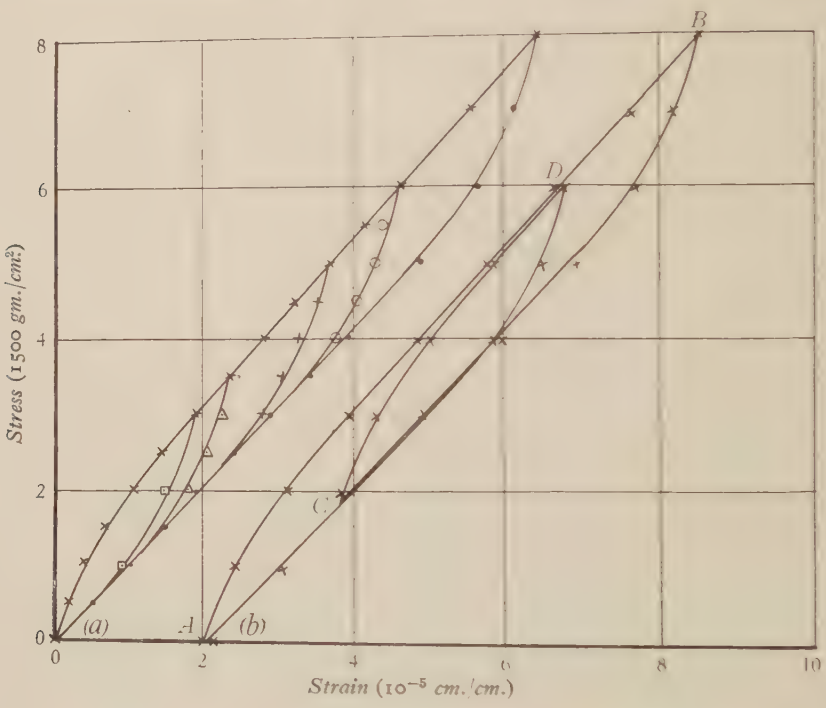

Figure 4.

the point *A*. Hence the same loop is obtained whether the lower reversal is made at zero stress or at some other stress. A further point of importance is that, although in these experiments stress is only being applied in one sense, i.e. tension and not compression, the loop is closed, and can be repeated a number of times without observable change.

The elastic limit. The constancy of the slope of the straight-line parts of the hysteresis loops is shown in figure 5, in which the change of length, in units of 10^{-7} cm./cm., corresponding to a change of stress of 1500 gm./cm.², is plotted against the total stress. The points marked by crosses indicate increasing stress, and the circles decreasing stress. The points lie very close to a straight line, with the exception of two points at the beginning of each set which correspond to the curvature which gives rise to the hysteresis loop. Apart from these points, the maximum

deviation from a horizontal straight line is three units, indicating a maximum difference of slope of the stress-and-strain line of 3 per cent from the mean. There is, however, no systematic deviation of the points from the horizontal line, and it follows that there is no change of slope above the limits of the experimental error. It is safe to say that the slope does not change by more than 1 per cent over the range of this curve.

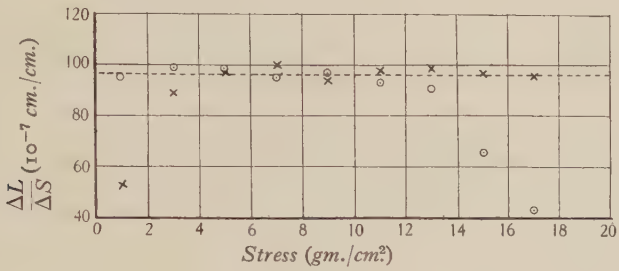

Figure 5.

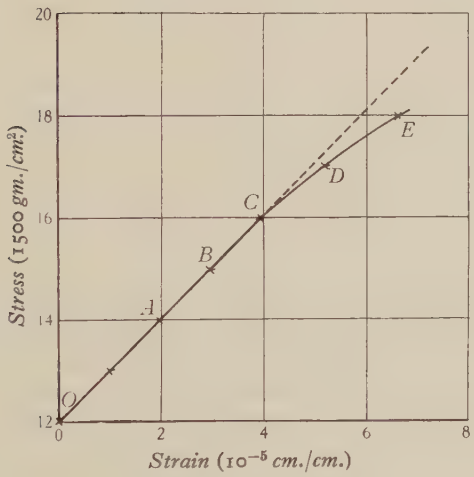

Figure 6.

Figure 6, however, shows that at a greater stress an abrupt departure from the straight line takes place. *OABC* represents the straight line part of the curve, and beyond *C* an obvious deviation occurs. Curves showing the elastic after-effect corresponding to increases of stress from *A* to *B*, *B* to *C*, *C* to *D* and *D* to *E* are given in figure 7. It is clear that the point *C* marks the transition between the two kinds of after-effect curve, as well as the end of the straight line. The points above *C* are not as definite as the points below *C*, because the after-effect curve shows no definite final value once *C* has been passed. It follows that the point *C* marks a definite change in the response of the metal to stress, and is the transition point between the elastic and the plastic parts of the curve. The point *C* is therefore taken as the elastic limit. It will be shown in § 4 that the after-effect occurring before this

point is due to thermal and not to plastic effects. The amount of stress corresponding to the elastic limit depends upon the history of the specimen, and so cannot be given a definite value. When the greatest strain to which the specimen has been subjected is comparatively small, i.e. not very much above the primitive elastic limit, the elastic limit of the strained specimen is low; when the maximum stress is high, the elastic limit is also high.

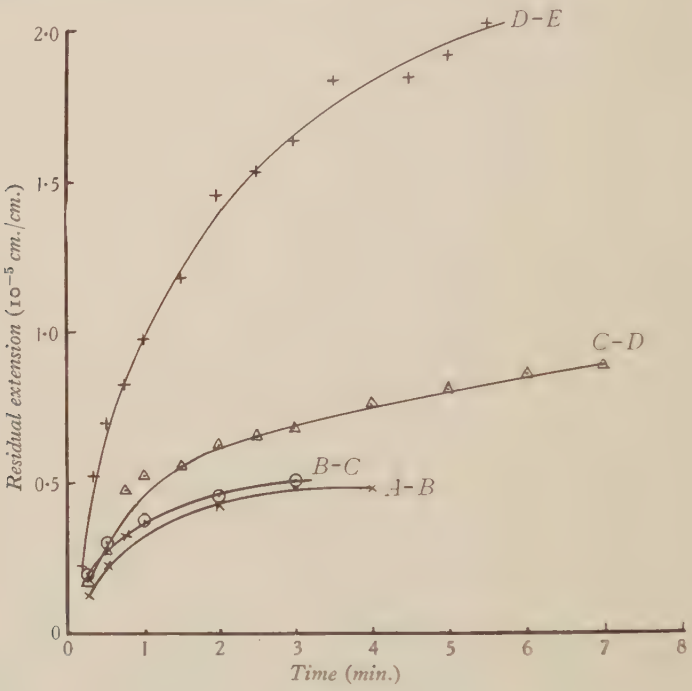

Figure 7.

§ 4. DISCUSSION OF THE RESULTS

The experimental study of elastic hysteresis and the allied effects has been pursued in the past chiefly by the use of torsional stresses and strains[3, 5, 8]. Such work, although of the greatest value from the practical point of view, cannot be made to give very much information regarding the fundamental relations between stress and strain. The effect of a torsional stress on a material which does not obey Hooke's law for the whole range of stress applied must be to set up a very complicated set of internal stresses and strains. The observed torsional deformation would be some function of the stress and of the deviation from Hooke's law. If, in addition, the stress acting on some part of the specimen, namely the outer shell, is above the limit of approximate adherence to Hooke's law, while the rest of the specimen is under stresses varying from zero to this limit, effects resembling the production of a hysteresis loop may result, the energy-loss in the loop being produced in the part of the material which is in the plastic state.

Much of the work done on elastic hysteresis in which a homogeneous stress (e.g. tension) is used is valueless from the present point of view owing to insufficient accuracy. Ewing[1] performed experiments on long wires with an accuracy of 10^{-7}, but his experiment only established the existence of a hysteresis loop without investigating its shape. Gough, Hanson and Wright[2] used tensile tests for part of their work, making their measurements with a Marten's extensometer, the limit of their accuracy being 2×10^{-6}.

In these cases, as in others in which the apparatus is constructed on a fairly large scale, sufficient temperature-control for an accuracy approaching 10^{-7} cannot be obtained.

The degree of accuracy obtainable with the present apparatus is necessary in order to establish the existence of a definite elastic range in the unstrained specimen. The elastic range is regarded as being definite because there appears to be a definite point at which three deviations from perfect elasticity first become discernible—departure from the straight line, permanent set, and true plastic flow. These deviations increase rapidly, and roughly in proportion to the amount by which the stress exceeds the elastic limit, when this limit has been passed. These observations indicate that a higher degree of accuracy would not indefinitely reduce the elastic limit.

After the specimen has been strained and allowed to recover from the immediate effects of the strain (which take the form of a continuous reduction of length towards a final value to which it approaches asymptotically and is sensibly equal after a few hours) its behaviour is quite different from the elastic behaviour discussed above. The slope of the stress-and-strain line at the origin is roughly equal to that of the straight line of the unstrained specimen, but further increase of stress reduces the slope of the line, so that there is less stress per unit strain, and the slope of the straight line which is eventually reached is between one-half and two-thirds of that of the primitive elastic line. Hence the general effect of applying a large stress to the specimen is to reduce its effective elastic modulus, bring it to a condition in which hysteresis loops can be obtained, and replace the low elastic limit of the unstrained specimen by an elastic-hysteresis limit which is much greater (the limiting stress being five or ten times as great) and shares all the properties of the actual elastic limit.

The type of hysteresis loop obtained in the investigations cited above, and discussed by Tomlinson[9] and by Prandtl[6], is that shown in figure 8. Such a loop depends upon the deviation of the line of increasing stress *ABCD* from a straight line at *C*. It requires, then, that the stress applied, at any rate to part of the specimen, should exceed the elastic limit. The loop is a result of permanent set of the specimen occurring at the extremes of stress, and can only be closed if equal stresses of opposite signs are applied alternately. Since it would presumably not exist if the reversal of the stress were made at the point *C*, it depends upon the material entering the plastic or overstrained state, and the name *plastic hysteresis* may be suggested for this type of loop.

The formation of the hysteresis loop observed in the present experiments differs

fundamentally from the plastic hysteresis loop referred to above. An elastic hysteresis loop, such as that shown in figure 4, depends upon the fact that the stress-and-strain line is curved either when the stress is increased from a minimum value or decreased from a maximum value, irrespective of what these values are, provided that they do not exceed the elastic limit, i.e. that the stress is not sufficient to produce a sensible deviation from the straight-line part of the stress-and-strain curve, or to cause a true plastic after-effect exceeding 10^{-7} cm. cm. per minute after 5 minutes.

In a recent paper on the bending of marble, Lord Rayleigh[7] gives diagrams of the hysteresis loops he obtained by applying flexural stresses to specimens of marble that had been heated. The diagrams show loops very similar to those described in the present paper, and appear to be elastic rather than plastic in origin. Similar elastic hysteresis loops are given by Hanson[4] for zinc single crystals by bending. The difference between these loops and the plastic loops is not discussed in either of the papers cited.

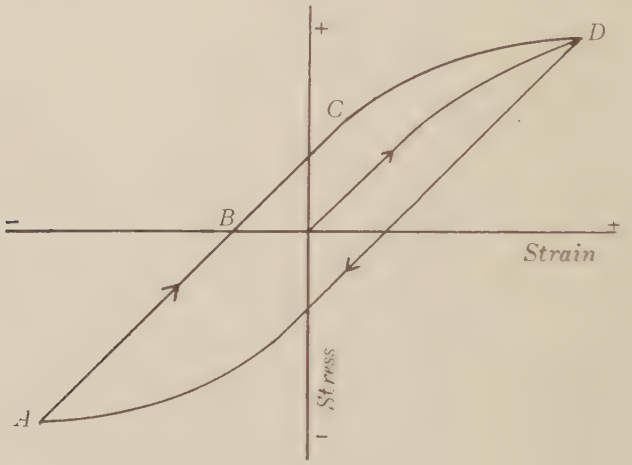

Figure 8.

Before discussing the significance of these loops it is necessary to enquire into the possibility of their existence being only apparent, and due to some defect in the apparatus. Various experiments have been made with a view to eliminating this possibility. Any cause which would prevent the upper plate of the interferometer from moving freely, so that it lagged behind its true position, would cause a loop such as was found to appear. Two possible ways in which this might happen suggest themselves, the first being that some friction might prevent free movement of the upper plate, and that the upper interferometer mirror might not move in proportion to the movement of R (figure 1) until R had moved by a certain amount. This would cause the length to appear too small when it was increasing and too large when decreasing. A similar effect on the lower plate would give the reverse effect, and a loop of apparently negative area would result.

The effect of friction is usually to prevent all movement until a limiting force is reached, when movement suddenly starts; this is not what happens with the

ysteresis loops, since the ends of the loops are curved and not flat. Further, if uch a frictional force existed, there would be a range of positions in which the pper interferometer plate would be in equilibrium between the frictional force and he force acting on it at its point of contact with the specimen. It is found, however, hat if the plates are set in vibration by lightly tapping the bench on which the pparatus stands, after the broadening of the fringes due to vibration has disappeared, he fringes are in the same position as before, to an accuracy of 0·01 of a fringe. This ndicates that there is only one position of equilibrium, and that friction does not ffect the position of the fringes to more than 0·01 of a fringe. It was also found hat if the plate R was moved by amounts corresponding to a movement of one or wo fringes by pressure of the finger on R, T or V, it returned to its original position vhen the pressure was removed.

The second way in which spurious loops might appear is that the contact at R night not be effective, and might be different when the specimen was moving pwards and when it was moving downwards. On one or two occasions when the pparatus had been set up so that contact at R was definitely unsatisfactory, it was mpossible to get the fringes steady, owing to chance vibrations of the upper plate. t follows that when the fringes are steady contact is satisfactory. A further test was nade as follows. Normally the upper interferometer plate was balanced and applied no force to the specimen; stress-and-strain curves were taken after altering the balancing so that R applied first a slight upward force on the specimen at the point of contact, and then a downward force. Identical loops were obtained in the various cases.

A further consideration is that the appearance of the loops did not depend upon he particular setting of the apparatus, for they were not altered by taking the specimen out, taking the apparatus to pieces and putting it together again, and replacing the specimen.

The most positive consideration, however, is that it is possible to get either the straight line or the hysteresis loop with the same specimen without removing it from he apparatus or making any other alteration except applying a larger stress to the specimen. In no case did a specimen which normally gave a straight line give a loop, and a specimen normally showing a loop was never observed to give a straight line. It must be concluded that it is not the instrument but the specimen which causes the loop to be observed, and that the hysteresis loop is an actual property of the specimen.

It is next necessary to discuss the significance of the elastic hysteresis loop. In the first place, the magnitude of the loop can be expressed as the ratio of the work transformed into heat during the cycle to work done on the specimen during its extension. In the series of loops given in figure 4 (*a*) this ratio varies from 0·21 for the largest loop to 0·33 for the smallest loop.

It follows that if a specimen of lead which has previously been strained is set in vibration, up to about one-third of the energy of the specimen in a single vibration may be lost if the amplitude is small. This conclusion will account for the fact that elastic vibrations in lead die away very quickly, and may account for the observation of Waller[10] that lead does not share the property of most other metals of being set into acoustic vibration by contact with solid carbon dioxide. This observation

must be distinguished from the decay of torsional vibrations of wires, in which plastic losses are probably concerned.

The general cause of the loss of energy involved in the hysteresis loops must be some kind of internal friction that causes a difference in the equilibrium between stress and strain when the stress is increasing or decreasing. It would be unprofitable, however, to attempt to picture the mechanism involved until the way in which the effect varies with crystalline arrangement has been investigated much more fully and, in particular, until it has been established whether the hysteresis loop can be obtained with a specimen consisting of a single crystal.

Although the elastic after-effect described above in connexion with figure 3 superficially resembles the true plastic after-extension, it can be shown that it may be due to thermal changes and not to plastic flow. It was pointed out by Joule that if a substance expands when heated, then if that substance is subjected to pressure its temperature will rise. Conversely, if a tension be applied the temperature will fall. Calculation shows that the thermal expansion due to the rise of temperature required to bring the specimen back to the temperature of its surroundings, after a fall in temperature due to the application of a tension, is of the right magnitude to account for the observed after-extension. A reduction of the tension gives a corresponding effect with the sign changed. The calculation only applies while the stress applied is less than that required to cause deviations from the straight line *OAB*, figure 6.

The fourth thermodynamic relation of Maxwell states that

$$\left(\frac{dH}{dp}\right)_T = -v\alpha T,$$

where dH is the heat entry during an isothermal change due to a change of pressure dp of a volume v at a temperature T, the coefficient of expansion being α. The isothermal heat entry dH is also the heat that will enter during the return to the original temperature if the first change is adiabatic, and that is approximately the condition of the experiment. Hence the fall in temperature of the specimen during an adiabatic extension can be calculated, and so the subsequent extension due to rise in temperature can also be determined.

$$dH = -v\alpha T dp,$$

or

$$\Delta H = -v\alpha T \Delta p,$$

where Δp is the change in tension in dynes/cm.^{2},

$$H = -\alpha T \text{ erg/cm.}^3 \text{ per dyne/cm.}^2,$$

or

$$H = -\alpha T D/J \text{ cal./gm. per dyne/cm.}^2,$$

where J is Joule's Equivalent and D is the density. The corresponding change in temperature ΔT is given by

$$\Delta T = -\alpha T D g/JS \text{ deg. per gm./cm.}^2,$$

where S is the specific heat.

Hence the subsequent increase ΔL of unit length is

$$\Delta L = -\alpha^2 TDg/JS \text{ cm. per gm./cm.}^2$$

Evaluating this for lead we get

$$\Delta L = 1{\cdot}937 \times 10^{-9}.$$

When the increase of tension is 3000 gm./cm.^{2},

$$\Delta L = 3000 \times 1{\cdot}937 \times 10^{-9}$$
$$= 5{\cdot}811 \times 10^{-6} \text{ cm./cm.},$$

which is about the extension required to give a shift of one half-fringe.

It was always found that a change of tension of 3000 gm./cm.^{2} within the elastic limit gave an after-effect of less than 0·5 of a fringe, see curve *A*, figure 4. For greater changes of tension greater after-effects were found, but never greater than the value calculated as above. There are two reasons why the observed after-effect should be less than that calculated. The first is that the change is not strictly adiabatic, as it takes a definite time to apply the stress; hence the fall in temperature T is not as large as is found in the calculation. Secondly, observations of the positions of the fringes cannot be taken immediately after the stress is applied, so the full extent of the after-effect is not observed.

The slight variation in the shape of the curves *A*, *B*, *C*, *D*, figure 4, is probably due to the fact that the rate of loss of heat from the surface of the specimen depends upon the speed of circulation of the water surrounding it. This varied according to the speed of the stirring-motor. Hence the shape, but not the final extension, may vary.

The variation of temperature of a cylinder with time, if the cylinder loses heat radially to its surroundings, can be derived from a Bessel-Fourier function. The variation of mean temperature with time can be shown to follow an exponential law. When one of the curves of figure 3 is plotted logarithmically (i.e. when $\log \{(L-L_\infty)/(L_0-L_\infty)\}$ is plotted against t, where L is the length at time t, L_0 the length when $t=0$, and L_∞ the final length) the curve of figure 3 (*b*) is obtained. The fact that this curve is straight shows that the law of the thermal after-effect is exponential.

It is concluded, therefore, that within the elastic limit as indicated by the straight-line part of the stress-and-strain curve, the after-effect does not exceed the amount that can be accounted for on thermodynamic grounds. It appears probable that plastic flow commences at the elastic limit.

The curves of figure 7 show quite clearly that the after-extension completely changes its character when the point *C*, figure 6, has been passed, and that the rate of this plastic extension increases rapidly with increase of stress beyond that corresponding to the point *C*, figure 6. This applies in both the strained and the unstrained conditions.

Although Hooke's law is not obeyed with lead after straining, it is possible to express a value for Young's modulus for the specimen concerned; such a value refers to the slope of the straight-line portions of the stress-and-strain loop. Since the slope of these lines varies in some manner as yet unknown with the conditions that

affect the crystalline arrangement of the metal, it is useless to attempt to evaluate Young's modulus to a high degree of accuracy. The values obtained are

$$Y = 1{\cdot}7 \times 10^{11} \text{ dyne/cm}^2 \text{ for a strained specimen}$$

and

$$Y = 2{\cdot}7 \times 10^{11} \text{ dyne/cm}^2 \text{ for an unstrained specimen.}$$

Although the actual stress corresponding to the elastic limit varied somewhat, it was found to be of the order of 30,000 gm. cm^{-2}, and the limit of the elastic extension was in the neighbourhood of 2×10^{-4} cm. cm. for a strained specimen. The corresponding values were 9000 gm. cm^{-2} and 4×10^{-5} cm. cm. for the unstrained specimen.

REFERENCES

(1) Ewing. *Brit. Ass. Report*, p. 502 (1889).
(2) Gough, Hanson and Wright. *Philos. Trans.* A, **226**, 1 (1925).
(3) Guest and Lea. *Proc. roy. Soc.* A, **93**, 313 (1917).
(4) Hanson. *Phys. Rev.* **45**, 5, 331 (1934).
(5) Kimball and Lovell. *Phys. Rev.* **30**, 948 (1927).
(6) Prandtl. *Z. angew. Math. Mech.* **8**, 85 (1928).
(7) Rayleigh. *Proc. roy. Soc.* A, **144**, 266 (1934).
(8) Rowett. *Proc. roy. Soc.* A, **89**, 828 (1914).
(9) Tomlinson. *Phil. Mag.* **17**, 113, 634 (1934).
(10) Waller. *Proc. phys. Soc.* **46**, 116, 252 (1934).

DISCUSSION

Prof. Andrade. I understand that the strained rods recovered their unstrained condition, in which they showed no hysteresis, if kept at air temperature for a time. Is that so, and, if so for how long must they be kept? Did the author carry out any experiments on annealing strained rods, and what kind of strains did he employ? Were they simple extensions only? What were the magnitudes of the strains?

Comparison of figures 2 and 4 seems to show that the strained rods have a higher modulus than the unstrained to begin with, but a lower one when they reach their steady state, corresponding to the straight-line portion of the curve. Are figures 2 and 4 strictly comparable?

Has the author studied the flow when the rods are subjected to such a stress that the creep continues for hours? The thermodynamic cooling cannot, of course, be calculated on simple lines in this irreversible case, but must be exceedingly small. It would much interest me to be able to compare the flow at such relatively small stresses with that at much higher stresses which I measured many years ago. In the case of these small extensions no special device is needed to keep the stress constant as the rod extends.

As regards the propagation of sound, it looks as if an unstrained piece of lead should conduct sound quite well, as there is no hysteresis: the velocity will, of course, be that corresponding to adiabatic compressions and tensions, unless the

equency is very low. A strained piece of lead, however, exhibits hysteresis, and ould dissipate energy and show marked attenuation.

Dr F. D. Smith. It is difficult to find an entirely satisfactory definition of oung's modulus for a material like lead, which exhibits elastic hysteresis. We are ot justified in calculating it from one part of the hysteresis loop, figure 4, rather an another. The velocity of propagation of elastic vibrations of large amplitude ust be subject to a similar complexity. Certainly such vibrations will be rapidly storted and attenuated.

Elastic vibrations of small amplitude travel well in lead, as Dr Wood and I have oticed in our experiments. It may be that the hysteresis observed by the author oes not occur unless the strain is large.

Does the strain ever increase discontinuously? We know that intensity of agnetization sometimes increases discontinuously (Barkhausen effect). The xtensometer must, of course, be undamped for this test.

It would be preferable to plot stress (cause) as abscissa and strain (effect) as rdinate.

Dr A. B. Wood. The paper gives values of Young's modulus for lead ranging om $1{\cdot}7 \times 10^{11}$ dyne cm^{-2} for a strained specimen to $2{\cdot}7 \times 10^{11}$ for an unstrained ecimen. It is interesting to compare these values with those deduced from the elocity of sound in rolled lead sheet, as measured by a method recently described the *Proceedings**. The velocity of sound in rolled sheet (presumably overstrained) as found to be $1{\cdot}56 \times 10^{5}$ cm./sec., which gives for the elastic modulus $E/(1-\sigma^2)$ value of $2{\cdot}73 \times 10^{11}$ dyne/cm^2. Assuming a value 0·446 of Poisson's ratio σ, this ives $2{\cdot}35 \times 10^{11}$ dyne/cm^2 for Young's modulus E. It would be a very simple matter determine by the velocity method the variation of elasticity due to work-ardening of lead sheet. This method has the advantage that the strains superposed n the permanent strain in making the measurement are always very small.

Dr Mary D. Waller. I notice that the temperature is kept constant to within ·5° C. The temperature coefficient of variation of plasticity (possibly also that of lasticity) in the case of lead is probably considerable: would it not therefore be esirable to state the actual temperature of the experiments? The value of Young's odulus is higher than that usually quoted. Do wires of different diameters give onstant results? The large diminution in Young's modulus as a result of straining s interesting and may be characteristic of this peculiarly plastic metal. It appears o be much greater than that of other metals for which data are available.

Author's reply. In reply to Prof. Andrade: the question of annealing at room emperature and higher temperatures has not yet been dealt with quantitatively, but my results show that a strained specimen reverts to the unstrained state when kept at room temperature for some days. The curves in figures 2 and 4 are strictly comparable, being plotted in the same units, and the conclusions drawn from a

* *Proc. phys. Soc.* **47**, 149 (1935).

comparison are valid. I have not yet obtained creep curves over long periods time, but this should not present any particular difficulty, and it will be interesti to see whether these results agree with Prof. Andrade's empirical law for mu faster rates of creep.

In connection with the transmission of sound by lead, mentioned by Pr Andrade, Dr Wood and Dr Smith, it seems possible that the adiabatic stress-an strain curve may not exhibit the hysteresis loop even when the isothermal stres and-strain curve does so. This cannot easily be tested directly, but can perhaps l concluded from such considerations as those mentioned.

The importance of grain-size and the distribution of impurities in the materi is probably considerable in connection with the elastic properties, and may rend a comparison such as that suggested by Dr Wood of little value when the materia used have undergone very different treatments in their preparation.

No discontinuous increases in strain have been observed, and the experiment results give no indication even of a discontinuity of the slope of the stress-and-stra curve, except perhaps at the elastic limit.

In reply to Dr Waller: the experiments were all carried out at temperatures about 15° C. Wires of different diameters have not been compared: such a com parison would serve no useful purpose as the possible differences in the crystalli arrangements of the different specimens due to different mechanical treatmen would vitiate any conclusions drawn from the results.

REVIEWS OF BOOKS

xperimental Physics: A Selection of Experiments, by G. F. C. Searle. Pp. xiv + 363. (Cambridge University Press.) 16*s*.

In welcoming the publication of another manual of practical physics by the doyen of monstrators, Dr G. F. C. Searle, we regret to learn that this, the fourth volume in his ries of laboratory text-books, is not to be followed by another on experimental electricity d magnetism. From our knowledge of the excellence of the four volumes published we ould have known that the completed pentateuch would have been a final authority on boratory investigations of physical laws and principles. The clarity of exposition and the nple practical details which are given will prevent much wandering in the wilderness on e part of teachers and others who wish to set up any of these original experiments. It is ot suggested that such wandering should be condemned as being any more unprofitable a physical laboratory than, as history shows, it was in the desert of Et Tih, but the great xperience and the genius of Dr Searle are so very evident in each one of the experiments, oth in the theoretical discussion of a problem and in the design of the apparatus used investigate it, that these records of his methods of dealing with specific problems stand ut as models for all. The present volume contains accounts of experiments in mechanics, lasticity, surface tension, viscosity, heat and sound, none of which occurs in the three anuals already published, together with other experiments which have not been described reviously by Dr Searle except in the manuscripts written for use by his students in the avendish Laboratory.

A practical example, with numerical data, follows each experiment. It is not always ear that the order of accuracy to which a result is stated is that to be expected from the easurements on which the result is based. For example, in determining the viscosity of ater by flow through a capillary tube only two observations of the time of flow of unit ass, t/M, were made. These differ by about two per cent. The mean value is taken and the rude result is worked out. Corrections for calibration of the flow tube, buoyancy, etc., re then made by means of a factor 0·9915, better expressed as $(1 - \cdot 0085)$, and the final sult is stated as 0·01066 c.g.s. units. A little more time spent in settling the value of M more accurately would have been time well spent. J. H. B.

A Study of Crystal Structure and its Applications, by Wheeler P. Davey, Ph.D. Pp. xi + 695, with numerous illustrations. (McGraw Hill Book Co., 1934.) 45*s*. net.

This book is a review of the technique of crystal analysis, and the author states that it s intended for college graduates who wish to read the literature and do independent xperimental work. It is based on lectures given over fourteen semesters in the Penn-sylvania State College. It is divided into three main sections containing the necessary preliminary information about diffraction and crystal structure, a description of methods of crystal analysis, and a description of its applications in physics, chemistry and metallurgy. The appendices deal with X-ray apparatus, charts for the powder method, and space groups.

A book of this kind may either be a concise review of the main principles of the subject, which refers the student to the original papers for a detailed description of technique, or a comprehensive treatise for the X-ray worker which selects for description the most

recent and successful methods and theoretical advances. It seems to the reviewer that th present work does not achieve either of these objects. So long a book falls into the categor of the comprehensive treatise, yet in many cases it goes in great detail into descriptions o early methods and ideas without mentioning the simpler and better ones that have sinc replaced them. This applies both to questions of technique and to theoretical discussion which must surely now be based on quantum mechanics and not on the semi-classical ide of the Lewis-Langmuir and first Bohr atom, invaluable though these conceptions were i their time. To put it briefly, many sections of the book are years behind the times, and in subject which is growing so fast this is a serious defect.

The work of Zwicky on secondary structure in crystals has been described at lengt without reference to the subsequent work of Pauling, Orowan, and Smekal which claim to show that it is based on very erroneous calculations of lattice energy. In the chapter on the powder method the use of molybdenum K rays is described, with bare reference to the vast literature on the use of rays from anticathodes in the calcium-zinc range which has resulted in so enormous an improvement of accuracy. M_{α} rays have only been used becaus X-ray tubes with this anticathode are easily available; they are quite unsuited to accurate work. The description of the structure of Ag_3Al (p. 549) is based on a reference in the *International Critical Tables* of 1926, apparently in ignorance of its solution by Westgren and Bradley two years later. Probably few workers in this field would agree with the author's censure of the new nomenclature of space groups adopted by international agreement, which is widely held to be conspicuously successful in meeting the needs of X-ray analysis. The adoption of its rational system might have saved the author from giving in his list of screw axes (p. 213) only four of the eleven possible types, and listing as monoclinic (p. 21) the face-centred orthorhombic lattice. These are small points, but they are indicative of a want of balance and sense of proportion which mars the book. It contains many suggestive and interesting ideas, and is attractively illustrated. It does not appear to the reviewer, however, to present an accurate picture of the present state of the subject.

Electrolytes, by Hans Falkenhagen. Translated by R. P. Bell. Royal 8vo, pp. 346. (Oxford University Press.) 25*s*. net.

The volume gives an admirable account of a subject which is receiving but little attention from physicists in this country. The foundations laid by Faraday have been built upon by Debye and other workers abroad. In the book will be found a comprehensive survey of the modern theory of electrolytes and an indication of the experimental investigations and the data obtained.

The early chapters are devoted to a consideration of the theory of dilute solutions following on the lines laid down by Planck and Arrhenius. This theory is only valid for weak electrolytes, and the author then proceeds to consider strong electrolytes. The behaviour of strong electrolytes shows considerable departures from Arrhenius's theory, and to explain these account must be taken of interionic action. It is only with difficulty that the theory can be extended from the field of dilute solutions to embrace concentrated solutions. Such an extended theory must take into account the polarization, dispersion and repulsive forces between the ions, as well as the forces of interaction between the ions and the solvent molecules. The theoretical treatment of these complicated factors has so far been only partially successful. An account is given of the various attempts that have been made to treat theoretically the properties of concentrated solutions and the question of the true degree of dissociation of an electrolyte is closely connected with this problem. A section of the book is devoted to points connected with the optics of electrolytes and the detection of the undissociated part. It is of interest to note that attempts have been made to study the structure of electrolyte solutions by means of the Raman effect. Prof. R. H.

owler contributes an appendix on recent applications of quantum mechanics to the theory electrode processes.

The volume is to be strongly recommended to students wishing to enter this promising eld of enquiry. A word of praise is also due to Mr Bell for the excellence of his translation.

E. G.

Magnetism and Matter, by E. C. STONER, Ph.D. Pp. xv + 575, with 87 diagrams. (Methuen and Co., Ltd., 1934.) 21*s*. net.

Progress in the study of magnetic phenomena has been particularly rapid since the scovery of the electron, but at no period has it been more rapid than in the eight years hich have elapsed since the publication of Stoner's *Magnetism and Atomic Structure*. The te of progress has been such that the new book, *Magnetism and Matter*, is virtually a new ork. It takes a very definite and important place in the literature of magnetism, for it ccupies a position somewhere between the purely descriptive accounts of experimental cts and procedure and the more rigorous theoretical treatises such as Van Vleck's *Theory f Electric and Magnetic Susceptibilities*.

Consequently one must not turn to Stoner for the most comprehensive experimental tails, although complete references and many useful accounts of experimental methods e to be found in his work. The experimental sections have been brought up to date by ne inclusion of descriptions of the Sucksmith ring balance (which might, incidentally, be mended in the next edition) and of Kapitza's work with intense magnetic fields. But one ust turn to Stoner for an outline of the more important experimental facts and their ossible interpretations in the light of modern theories. Thus, those readers who require n easy approach to the present-day theory of paramagnetism will find it here. Here, too, a readable outline of the modern theory of ferromagnetism and a treatment of the modern spect of magnetoelastic and magnetoelectric effects. There is very much to be said in vour of such an adequate guide, as a preliminary to the more advanced mathematical reatises and works on modern magnetism.

In his preface the author states that the selection of investigations for detailed con-deration has necessarily been somewhat arbitrary, but there must be singularly few mpetent persons who will find fault with his selection. The book is an important ddition to the standard works on physics and is heartily commended to the Fellows of the hysical Society.

L. F. B.

The Kinetic Theory of Gases (Second Edition), by L. B. LOEB. Pp. xx + 687. (McGraw-Hill Book Co., 1934.) 36*s*. net.

In reviewing a *Kinetic Theory* of the scope of this book some comparison with the well-nown treatise of Jeans seems almost unavoidable, and in any case there is no reason why o useful a comparison should be avoided.

Though much of the same ground is covered in the two treatises, Loeb lays much nore emphasis than Jeans on the experimental side of the kinetic theory, and he deals xhaustively with a great many modern applications and developments of the subject. On ne mathematical side the treatment is less systematic and less elegant than that of Jeans. o use a possibly far-fetched analogy, Jeans climbs his mathematical hills quietly and asily in top gear and then in special physical chapters tells his humbler readers exactly hat is visible from the hill-tops. Loeb, on the other hand, takes the experimental hysicist and chemist with him up such hills as he elects to climb. The load being heavier, nis choice makes for a certain amount of gear-grinding, but on the whole there is much to e said for it.

Prof. Loeb clearly writes with a real enthusiasm for his subject. The book is of special value in that it combines in a single volume accounts of the classical kinetic theory and of the most recent developments. It thus provides, both for undergraduate and for advanced students, a valuable compendium of information, much of which is not elsewhere available in text-book form. In particular mention must be made of the chapter, nearly 100 pages long, on the applications of kinetic theory to problems in electrical conduction through gases, where Prof. Loeb can write freely as a leading authority.

There are, unfortunately, some minor blemishes in the work. There are some slips which should not have appeared in a second edition, and some errors—for example, the derivation of Poiseuille's formula on the assumption that a gas behaves as an incompressible fluid. There is also some carelessness in the writing of proper names. Most of these are too trivial for comment, but it is not in human nature to overlook the reference in the index to "Sir W. Rayleigh"—which suggests an ingenious telescoping, across almost exactly three centuries, of a great physicist and a great Elizabethan seaman. It must, however, be added that if Prof. Loeb is slightly inaccurate in some of his references, he is precise and very generous in his acknowledgments.

Prof. Loeb deserves credit for emphasizing the historical side of the subject, but the weight of evidence is against some of his historical notes. Brown, for instance, would have been much in advance of the other botanists of his time if in 1827 he had been led (p. 390) "to venture the idea that the (Brownian) motion was due to the unequal bombardment of the particles on various sides by the molecules of the liquid executing their heat motions and that they were therefore a manifestation of molecular heat motions." The kinetic-molecular explanation is generally attributed to Wiener (1863), and in his paper of 1829 Brown speaks of "motions for which I am unable to account." There is little evidence of any strong interest in the motions, and still less of any "violent controversy," for some years after Brown's discovery.

Again (pp. 84, 139) there has been some misapprehension concerning the date of publication of Waterston's paper on "The Physics of Media that are Composed of Free and Perfectly Elastic Molecules in a State of Motion." This was communicated to the Royal Society in 1845 by Beaufort, but it was not until nearly fifty years later that Rayleigh, then Secretary, rescued it from the Archives and caused it to be printed in the *Phil. Trans.* for 1892. It is not likely that Rayleigh, who was born in 1842, had in 1845 any very pertinent comment to make on the importance of the paper. If he had, his precocity would have been almost as remarkable as the vitality and versatility of Robert Brown, who was in his fifties when he discovered the Brownian movements, but who is shown in the index as O. W. Richardson's collaborator more than eighty years later.

These minor sources of irritation or amusement apart, this is a very good book.

H. R. R.

Bessel Functions for Beginners, by N. W. McLachlan, D.Sc., M.I.E.E. Pp. xi + 192. (Clarendon Press, 1934.) 15*s*. net.

The object of this book is to provide engineers and engineering students with a course of Bessel functions sufficiently advanced to enable them to employ the functions in practice in their physical and engineering researches. The book is well written and a great deal of labour has obviously been expended on it. Besides the worked-out examples there are 600 other examples set with answers. It will thus be as useful to students of pure as to students of applied mathematics. A graduate student looking out for a mathematical or physical subject as a thesis for a doctor's degree would find this a suggestive book. We can thoroughly recommend it.

A. R.

s Appareils à Fil Chaud, by E. G. RICHARDSON. Pp. 67. (Paris: Gauthier-Villars, 1934.) 20 fr.

This memoir contains in an expanded form the substance of a lecture given during 32 by its author at the Institut de Mécanique des Fluides of the University of Paris. is divided into two parts, the first of which contains an outline of the history and eory of hot-wire anemometers together with instructions for their use including par-ulars of precautions and corrections to be observed and made. In the second part the sults of investigations making use of such instruments are described: these investigations e concerned with such phenomena as the flow around aerofoils, vortex formation and rbulence, the distribution of air-velocity in acoustical resonators, flow in tubes, and the scosity of colloids.

The book summarizes conveniently the advances made by the author (who in many of s researches has collaborated with Dr Piercy of the Aeronautical Department at East ondon College and Dr Tyler of Leicester Technical College), while a bibliography of me sixty references ensures that adequate weight is given to the results of other workers this field. All those who contemplate using a hot wire will be well advised to onomize in both time and trouble by securing a copy of this book. E. J. I.